Systems vaccinology : molecular signatures of immunity to Bordetella pertussis

Raeven, R.H.M.

Systems vaccinology

Molecular signatures of immunity to *Bordetella pertussis*

René Raeven

The research described in this thesis was performed at the Research department of the Institute of Translational Vaccinology (Intravacc), Bilthoven, The Netherlands

ISBN: 978-90-8219-686-3

Printing of this thesis was financially supported by the Institute of Translational Vaccinology (Intravacc) and the MicroArray Department (MAD) of the UvA

Cover design: René Raeven
Layout: René Raeven
Photography: Guido Raeven & René Raeven
Printed by: PrintSupport4U

About the cover: "*Exploring the Mountains and Seas of Data*". Mount Fuji, its surrounding sea, and a blossomed cherry tree illustrated in Ukiyo-e style. All are dissected into smaller pieces and connected into a network using a Systems approach. Based on the "*Great Wave off Kanagawa*", which is part of the series "*Thirty-six Views of Mount Fuji*", by Japanese artist *Katsushika Hokusai*.

Systems vaccinology

Molecular signatures of immunity to *Bordetella pertussis*

Proefschift

ter verkrijging van
de graad van Doctor aan de Universiteit Leiden
op gezag van Rector Magnificus Prof. mr. C.J.J.M. Stolker,
volgens besluit van het College voor Promoties
te verdedigen op donderdag 22 september 2016
klokke 15.00 uur

door

René Henri Maria Raeven
geboren op 18 augustus 1982
te Geleen

Promotoren:
Prof. Dr. G.F.A. Kersten (Intravacc & Universiteit Leiden)
Prof. Dr. W. Jiskoot (Universiteit Leiden)

Copromotor:
Dr. B. Metz (Intravacc)

Promotiecommissie:
Prof. Dr. P. v. d. Graaf (Voorzitter)
Prof. Dr. M. Danhof (Secretaris)
Prof. Dr. A. Meijer (Universiteit Leiden)
Prof. Dr. F. Mooi (RIVM & Universiteit Utrecht)(Emeritus)
Dr. C. Locht (Institute Pasteur Lille)
Dr. M. de Jonge (Radboud UMC, Nijmegen)

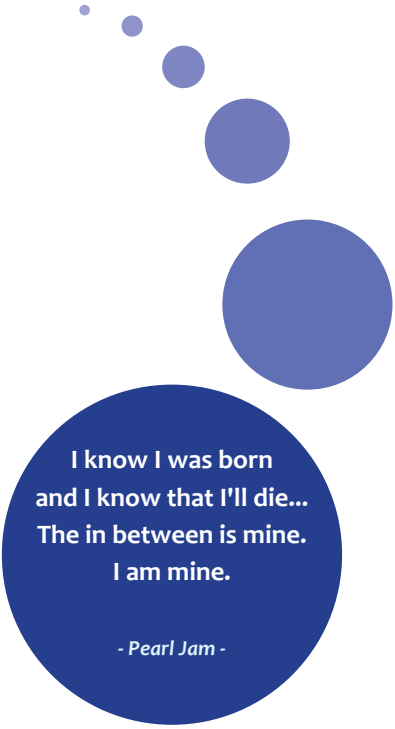
I know I was born
and I know that I'll die...
The in between is mine.
I am mine.
- Pearl Jam -

Table of contents

About the cover: Kinkaku-ji ("Golden Pavilion"), part of the Rokuon-ji temple complex in Kyoto, Japan. The Buddhist temple dates from 1397 and is covered in gold leaf.

CHAPTER 1

General introduction

Bordetella pertussis

Whooping cough, or pertussis, is a highly contagious respiratory disease that is caused by the gram-negative bacterium *Bordetella pertussis*. *B. pertussis* was discovered and isolated by Bordet and Gengou in 1906 [1]. It is a strictly human pathogen and all age groups can be infected. However, infants are the main risk group. Diagnosis of pertussis is often difficult in the early stage with only a mild cough, and fever is uncommon. Later, the severity of the disease increases with pneumonia, vomiting and increased coughing that in infants can lead to death [2]. The most profound characteristic of pertussis is the "whooping" sound during coughing. In patients with severe disease, the cough can last for a long period, which made the Chinese call pertussis the "100 day cough". Diagnostics of pertussis is performed indirectly with serology or direct bacterial detection in sputum by culturing or PCR [3]. For serological diagnosis IgG antibodies against pertussis toxin (Ptx) are used [4].

B. pertussis contains many virulence factors (proteins associated with pathology) that are regulated by the Bordetella virulence regulon (Bvg) [5]. These virulence factors have different locations and functions in the bacterium (**Figure 1A**). During colonization, *B. pertussis* excretes Ptx and other toxins, such as adenylate cyclase toxin (Act), dermonecrotic toxin (Dnt), and tracheal cytotoxin (Tct). Moreover, the bacterial membrane contains virulence factors, such as BrkA, filamentous hemagglutinin (FHA), pertactin (Prn), fimbriae 2 and 3 (Fim 2 and 3) and Vag8. These virulence factors facilitate adhesion of the bacteria in the respiratory tract. Some virulence factors arm *B. pertussis* with immune evasive strategies that increase the chances of bacterial survival in the respiratory tract [6]. The virulence factor expression depends on the state of the bacteria, i.e. colonizing or resting, but also varies among *B. pertussis* isolates probably because of host defense induced selection [7].

Pertussis vaccines and vaccination

Pertussis is a vaccine-preventable disease. However, *B. pertussis* is endemic around the world and epidemic cycles occur every 2 to 5 years [8] (**Figure 2A-B**). Vaccination against *B. pertussis* in the 1940s resulted in an impressive decrease of pertussis cases worldwide (**Figure 2A**). Global pertussis vaccine coverage among infants that received three doses was estimated at 86% (115 million infants) in 2014. However, low vaccination coverage is observed in some low-income countries (**Figure 2C**). Vaccination has resulted in the prevention of almost 700,000 deaths in 2008, as estimated by the WHO [9].

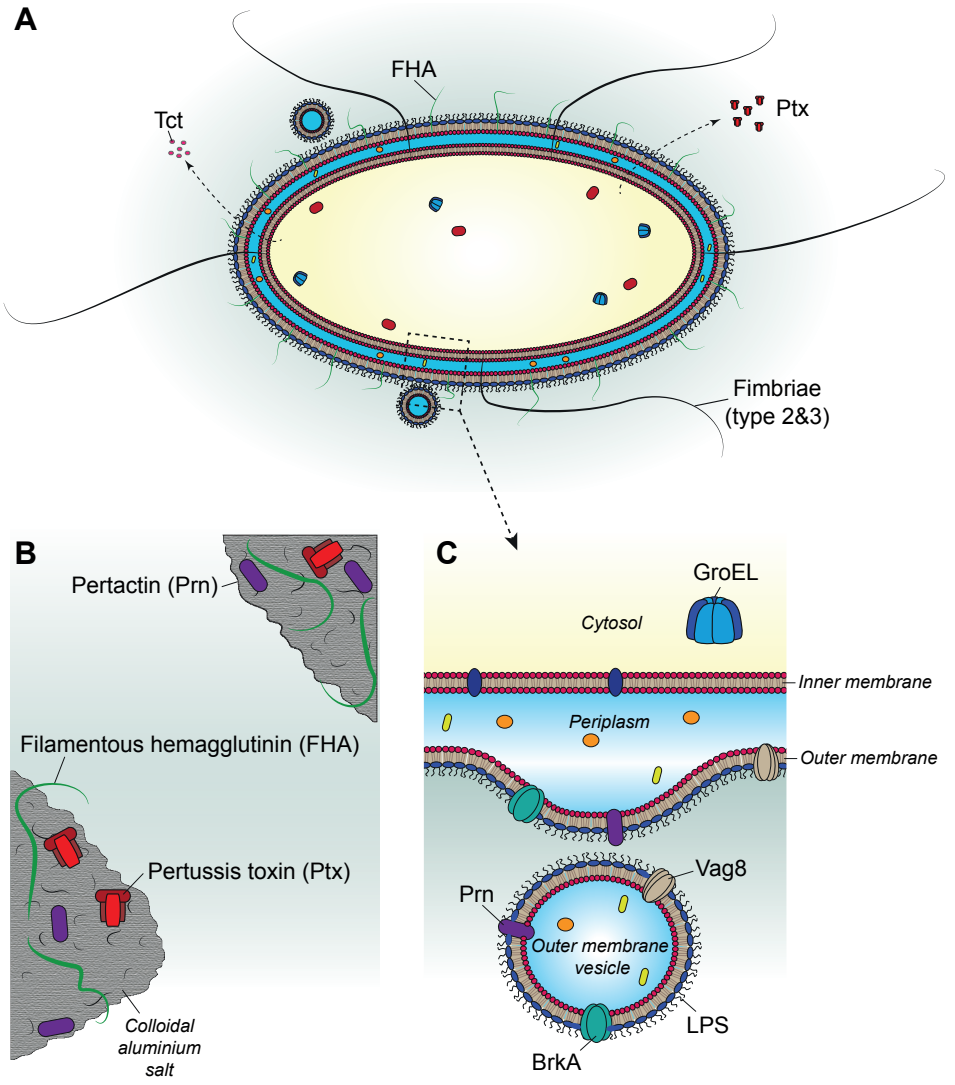

Figure 1 - *B. pertussis* and different pertussis vaccines. Schematic illustration of **(A)** *B. pertussis*, **(B)** acellular pertussis vaccine, and **(C)** outer membrane vesicle pertussis vaccine.

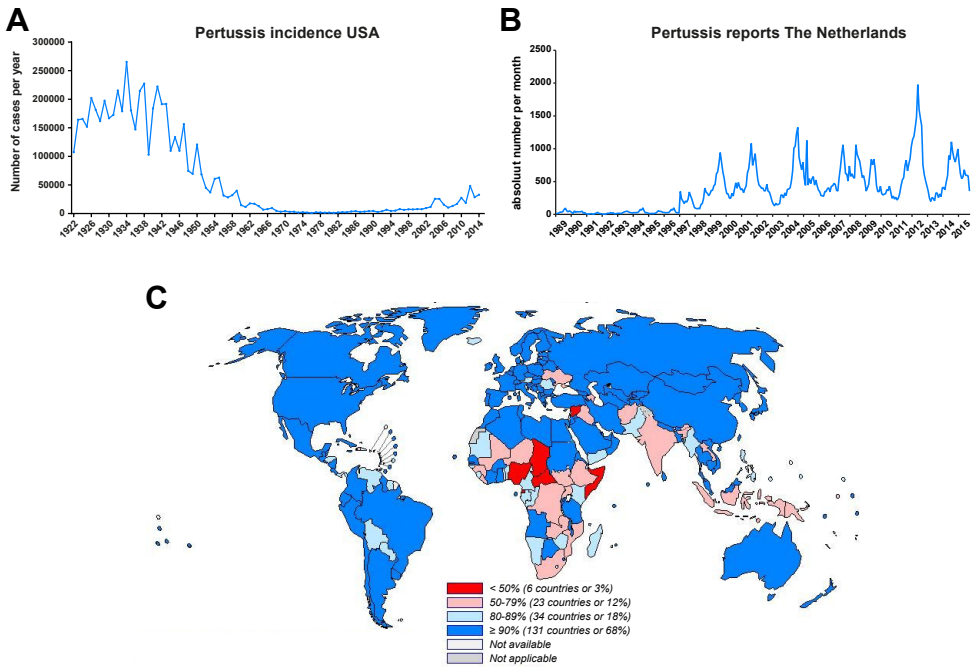

Figure 2 - Pertussis incidence and DTP3 vaccination coverage. **(A)** The number of pertussis cases registered each year in the USA in the period 1922-2014. *Figure adapted from www.cdc.gov, accessed July 2016.* **(B)** The absolute number of pertussis reports in The Netherlands for each month in the period January 1989 – September 2015. Source: Pertussis reports in Osiris, adapted by RVP-EPI-RIVM. **(C)** The global immunization coverage among infants that received three vaccinations with DTP3 according to the WHO in 2012. The colors illustrate the coverage per nation. *Illustration adapted from www.who.int, accessed July 2016.*

Antibodies are essential for protection against pertussis. Antibodies have therefore been marked as potential correlates of protection against *B. pertussis* [10, 11]. Anti-Ptx IgG antibody serology is commonly used for epidemiological screening of protection [12]. However, the contribution of antigen-specific T-cells is not to be underestimated [13, 14]. Currently two types pertussis vaccine are marketed, the whole-cell and acellular pertussis vaccine, and at least two vaccine concept are under development, a live attenuated vaccine and a vaccine based on outer membrane vesicles, that are discussed below.

Whole cell pertussis vaccines (wPVs)

The first pertussis vaccines on the market were the cellular vaccines, also known as whole-cell pertussis vaccines (wPVs). Currently, still 75% of the world population receives these vaccines. These vaccines contain dead *B. pertussis* bacteria that are physically (heat) or chemically (formaldehyde) inactivated. The wPVs contain lipopolysaccharide (LPS), acting as an intrinsic adjuvant, as well as other pathogen-associated molecular patterns (PAMPs). Some wPVs contain colloidal aluminium salts (alum) as an added adjuvant. As wPVs contain the whole bacteria, a diverse range of virulence factors, particularly membrane bound proteins, such as FHA, Prn, Fim2, and Fim3, are present in the vaccine. However, the composition of wPVs may

vary depending on the type of strain, culture conditions, and type of inactivation. This variation in production leads to vaccines with a varying efficacy [15]. The use of wPV is associated with mild adverse effects, such as local swelling and fever after vaccination [15, 16]. The adverse effects tend to increase with the number of vaccinations and the age. Therefore, wPV is not recommended for vaccination of adolescents and adults. The suspected correlation between wPV and serious acute neurological illness in children [17, 18] has led to a call for safer pertussis vaccines.

Acellular pertussis vaccines (aPVs)

The need for safer and better-defined pertussis vaccines stimulated the development of the acellular pertussis vaccines (aPVs). These were first developed and introduced in Japan [19] and slowly afterwards in other developed countries [20, 21]. The marketed aPVs contain purified proteins from *B. pertussis* that are adsorbed onto colloidal aluminium salts and vary in antigen composition (**Figure 1B**). They contain one to five antigens, i.e. FHA, Fim 2, Fim 3, Prn and/or Ptx. In the Netherlands, a trivalent aPV (FHA, Prn, Ptx) is used, whereas in Denmark a monovalent Ptx vaccine is used. The high cost of aPVs limits their widespread use in developing countries.

Live-attenuated pertussis vaccine (BPZE1)

One of the vaccines under development is a live attenuated *B. pertussis* strain, BPZE1 [22]. This strain is genetically attenuated by altering or removing three virulence factors involved in pertussis pathogenesis. Dermonecrotic toxin (Dnt) was completely removed, whereas the ability to secrete pertussis toxin (Ptx), and tracheal cytotoxin (Tct) was reduced. Similar as wPV, BPZE1 also consists of a broad range of antigens and PAMPs. In contrast to other pertussis vaccines, BPZE1 is administered intranasally and is still able to replicate in the upper and lower respiratory tract. A single nasal dose provides protection in mice [22] with long-term immunity [23, 24]. BPZE1 is in early clinical development. A phase 1 study revealed no safety issues in healthy adults [25]. Moreover, increased B-cell responses were detected, indicating that BPZE1 is immunogenic [26].

Outer membrane vesicle pertussis vaccines (omvPVs)

Many gram-negative bacteria produce outer membrane vesicles (OMVs) [27, 28]. Naturally, they serve as transport system between bacteria and function as decoy for the host immune system [27, 28]. Also *B. pertussis* releases OMVs [29]. These OMVs are a potential vaccine candidate. Outer membrane pertussis vaccine (omvPV) confers protection in mice after parenteral immunization [30] with long-lasting immunity [31]. The omvPV mainly consists of outer membrane proteins, lipids, phospholipids and LPS (**Figure 1C**). In addition, proteins may be present that are encapsulated during the OMV formation. The composition of omvPV also depends on the production method [32]. OMVs form spontaneously in low amounts

during cultivation. Constructing high-blebbing mutants can increase the yield of OMVs. Often membrane-destabilizing agents, such as EDTA and non-ionic detergents, are used to obtain high yields.

Vaccination against *B. pertussis*

Despite the high vaccine coverage, pertussis still ranks in the top 10 of vaccine-preventable diseases according to the WHO. Many countries experience resurgence of *B. pertussis* [33, 34]. In addition to infants, older age groups are increasingly affected [35, 36]. Adaptation of circulating strains is one of the causes of this resurgence [37]. This selection may be vaccine induced. The current increased circulation of Prn-deficient strains is an example of vaccine-induced strain adaptation that leads to antigen-mismatch [38, 39]. Although current licensed vaccines induce high antibody levels, the potential correlate of protection for pertussis [10, 11], the duration of protection is with 4-12 years relatively short [40, 41]. Increasing the number of immunizations with aPV does not solve this [42]. Studies in baboons [43] have demonstrated that the aPVs prevent the disease, but in contrast to wPVs, they are incapable to prevent transmission of *B. pertussis* [44]. Healthy aPV-vaccinated people can carry and transmit pertussis to very young, still unprotected children. The most recent strategy to prevent pertussis in this vulnerable group, is maternal vaccination with aPV [45]. Maternal immunization allows protection of the newborn in the period between birth and primary vaccination by placental transfer of antibodies from the mother to the child. This strategy significantly reduces the risk of death among the main target group, infants [46]. However, the problem of strain adaptation and protection of other target groups require additional measures. The switch from aPV back to wPV is highly unlikely in high-income countries because of the safety issues with wPV. However, wPVs remain the first choice for many low-income countries because of their high efficacy and low cost.

The current state of knowledge with respect to immunity to *B. pertussis* is that the induction of specific IgG antibodies and T-helper (Th) 2 cells is sufficient for short-term protection. However, the presence of Th1 and Th17 cells may be beneficial. Additionally, mucosal immunity may contribute to better protection based on the results after local administration of BPZE1 or a natural infection. Interestingly, infection-induced immunity in humans is estimated to last 4-20 years [40] or even up to 50 years [41] which is longer than by vaccination with marketed pertussis vaccines [40, 41]. This indicates the possibility to improve vaccine-induced pertussis immunity. An unbiased and comprehensive investigation in infection-induced and vaccine-induced immune responses could provide insight in molecular signatures that enables vaccinologists to improve pertussis vaccines. This thesis describes the findings of a systems vaccinology approach in pertussis research and the molecular signatures that were discovered related to *B. pertussis* immunity.

Systems vaccinology

Vaccine development has reached a point where the 'easy' vaccines have been developed. Still no effective vaccines are available for some diseases, i.e. AIDS and tuberculosis, while some pathogens require improved vaccines, i.e. *B. pertussis*. Moreover, the development of vaccines against new emerging diseases requires immediate action, yet the lack of in-depth knowledge on the pathogen and immunity often leads to hampered development [47]. This situation calls for innovative strategies in vaccine development. Systems vaccinology is a new approach that provides comprehensive insight in immune responses induced by the pathogen or vaccine candidates [48, 49]. Systems vaccinology is a part of systems biology. According to Alan Adrem the definition of systems biology is a "comprehensive quantitative analysis of the manner in which all the components of a biological system interact functionally over time that is executed by an interdisciplinary team of investigators" [50]. In analogy, systems vaccinology could be defined as a "comprehensive quantitative analysis of the manner in which all the components of the immune system interact functionally over time during progression of the response to infection or vaccination". Systems vaccinology can potentially fill the gap for vaccine development by contributing in-depth knowledge on vaccine-induced responses, which will be described hereafter.

Systems vaccinology aims at in-depth understanding how vaccines work, or why some vaccines do not work. A biological system can vary from the human body to a single cell. An important first task for a systems vaccinologist is setting boundaries on the system. In this case, this thesis was mainly limited to the host immune system. However, vaccine composition was not neglected and characterized for better understanding of the interaction of vaccine components with the host immune systems. The immune system consists of many different layers, such as organs, tissue, cells, proteins and genes that interact with each other. These biological processes have different kinetics, which makes time an essential parameter of the investigation. Information on the immune status can be acquired by analysis of gene expression (transcriptomics), protein synthesis (proteomics), lipid secretion (lipidomics), and production of metabolites (metabolomics), or change in cellular composition and morphology. To study the relationship and interaction between all distinct levels of a biological system, a comprehensive analysis is required using analytical techniques (**Figure 3**).

Systems vaccinology can be applied at many stages of vaccine R&D (**Table 1**). The pioneer studies in the field demonstrated the advantage of systems vaccinology to identify molecular signatures that predict vaccine efficacy in an early stage after i.e. yellow fever and influenza vaccination [51-53]. The yellow fever vaccine has a high efficacy and the correlates of protection, antigen-specific $CD8^+$ T-cells and antibody titers, are known. Whereas regular efficacy studies require 60 days before these correlates could be determined in blood,

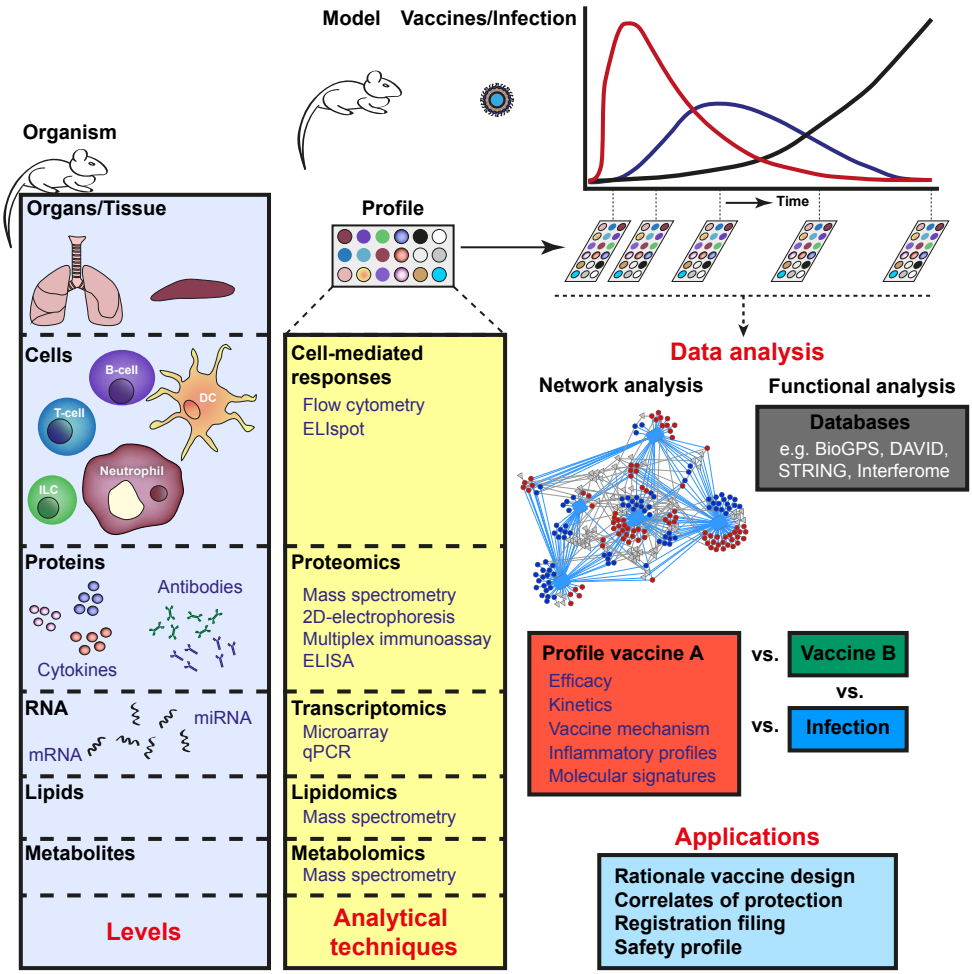

Figure 3 – Systems vaccinology approach. Data, preferably obtained during a time course of the same subject are combined for further analysis. Network analysis (e.g. Cytoscape) is performed to determine co-expression profiles, indicating interdependence. Functional analysis is executed in public databases, e.g. DAVID (www.david.ncifcrf.gov), STRING (www.string-db.org), BioGPS (www.biogps.org), and Interferome (www.interferome.org). Combined data form a response profile for a vaccine. Vaccine profiles can be compared to other vaccine or infection profiles and used for multiple applications as mentioned in **Table 1**.

molecular signatures were retrieved from the gene expression profiles in blood obtained 1, 3, and 7 days after vaccination. These studies with clinical data facilitate in further clinical development and post-marketing surveillance. Unfortunately, this predictive approach is only applicable for vaccines with well-known correlates of protection. For many vaccines, including all new vaccines, the correlates of protection are not known [54].

Nevertheless, systems vaccinology can be deployed for multiple other applications to assist vaccine R&D (**Table 1**). Systems vaccinology can assist in better understanding of adjuvants like MF59, alum, CpG ODN, and α-GalCer [61, 62]. Furthermore, the safety of vaccines can be explored by investigating adverse effects like fever, seizures, and decreased body weight [60, 64, 65]. Moreover, vaccine development may benefit from detailed insight into infection-induced responses as was done for respiratory syncytial virus (RSV) [66], tuberculosis [67], and influenza [68, 69]. This provides insight in the host-pathogen responses and isolation of potential targets for vaccine development. Finally, datasets from vaccine responses against different pathogens in combination with integrative network modeling can reveal detailed insight in critical or universal signatures [58-60]. Li *et al.* compared molecular signatures, induced by five different human vaccines against specific bacterial or viral infections, which could predict antibody responses [59]. These universal markers can be used as benchmark for vaccine development against new emerging diseases.

Table 1. Actual and potential use of systems vaccinology

Aim, deliverables	Benefits	Examples
Predicting responses	Clinical development, post-marketing surveillance	[48, 49, 51, 53, 55, 56]
Understand mode of action of vaccines	Risk mitigation: less late stage failure	[52, 56, 57]
Identify universal vaccine signatures	Improve vaccine development	[58-60]
Select new immune modulators and delivery systems	Risk mitigation: less early stage failure Better vaccines	[61-63]
Assess vaccine safety and adverse effects	Clinical development, post marketing surveillance	[60, 64, 65]
Understand mode of action of infection	Host-pathogen interaction	[66-69]
Rational vaccine design	Risk mitigation: less early stage failure Facilitates regulatory acceptance	N.A.
Development of animal models	Improved early development Risk mitigation: facilitates preclinical to clinical decision.	[60]

Thesis scope and outline

The scope of this thesis is the implementation of a systems vaccinology approach to aid the development of better vaccines against *Bordetella pertussis*. This includes the following sub-aims:

- Develop a systems approach for pertussis vaccine research
- Explore the infection-induced immunity and use *B. pertussis* infection as benchmark for vaccination studies
- Investigate vaccine-induced responses of different pertussis vaccines
- Connect innate and adaptive immunity with vaccine-induced responses.
- Examine the change in vaccine-induced responses with respect to different routes of administration and/or adjuvants.
- Compare and connect the different datasets to obtain a comprehensive overview of the molecular signatures involved in pertussis immunity

In this thesis, we investigate and compare the immunogenicity of different pertussis vaccines concepts, with emphasis on omvPV, with respect to vaccine composition and administration route. Important aspects are the inclusion of *B. pertussis* infection as benchmark and multiple time points of evaluation. The challenge experiments and vaccine production in this thesis are performed with the B1917 strain, a clinical isolate from The Netherlands [70]. All concepts are tested in a mouse challenge model [14].

In **Chapter 2**, a systems approach was applied on a primary *B. pertussis* infection in a murine model. We investigate the immune response on transcriptomic and functional level with respect to cytokine profile, antibody levels, and cellular responses to create a comprehensive overview of innate and adaptive responses after intranasal infection.

Mice develop sterilizing immunity in the lungs after infection. **Chapter 3** describes the immunological signatures of infection-induced immunity that contribute to sterilizing immunity in the lungs of mice. The pulmonary and systemic environments are investigated in protected mice with infection-induced immunity in comparison with non-immunized unprotected mice following a *B. pertussis* challenge.

Whole-cell and OMV vaccines are not well-defined biologicals, as they contain many bacterial proteins. Most antibodies induced by *B. pertussis* infection and whole-cell and OMV vaccines used in this thesis are not directed against antigens present in acellular vaccines. In **Chapter 4**, a method is developed for immunoproteomic profiling of humoral responses to identify immunogens. This method combines protein separation by two-dimensional gel electrophoresis and identification of immunogenic proteins by Western blotting, with

antisera of infected or immunized mice, together with mass spectrometry. The antibody specificity and antibody subclass distribution elicited by aPV, omvPV, wPV, and *B. pertussis* infection are assessed.

In **Chapter 5** vaccine-induced responses of a candidate omvPV are compared with those elicited by a classical wPV after systemic immunization. This comparison includes an assessment of bacterial lung clearance and immunological signatures in both immunized groups following a *B. pertussis* challenge.

It was previously shown that addition of a non-toxic TLR4 ligand, Lpxl1, to a licensed aPV adjuvanted with colloidal alum, leads to a distinct distribution of T-helper subsets in mice [71]. In **Chapter 6** we investigate the molecular signatures of these isolated $CD4^+$ T-cells of mice that were immunized with aPV or aPV+Lpxl1.

In **Chapter 7** we investigate the effect of administration route on protection and the immune responses underlying this immunity. To that end, pulmonary administration of an omvPV is compared with traditional subcutaneous administration. Innate and adaptive immune responses are compared on systemically (blood, spleen) and locally (lung, draining lymph nodes). Analyses are done and on transcriptomic, proteomic, and cellular level.

An *in silico* comparison is made in **Chapter 8** by using datasets of the pulmonary transcriptome following *B. pertussis* challenge of non-immunized unprotected mice and mice with infection-induced immunity from **Chapter 3** together with the mice immunized systemically with omvPV or wPV from **Chapter 5**.

The findings of these studies are summarized in **Chapter 9**. Moreover, the perspectives of systems vaccinology in pertussis research are discussed.

References

1. Bordet, J. and O. Gengou, Le microbe de la coqueluche. Ann. Inst. Pasteur, 1906. 20: p. 48-68.
2. Mattoo, S. and J.D. Cherry, Molecular pathogenesis, epidemiology, and clinical manifestations of respiratory infections due to *Bordetella pertussis* and other Bordetella subspecies. Clin Microbiol Rev, 2005. 18(2): p. 326-82.
3. Wirsing von Konig, C.H., Pertussis diagnostics: overview and impact of immunization. Expert Rev Vaccines, 2014. 13(10): p. 1167-74.
4. Guiso, N., *et al.*, What to do and what not to do in serological diagnosis of pertussis: recommendations from EU reference laboratories. Eur J Clin Microbiol Infect Dis, 2011. 30(3): p. 307-12.
5. Uhl, M.A. and J.F. Miller, Autophosphorylation and phosphotransfer in the *Bordetella pertussis* BvgAS signal transduction cascade. Proc Natl Acad Sci U S A, 1994. 91(3): p. 1163-7.
6. de Gouw, D., *et al.*, Pertussis: a matter of immune modulation. FEMS Microbiol Rev, 2011. 35(3): p. 441-74.
7. Bart, M.J., *et al.*, Global population structure and evolution of *Bordetella pertussis* and their relationship with vaccination. MBio, 2014. 5(2): p. e01074.
8. Pertussis vaccines: WHO position paper - September 2015. Wkly Epidemiol Rec, 2015. 90(35): p. 433-58.
9. Pertussis vaccines: WHO position paper. Wkly Epidemiol Rec, 2010. 85(40): p. 385-400.
10. Cherry, J.D., *et al.*, A search for serologic correlates of immunity to *Bordetella pertussis* cough illnesses. Vaccine, 1998. 16(20): p. 1901-6.
11. Plotkin, S.A., Correlates of protection induced by vaccination. Clin Vaccine Immunol, 2010. 17(7): p. 1055-65.
12. Taranger, J., *et al.*, Correlation between pertussis toxin IgG antibodies in postvaccination sera and subsequent protection against pertussis. J Infect Dis, 2000. 181(3): p. 1010-3.
13. Leef, M., *et al.*, Protective immunity to *Bordetella pertussis* requires both B cells and CD4(+) T cells for key functions other than specific antibody production. J Exp Med, 2000. 191(11): p. 1841-52.
14. Mills, K.H., *et al.*, A murine model in which protection correlates with pertussis vaccine efficacy in children reveals complementary roles for humoral and cell-mediated immunity in protection against *Bordetella pertussis*. Infect Immun, 1998. 66(2): p. 594-602.
15. Jefferson, T., M. Rudin, and C. DiPietrantonj, Systematic review of the effects of pertussis vaccines in children. Vaccine, 2003. 21(17-18): p. 2003-14.
16. David, S., P.E. Vermeer-de Bondt, and N.A. van der Maas, Reactogenicity of infant whole cell pertussis combination vaccine compared with acellular pertussis vaccines with or without simultaneous pneumococcal vaccine in the Netherlands. Vaccine, 2008. 26(46): p. 5883-7.
17. Miller, D.L., *et al.*, Pertussis immunisation and serious acute neurological illness in children. Br Med J (Clin Res Ed), 1981. 282(6276): p. 1595-9.
18. Armstrong, M.E., *et al.*, IL-1beta-dependent neurological effects of the whole cell pertussis vaccine: a role for IL-1-associated signalling components in vaccine reactogenicity. J Neuroimmunol, 2003. 136(1-2): p. 25-33.
19. Sato, Y., M. Kimura, and H. Fukumi, Development of a pertussis component vaccine in Japan. Lancet, 1984. 1(8369): p. 122-6.
20. Greco, D., *et al.*, A controlled trial of two acellular vaccines and one whole-cell vaccine against pertussis. Progetto Pertosse Working Group. N Engl J Med, 1996. 334(6): p. 341-8.
21. Olin, P., *et al.*, Randomised controlled trial of two-component, three-component, and five-component acellular pertussis vaccines compared with whole-cell pertussis vaccine. Ad Hoc Group for the Study of Pertussis Vaccines. Lancet, 1997. 350(9091): p. 1569-77.
22. Mielcarek, N., *et al.*, Live attenuated *B. pertussis* as a single-dose nasal vaccine against whooping cough. PLoS Pathog, 2006. 2(7): p. e65.
23. Feunou, P.F., *et al.*, Long-term immunity against pertussis induced by a single nasal administration of live attenuated *B. pertussis* BPZE1. Vaccine, 2010. 28(43): p. 7047-53.
24. Skerry, C.M. and B.P. Mahon, A live, attenuated *Bordetella pertussis* vaccine provides long-term protection against virulent challenge in a murine model. Clin Vaccine Immunol, 2011. 18(2): p. 187-93.
25. Thorstensson, R., *et al.*, A phase I clinical study of a live attenuated *Bordetella pertussis* vaccine--BPZE1; a single centre, double-blind, placebo-controlled, dose-escalating study of BPZE1 given intranasally to healthy adult male volunteers. PLoS One, 2014. 9(1): p. e83449.
26. Jahnmatz, M., *et al.*, B-cell responses after intranasal vaccination with the novel attenuated *Bordetella pertussis* vaccine strain BPZE1 in a randomized phase I clinical trial. Vaccine, 2014. 32(27): p. 3350-6.
27. Kuehn, M.J. and N.C. Kesty, Bacterial outer membrane vesicles and the host-pathogen interaction. Genes Dev, 2005. 19(22): p. 2645-55.
28. Amano, A., H. Takeuchi, and N. Furuta, Outer membrane vesicles function as offensive weapons in host-parasite interactions. Microbes Infect, 2010. 12(11): p. 791-8.
29. Hozbor, D., *et al.*, Release of outer membrane vesicles from *Bordetella pertussis*. Curr Microbiol, 1999. 38(5): p. 273-8.
30. Roberts, R., *et al.*, Outer membrane vesicles as acellular vaccine against pertussis. Vaccine, 2008. 26(36): p. 4639-46.
31. Gaillard, M.E., *et al.*, Acellular pertussis vaccine based on outer membrane vesicles capable of conferring both long-lasting immunity and protection against different strain genotypes. Vaccine, 2014. 32(8): p. 931-7.
32. van de Waterbeemd, B., *et al.*, Quantitative proteomics reveals distinct differences in the protein content of outer membrane vesicle vaccines. J Proteome Res, 2013. 12(4): p. 1898-908.
33. Cherry, J.D., Epidemic pertussis in 2012--the resurgence of a vaccine-preventable disease. N Engl J Med, 2012. 367(9): p. 785-7.
34. Celentano, L.P., *et al.*, Resurgence of pertussis in Europe. Pediatr Infect Dis J, 2005. 24(9): p. 761-5.
35. Spokes, P.J., H.E. Quinn, and J.M. McAnulty, Review of the 2008-2009 pertussis epidemic in NSW: notifications and hospitalisations. N S W Public Health Bull, 2010. 21(7-8): p. 167-73.
36. van der Maas, N.A., *et al.*, Pertussis in the Netherlands, is the current vaccination strategy sufficient to reduce

disease burden in young infants? Vaccine, 2013. 31(41): p. 4541-7.
37. Mooi, F.R., N.A. Van Der Maas, and H.E. De Melker, Pertussis resurgence: waning immunity and pathogen adaptation - two sides of the same coin. Epidemiol Infect, 2014. 142(4): p. 685-94
38. Pawloski, L.C., *et al.*, Prevalence and molecular characterization of pertactin-deficient *Bordetella pertussis* in the United States. Clin Vaccine Immunol, 2014. 21(2): p. 119-25.
39. Lam, C., *et al.*, Rapid increase in pertactin-deficient *Bordetella pertussis* isolates, Australia. Emerg Infect Dis, 2014. 20(4): p. 626-33.
40. Wendelboe, A.M., *et al.*, Duration of immunity against pertussis after natural infection or vaccination. Pediatr Infect Dis J, 2005. 24(5 Suppl): p. S58-61.
41. Campbell, P.T., *et al.*, Defining long-term drivers of pertussis resurgence, and optimal vaccine control strategies. Vaccine, 2015. 33(43): p. 5794-800.
42. Klein, N.P., *et al.*, Waning protection after fifth dose of acellular pertussis vaccine in children. N Engl J Med, 2012. 367(11): p. 1012-9.
43. Warfel, J.M., *et al.*, Nonhuman primate model of pertussis. Infect Immun, 2012. 80(4): p. 1530-6.
44. Warfel, J.M., L.I. Zimmerman, and T.J. Merkel, Acellular pertussis vaccines protect against disease but fail to prevent infection and transmission in a nonhuman primate model. Proc Natl Acad Sci U S A, 2014. 111(2): p. 787-92.
45. Mooi, F.R. and S.C. de Greeff, The case for maternal vaccination against pertussis. Lancet Infect Dis, 2007. 7(9): p. 614-24.
46. Amirthalingam, G., *et al.*, Effectiveness of maternal pertussis vaccination in England: an observational study. Lancet, 2014. 384(9953): p. 1521-8.
47. Wack, A. and R. Rappuoli, Vaccinology at the beginning of the 21st century. Curr Opin Immunol, 2005. 17(4): p. 411-8.
48. Oberg, A.L., *et al.*, Systems biology approaches to new vaccine development. Curr Opin Immunol, 2011. 23(3): p. 436-43.
49. Pulendran, B., S. Li, and H.I. Nakaya, Systems vaccinology. Immunity, 2010. 33(4): p. 516-29.
50. Aderem, A., Systems biology: its practice and challenges. Cell, 2005. 121(4): p. 511-3.
51. Querec, T.D., *et al.*, Systems biology approach predicts immunogenicity of the yellow fever vaccine in humans. Nat Immunol, 2009. 10(1): p. 116-25.
52. Gaucher, D., *et al.*, Yellow fever vaccine induces integrated multilineage and polyfunctional immune responses. J Exp Med, 2008. 205(13): p. 3119-31.
53. Nakaya, H.I., *et al.*, Systems biology of vaccination for seasonal influenza in humans. Nat Immunol, 2011. 12(8): p. 786-95.
54. Plotkin, S.A., Complex correlates of protection after vaccination. Clin Infect Dis, 2013. 56(10): p. 1458-65.
55. Furman, D., *et al.*, Apoptosis and other immune biomarkers predict influenza vaccine responsiveness. Mol Syst Biol, 2013. 9: p. 659.
56. Nakaya, H.I., *et al.*, Systems Analysis of Immunity to Influenza Vaccination across Multiple Years and in Diverse Populations Reveals Shared Molecular Signatures. Immunity, 2015. 43(6): p. 1186-98.
57. Bucasas, K.L., *et al.*, Early patterns of gene expression correlate with the humoral immune response to influenza vaccination in humans. J Infect Dis, 2011. 203(7): p. 921-9.
58. Obermoser, G., *et al.*, Systems scale interactive exploration reveals quantitative and qualitative differences in response to influenza and pneumococcal vaccines. Immunity, 2013. 38(4): p. 831-44.
59. Li, S., *et al.*, Molecular signatures of antibody responses derived from a systems biology study of five human vaccines. Nat Immunol, 2014. 15(2): p. 195-204.
60. Wang, I.M., *et al.*, Transcriptional profiling of vaccine-induced immune responses in humans and non-human primates. Microb Biotechnol, 2012. 5(2): p. 177-87.
61. Mosca, F., *et al.*, Molecular and cellular signatures of human vaccine adjuvants. Proc Natl Acad Sci U S A, 2008. 105(30): p. 10501-6.
62. Lindqvist, M., *et al.*, Unraveling molecular signatures of immunostimulatory adjuvants in the female genital tract through systems biology. PLoS One, 2011. 6(6): p. e20448.
63. Nakaya, H.I., *et al.*, Systems biology of immunity to MF59-adjuvanted versus nonadjuvanted trivalent seasonal influenza vaccines in early childhood. Proc Natl Acad Sci U S A, 2016. 113(7): p. 1853-8.
64. Lewis, D.J. and M.P. Lythgoe, Application of "Systems Vaccinology" to Evaluate Inflammation and Reactogenicity of Adjuvanted Preventative Vaccines. J Immunol Res, 2015. 2015: p. 909406.
65. Mizukami, T., *et al.*, System vaccinology for the evaluation of influenza vaccine safety by multiplex gene detection of novel biomarkers in a preclinical study and batch release test. PLoS One, 2014. 9(7): p. e101835.
66. Mejias, A., *et al.*, Whole blood gene expression profiles to assess pathogenesis and disease severity in infants with respiratory syncytial virus infection. PLoS Med, 2013. 10(11): p. e1001549.
67. Berry, M.P., *et al.*, An interferon-inducible neutrophil-driven blood transcriptional signature in human tuberculosis. Nature, 2010. 466(7309): p. 973-7.
68. Brandes, M., *et al.*, A systems analysis identifies a feedforward inflammatory circuit leading to lethal influenza infection. Cell, 2013. 154(1): p. 197-212.
69. Tam, V.C., *et al.*, Lipidomic Profiling of Influenza Infection Identifies Mediators that Induce and Resolve Inflammation. Cell, 2013. 154(1): p. 213-27.
70. Bart, M.J., *et al.*, Complete Genome Sequences of *Bordetella pertussis* Isolates B1917 and B1920, Representing Two Predominant Global Lineages. Genome Announc, 2014. 2(6).
71. Brummelman, J., *et al.*, Modulation of the CD4(+) T cell response after acellular pertussis vaccination in the presence of TLR4 ligation. Vaccine, 2015. 33(12): p. 1483-91.

About the cover: Mount Fuji ("Fujisan") seen from Lake Kawaguchi-ko. With 3,776 metres this snow capped active volcano is the highest mountain in Japan. It is considered a holy mountain and frequent subject of Japanese art. Every year, thousands make the ascent to the top. A well-known Japanese saying states that a wise person will climb Mt. Fuji once in their lifetime, but only a fool would climb it twice.

CHAPTER 2

Molecular signatures of the evolving immune response in mice following a *Bordetella pertussis* infection

René H. M. Raeven[1,2], Jolanda Brummelman[3], Jeroen L. A. Pennings[4], Olaf E. M. Nijst[1], Betsy Kuipers[3], Laura E. R. Blok[1], Kina Helm[3], Elly van Riet[1], Wim Jiskoot[2], Cécile A. C. M. van Els[3], Wanda G. H. Han[3], Gideon F. A. Kersten[1,2], Bernard Metz[1]

[1]Institute for Translational Vaccinology (Intravacc), Bilthoven, The Netherlands,
[2]Division of Drug Delivery Technology, Leiden Academic Centre for Drug Research, Leiden, The Netherlands,
[3]Centre for Infectious Disease Control, National Institute for Public Health and the Environment, Bilthoven, The Netherlands,
[4]Centre for Health Protection, National Institute for Public Health and the Environment, Bilthoven, The Netherlands

PLoS One. 2014 19;9(8):e104548

Abstract

Worldwide resurgence of pertussis necessitates the need for improvement of pertussis vaccines and vaccination strategies. Since natural infections induce a longer-lasting immunity than vaccinations, detailed knowledge of the immune responses following natural infection can provide important clues for such improvement. The purpose was to elucidate the kinetics of the protective immune response evolving after experimental *Bordetella pertussis* (*B. pertussis*) infection in mice. Data were collected from (i) individual analyses, i.e. microarray, flow cytometry, multiplex immunoassays, and bacterial clearance; (ii) twelve time points during the infection; and (iii) different tissues involved in the immune responses, i.e. lungs, spleen and blood. Combined data revealed detailed insight in molecular and cellular sequence of events connecting different phases (innate, bridging and adaptive) of the immune response following the infection. We detected a prolonged acute phase response, broad pathogen recognition, and early gene signatures of subsequent T-cell recruitment in the lungs. Activation of particular transcription factors and specific cell markers provided insight into the time course of the transition from innate towards adaptive immune responses, which resulted in a broad spectrum of systemic antibody subclasses and splenic Th1/Th17 memory cells against *B. pertussis*. In addition, signatures preceding the local generation of Th1 and Th17 cells as well as IgA in the lungs, considered key elements in protection against *B. pertussis*, were established. In conclusion, molecular and cellular immunological processes in response to live *B. pertussis* infection were unraveled, which may provide guidance in selecting new vaccine candidates that should evoke local and prolonged protective immune responses.

Introduction

The Gram-negative bacterium *Bordetella pertussis*, the causative agent of whooping cough (pertussis), accounted for high mortality rates among infants in the pre-vaccine era. Whole-cell and acellular vaccines have drastically decreased the number of cases [1]. However, recently resurgence of pertussis in the vaccinated population has been observed in the USA [2, 3] and in European countries [4, 5]. Currently pertussis is still endemic, ranking in the top-ten of vaccine preventable diseases worldwide, according to the WHO. Next to improved diagnostics and public awareness, also strain adaptation and waning immunity are thought to be responsible for this increase in disease cases [6]. Thus, a call for vaccines with improved efficacy is evident.

As a main feature of the innate immune response upon *B. pertussis* infection in mice the recognition of lipopolysaccharide (LPS) by TLR4 has been acknowledged [7, 8]. This activation of TLR4 by *B. pertussis* leads to upregulation of cytokine gene expression and recruitment of neutrophils into the lungs [9, 10]. It was found in animal models that *B. pertussis* infection results in formation of T helper (Th) 1 and Th17 cells [11-13]. Since immunity induced by natural infections provides faster clearance upon reinfection and is longer lasting compared to both acellular and whole-cell pertussis vaccination [14, 15], immune mechanisms induced upon infection or vaccination have been compared. In human and murine studies, immunization with whole-cell or acellular pertussis vaccines results predominantly in a Th1 or a Th2 response, respectively [11, 16]. In addition, in both the intramuscular (human) or subcutaneous (mice) administered acellular and whole cell pertussis vaccines, the humoral response is characterized by systemic IgG antibodies [17, 18], while mucosal immune responses seem absent. Despite the absence of direct evidence for correlates of protection against *B. pertussis*, both Th1 and Th17 type of $CD4^+$ T-cells as well as IgA-producing B-cells seem to play an important role in a protective immune response against *B. pertussis* [12, 15, 19-22]. Since these responses are not induced by the currently available vaccines [23], but more resemble responses induced by infection, a better understanding of the immune response induced in the host following *B. pertussis* infection is needed. Despite knowledge on particular elements of the immune response generated by a *B. pertussis* infection, little is known about the kinetics and sequential relation of these elements. For this, systems biology can be an important tool, as was shown for tuberculosis and influenza infection [24-26].

Here, systems biology was applied to elucidate molecular and cellular events in the different phases of the immune response after primary *B. pertussis* infection in a murine model. To this end, innate and adaptive immune responses were investigated over a period of 66 days post infection. Gene expression profiles in spleen and lungs, cytokine profiles in sera, and

cellular composition of the spleen were determined at twelve time points. Furthermore, cellular and antibody mediated immune responses against *B. pertussis* were investigated. Herewith, we revealed a chronological cascade of immunological processes consisting of recognition, processing, presentation and clearance of *B. pertussis*. The extensive insights into the immune response upon *B. pertussis* infection generated in this study may serve as a solid base for future research on pertussis vaccines and vaccination strategies.

Results

Lung clearance of infected mice

The presence of *B. pertussis* in lungs of mice was examined during a period of 28 days post infection (p.i.), providing the benchmark for this study (**Figure 1A**). Therefore, mice were intranasally infected with *B. pertussis* using a dose of 10^5 colony forming units (cfu). Approximately 13% of the intranasal dose was traceable in the lungs of mice 2 hours p.i. The number of bacteria remained fairly constant for one day, and increased from the second day to a maximum 7 days p.i. (10^7 cfu). Subsequently, a decrease in the number of bacteria was observed and complete clearance in 2 out of 3 mice was achieved 28 days p.i. To determine whether single intranasal infection with *B. pertussis* leads to protection, mice were reinfected 56 days after primary infection (**Figure 1B**). A similar number of viable bacteria was detected 4 hours p.i. in lungs of both reinfected and naive mice. Reinfected mice were able to clear *B. pertussis* from the lungs within 2 days p.i., whereas naive mice showed a similar pattern as observed before. In conclusion, naive mice can clear *B. pertussis* from the lungs in about 28 days. Furthermore, mice previously infected with *B. pertussis* had developed sterilizing immunity, which clears the lungs in two days.

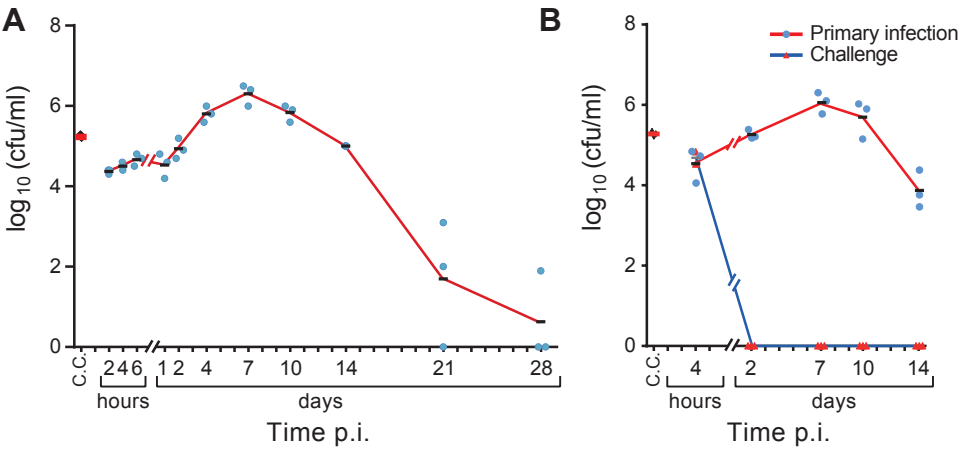

Figure 1 - Lung clearance of naive and reinfected mice after *B. pertussis* infection. **(A)** Number of colony forming units (cfu) in challenge culture (C.C.) was confirmed before challenge. All other cfu were determined in lung of challenged mice (mean n = 3). A large fraction of the original infection dose was traceable in the lungs of mice 2 hours p.i. Bacteria were able to colonize and multiply approximately 100-fold at 7 days p.i. After one week, the mice were able to clear bacteria, which resulted in cleared lungs (2 out of 3 mice) at the last time point (day 28 p.i.). **(B)** Reinfection was performed at 56 days after primary infection and the number of cfu were counted after 4 hours p.i. While reinfected mice were able to clear *B. pertussis* from the lungs within 2 days p.i., naive mice showed a similar pattern as observed in **Figure 1A**.

Gene expression in lung tissue

The gene expression in lung tissue of infected mice was monitored over a period of 28 days. In total, 558 genes of the genome were differentially regulated (*p*-value ≤ 0.001, fold ratio (FR) ≥ 1.5): 446 genes were upregulated and 112 genes were downregulated (**Figure 2**). A complete list of gene names is given in **Table S1**. Gene expression profiles changed already 4 hours p.i. with largest differences at 14 days p.i. (377 responsive genes). The number of genes with an altered expression had declined 21 and 28 days p.i. However, the expression of many genes had not yet returned to naive basal levels. Principal component analysis confirmed the largest differences at 14 days p.i. and the decline at 21 and 28 days p.i. (**Figure 3**). Interestingly, the time point with the least changes in gene expression (2 days p.i.) preceded the increase in cfu in the lungs (**Figure 1**).

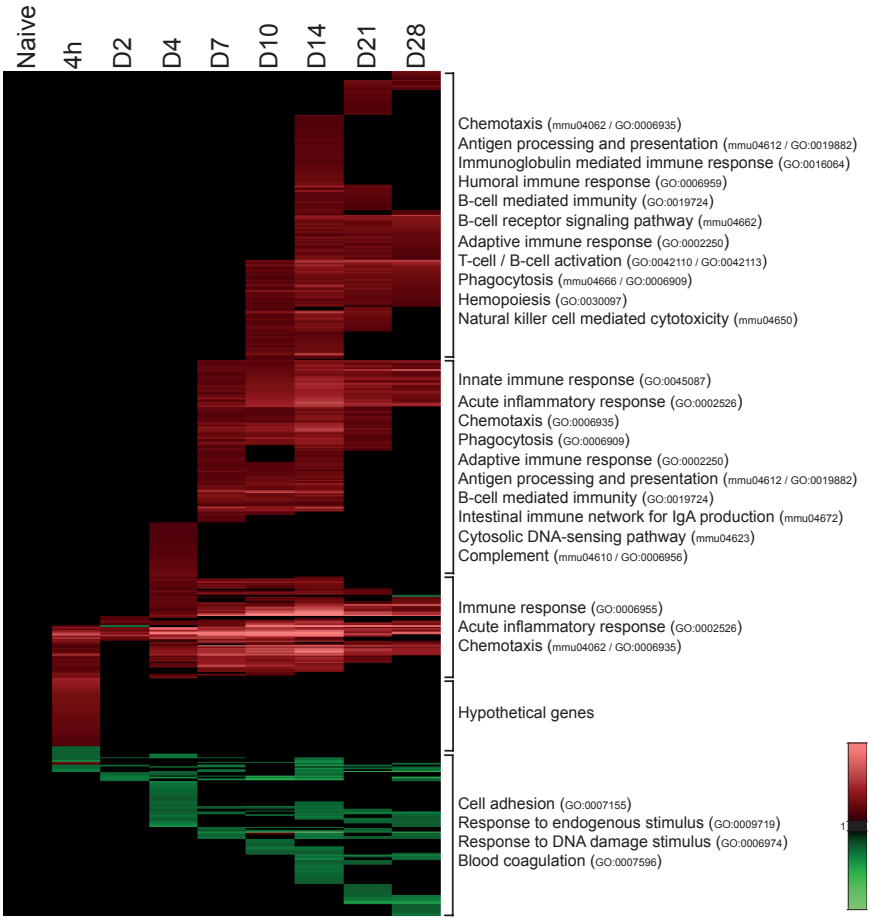

Figure 2 - Pulmonary gene expression profiles as function of time after *B. pertussis* infection. Fold changes in expression were calculated compared to naive mice and significant gene expression results (*p*-value ≤ 0.001, FR ≥ 1.5) are visualized as heatmap (mean of n = 3). In total, 558 genes were found to be differentially regulated, divided in 446 upregulated genes (red) and 112 downregulated genes (green). Genes not exceeding a fold change of 1.5 are depicted as basal level (black). Results are divided in 5 clusters representing up-/downregulation and time of involvement including corresponding GO-BP terms and KEGG pathways.

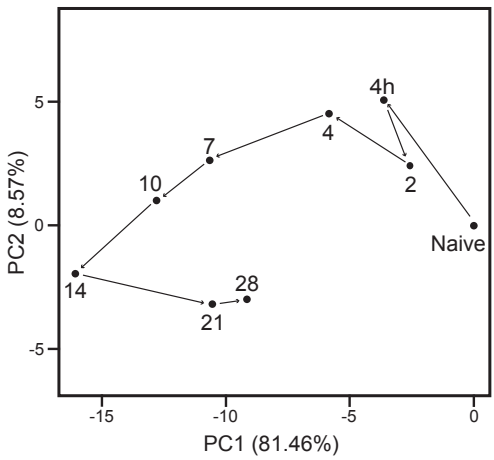

Figure 3 - Principal component analysis of pulmonary gene expression. An evolving gene expression profile was indicated after *B. pertussis* infection of naive mice (mean of n = 3), illustrated as principal- component analysis (PCA). PCA is a mathematical algorithm [117], which describes data based on (dis)similarity. Therefore, a greater distance between points in the plot corresponds to a greater dissimilarity. In this figure, the similarity of the 10 time points are compared based on the expression profiles of the 558 differentially expressed genes. Results indicate that 81% and 9% of the variance between time points could be addressed by principal component 1 (PC1) and PC2, respectively. The next principle components contribute for the residual variances. The plot revealed a notable change in gene expression at 2 days p.i. compared to 4 hours p.i., and largest differences at 14 days p.i. The gene expression at 28 days p.i. was still far from the naive state.

To determine which biological processes were involved, functional analysis of all 558 genes was performed using DAVID. Over-representation analysis (ORA) (Benjamini-corrected *p*-value ≤ 0.05) in GO-BP and KEGG databases resulted in respectively 122 terms and 20 pathways significantly enriched. A selection of these terms is presented in **Figure 4**. The selection is based on immunological relevance and by exclusion of overlapping terms. Acute phase response and chemotaxis were observed right after infection (4 hours p.i.) (**Figure 2**). Subsequently, innate immune response, phagocytosis, antigen processing and antigen presentation were initiated (7 days p.i.). Involvement of B-cell mediated immunity in this stage is mainly demonstrated by the expression of complement related genes. Eventually, the gene expression showed initiation of the adaptive immune response, such as activation of B-cells and T-cells, B-cell receptor (BCR) signaling, humoral immune response (complement activation) and immunoglobulin-mediated immunity from 10 until 28 days p.i.

The gene expression data was compared with the BioGPS database to identify the influx, presence or activation of particular immunological cells in the lungs (**Figure S1**). Sixty-one genes, which are predominantly expressed in macrophages, suggest two events: (i) triggering of alveolar macrophages 4 hours p.i. and (ii) recruitment of macrophages in the lungs 7 days p.i. The influx of macrophages was observed on cellular level using fluorescence microscopy [27]. In addition, the increased expression of 29 genes was attributed to the presence of neutrophils in the lungs 4 days p.i. Moreover, data suggests altered expression of 32, 48, and 17 genes of B-cells, dendritic cells (DCs) and mast cells, respectively, 7 days p.i., and 19 T-cell genes 14 days p.i.

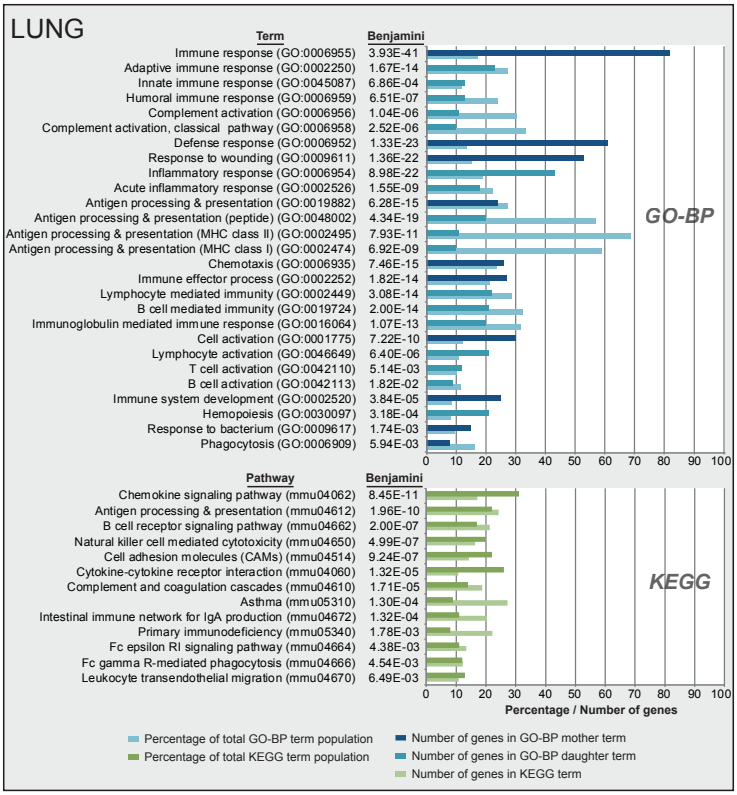

Figure 4 - Functional annotation of pulmonary gene expression data after *B. pertussis* infection. Over-representation analysis (Benjamini- corrected *p*-value ≤ 0.05) in GO-BP and KEGG databases of pulmonary gene expression data resulted in respectively 122 terms and 20 pathways significantly enriched. A selection of terms and pathways, based on immunological relevance and exclusion of overlapping terms, is given in this figure. GO-BP terms were divided in mother terms (dark blue) and corresponding daughter terms (light blue). For each term the amount of genes, the percentage of the total term population and the Benjamini-corrected *p*-value are shown.

Differentially regulated genes in lung tissue after the infection with *B. pertussis* were classified according to function, pathway and cell type. For eleven different groups details are described below.

(1) Cytokines. Twenty-one cytokine-encoding genes were differentially expressed in the lungs during *B. pertussis* infection (**Figure 5**). Sixteen cytokines are associated with a chemotactic function. The other five genes (*Flt3l, Ifng, Il17a, Il17f, Il16*) reflect cytokines involved in the activation of T-cells, such as Th1 and Th17 cells.

(2) Membrane receptors. Forty-six membrane receptors were identified with altered gene expression (**Figure 5**). The receptors were divided in eight groups: cytokine receptors, C-type lectins (CLRs) [28], Fc-receptors, epithelial cell specific receptors, including the IgA transporter (*Pigr*), myeloid-associated immunoglobulin-like receptors, semaphorins [29],

lymphocyte receptors (e.g., *Pdl1*) [30, 31] and the mucosal-homing receptor (*Itgb7*). Other membrane receptors are collected in one group (Figure 5). Gene expression profiles of both cytokines and cytokine receptors enabled early prediction of immune cell recruitment

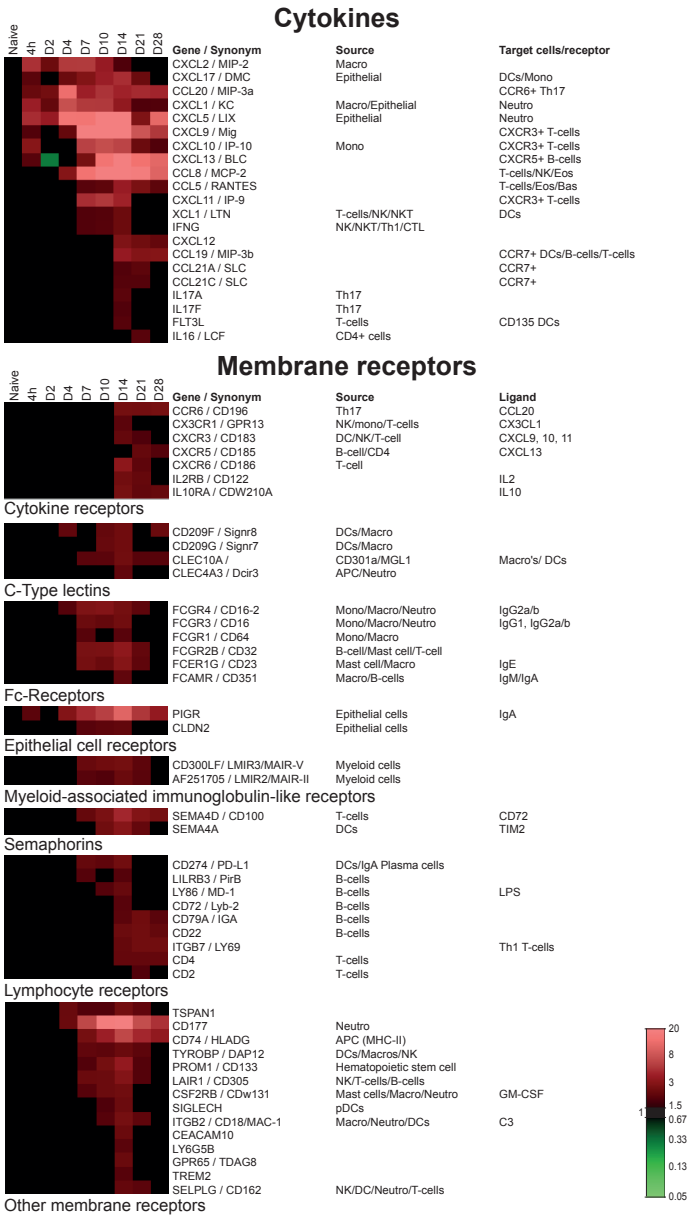

Figure 5 - Gene expression profiles of pulmonary cytokines and membrane receptors after *B. pertussis* infection. Results (mean of n = 3) for cytokines and membrane receptors include expected source and known corresponding receptors, target cells and receptor ligands. Membrane receptors are divided in eight different groups according to function.

towards the lungs on transcriptomic level in this study. Increased expression of *Cxcl13* and *Ccl20* was followed by the upregulation of receptors *Cxcr5* and *Ccr6*. These chemokines lead to the recruitment of CXCR5$^+$ B-cells, CXCR5$^+$ T-cells, CCR6$^+$ DCs and CCR6$^+$ Th17 cells into the lungs [32-34]. Likewise, the expression of *Cxcl9*, *Cxcl10* and *Cxcl11*, induced by interferon gamma (IFNγ), is associated with recruitment of CXCR3$^+$ T-cells or CXCR3$^+$ pDCs [35].

(3) Antimicrobial peptides (AMPs). AMPs have defensive properties against bacterial infections, recruit immune cells and model subsequent immune responses [36]. Gene expression of four AMPs was elevated for 21 days p.i. (**Figure 6**). These four AMPs recruit neutrophils or protect against respiratory pathogens [37-40]. Interestingly, the chemokine *Cxcl17*, primarily expressed in the lungs, was described as an antimicrobial mucosal chemokine that recruits DCs and CD14$^+$ monocytes and protects against pathogenic bacteria [41, 42].

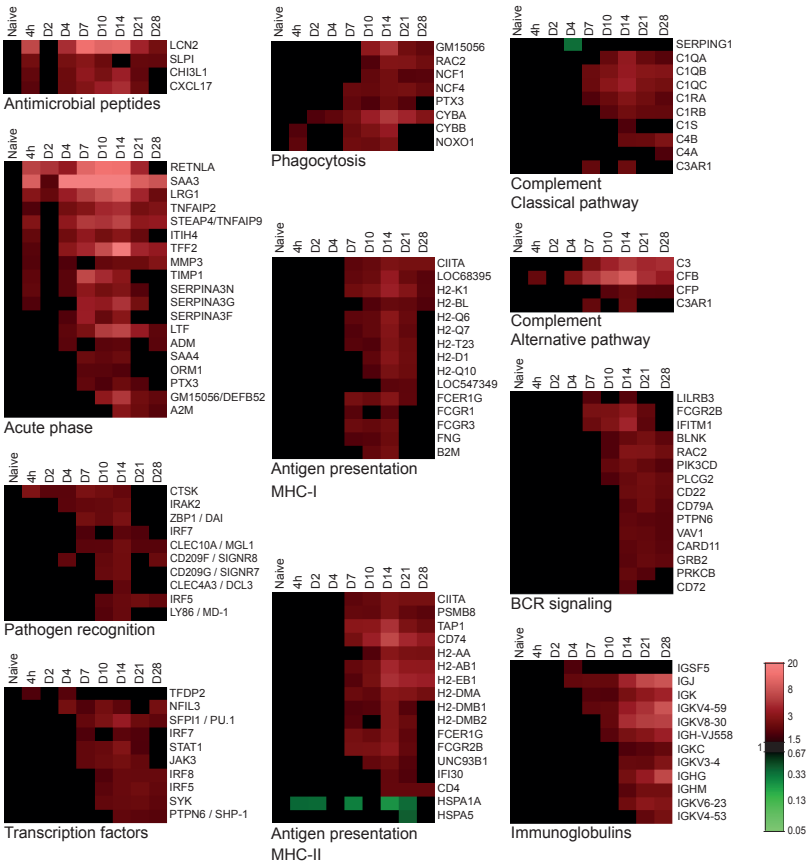

Figure 6 - Pulmonary gene expression representing immunological pathways as function of time after *B. pertussis* infection. Details on pulmonary gene expression profiles (mean of n = 3) indicated expression of antimicrobial peptides, acute phase proteins, pathogen recognition, phagocytosis, both classical and alternative pathways of complement cascade, transcription factors, antigen presentation via both MHC-I and MHC-II, B-cell receptor (BCR) signaling ,and immunoglobulin related genes.

(4) Acute phase response. Primary reaction to an infection is the acute phase response, which leads to the release of pro-inflammatory cytokines and activation of inflammatory cells. Strong upregulation of 19 genes involved in the acute phase response was detected at 4 hours p.i. Remarkably, the gene expression of the acute phase response remained highly expressed at least until day 28 p.i. (**Figure 6**).

(5) Pathogen recognition. Enhanced gene expression suggested activation of TLR4, TLR9, DAI and CLR signaling pathways, implying pathogen recognition by several ligands of *B. pertussis* (**Figure 6**). The induction of *Md-1* and transcription factor *Irf5* genes suggested TLR4 signaling upon sensing of LPS [43]. Upregulation of *Ctsk* and the downstream transcription factor *Irf7* assumes activation of TLR9 by sensing of unmethylated CpG sequences in bacterial DNA [44]. In addition, the cytosolic DNA sensor (DAI) was induced [45]. Elevated gene expression of several CLRs was noticed, such as *Mgl1* and the mouse DC-SIGN-related proteins *Signr7* and *Signr8* [46]. Mgl1 recognizes N-acetylgalactosamine (GalNAc), which is present in *B. pertussis*. Mgl1 has recently been linked to *B. pertussis* mast cell interaction [47].

(6) Transcription factors. Ten transcription factors were differentially expressed in the lungs (**Figure 6**). These include genes of factors *Pu.1, Shp-1, Nfil3, Syk, Irf5, Irf7,* and *Irf8*. All of these transcription factors have been designated as regulators of immunological processes, thereby defining the direction of the host immune response upon bacterial infection [48-54].

(7) Phagocytosis. Six genes representing subunits of NADPH oxidase (NOX) were activated between 4 hours and 28 days p.i. (**Figure 6**). The activation suggests the production of reactive oxygen species, which are involved in a phagocyte respiratory burst to assist in the killing of bacteria during phagocytosis [55].

(8) Antigen presentation. Twenty-eight genes representing antigen presentation were upregulated between 7 and 28 days p.i. (**Figure 6**). Results indicate that both antigen presentation via MHC class I and class II were included. This suggests antigen presentation to both $CD4^+$ T-cells and cytotoxic $CD8^+$ T-cells (CTLs). In line with these findings, the upregulation of *Cd4* and *Ctsw* gene expression in lung tissue was observed, which may indicate presence of $CD4^+$ T-cells [56] and CTLs [57], respectively (**Figure S1**).

(9) Complement activation. Twelve genes of the complement system were more abundantly expressed between 7 and 28 days p.i. (**Figure 6**). Increased gene expression was observed for the complement components C1 and C4, which belong to the classical pathway. In contrast, reduced gene expression of the C1-inhibitor (*Serping1*) was observed day 4 p.i. Furthermore, strong up-regulation of *Cfb* suggests activation of the alternative complement pathway.

(10) BCR signaling. Fifteen genes of the BCR signaling pathway were upregulated between 7 and 28 days p.i. (**Figure 6**). BCR activation was detected by elevated gene expression of eight downstream proteins (*Blnk, Card11, Grb2, Pik3cd, Plcg2, Prkcb, Rac2,* and *Vav1*). Furthermore, the gene expression of the BCR signaling pathways indicates a balanced B-cell response because of an interplay of stimulation by *Cd79a* and *Ifitm1*, and inhibition by *FcgrIIb*, *Lilrb3* (*Pirb*), *Cd22*, *Cd72*, and *Shp-1*. These co-inhibitors prevent overstimulation of B-cells [58].

(11) Immunoglobulins. Gene expression associated with antibody formation was observed after 4 days p.i. and was increased up to 28 days p.i. (**Figure 6**). The microarray data revealed gene expression of seven kappa (κ) light chain genes, heavy chain Ig alpha chain C (*Ihg-vj558*), *Ighm* and *Ighg*, indicating the formation of IgA, IgM and IgG antibodies.

In summary, approximately 40% of the genes expressed in the lungs could be annotated according to function. The chronology of immunological processes comprises broad pathogen recognition, prediction of cell recruitment by cytokine and receptor expression, MHC class I and II antigen presentation, and markers for both antibody and cell-mediated immunity.

Cytokine profiles in mouse sera

The concentrations of thirty-three cytokines were determined in mouse sera by ELISA and multiplex immunoassay (MIA). *B. pertussis* infection induced nine cytokines: CCL11, CCL20, CXCL9, CXCL10, G-CSF, IL-1α, IL-6, IL-9 and IL-17A (**Figure 7**). The pro-inflammatory cytokines, IL-1α and IL-6, are both involved in the acute phase response. The concentration of IL-1α was significantly increased 1 day p.i. Enhanced concentrations of IL-6 were detected at three different time points: 2 hours (not significant), 4 days, and 7 days p.i. (**Figure 7A-B**). Remarkably, IL-6 concentrations returned to basal level 6 hours p.i. Production of IL-1α by epithelial cells was most likely a result of LPS or tracheal cytotoxin (TCT) exposure [59]. The enhanced concentration of IL-6 2 hours p.i. was most likely caused by lung-resident immune cells, such as macrophages and mast cells. These cells are the first to recognize bacterial infection [13]. Elevated concentrations of chemokines CXCL9 (MIG) and CXCL10 (IP-10) were measured between 14–28 days p.i. (**Figure 7D and G**), which suggests a Th1 response [60]. CCL11 (Eotaxin) was enhanced at 14 days p.i. (**Figure 7C**). Eotaxin is involved in allergic inflammation and is chemoattractive for eosinophils [61] and $CCR3^{+}$ Th2 cells [62]. IL-9 was increased 7 days p.i. (**Figure 7F**). IL-9 is mainly produced by T-cells and originally associated with Th2 responses [63]. However, there is evidence that IL-9 is produced by a specific Th subset: Th9 cells [64] and Th17 cells [65]. A Th17 response was identified by markers, such as IL-17A, CCL20 (MIP-3a) and granulocyte colony-stimulating factor (G-CSF) [34]. Enhanced concentrations of IL-17A and CCL20 were determined in mouse sera 14 days p.i. (**Figure 7E,H and I**). CCL20 binds exclusively to CCR6, which is highly expressed on Th17 cells [32, 33]. G-CSF

was produced between 4 and 28 days p.i. G-CSF is important for recruitment, differentiation and proliferation of neutrophils [66] and is linked to a Th17 response [67]. No significant changes in concentrations were detected for the other twenty-four cytokines.

In conclusion, serum cytokine profiles indicate the induction of an acute phase response (IL-1α and IL-6) followed by a multi-flavored immune response with Th1 (CXCL9 and CXCL10), Th2 (CCL11 and IL-9) and Th17 signatures (G-CSF, CCL20, IL-9 and IL-17A).

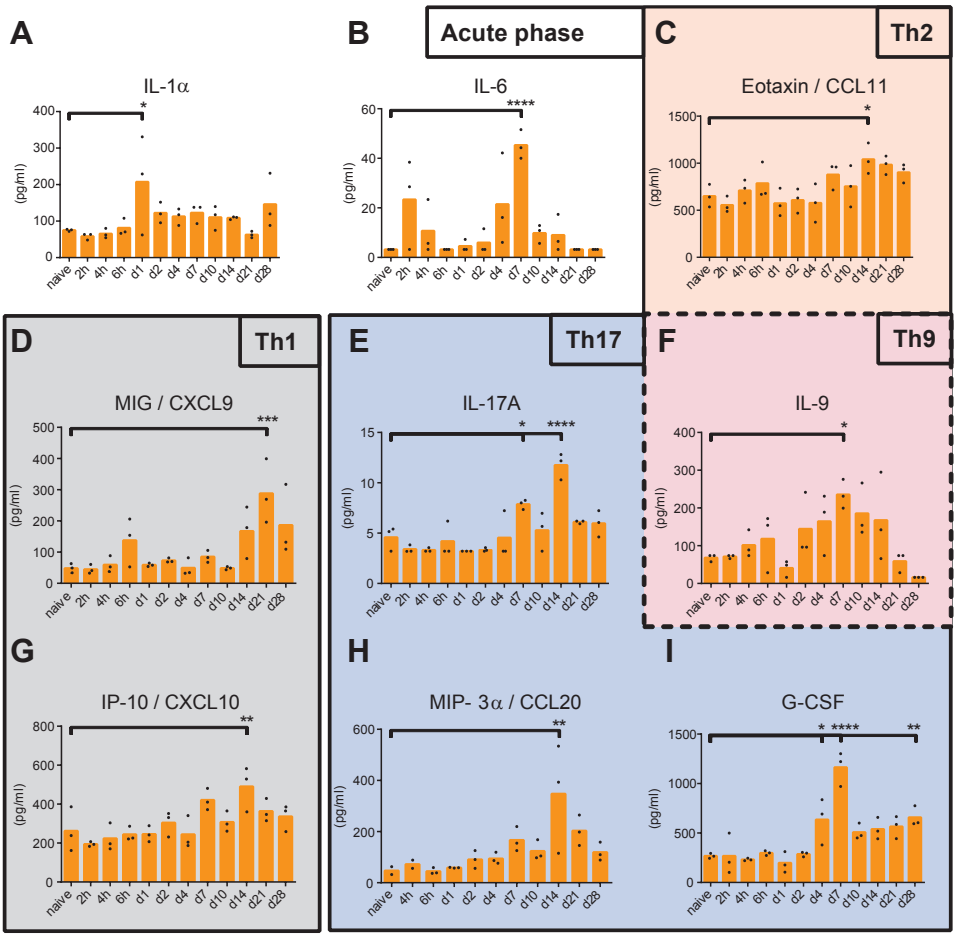

Figure 7 - Serum cytokine concentrations as function of time after *B. pertussis* infection. The concentrations of **(A)** IL-1α, **(B)** IL-6, **(C)** CCL11, **(D)** CXCL9, **(E)** IL-17A, **(F)** IL-9, **(G)** CXCL10, **(H)** CCL20, and **(I)** G-CSF in serum were analyzed over time. Results indicated that after the acute phase response (IL-1α and IL-6) a multi-flavored immune response with Th1 (CXCL9 and CXCL10), Th2 (CCL11 and IL-9), and Th17 (G-CSF, CCL20, IL-9, and IL-17A) was induced. Data represented as mean concentrations including individual values (n = 3). *p*-values were determined by one-way ANOVA with multiple comparison compared to naive mice, * $p \leq 0.05$, ** $p \leq 0.01$, *** $p \leq 0.001$ and **** $p \leq 0.0001$).

Cellular composition of the spleen

The cellular composition of the spleen was examined (**Figure 8A and Figure S2**) by flowcytometry with a panel of fluorescence-labeled monoclonal antibodies binding to cell-specific membrane markers (**Figure S3 and Figure S4**). Results indicate that in the naive situation, the majority of splenocytes consist of B-cells and T-cells (approximately 40% each). Upon *B. pertussis* infection, the ratio between B-cells and T-cells changed, since an increased percentage of T-cells and decreased percentage of B-cells was observed on day 2–4 p.i. However, this ratio was restored on day 7 p.i. The distribution of minor cell populations in the spleen, such as DCs, neutrophils and $CD14^+$ cells, changed over time upon *B. pertussis* infection. Here, we observed an early increased percentage of $CD14^+$ cells (day 1 p.i.) and DCs (day 1 and day 7–14 p.i.). Furthermore, a gradual increased percentage of neutrophils from day 4 until day 21 p.i. was observed. Importantly, enlargement of the spleen was observed during the course of infection (not quantified), suggesting influx or proliferation of cells. This might explain the observed changes in cellular distribution. In conclusion, cellular composition of the spleen indicates fluctuations over time upon *B. pertussis* infection.

Gene expression in the spleen

Gene expression in the spleen of infected mice was determined by microarray analysis. The study identified 798 genes of the whole genome that were differentially regulated (p-value ≤ 0.001, FR ≥ 1.5): 342 genes were upregulated, 425 genes were downregulated, and 31 genes that were initially downregulated and subsequently upregulated (**Figure 8B**). All involved genes are listed in **Table S2**. A limited set of genes showed altered gene expression between 4 hours and 7 days p.i. However, large changes in gene expression were observed 21 days p.i., while the gene expression was almost back to the original values 28 days p.i. Only eight genes still showed altered expression. ORA of the 798 differentially expressed genes in the spleen revealed 66 GO-BP terms and two KEGG pathways. A selection of 16 terms and 2 pathways is presented in **Figure 9**, which are involved in transcription, cell cycle, chromatin assembly and a number of immunological processes. The corresponding proteins are involved in proliferation, differentiation or activation of immune cells in the spleen. Downregulated genes encode proteins that are involved in transcription, adaptive immune responses, antigen processing, antigen presentation and chemokine signaling (**Figure 8B and Figure 10**). Downregulation of these genes suggests suppression of the immune response or migration of immune cells.

(1) Immune response. Forty-one immune response genes were identified (**Figure 10**), 13 of which are associated with the adaptive immune response. Interestingly, downregulation of genes involved in T-cell activation, B-cell activation, antigen processing and presentation, and the subsequent BCR signaling pathway were observed 21 days p.i. (**Figure 10**). Upregulation of genes encoding immunoglobulin heavy chains *Ighg*, *Igha* and *Igh-vj558* indicate production

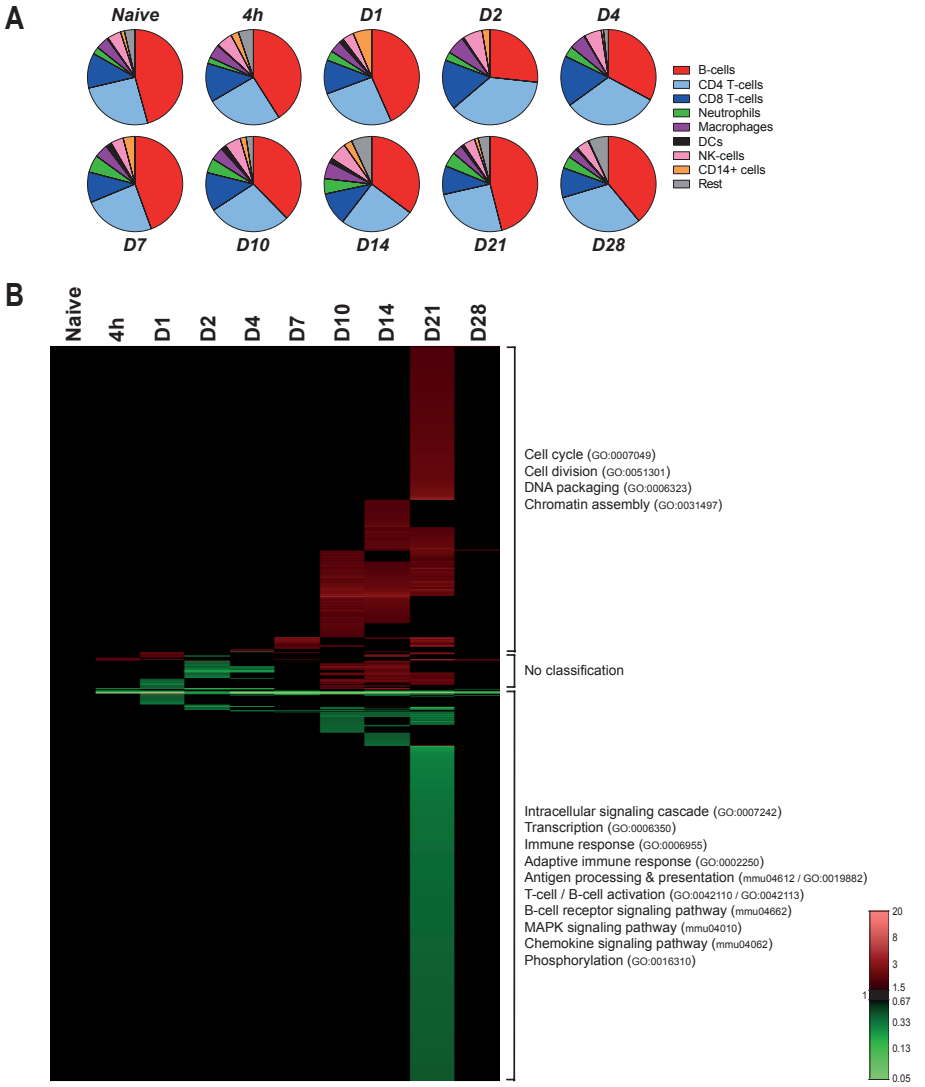

Figure 8 - Splenic cellular composition and gene expression profiles as function of time after *B. pertussis* infection. **(A)** The distribution of the splenic cellular composition illustrated as pie charts at a selection of time points during the *B. pertussis* infection. FACS was used to determine the percentage (mean of n = 3) of B-cells ($CD19^+$), $CD4^+$ T-cells, $CD8^+$ T-cells, neutrophils ($Gr\text{-}1^+$), macrophages ($CD11b^+$), dendritic cells ($33D1^+$), NK cells ($DX5^+$), and $CD14^+$ cells in splenocytes. **(B)** Fold changes of expression were calculated compared to naive mice and significant gene expression results (*p*-value ≤ 0.001, FR ≥ 1.5) were visualized as a heatmap (mean of n = 3). This test was performed for each gene at each time point. In total, 798 genes were differentially regulated (*p*-value ≤ 0.001, FR ≥ 1.5) compared to naive mice, divided in 342 upregulated (red) and 425 down-regulated genes (green). Additionally, a distinct group of 31 genes showed downregulation between 4 hours and 4 days p.i., but were upregulated between 10 and 21 days p.i. Genes not exceeding a fold change of 1.5 are depicted as basal level (black) at this time point. Results are divided in 3 clusters representing up/down-regulation and time of involvement and included corresponding GO-BP terms and KEGG pathways.

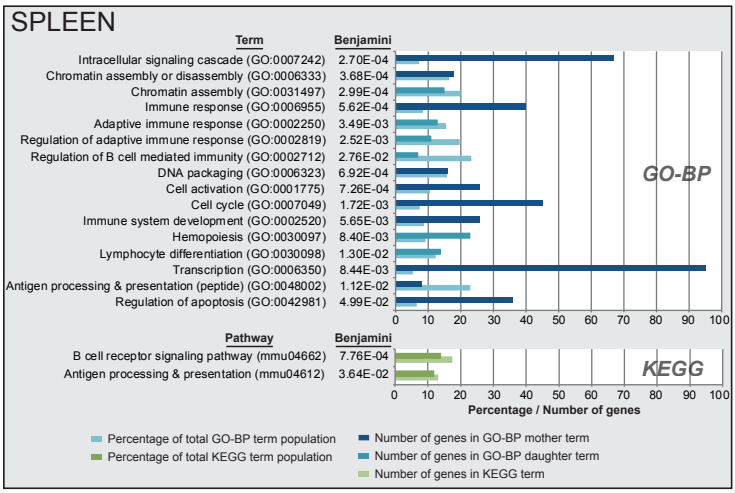

Figure 9 - Functional annotation of splenic gene expression data after *B. pertussis* infection. Over-representation analysis (Benjamini- corrected *p*-value ≤ 0.05) of all 798 differentially expressed genes in the spleen in GO-BP and KEGG databases, This resulted in respectively 66 terms and 2 pathways significantly enriched of which a selection, based on immunological relevance and exclusion of overlapping terms, of 16 terms and 2 pathways are presented. GO-BP terms were divided in mother terms (dark blue) and corresponding daughter terms (light blue). For each term the amount of genes, the percentage of the total term population and the Benjamini-corrected *p*-value are shown.

of immunoglobulins IgG and IgA by B-cells (Figure 10). Downregulation of the *Ighm* gene suggests a suppressed IgM production or a class-switch to IgG or IgA.

(2) Membrane receptors. Upregulation of genes encoding myeloid cell membrane markers, Fc-receptors and membrane attack complex (MAC) inhibitory proteins (*Cd59a*/*Cd59b*) suggests increased presence of myeloid cells, such as neutrophils, between 10 and 21 days p.i. (Figure 10). The induction of the MAC-inhibitory genes suggests inhibition of MAC formation, which is part of the complement cascade. In addition, BioGPS analysis (Figure S5) revealed the presence of myeloid cell markers that are expressed on neutrophils (*Trem3* and *Clec4e*) or macrophages (*Clec4e*). Downregulated gene expression of membrane markers of B-cells (*Cd22, Cd72, Cd74,* and *Siglecg*) and T-cells (*Sema4d, Tcra*) implies decreased presence of lymphocytes 21 days p.i. (Figure 10).

(3) Transcription. Ninety-five genes that were differentially regulated in the spleen turned out to be involved in transcription (Figure 9), of which 70 genes were downregulated (data not shown).

(4) Cell cycle. Most of the genes involved in the cell cycle process (31 out of 45) were upregulated (Figure 10) which suggest increased cell replication between 10 and 21 days p.i. in the spleen.

(5) Regulation of apoptosis. Apoptosis was characterized by upregulation of 12 genes (between 7 and 21 days p.i.) and downregulation of 24 genes (21 days p.i.) (**Figure 10**). The role of apoptosis is especially interesting because of the recently described link between apoptotic markers and influenza vaccine responsiveness [68]. However, no overlap was found between the markers from the study of Furman *et al.* and the current study.

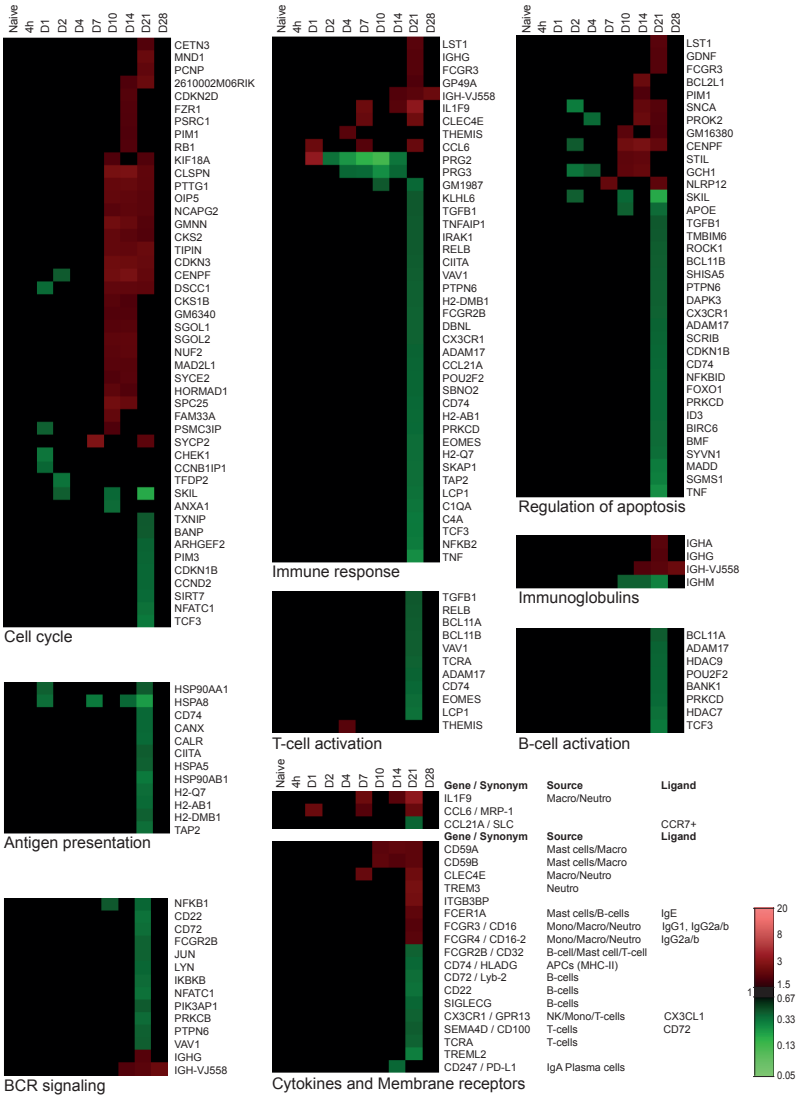

Figure 10 - Splenic gene expression profiles of specific processes as function of time after *B. pertussis* infection. Expression profiles (mean of n = 3) are summarized for immune response, cell cycle, regulation of apoptosis, T-cell activation, B-cell activation, immunoglobulin, B-cell receptor (BCR) signaling, antigen processing, cytokines and membrane receptors in spleen.

In summary, most prominent differences in gene expression in the spleen were found around 21 days p.i. These differences point to downregulation of immunological processes. After 28 days p.i. the expression profiles returned to basal level, at the same moment that the bacteria were almost cleared from the lungs. Interestingly, when combining cellular composition (**Figure 8A**) with gene expression profiles (**Figure 8B and Figure S5**), the increase in neutrophils (10–21 days p.i.) was observed with both techniques. However, changes in the distribution of B-cells and T-cells on day 2 and 4 p.i. were not detected on gene expression level. Overall, these findings suggest that gene expression profiles cannot directly be translated in cellular fluctuations in the spleen.

Overlap of transcriptomic responses in lungs and spleen

A comparison of transcriptomic datasets was made to determine the related biological processes that occurred in both spleen and lungs (**Figure S6**). Seventy-two genes were differentially expressed in spleen and lungs, which were divided in four groups: (i) 20 genes that were upregulated in both tissues, (ii) 42 genes that were upregulated in lungs and downregulated in the spleen, (iii) 2 genes that were downregulated in lungs and upregulated in the spleen, and (iv) 8 genes that were downregulated in both tissues. Fifteen genes of the second group were involved in the immune response, such as leukocyte activation, BCR signaling pathway, antigen processing and presentation, and chemotaxis. Remarkably, the immunoglobulin-mediated immune response was the only process upregulated in both tissues, suggesting local and systemic antibody production.

In summary, both tissues showed activation of antibody-mediated immunity upon a *B. pertussis* infection. In addition, most differentially expressed genes representing immunological processes were observed upregulated in the lungs and downregulated in the spleen.

B. pertussis-specific IgM, IgG and IgA antibody responses

Antibody isotypes, IgM, IgG and IgA against *B. pertussis* were analyzed for a period of 28 days p.i. The formation of IgM against *B. pertussis* antigens present in outer membrane vesicles (OMV) was not observed during the course of infection (**Figure 11A**). Contrarily, anti-*B.pertussis* IgG in mouse sera was detectable from 10 days p.i. and the responses were progressively increased until 28 days p.i. (**Figure 11B**). Notably, no IgG titers were detectable against the individual purified *B. pertussis* antigens pertactin (Prn), pertussis toxin (Ptx), filamentous hemagglutinin (FHA) or fimbria type 2 and 3 (Fim2/3) (**Figure S7**). However, anti-OMV IgG was significantly increased at 14, 21 and 28 days p.i. (**Figure 11C**) and consisted of IgG1, IgG2a and IgG2b subclasses, but not IgG3. (**Figure 11D–G**), Remarkably, IgG1 levels dropped significantly at 28 days p.i. compared to 21 days p.i. In addition, significantly increased anti-OMV IgA responses were measured in sera (**Figure 11H**) as well as in lung lysates (**Figure 11I**) 28 days p.i.

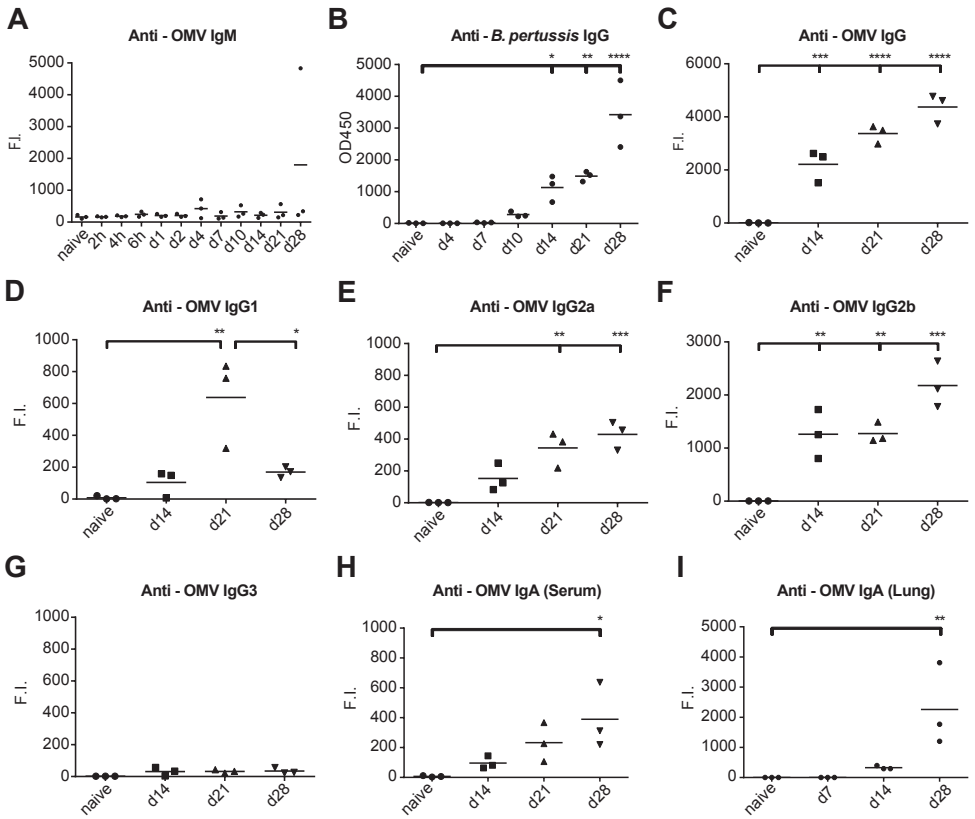

Figure 11 - Antibody profiling after *B. pertussis* infection. **(A-H)** Antibody responses were determined in mouse sera after intranasal infection by whole-cell *B. pertussis* ELISA or MIA and expressed as OD450 or Fluorescent Intensity (F.I.), respectively (mean of n = 3). **(A)** IgM antibodies against OMV B1917 were absent. **(B)** Whole-cell *B. pertussis* ELISA indicated IgG antibody formation 10-14 days p.i., which increased until day 28 days p.i. **(C-G)** Levels of total IgG antibodies and individual subtypes (IgG1, IgG2a, IgG2b, and IgG3) against OMV B1917 indicated presence of multiple subclasses. **(H)** Anti-OMV IgA antibodies in serum were induced after 14-28 days p.i. **(I)** In lung lysates, anti-OMV IgA antibodies were detected 14 and 28 days p.i. *p*-values were determined by one-way ANOVA with multiple comparison compared to naive mice, * $p \leq 0.05$, ** $p \leq 0.01$, *** $p \leq 0.001$, and **** $p \leq 0.0001$.

In conclusion, intranasal infection leads to a broad spectrum of systemic antibody subclasses against outer membrane proteins of *B. pertussis* within 14 days p.i., but responses against purified virulent antigens Ptx, Prn, FHA and Fim2/3 remain undetectable until 28 days p.i. Moreover, *B. pertussis*-specific anti-OMV IgA antibodies were secreted in the lungs.

CD4⁺ T-cell responses after *B. pertussis* infection

Cytokine profiles of antigen-specific memory CD4⁺ T-cells in the spleen were determined 66 days p.i. Splenocytes of naive and infected mice were stimulated for 8 days with Ptx, FHA or Prn, important virulence factors present in the acellular pertussis vaccine. Cytokine profiling on single cell level was established by using intracellular cytokine straining (ICS), while cytokine concentrations in splenic culture supernatants were determined by using a

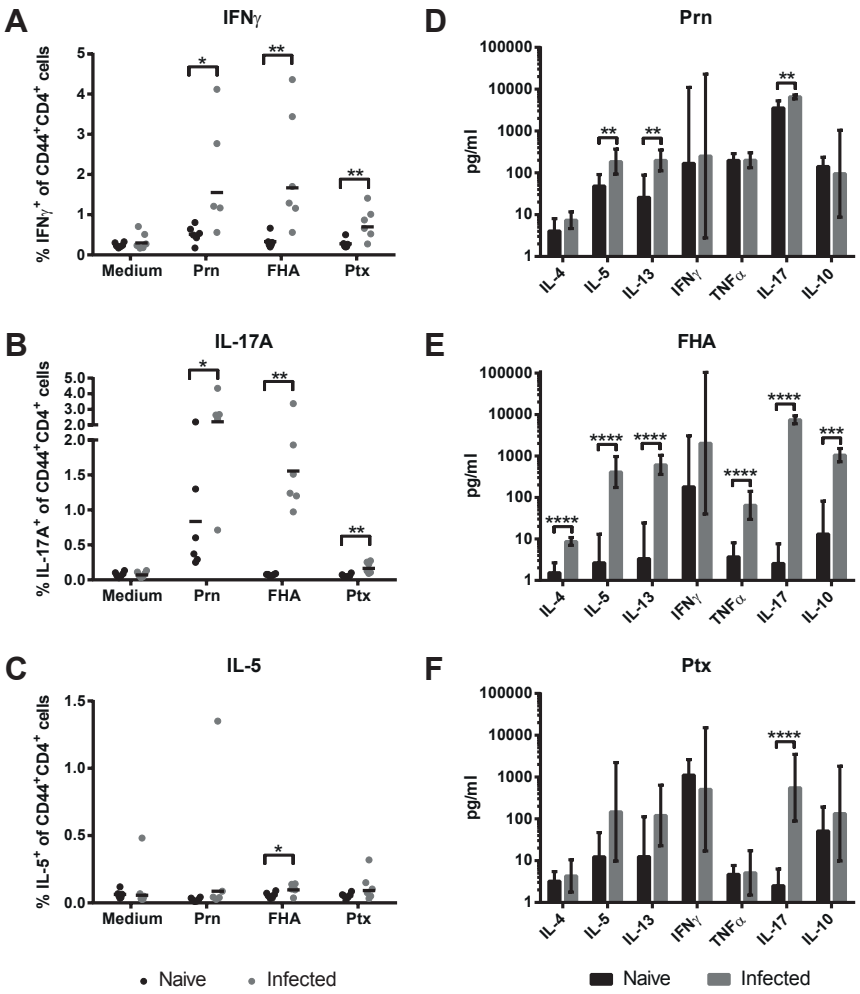

Figure 12 - Systemic memory Th cytokine profiles. **(A-C)** Splenocytes of naive and infected mice were collected 66 days p.i. and *in vitro* restimulated with Prn, FHA, or Ptx for 8 days. The percentages of IFNγ-, IL-17A-, and IL-5-producing $CD4^+CD44^+$ T-cells were determined using ICS (mean of n = 6). **(D-F)** Cytokine levels in supernatant after 7 days of stimulation were determined by using a MIA. Results (mean of n = 6) are corrected for the background level in the presence of medium as control. Statistical differences between the groups were detected for the ICS with a non-parametric Mann-Whitney test and for the MIA with a Student t-test on the log-transformed data. * $p \leq 0.05$, ** $p \leq 0.01$, *** $p \leq 0.001$, **** $p \leq 0.0001$.

MIA. CD44 expression was used to focus on activated $CD4^+$ T-cells. Results of ICS indicate a significant increase in IFNγ- and IL-17A-producing Prn-, FHA-, and Ptx-specific $CD4^+CD44^+$ T-cells after infection (**Figure 12A-B**). Except for FHA-stimulation, no evidence was found for specific IL-5-producing $CD4^+CD44^+$ T-cells (**Figure 12C**). Cytokine profiles in culture supernatant revealed a significant increase in TNFα production by splenocytes of infected mice after FHA stimulation and IL-17A production after Prn, Ptx, or FHA stimulation (**Figure 12D-F**). No changes were observed in IFNγ production in culture supernatants (**Figure 12D-F**). Notably,

FHA stimulation induced besides Th1 and Th17 cytokines an increase in IL-5, IL-13, IL-4, and IL-10 production by splenocytes of infected mice (**Figure 12E**). IL-5 and IL-13 production occurred also after Prn stimulation (**Figure 12D**). This might indicate that these three *B. pertussis* antigens induce a mixed Th response, of which Th1 and Th17 are the major components. While ICS specifically focuses on $CD4^+CD44^+$ T-cells, multiple cell types can produce the accumulated cytokines present in the splenic culture supernatants after stimulation. The production of IL-17A is exclusive for Th17 cells [69]. Besides Th1 cells, IFNγ could also be produced by CTLs and NK cells. The high levels of IFNγ produced by splenocytes of naive mice after Ptx stimulation may be explained by TLR4 activation on innate cells by Ptx [70]. A high background of Prn-responding $IL\text{-}17A^+CD4^+CD44^+$ T-cells and IL-17A in supernatant was seen in two out of six naive mice, indicating Prn-activated IL-17A production in unprimed splenocytes.

In summary, $CD4^+$ memory T-cell analysis revealed that infection with *B. pertussis* primarily generates specific Th1 and Th17 responses, regarded essential in protection against a *B. pertussis* infection [12, 20, 21].

Figure 13 (Right) - Overview of immune response evolving after *B. pertussis* infection. Merging data from a wide array of functional analyses reveals a comprehensive overview of the immune response of mice upon *B. pertussis* infection. (i) Innate phase, (ii) bridging phase and (iii) adaptive phase are indicated in the response facing variable levels of *B. pertussis* present in the initial inoculum, the exponential growth phase, and in the clearance phase, respectively. Highlights of the study are given, based on lung clearance, relative gene expression levels (lungs), cytokine profiles (serum), cellular response (spleen) and pertussis-specific responses in serum and spleen as depicted in the figure legend.

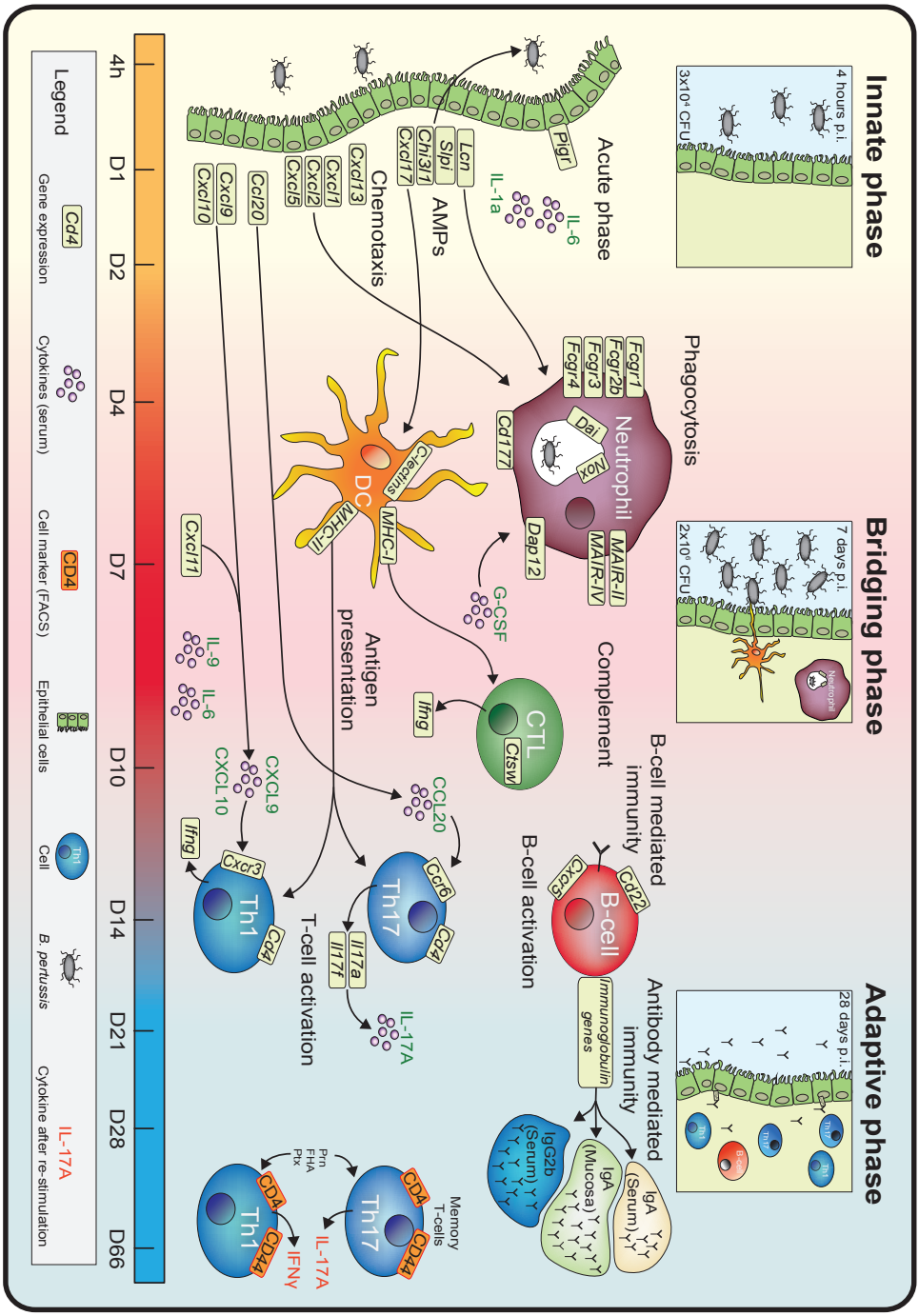
Innate phase
Bridging phase
Adaptive phase
4 hours p.i.
3x10⁴ CFU
7 days p.i.
2x10⁶ CFU
28 days p.i.
Neutroph
Th1
Th17
B-cell
Acute phase
IL-6
IL-1a
Pigr
Lcn
Slpi
Chi3l1
Cxcl17
AMPs
Cxcl1
Cxcl2
Cxcl5
Cxcl13
Chemotaxis
Ccl20
Cxcl9
Cxcl10
Phagocytosis
Fcgr1
Fcgr2b
Fcgr3
Fcgr4
Dai
Nox
Cd177
Neutrophil
MAIR-II
MAIR-IV
Dap12
G-CSF
DC
C-lectins
MHC-II
MHC-I
Cxcl11
IL-9
IL-6
Ifng
CTL
Ctsw
Complement
B-cell mediated immunity
Cxcr5
Cd22
B-cell
Immunoglobulin genes
B-cell activation
Antibody mediated immunity
IgA (Serum)
IgA (Mucosa)
IgG2b (Serum)
Antigen presentation
CCL20
Ccr6
Rorγt
Il17a
Il17f
IL-17A
T-cell activation
CXCL9
CXCL10
Cxcr3
Tbx21
Memory T-cells
CD4
CD44
Prn
FHA
Plx
IL-17A
IFNγ
Legend
Cd4
Gene expression
Cytokines (serum)
CD4
Cell marker (FACS)
Epithelial cells
Cell
B. pertussis
IL-17A
Cytokine after re-stimulation
4h
D1
D2
D4
D7
D10
D14
D21
D28
D66

Discussion

An integrated systems biology approach was applied to investigate the evolving immune response of mice following a primary intranasal *B. pertussis* infection, considered capable of inducing sterilizing immunity. Data sets from individual analytical platforms, such as microarray, flow cytometry, multiplex immunoassays, and colony counting, addressing different biological samples taken at multiple time points during the immune response were merged. Altogether, a comprehensive overview of immunological processes occurring upon primary infection of mice with *B. pertussis* was constructed in three consecutive phases, as shown in **Figure 13**: (i) the innate phase, (ii) the bridging phase, and (iii) the adaptive phase.

Highlights featured in this study are: (i) a protracted acute phase response, as part of the innate phase, lasting for at least 28 days, which co-occurred with prolonged antigen exposure; (ii) the recognition of several *B. pertussis* pathogen-associated molecular patterns (PAMPs), i.e. LPS, DNA, and GalNac, (iii) early signatures for recruitment of adaptive immune cells e.g. the cytokine CCL20 that attracts $CCR6^+$ Th17 cells, (iv) expression of specific membrane markers (e.g. DAP12) and transcription factors that determine the strength and direction of the adaptive immune response. Furthermore, features of adaptive immunity consisted of: (v) IgA secretion in the lungs; (vi) a broad systemic antibody response; (vii) a Th1 and Th17-mediated response in the lungs and systemic formation of specific memory Th1 and Th17 cells.

Various signatures, associated with the induced protective immune response as presented in **Figure 13**, are discussed in detail hereafter. The innate phase was characterized by the presence of AMPs, acute phase proteins and chemotactic cytokines as detected by microarray analysis and MIA (**Figure 5–7**). Expression of the involved genes is most likely initiated by activation of TLR2 and TLR4 by LPS of *B. pertussis* [8, 10]. Upregulated gene expression of four AMPs (*Chi3l1, Cxcl17, Lcn2,* and *Spli*) was found in the lungs during the whole course of infection. These AMPs contribute to innate protection as was shown for other respiratory pathogens [38-40, 42]. In addition, these AMPs have the capacity to recruit immune cells, such as neutrophils, DCs, and monocytes [37, 41] and are therefore important for the induction of subsequent immune responses [36].
Furthermore, the expression of particular cytokines on gene and protein level in the innate phase (**Figure 5 and Figure 7**), in combination with increased gene expression of cytokine receptors and the change in cellular composition of the spleen (**Figure 5 and Figure 8A**), gave detailed insight into the immunological processes during the course of infection, as depicted in **Figure 13**. For example, the gene expression levels of the cytokine *Cxcl1, Cxcl2, Cxcl5,* and *Cxcl17* was in agreement with the recruitment of neutrophils and DCs towards the site of infection [41, 71, 72]. Furthermore, the gene expression of the cytokines *Cxcl9, Cxcl10, Cxcl11* and *Ccl20* was increased early after infection. CXCL9, CXCL10 and CXCL11 are known to be

involved in the recruitment of $CXCR3^+$ Th1 cells, and CCL20 in the recruitment of $CCR6^+$ Th17 cells [32, 33, 60]. The upregulation of *Ccr6* and *Cxcr3* genes was observed at day 14 p.i. in the lung (**Figure 13**).
Remarkably, gene expression of cytokines, acute phase proteins, and AMPs was temporary suppressed at 2 days p.i. Simultaneously, the proliferation of bacteria started in the lungs. These results indicate temporary suppression of the immune system by *B. pertussis*. Several immune evasion strategies of *B. pertussis* have been described in literature [73-77]. The evasion is attributed to virulence factors, such as adenylate cyclase toxin (ACT), Ptx, TCT, and FHA. These investigators demonstrated enhanced production of IL-10 and regulatory T-cells, delay of neutrophil recruitment, and inhibition of early chemokine production in mice in relation to secretion of *B. pertussis* virulence factors. In the present study, these immunosuppressive properties of *B. pertussis* might explain the suppression of the differential gene expression observed 2 days p.i. In addition, secretion of OMVs occurs during bacterial colonization [78]. These OMVs are thought to serve as decoy for the host immune response and their immunomodulatory properties support survival of the bacteria [79, 80].

During the bridging phase, the number of bacteria in the lungs increased (**Figure 1**). The highest number of bacteria in the lungs was found at 7 days p.i. followed by a decrease, suggesting that day 7 is the turning point in the progress of the infection. Simultaneously, microarray analysis suggests the presence of neutrophils, macrophages, and DCs in the lungs based on BioGPS analysis (**Figure S1**). These cells are likely responsible for (i) phagocytosis, (ii) pathogen recognition, (iii) antigen presentation, and (iv) differentiation by expression of cell receptors in the period between 4-10 days p.i. (**Figure 13**).
The innate immune cells appeared to cause the initial decrease in numbers of bacteria in the lungs from 7 days p.i., because a strong antibody response (IgM, IgG, IgA) (**Figure 11**) and $CD4^+$ T-cell response were not yet present. Based on gene expression of neutrophil markers, the neutrophil invasion in the lungs probably occurred from 4 days p.i., which is observed on cellular level by McGuirk *et al.* [81]. This influx of cells is most likely orchestrated by IL-17A and G-CSF [66, 67, 69]. In the present study, both cytokines were enhanced in the sera of infected mice. Furthermore, genes involved in phagocytosis were found to be upregulated (**Figure 6**) which is important for protection against *B. pertussis* [55, 82].
This study demonstrated also that *B. pertussis* infection activates different pattern recognition receptor (PRR) pathways, such as TLR4, TLR9, DAI, and several CLRs (**Figure 6**). Bacterial ligands, e.g. LPS, DNA, and GalNAc trigger these signaling pathways [8, 45, 47]. Upregulation of genes involved in TLR4-signalling (*Md-1, Irf5*) is probably caused by detection of bacterial LPS [8, 10, 43]. Bacterial DNA recognition occurred through the TLR9 pathway (*Ctsk, Irf7*) and the cytosolic DNA sensor (*Dai*). The receptor DAI recognizes both host DNA, upon tissue damage, and bacterial DNA, which leads to an innate immune response [45]. Furthermore, increased gene expression of the CLRs, *Signr7*, *Signr8*, and *Mgl1* was observed, which are

predominantly expressed on DCs [28, 83]. The enhanced expression of mouse DC-SIGN-related genes *Signr7* and *Signr8* during the *B. pertussis* infection is a novel finding. Despite indications of sensing of 6-sulfo-sialyl Lewis(x) oligosaccharide by Signr7, the exact ligands and role of these receptors remains to be discovered [46]. Recognition of GalNAc via Mgl1 has recently been associated with mast cell activation by *B. pertussis* [47]. An important conclusion is that ligands of *B. pertussis* activate multiple PPRs during the infection. This may be important for the induction of a broad adaptive immune response, including Th1 as well as Th17 cells, mucosal IgA and systemic IgG.

During the bridging phase, upregulation of MHC class I and II genes were measured, enabling antigen presentation to both $CD4^+$ Th cells and cytotoxic $CD8^+$ T-cells (CTLs). Several studies focused on the role of Th cells because of their important contribution to protect against *B. pertussis* [12, 20, 21]. Nevertheless, the CTLs seem also important for protection against *B. pertussis*, indicated by CTL infiltration, based on upregulation of *Ctsw*, in lungs in our study by formation of FHA-specific IFNγ-producing CTLs upon B. pertussis infection in other studies in mice and humans [81, 84].

In addition, the bridging phase was characterized by simultaneous gene expression of several receptors on innate immune cells in the lungs and spleen. Interestingly, this included MAIRs, TREMs, semaphorins, and DAP12, which is the first evidence that these receptors might play a role in *B. pertussis* infection. Especially DAP12, which is abundantly expressed in lungs, interacts with other membrane receptors and influences cytokine expression [85]. Coupled to MAIR-II, DAP12 is an inhibitor of B-cell responses [86]. Together with TREM2, DAP12 downregulates TLR and FcR expression [87]. Overall, these former receptors function as an important bridge between innate and adaptive immune responses, determining the strength and direction of the adaptive immune response by the successive activation of lymphocytes, such as CTLs, Th cells, and B-cells [29, 88-91]. Since the exact role of these receptors in the protection against *B. pertussis* remains unresolved, additional research is needed to find whether targeting of these receptors might be a viable strategy to elicit desired immune responses. In summary, the bridging phase suggests the presence of APCs and myeloid cells, such as DCs and neutrophils based on gene expression of membrane markers. However, this was not validated by histological data.

Finally, the adaptive phase was recognized by the formation of T and B-cell responses and a broad antibody response (**Figure 13**). In this same period, the naive mice were able to clear *B. pertussis* from their lungs. Gene expression, cytokine secretion and cellular analysis revealed presence of activated $CD4^+$ T-cells. The highest number of $CD4^+$ T-cells was detected at 14 days p.i., which is in agreement with a study showing the largest influx of Th17 cells in the lungs after *B. pertussis* infection at 14 days p.i. [12]. Phenotyping of $CD4^+$ T-cells, based on cytokine profiles in serum (protein) and lung (genes) and expression of specific transcription factors or membrane markers, suggests a broad Th response in the present study. The Th1 response

in the lungs was characterized by *Ifng* and *Stat1* expression [92]. Gene expression of the mucosal homing receptor *Ccr6, Card11, Ccl19, Ccl21a, Ccl21c,* and signature cytokines *Il17a* and *Il17f* might indicate Th17 cells in the lungs [32, 69, 93-96]. Upon re-stimulation of splenocytes with purified *B. pertussis* antigens, Prn- and FHA-specific Th1 and Th17 type $CD4^+$ T-cells could be detected in the memory phase (66 days p.i.) (**Figure 12**). In addition, enhanced IL-9 levels in serum suggest activation of Th9 cells and Th17 cells as these cells produce large amounts of IL-9 [64, 65]. However, Tregs, NKT-cells and mast cells are also sources of IL-9. In summary, the different phases of T-cell development were mapped; the expansion phase of naive T-cells in the spleen (2 days p.i.), the effector phase in the lungs (14 days p.i.), contraction phase in the spleen (21 days p.i.) and finally the specific memory T-cells (66 days p.i.) (**Figure 5, 8A, 10 and 12**). Data from this study suggests generation of local specific Th1/Th17 cells in the lungs. Th1 cells, which produce IFNγ are important for clearance of *B. pertussis*. Postponed clearance was shown in IFNγ-depleted mice [97]. Th17 cells have been indicated as key cells to control bacterial infections at mucosal sites [98]. Recent studies revealed that Th17 cells increase the clearance of *B. pertussis* after an intranasal infection in animals [12, 13, 99].

Infection with *B. pertussis* induces also B-cell and antibody mediated immunity. Microarray analysis showed increased gene expression of the BCR in the lungs. In addition, gene expression of IgM, IgG, and IgA was observed in lungs and spleen. Whereas, most genes for antibody isotypes were found upregulated in both tissues, IgM was downregulated in the spleen (**Figure 6 and Figure 10**). This was confirmed by the detection of IgA and IgG (IgG1, IgG2a and IgG2b) antibodies after 14 days p.i. However, IgM antibodies were not found systemically (**Figure 11**). In mice, IgG1 is associated with a Th2-like response, while IgG2a (in Balb/c mice) and IgG2b suggest induction of a Th1 response [100]. IgG2b is also linked to Th17 lymphocytes [101]. All antibody responses in the present study were directed against whole-cell *B. pertussis* and outer membrane vesicles, but not against the *B. pertussis* antigens that are typically present in acellular vaccines: Ptx, Prn, FHA and Fim2/3. However, memory Th1/Th17 cells were detected upon re-stimulation with Prn and FHA (**Figure 12**). The polymeric immunoglobulin receptor (pIgR) was highly expressed during the whole course of *B. pertussis* infection in the lungs. pIgR is essential for the transport of IgA into the mucus and is seen as a bridge between innate and adaptive mucosal responses [102, 103]. The expression of pIgR was drastically enhanced 14 days p.i., leading to secretion of mucosal IgA in the lungs (**Figure 5 and Figure 11**). Interestingly, the increased pIgR expression coincided with IL-17A production in the lungs and sera (**Figure 5 and Figure 7**), which is in agreement with the finding that Th17-mediated responses influence the local humoral response by inducing pIgR expression and elevating secretory IgA levels [104]. Therefore, the transport of IgA to the mucosa, which is orchestrated by IL-17A via the induction of pIgR, supports an important role for local immunity. In summary, *B. pertussis* infection induces a broad humoral response, which was observed by gene and protein expression.

Our study also contains several conceptual points for discussion. First, altered gene expression in the spleen caused by *B. pertussis* infection was modest, except for 21 days p.i. Two possible reasons can be given: (i) the infection initiated a local immune response in the lungs and (ii) gene expression is required to be rather strong to exceed the significance threshold. After the lungs and the draining lymph nodes, the spleen is the third organ in line involved in the generation of the immune response. Therefore, gene expression effects could be less abundant. Furthermore, the spleen consists of many cell types with different gene expression profiles, so changes in expression levels in a single cell type might not have been detected. Cell sorting of individual cell types and subsequent gene expression profiling could overcome this problem. Second, specific antibody and T-cell responses were only measured for a limited set of available purified antigens. The inclusion of other antigens, such as outer membrane proteins, would perhaps have allowed a more detailed analysis. Third, in this study we propose murine infection-induced immune signatures as a benchmark to be used in the development of improved human pertussis vaccines. Since *B. pertussis* is not a natural pathogen for mice, translation of the results obtained in this study to the human situation remains to be interpreted with caution. Nevertheless, using a (naive) murine model has several advantages. It is regarded an important small animal model for pertussis vaccine development [105] and enables to dissect the local and systemic immune response in great detail, as shown in this study, rather than using blood or nasal washes from humans undergoing a *B. pertussis* infection. Furthermore, the role of individual gene signatures and products could be assessed in future research in mice by using knock-in or knock-out strains, or by functional interventions. Encouraging is that many observations made in this study, such as the rapid clearance upon reinfection and involvement of Th17 and Th1 responses, are in line with recent studies on *B. pertussis* infection in baboons, which resemble the human situation more closely [13, 15]. Translation of biomarkers from mouse to man however should be performed with care.

Overall, our study describes the molecular and cellular sequence of events that eventually lead to the induction of protective immunity to *B. pertussis*, including local immunity in the lungs, which is not induced by current vaccines. Especially the inductions of Th1 and Th17 cells and IgA antibodies in the lungs are regarded key elements in superior immunity. Our data can be used to select vaccine concepts that resemble infection, with respect to e.g. administration route and prolonged antigen exposure, and immune signatures elicited. Local delivery of vaccines may be an important advancement for improved protection as was previously demonstrated with a live attenuated pertussis vaccine [106]. Also adjuvants could be selected and optimized that can steer host immunity of inactivated vaccines towards an infection-like immune response with minimal adverse effects. The molecular and cellular fingerprint of the local immune response discovered in *B. pertussis* infected mice thus can provide a strong guidance for developing improved pertussis vaccines.

Materials and methods

Ethics Statement

The independent ethical committee for animal experimentations 'Dierexperiment Commissie (DEC)' of the National Institute for Public Health and the Environment (RIVM) reviewed the animal experiments in this study according to the guidelines provided by the Dutch Animal Protection Act. The committee approved documents with the identification numbers 'DPA201100230' and 'DPA201100348'.

Materials

Bordetella pertussis strain B1917 [107] was isolated in The Netherlands in 2000 and was kindly provided by Frits Mooi. Bordet-Gengou agar plates with 15% sheep blood were purchased from BD (Cat. No. 254400, BD, The Netherlands). Verweij medium was obtained from Bilthoven Biologicals (BBio, Bilthoven, The Netherlands). PBS (pH 7.2) and Roswell Park Memorial Institute Media 1640 (RPMI) were purchased from Invitrogen (Gibco, Invitrogen). All RPMI media used in this experiment were supplemented with 10% fetal calf serum (FCS, Hyclone, New Zealand), 100 units penicillin, 100 units streptomycin, and 2.92 mg/ml L-glutamine (p/s/g; Invitrogen). Shockbuffer for splenocyte isolation consisted of 8.3 g/L NH_4CL, 1 g/L $NaHCO_3$, and 5000 IE/L Heparine dissolved in dH_2O (pH 7.4; ice cold) and was filtered (0.22 µm) before use. FACS buffer consisted of PBS pH 7.2 supplemented with 0.5% BSA (A3803, Sigma Aldrich, Germany) and 0.5 mM EDTA (ICN Biomedicals). Horseradish peroxidase (HRP) labelled goat-anti-mouse IgG and *R*-Phycoerythrin (RPE)-conjugated goat-anti-mouse IgM, IgA, IgG, IgG1, IgG2a, IgG2b, and IgG3 were obtained from Southern Biotech (Southern Biotech, United States). Fluorescently labeled antibodies for flow cytometry, anti-CD3-Pacific blue (17A2), anti-CD4- Pacific blue (GK1.5), anti-IA-IE-PerCP-Cy5.5 (M5/114.15.2), anti-33D1-APC (33D1), and anti-IL-5-APC were purchased from Biolegend (ITK, The Netherlands). Fluorescently labeled antibodies, anti-CD4-APC (RM4-5), anti-CD8a-PerCP (53 6.7), anti- CD69-FITC (H1.2 F3), anti-Gr-1-PE (RB6-8C5), anti-CD19- FITC (1D3), anti-CD14-PE (rmC5-3), anti-DX5-APC (DX5), anti-CD11b-PE (M1/70), anti-CD40-FITC (HM40-3), anti-CD44-FITC (IM7), and anti-IFNγ-PE were purchased from BD (BD Biosciences, The Netherlands). Fluorescently labeled antibodies CD11c-PE-Cy7 (N418) and anti-IL-17A-PerCP-Cy5.5 were obtained from eBioscience (eBioscience, Austria). Live/dead staining was purchased from Invitrogen (LIVE/DEAD Fixable Aqua Dead Cell Stain Kit; Invitrogen). Anti-CD16/CD32 was purchased from BD (BD, The Netherlands).

Cultivation of *B. pertussis*

B. pertussis strain B1917 was grown on Bordet-Gengou agar plates for 4 days at 35ºC. Subsequently, multiple colonies were transferred onto new plates and grown for 24 hours at 35ºC, which was repeated 3 times. Colonies on each plate were harvested in 1.5 ml Verweij medium [108] and the suspensions were pooled. After centrifugation (30 min, 1932

g), cells were washed with 15 ml Verweij medium. Subsequently, bacterial suspensions of approximately $2x10^{10}$ cfu/ml were resuspended in Verweij medium containing 15% glycerol (v/v) and aliquots of 0.25 ml were flash frozen in ethanol and dry ice and stored at -80ºC.

Challenge culture

A stock of *B. pertussis* B1917 was diluted with Verweij medium to a final concentration of $5x10^6$ cfu/ml. The number of cfu was confirmed by plating 100 µl of the infection suspension (1:2000 in Verweij medium) on Bordet-Gengou agar plates. Plates were incubated for 4 days at 35ºC and cfu were counted by using a colony counter (ProtoCOL, Synbiosis, Cambridge, United Kingdom).

Animal experiment

Female BALB/c mice (Harlan, The Netherlands), 8-weeks-old, were divided in groups of three animals and housed in cages (macrolon III including filter top). Three healthy mice were euthanized at day 0 and considered as naive group. Other mice were intranasally infected under anesthesia (isoflurane/oxygen), with $2x10^5$ cfu *B. pertussis* B1917 in 40 µl Verweij medium at day 0. Groups of animals (n = 3) were euthanized after 2, 4, 6 hours, and after 1, 2, 4, 7, 10, 14, 21, and 28 days of infection, respectively. At 56 days p.i. five groups of primary infected animals and five groups of naive animals (n = 3) were infected as previously described and euthanized after 4 hours, and after 2, 7, 10, and 14 days of infection. In addition, six infected and six healthy mice were euthanized at day 21 and day 66 for the analysis of $CD4^+$ T-cell responses. Mice were bled, under anesthesia (isoflurane/oxygen), by orbital bleeding and sacrificed by cervical dislocation. Whole blood from each mouse was collected in a blood collection tube (MiniCollect 0.8 ml Z Serum Sep GOLD, Greiner Bio-One, Austria). After coagulation (10 min at room temperature), sera were taken after centrifugation (10 min, 3000 g) and stored at -80ºC. Lung lobes were excised. The right lobe was placed in 900 µl Verweij medium and kept at room temperature. The left lobe was placed in 1 ml RNAlater (Qiagen), incubated overnight at 4ºC and stored at -80ºC. The spleen was excised and divided in two equal parts. One piece was placed in 5 ml of RPMI medium and kept on ice. The other piece was placed in 1 ml RNAlater (Qiagen), incubated overnight at 4ºC and stored at -80ºC. For the analysis of $CD4^+$ T-cell responses, whole spleen was collected and placed in 5 ml of RPMI medium and kept on ice.

Colonization assay

Lung tissue in 900 µl Verweij medium was homogenized for 15 seconds using a Labgen 7 Homogenizer (Cole Palmer, Schiedam, The Netherlands). Homogenizer was sanitized between samples with ethanol (80%) and water. Lung homogenates were serially diluted (undiluted, 1:10, 1:100 or 1:1000) in Verweij medium depending on the expected number of cfu. Suspensions of 100 µl were plated on Bordet-Gengou agar plates and incubated for 4

days at 35ºC. The numbers of colonies were counted by using a colony counter (ProtoCOL, Synbiosis, Cambridge, United Kingdom) and calculated as cfu per mouse.

RNA isolation

Lung and spleen tissues were homogenized by using a Labgen 7 Homogenizer (Cole Palmer, Schiedam, The Netherlands) in 700 and 2100 µl Qiazol (Qiagen Benelux, Venlo, The Netherlands), respectively. RNA isolation was performed using a miRNeasy Mini Kit with DNAse treatment (Qiagen Benelux, Venlo, The Netherlands) according to the manufacturer's protocol. RNA concentrations were determined by UV spectroscopy (Tech3 module, Synergy Mx, BioTek, Winooski, United States). RNA quality was determined by using electrophoresis (RNA nano 6000 kit, 2100 Bioanalyzer, Agilent Technologies, Amstelveen, The Netherlands). Results were given as RNA integrity numbers (RIN) between 1 and 10 (manual Bioanalyzer). Samples with a RIN of 7 or higher were used for microarray analysis. For microarray analysis of lung tissue, RNA concentrates of individual mice were analyzed for the following time points: naive, 4 hours, 2 days, 4 days, 7 days, 10 days, 14 days, 21 days, and 28 days post infection (p.i.). For spleen tissue, samples of individual mice were analyzed for the following time points: naive, 4 hours, 1 day, 2 days, 4 days, 7 days, 10 days, 14 days, 21 days, and 28 days p.i.

Microarray analysis

Amplification, labeling and hybridization of RNA samples to microarray chips was carried out at the Microarray Department of the University of Amsterdam, The Netherlands, as described previously [109].

Briefly, 500 ng total RNA of each sample was amplified (aRNA) according to the Agilent QuickAmp kit manual (Agilent technologies). A common reference sample for either lung or spleen tissue was made by pooling equimolar amounts of aRNA from individual samples of the respective tissues. Cy3 and Cy5 monoreactive dyes (GE Healthcare) were used to label individual samples and the common reference sample, respectively. Labeling was performed with 10 ml of CyDye solution and incubated for 1 hour before the reaction was quenched by adding 5 ml 4 M hydroxylamine (Sigma-Aldrich). Purification was performed by using a clean-up kit (E.Z.N.A. MicroElute RNA Clean Up Kit, Omega Bio-Tek, Norcross, United States). The yields of amplified RNA and incorporation of CyDye were determined by using a spectrophotometer (NanoDrop ND-1000, NanoDrop products, Wilmington, United States).

Hybridization mixture was prepared by adding a dried mixture (1:1) of sample (Cy3) and common reference (Cy5) together with sample tracking control (STC, Roche NimbleGen) and hybridization cocktail (NimbleGen Arrays User's Guide - Gene Expression Arrays Version 5.0, Roche NimbleGen). Samples were incubated successively for 5 min at 95ºC and 5 min at 42ºC. Hybridization was performed by loading a sample onto a microarray (NimbleGen 126135 k Mus musculus, Roche, Germany) containing probes for 44,170 genes with 3 spots per target probe. Hybridization was performed with a NimbleGen Hybridization System 4 (Roche

NimbleGen) for 20 hours at 42°C. After washing (NimbleGen Arrays User's Guide - Gene Expression Arrays Version 5.0), slides were scanned in an ozone-free room with a microarray scanner (Agilent DNA microarray scanner G2565CA, Agilent Technologies). Each microarray corresponded to labeled RNA from specific tissue (lung or spleen) from one individual mouse. Feature extraction was performed with NimbleScan v2.5 (Roche NimbleGen) resulting in a table containing individual probe signal intensities for both dyes. Complete raw and normalized microarray data and their MIAME compliant metadata from this publication have been submitted to the GEO database (www.ncbi.nlm.nih.gov/geo) and assigned the identifier GSE53294.

Data analysis of gene expression

Quality control was performed on raw data by means of Cy3-Cy5 scatter plots, and by comparing signal average and distribution across slides. All slides passed quality control. Raw microarray data for gene-coding probes were normalized in R (www.r-project.org), by using a four step approach [109]: (1) natural log-transformation, (2) quantile normalization of all scans, (3) correcting the sample spot signal for the corresponding reference spot signal and (4) averaging data from replicate probe spots. Further analysis of normalized data of 44,170 probes was performed in R and Microsoft Excel.

Genes differentially expressed between experimental groups (naive and various time points p.i.) were identified by using ANOVA. Fold ratio induction or repression of individual genes was calculated by comparing mean gene expression levels of infected groups to the group with naive mice. Data are presented as the average normalized gene expression levels of three mice per group. Probes were considered differentially expressed if they met the following two criteria: (i) a *p*-value ≤ 0.001 (ANOVA), which corresponds to a Benjamini-Hochberg False discovery rate (FDR) [110] of < 5%; and (ii) an absolute fold ratio ≥ 1.5 (infected compared to naive mice) for at least one time point. If multiple probes corresponding to the same gene were significant, their data were averaged to remove redundancy for further analysis. Gene expression of each group was compared with the group of naive mice. Differences in gene expression were visualized in heat maps (GeneMaths XT, Applied Maths, St-Martens-Latem, Belgium). Genes were arranged according to similar expression patterns in time at which genes exceeded the fold ratio cut-off of 1.5. To facilitate visual interpretation of heat maps, only induction (red) and repression (green) of gene expression levels with fold ratios ≥ 1.5 are visualized, therefore presenting fold ratios < 1.5 as naive level (black).

Functional enrichment with an over-representation analysis (ORA) was carried out by using DAVID [111] based on Gene Ontology Biological Processes (GO-BP) and Kyoto Encyclopedia of Genes and Genomes (KEGG). Cell-specific or tissue-specific gene sets were obtained by using data from BioGPS [112, 113]. For each cell type or tissue, gene expression data were compared to the average of all tissues included in the data set. The top 100 genes, which had the highest tissue-specific expression and were included on the NimbleGen array, were selected. If the

BioGPS dataset included multiple entries for the same cell type (e.g., $CD4^+$ and $CD8^+$ T-cells), the resulting sets were combined in our subsequent analysis.

Whole-cell *B. pertussis* ELISA

Immunoglobulin G responses against *B. pertussis* were determined in sera by an ELISA. Therefore, *B. pertussis* B1917 was heat-inactivated for 45 min. at 56ºC, after which ELISA plates (Immunolon 2HB, Thermo Scientific) were coated overnight at room temperature with 100 µl/well whole-cell *B. pertussis* ($OD_{590\ nm}$ = 0.1 in PBS). Plates were washed with 0.03% (v/v) Tween 80 in water. Then, plates were incubated for 1 hour at 37ºC with 100 µl/well serial dilutions of serum samples in PBS, pH 7.2 (Gibco) with 0.1% (v/v) Tween 80. Plates were washed twice and incubated (1 hour, 37ºC) with 100 µl/well of HRP-conjugated goat-anti-mouse IgG (1:5000) in PBS with 0.1% (v/v) Tween 80 and 0.5% (w/v) Protifar (Nutricia). After washing twice, 100 ml/well peroxidase substrate (4.2 mM Tetra Methyl Benzidine and 0.012% H_2O_2 in 0.11 M sodium acetate buffer, pH 5.5.) was added, plates were incubated at room temperature and the reaction terminated after 10 min by adding 100 µl/well, 2 M H_2SO_4 (BBio, Bilthoven, The Netherlands). Finally, the absorbance was recorded at 450 nm with a plate reader (BioTek reader EL808, Bio-Tek, USA) and antibodies against whole-cell *B. pertussis* are presented in OD450 signal, because a reference is not available.

Multiplex immunoassay (MIA) for antibody response

Responses of IgM, IgA, total IgG, and the IgG subclasses (IgG1, IgG2a, IgG2b and IgG3) against *B. pertussis* antigens P.69 pertactin (P.69 Prn), filamentous hemagglutinin (FHA), pertussis toxin (Ptx), combined fimbria type 2 and 3 antigens (Fim2/3), and outer membrane vesicles B1917 (OMV B1917) were determined in sera by using a MIA. Outer membrane vesicles from *B. pertussis* B1917 were produced as previously described [114] with additional changes. Conjugation of antigens and OMVs to beads was performed as described previously [115]. Serum was diluted 1:100 in PBS containing 0.1% Tween 20 and 3% bovine serum albumin and mixed 1:1 with conjugated beads. After incubation with *R*-Phycoerythrin (RPE)-conjugated anti-mouse IgM (1:100), IgA (1:100), IgG (1:200), IgG1 (1:200), IgG2a (1:40), IgG2b (1:200), and IgG3 (1:200), samples were analyzed by using a Bio-Plex system (Bio-Plex 200, BioRad). Total IgG titers (U/ml) against *B. pertussis* antigens were calculated from mean fluorescent intensity (MFI) by using a reference from the National Institute for Biological Standards and Control (Code 99/520, NIBSC, England) in the Bio-Plex Manager software (Bio-Rad Laboratories). Results for IgM, total IgG, IgG subclasses, and IgA antibodies against OMV B1917 are presented in fluorescent intensity (F.I.), because a reference is not available.

Lung lysate preparation and IgA antibody assay

The lung lysates used for the colonization assay were centrifuged (10 min, 2000 g) and filtered (0.22 µm Millex-GV, Merck KGaA, Darmstadt, Germany) to remove cell debris and

bacteria. Filtrates were stored at -80ºC. Prior to analysis, lung lysates were diluted 1:10 in PBS containing 0.1% Tween 20 and 3% bovine serum albumin. Analysis of IgA antibodies in the lung lysate was performed against *B. pertussis* antigens (Ptx, Prn, FHA, and Fim2/3) and OMV B1917 as described in the section multiplex immunoassay (MIA) for antibody response.

Splenocyte isolation

Spleen tissue was forced through a 70-µm cell strainer (BD Falcon, BD Biosciences, USA) and washed two times with 5 ml medium (RPMI, FCS, p/s/g) to obtain a single cell suspension. After centrifugation (5 min, 550 g), 1 ml shock buffer was added to cell pellet to lyse erythrocytes. After one minute, shock incubation was stopped by adding 25 ml medium. For cell count (CASEY model TT, Innovatis, Roche, Germany), cells were centrifuged and resuspended in 1 ml medium.

Cellular composition of spleen

Splenocytes were transfered to each well of a V-bottom 96-wells plate. After centrifugation (3 min, 400 g), pellets were washed with 100 µl FACS buffer. Fc-specific receptors on cells were blocked with anti-CD16/CD32 in FACS buffer (2%, v/v) by 5 min. incubation on ice to prevent aspecific binding of labeled antibodies to cells. Cells were stained after centrifugation by using a mixture (100 µl) of labeled antibodies (30 min, 4ºC). To determine the number and identity of cells, three different panels of labeled antibodies were used to prevent overlapping fluorescence spectra. Panels consisted of 1) total T-cell population (CD3), CD4 T-cell (CD4), CD8 T-cell (CD8), early activated T-cell (CD69), and neutrophil (Gr-1); 2) T-cell (CD3), B-cell (CD19), monocyte (CD14), and natural killer cell (DX5); 3) T-cell (CD3), macrophage (CD11b), DC (33D1, CD11c), MHC class II (IA/IE), and activation marker (CD40). Data acquisition was performed with a FACSCanto II (BD Biosciences, USA) and data analysis was done by using FlowJo software (Tree Star Inc., USA). Debris and dead cells were excluded by using forward/side scatter characteristics and live/dead staining, respectively.

Stimulation of splenocytes

Splenocytes were resuspended in the culture medium IMDM (Gibco) + 8% FCS + p/s/g + 20 µM β-mercaptoethanol (Sigma) and cultured (24-wells plate; $6x10^6$ cells/well) for 7 days at 37ºC in a humidified atmosphere containing 5% CO_2. Culturing was in the presence of either the culture medium, or the culture medium supplemented with Prn P.69 (in house expressed and purified as described previously [116]), heat-inactivated (15 min. at 95ºC) Ptx (Kaketsuken, Japan) or FHA (Kaketsuken, Japan), at a final concentration of 1 µg/ml. Supernatants were collected after 7 days for cytokine analysis. Subsequently, cells were transferred to U-bottom 96-wells plates ($5x10^6$ cells/well) and stimulated overnight by using the same antigens and conditions and used for intracellular cytokine staining.

Intracellular cytokine staining

The intracellular cytokine staining was performed on 8-days stimulated splenocytes by using a Cytofix/Cytoperm Fixation/ Permeabilization Solution Kit (BD Biosciences, USA). Briefly, cells were incubated during the last 5 hours of stimulation with 10 µg/ ml Golgiplug (BD Biosciences), 1 µg/ml αCD28 (BD Pharmingen), and 1 µg/ml αCD49d (BD Pharmingen). Cells were stained after washing with FACS buffer with anti-CD4-Pacific blue, anti-CD44-FITC, and live/dead staining. Subsequently, the cells were fixed, permeabilized, and stained with anti-IFNγ-PE, anti-IL-5-APC and anti-IL-17A-PerCP-Cy5.5. Data from fluorescence-activated cells were acquired on FACS Canto II (BD Biosciences) and analyzed with FlowJo software (Tree Star Inc., USA). CD44 was used to distinguish between naive and antigen experienced T- cells. IL-5 was used as a Th2 cytokine, IFNγ as a Th1 cytokine, and IL-17A as a Th17 cytokine.

Multiplex immunoassay (MIA) for cytokines

Cytokine (IL-4, IL-5, IL-10, IL-13, IL-17A, TNFα, and IFNγ) concentrations (pg/ml) were determined in culture supernatants of 7-days stimulated splenocytes of individual mice by using a MIA (Milliplex mouse cytokine 7-plex luminex kit; Merck KGaA, Darmstadt, Germany). Cytokine (Eotaxin, G-CSF, GM-CSF, IFNγ, IL-10, IL-12(p40), IL-12(p70), IL-13, IL-15, IL-17A, IL-1α, IL-1β, IL-2, IL-3, IL-4, IL-5, IL-6, IL-7, IL-9, IP-10, KC, LIF, LIX, M-CSF, MCP-1, MIG, MIP-1α, MIP-1β, MIP-2, RANTES, TNFα, VEGF) concentrations (pg/ml) present in serum were determined by using a MIA (Milliplex MAP Mouse Cytokine/ Chemokine - Premixed 32 Plex; Merck KGaA, Darmstadt, Germany) according to the manufacturer's instructions. Briefly, serum/ supernatant (25 µl) was diluted in supplied assay buffer (1/ 1; v/v), mixed with 25 µl conjugated beads and incubated overnight at 4ºC on a plate shaker. Subsequently, beads were washed twice with washing buffer by using a Bio-Plex handheld magnetic washer (BioRad, USA) and incubated with 25 µl detection antibodies (1 hour, 20-25ºC) followed by incubation with 25 µl streptavidin-phycoerythrin (30 min, 20-25ºC). After washing twice with 200 µl washing buffer, beads were resuspended in 150 µl PBS. Samples were analyzed using a multiplex system (Bio-Plex 200, BioRad, USA). In total, 50 beads per region were analyzed in 100 µl sample volume. Mean fluorescence intensity (MFI) of each cytokine was converted into pg/ml by using a dilution series of a standard (3.2–10,000 pg/ml) and Bio-Plex Manager software 5.0 (Bio-Rad, USA).

MIP-3α (CCL20) cytokine ELISA

Serum concentration of Macrophage Inflammatory Protein 3α (MIP3α/CCL20) was determined by ELISA (Mouse MIP-3α ELISA kit, RAB0061, Sigma-Aldrich, Germany) according to the manufacturer's manual. In short, serum (50 µl) was diluted in assay buffer A (1/1; v/v) and incubated in an antibody-coated ELISA plate (overnight, 4ºC, gentle shaking). After washing four times with 300 µl wash buffer, wells were incubated with 100 µl biotinylated antibody (1 hour, room temperature, gentle shaking). After washing four times with 300 µl wash buffer,

wells were incubated with 100 µl streptavidin solution (45 min, room temperature, gentle shaking). After washing four times, wells were incubated with 100 µl TMB one-step substrate reagent (30 min, room temperature) and reaction stopped with 50 µl stop solution. Finally, the absorbance was recorded at 450 nm with a plate reader (BioTek reader EL808, Bio-Tek) and converted to MIP-3α concentration by using a dilution series of a standard (2.06–1,500 pg/ml) and Gentech 5 software (BioTek).

Statistical analysis

Cellular composition of spleen, antibody titers and cytokines levels were analyzed by using a one-way ANOVA with multiple comparisons of all time points post infection vs. naive mice followed by a Dunnett t-test. ICS data was analyzed by using a Mann-Whitney t-test. For cytokine profiling after re-stimulation of splenocytes, MIA data was first log-transformed before t-test analysis. In all corresponding figures, *p*-values are represented as * $p \leq 0.05$, ** $p \leq 0.01$, *** $p \leq 0.001$ and **** $p \leq 0.0001$.

Acknowledgments

We thank employees of the Animal Research Centre (ARC) of Intravacc, in particular Dirk Elberts and Tanja Schouten, for the performance of animal experiments; Sylvia Reemers for fruitful discussions; Wichard Tilstra for the preparation of particular figures in this manuscript; Frits Mooi for providing the *Bordetella pertussis* B1917 strain. The authors thank the Microarray Department (MAD) of the University of Amsterdam for the performance of the microarray analyses.

References

1. Mattoo, S. and J.D. Cherry, Molecular pathogenesis, epidemiology, and clinical manifestations of respiratory infections due to *Bordetella pertussis* and other Bordetella subspecies. Clin Microbiol Rev, 2005. 18(2): p. 326-82.
2. Cherry, J.D., Epidemic pertussis in 2012--the resurgence of a vaccine-preventable disease. N Engl J Med, 2012. 367(9): p. 785-7.
3. Baxter, R., *et al.*, Effectiveness of pertussis vaccines for adolescents and adults: case-control study. BMJ, 2013. 347: p. f4249.
4. Celentano, L.P., *et al.*, Resurgence of pertussis in Europe. Pediatr Infect Dis J, 2005. 24(9): p. 761-5.
5. Kretzschmar, M., P.F. Teunis, and R.G. Pebody, Incidence and reproduction numbers of pertussis: estimates from serological and social contact data in five European countries. PLoS Med, 2010. 7(6): p. e1000291.
6. Mooi, F.R., V.D.M. NA, and H.E. De Melker, Pertussis resurgence: waning immunity and pathogen adaptation - two sides of the same coin. Epidemiol Infect, 2013: p. 1-10.
7. Mann, P.B., M.J. Kennett, and E.T. Harvill, Toll-like receptor 4 is critical to innate host defense in a murine model of bordetellosis. J Infect Dis, 2004. 189(5): p. 833-6.
8. Banus, H.A., *et al.*, Host genetics of *Bordetella pertussis* infection in mice: significance of Toll-like receptor 4 in genetic susceptibility and pathobiology. Infect Immun, 2006. 74(5): p. 2596-605.
9. Banus, S., *et al.*, Lung response to *Bordetella pertussis* infection in mice identified by gene-expression profiling. Immunogenetics, 2007. 59(7): p. 555-64.
10. Moreno, G., *et al.*, Toll-like receptor 4 orchestrates neutrophil recruitment into airways during the first hours of *Bordetella pertussis* infection. Microbes Infect, 2013.
11. Mills, K.H., *et al.*, Cell-mediated immunity to *Bordetella pertussis*: role of Th1 cells in bacterial clearance in a murine respiratory infection model. Infect Immun, 1993. 61(2): p. 399-410.
12. Ross, P.J., *et al.*, Relative contribution of Th1 and Th17 cells in adaptive immunity to *Bordetella pertussis*: towards the rational design of an improved acellular pertussis vaccine. PLoS Pathog, 2013. 9(4): p. e1003264.
13. Warfel, J.M. and T.J. Merkel, *Bordetella pertussis* infection induces a mucosal IL-17 response and long-lived Th17 and Th1 immune memory cells in nonhuman primates. Mucosal Immunol, 2013. 6(4): p. 787-96.
14. Wendelboe, A.M., *et al.*, Duration of immunity against pertussis after natural infection or vaccination. Pediatr Infect Dis J, 2005. 24(5 Suppl): p. S58-61.
15. Warfel, J.M., L.I. Zimmerman, and T.J. Merkel, Acellular pertussis vaccines protect against disease but fail to prevent infection and transmission in a nonhuman primate model. Proc Natl Acad Sci U S A, 2014. 111(2): p. 787-92.
16. Ausiello, C.M., *et al.*, Vaccine- and antigen-dependent type 1 and type 2 cytokine induction after primary vaccination of infants with whole-cell or acellular pertussis vaccines. Infect Immun, 1997. 65(6): p. 2168-74.
17. Mills, K.H., *et al.*, A murine model in which protection correlates with pertussis vaccine efficacy in children reveals complementary roles for humoral and cell-mediated immunity in protection against *Bordetella pertussis*. Infect Immun, 1998. 66(2): p. 594-602.
18. Canthaboo, C., *et al.*, Investigation of cellular and humoral immune responses to whole cell and acellular pertussis vaccines. Vaccine, 2000. 19(6): p. 637-43.
19. Hellwig, S.M., *et al.*, Immunoglobulin A-mediated protection against *Bordetella pertussis* infection. Infect Immun, 2001. 69(8): p. 4846-50.
20. Leef, M., *et al.*, Protective immunity to *Bordetella pertussis* requires both B cells and CD4(+) T cells for key functions other than specific antibody production. J Exp Med, 2000. 191(11): p. 1841-52.
21. Ryan, M., *et al.*, *Bordetella pertussis* respiratory infection in children is associated with preferential activation of type 1 T helper cells. J Infect Dis, 1997. 175(5): p. 1246-50.
22. Kirimanjeswara, G.S., P.B. Mann, and E.T. Harvill, Role of antibodies in immunity to Bordetella infections. Infect Immun, 2003. 71(4): p. 1719-24.
23. Hendrikx, L.H., *et al.*, Serum IgA responses against pertussis proteins in infected and Dutch wP or aP vaccinated children: an additional role in pertussis diagnostics. PLoS One, 2011. 6(11): p. e27681.
24. Brandes, M., *et al.*, A systems analysis identifies a feedforward inflammatory circuit leading to lethal influenza infection. Cell, 2013. 154(1): p. 197-212.
25. Tam, V.C., *et al.*, Lipidomic Profiling of Influenza Infection Identifies Mediators that Induce and Resolve Inflammation. Cell, 2013. 154(1): p. 213-27.
26. Berry, M.P., *et al.*, An interferon-inducible neutrophil-driven blood transcriptional signature in human tuberculosis. Nature, 2010. 466(7309): p. 973-7.
27. Vandebriel, R.J., *et al.*, Association of *Bordetella pertussis* with host immune cells in the mouse lung. Microb Pathog, 2003. 35(1): p. 19-29.
28. van Kooyk, Y., C-type lectins on dendritic cells: key modulators for the induction of immune responses. Biochem Soc Trans, 2008. 36(Pt 6): p. 1478-81.
29. Kikutani, H. and A. Kumanogoh, Semaphorins in interactions between T cells and antigen-presenting cells. Nat Rev Immunol, 2003. 3(2): p. 159-67.
30. Gianchecchi, E., D.V. Delfino, and A. Fierabracci, Recent insights into the role of the PD-1/PD-L1 pathway in immunological tolerance and autoimmunity. Autoimmun Rev, 2013.
31. Doi, T., *et al.*, IgA plasma cells express the negative regulatory co-stimulatory molecule programmed cell death 1 ligand and have a potential tolerogenic role in the intestine. Biochem Biophys Res Commun, 2012. 425(4): p. 918-23.
32. Alcaide, P., *et al.*, Difference in Th1 and Th17 lymphocyte adhesion to endothelium. J Immunol, 2012. 188(3): p. 1421-30.
33. Ito, T., *et al.*, CCR6 as a mediator of immunity in the lung and gut. Exp Cell Res, 2011. 317(5): p. 613-9.
34. Reibman, J., *et al.*, Airway epithelial cells release MIP-3alpha/CCL20 in response to cytokines and ambient particulate matter. Am J Respir Cell Mol Biol, 2003. 28(6): p. 648-54.

35. Kohrgruber, N., *et al.*, Plasmacytoid dendritic cell recruitment by immobilized CXCR3 ligands. J Immunol, 2004. 173(11): p. 6592-602.
36. Evans, S.E., *et al.*, Inducible innate resistance of lung epithelium to infection. Annu Rev Physiol, 2010. 72: p. 413-35.
37. Schroll, A., *et al.*, Lipocalin-2 ameliorates granulocyte functionality. Eur J Immunol, 2012. 42(12): p. 3346-57.
38. Nishimura, J., *et al.*, Potent antimycobacterial activity of mouse secretory leukocyte protease inhibitor. J Immunol, 2008. 180(6): p. 4032-9.
39. Saiga, H., *et al.*, Lipocalin 2-dependent inhibition of mycobacterial growth in alveolar epithelium. J Immunol, 2008. 181(12): p. 8521-7.
40. Dela Cruz, C.S., *et al.*, Chitinase 3-like-1 promotes Streptococcus pneumoniae killing and augments host tolerance to lung antibacterial responses. Cell Host Microbe, 2012. 12(1): p. 34-46.
41. Pisabarro, M.T., *et al.*, Cutting edge: novel human dendritic cell- and monocyte-attracting chemokine-like protein identified by fold recognition methods. J Immunol, 2006. 176(4): p. 2069-73.
42. Burkhardt, A.M., *et al.*, CXCL17 is a mucosal chemokine elevated in idiopathic pulmonary fibrosis that exhibits broad antimicrobial activity. J Immunol, 2012. 188(12): p. 6399-406.
43. Miyake, K., *et al.*, Innate recognition of lipopolysaccharide by Toll-like receptor 4/MD-2 and RP105/MD-1. J Endotoxin Res, 2000. 6(5): p. 389-91.
44. Asagiri, M., *et al.*, Cathepsin K-dependent toll-like receptor 9 signaling revealed in experimental arthritis. Science, 2008. 319(5863): p. 624-7.
45. Takaoka, A., *et al.*, DAI (DLM-1/ZBP1) is a cytosolic DNA sensor and an activator of innate immune response. Nature, 2007. 448(7152): p. 501-5.
46. Powlesland, A.S., *et al.*, Widely divergent biochemical properties of the complete set of mouse DC-SIGN-related proteins. J Biol Chem, 2006. 281(29): p. 20440-9.
47. Vukman, K.V., *et al.*, Mannose receptor and macrophage galactose-type lectin are involved in *Bordetella pertussis* mast cell interaction. J Leukoc Biol, 2013.
48. Turkistany, S.A. and R.P. DeKoter, The transcription factor PU.1 is a critical regulator of cellular communication in the immune system. Arch Immunol Ther Exp (Warsz), 2011. 59(6): p. 431-40.
49. Carotta, S., L. Wu, and S.L. Nutt, Surprising new roles for PU.1 in the adaptive immune response. Immunol Rev, 2010. 238(1): p. 63-75.
50. Male, V., *et al.*, E4BP4: an unexpected player in the immune response. Trends Immunol, 2012. 33(2): p. 98-102.
51. Perry, A.K., *et al.*, The host type I interferon response to viral and bacterial infections. Cell Res, 2005. 15(6): p. 407-22.
52. Miyagawa, F., *et al.*, Interferon regulatory factor 8 integrates T-cell receptor and cytokine-signaling pathways and drives effector differentiation of CD8 T cells. Proc Natl Acad Sci U S A, 2012. 109(30): p. 12123-8.
53. Shin, D.M., C.H. Lee, and H.C. Morse, 3rd, IRF8 governs expression of genes involved in innate and adaptive immunity in human and mouse germinal center B cells. PLoS One, 2011. 6(11): p. e27384.
54. Marquis, J.F., *et al.*, Interferon regulatory factor 8 regulates pathways for antigen presentation in myeloid cells and during tuberculosis. PLoS Genet, 2011. 7(6): p. e1002097.
55. Zurita, E., *et al.*, The Stimulated Innate Resistance Event in *Bordetella pertussis* Infection Is Dependent on Reactive Oxygen Species Production. Infect Immun, 2013. 81(7): p. 2371-8.
56. Gibbings, D. and A.D. Befus, CD4 and CD8: an inside-out coreceptor model for innate immune cells. J Leukoc Biol, 2009. 86(2): p. 251-9.
57. Stoeckle, C., *et al.*, Cathepsin W expressed exclusively in CD8+ T cells and NK cells, is secreted during target cell killing but is not essential for cytotoxicity in human CTLs. Exp Hematol, 2009. 37(2): p. 266-75.
58. Nitschke, L., The role of CD22 and other inhibitory co-receptors in B-cell activation. Curr Opin Immunol, 2005. 17(3): p. 290-7.
59. Flak, T.A., *et al.*, Synergistic epithelial responses to endotoxin and a naturally occurring muramyl peptide. Infect Immun, 2000. 68(3): p. 1235-42.
60. Clark-Lewis, I., *et al.*, Structure-function relationship between the human chemokine receptor CXCR3 and its ligands. J Biol Chem, 2003. 278(1): p. 289-95.
61. Jose, P.J., *et al.*, Eotaxin: a potent eosinophil chemoattractant cytokine detected in a guinea pig model of allergic airways inflammation. J Exp Med, 1994. 179(3): p. 881-7.
62. Sallusto, F., C.R. Mackay, and A. Lanzavecchia, Selective expression of the eotaxin receptor CCR3 by human T helper 2 cells. Science, 1997. 277(5334): p. 2005-7.
63. Schmitt, E., *et al.*, Establishment of different T cell sublines using either interleukin 2 or interleukin 4 as growth factors. Eur J Immunol, 1990. 20(8): p. 1709-15.
64. Veldhoen, M., *et al.*, Transforming growth factor-beta 'reprograms' the differentiation of T helper 2 cells and promotes an interleukin 9-producing subset. Nat Immunol, 2008. 9(12): p. 1341-6.
65. Nowak, E.C., *et al.*, IL-9 as a mediator of Th17-driven inflammatory disease. J Exp Med, 2009. 206(8): p. 1653-60.
66. Roberts, A.W., G-CSF: a key regulator of neutrophil production, but that's not all! Growth Factors, 2005. 23(1): p. 33-41.
67. Stark, M.A., *et al.*, Phagocytosis of apoptotic neutrophils regulates granulopoiesis via IL-23 and IL-17. Immunity, 2005. 22(3): p. 285-94.
68. Furman, D., *et al.*, Apoptosis and other immune biomarkers predict influenza vaccine responsiveness. Mol Syst Biol, 2013. 9: p. 659.
69. Liang, S.C., *et al.*, An IL-17F/A heterodimer protein is produced by mouse Th17 cells and induces airway neutrophil recruitment. J Immunol, 2007. 179(11): p. 7791-9.
70. Nishida, M., *et al.*, Pertussis toxin up-regulates angiotensin type 1 receptors through Toll-like receptor 4-mediated Rac activation. J Biol Chem, 2010. 285(20): p. 15268-77.
71. Jeyaseelan, S., *et al.*, Induction of CXCL5 during inflammation in the rodent lung involves activation of alveolar epithelium. Am J Respir Cell Mol Biol, 2005. 32(6): p. 531-9.
72. Bozic, C.R., *et al.*, Expression and biologic characterization of the murine chemokine KC. J Immunol, 1995. 154(11): p. 6048-57.
73. Boyd, A.P., *et al.*, *Bordetella pertussis* adenylate cyclase toxin modulates innate and adaptive immune responses: distinct roles for acylation and enzymatic activity in immunomodulation and cell death. J Immunol, 2005. 175(2): p. 730-8.

74. Carbonetti, N.H., Immunomodulation in the pathogenesis of *Bordetella pertussis* infection and disease. Curr Opin Pharmacol, 2007. 7(3): p. 272-8.
75. Kirimanjeswara, G.S., *et al.*, Pertussis toxin inhibits neutrophil recruitment to delay antibody-mediated clearance of *Bordetella pertussis*. J Clin Invest, 2005. 115(12): p. 3594-601.
76. Andreasen, C. and N.H. Carbonetti, Pertussis toxin inhibits early chemokine production to delay neutrophil recruitment in response to *Bordetella pertussis* respiratory tract infection in mice. Infect Immun, 2008. 76(11): p. 5139-48.
77. McGuirk, P., C. McCann, and K.H. Mills, Pathogen-specific T regulatory 1 cells induced in the respiratory tract by a bacterial molecule that stimulates interleukin 10 production by dendritic cells: a novel strategy for evasion of protective T helper type 1 responses by *Bordetella pertussis*. J Exp Med, 2002. 195(2): p. 221-31.
78. Hozbor, D., *et al.*, Release of outer membrane vesicles from *Bordetella pertussis*. Curr Microbiol, 1999. 38(5): p. 273-8.
79. Kuehn, M.J. and N.C. Kesty, Bacterial outer membrane vesicles and the host-pathogen interaction. Genes Dev, 2005. 19(22): p. 2645-55.
80. Ellis, T.N. and M.J. Kuehn, Virulence and immunomodulatory roles of bacterial outer membrane vesicles. Microbiol Mol Biol Rev, 2010. 74(1): p. 81-94.
81. McGuirk, P., *et al.*, Compartmentalization of T cell responses following respiratory infection with *Bordetella pertussis*: hyporesponsiveness of lung T cells is associated with modulated expression of the co-stimulatory molecule CD28. Eur J Immunol, 1998. 28(1): p. 153-63.
82. Rodriguez, M.E., *et al.*, Fc receptor-mediated immunity against *Bordetella pertussis*. J Immunol, 2001. 167(11): p. 6545-51.
83. den Dunnen, J., S.I. Gringhuis, and T.B. Geijtenbeek, Innate signaling by the C-type lectin DC-SIGN dictates immune responses. Cancer Immunol Immunother, 2009. 58(7): p. 1149-57.
84. Dirix, V., *et al.*, Both CD4(+) and CD8(+) lymphocytes participate in the IFN-gamma response to filamentous hemagglutinin from *Bordetella pertussis* in infants, children, and adults. Clin Dev Immunol, 2012. 2012: p. 795958.
85. Aoki, N., *et al.*, Differential regulation of DAP12 and molecules associated with DAP12 during host responses to mycobacterial infection. Infect Immun, 2004. 72(5): p. 2477-83.
86. Nakano-Yokomizo, T., *et al.*, The immunoreceptor adapter protein DAP12 suppresses B lymphocyte-driven adaptive immune responses. J Exp Med, 2011. 208(8): p. 1661-71.
87. Hamerman, J.A., *et al.*, Cutting edge: inhibition of TLR and FcR responses in macrophages by triggering receptor expressed on myeloid cells (TREM)-2 and DAP12. J Immunol, 2006. 177(4): p. 2051-5.
88. Takagi, H., *et al.*, Plasmacytoid dendritic cells are crucial for the initiation of inflammation and T cell immunity in vivo. Immunity, 2011. 35(6): p. 958-71.
89. Borrego, F., The CD300 molecules: an emerging family of regulators of the immune system. Blood, 2013. 121(11): p. 1951-60.
90. Clark, G.J., *et al.*, The CD300 family of molecules are evolutionarily significant regulators of leukocyte functions. Trends Immunol, 2009. 30(5): p. 209-17.
91. Nimmerjahn, F. and J.V. Ravetch, Fc-receptors as regulators of immunity. Adv Immunol, 2007. 96: p. 179-204.
92. Afkarian, M., *et al.*, T-bet is a STAT1-induced regulator of IL-12R expression in naive CD4+ T cells. Nat Immunol, 2002. 3(6): p. 549-57.
93. Acosta-Rodriguez, E.V., *et al.*, Surface phenotype and antigenic specificity of human interleukin 17-producing T helper memory cells. Nat Immunol, 2007. 8(6): p. 639-46.
94. Liao, F., *et al.*, CC-chemokine receptor 6 is expressed on diverse memory subsets of T cells and determines responsiveness to macrophage inflammatory protein 3 alpha. J Immunol, 1999. 162(1): p. 186-94.
95. Molinero, L.L., *et al.*, T cell receptor/CARMA1/NF-kappaB signaling controls T-helper (Th) 17 differentiation. Proc Natl Acad Sci U S A, 2012. 109(45): p. 18529-34.
96. Kuwabara, T., *et al.*, CCR7 ligands are required for development of experimental autoimmune encephalomyelitis through generating IL-23-dependent Th17 cells. J Immunol, 2009. 183(4): p. 2513-21.
97. Barbic, J., *et al.*, Role of gamma interferon in natural clearance of *Bordetella pertussis* infection. Infect Immun, 1997. 65(12): p. 4904-8.
98. Khader, S.A., S.L. Gaffen, and J.K. Kolls, Th17 cells at the crossroads of innate and adaptive immunity against infectious diseases at the mucosa. Mucosal Immunol, 2009. 2(5): p. 403-11.
99. Fedele, G., *et al.*, Attenuated *Bordetella pertussis* vaccine candidate BPZE1 promotes human dendritic cell CCL21-induced migration and drives a Th1/Th17 response. J Immunol, 2011. 186(9): p. 5388-96.
100. Germann, T., *et al.*, Interleukin-12 profoundly up-regulates the synthesis of antigen-specific complement-fixing IgG2a, IgG2b and IgG3 antibody subclasses in vivo. Eur J Immunol, 1995. 25(3): p. 823-9.
101. Mitsdoerffer, M., *et al.*, Proinflammatory T helper type 17 cells are effective B-cell helpers. Proc Natl Acad Sci U S A, 2010. 107(32): p. 14292-7.
102. Norderhaug, I.N., *et al.*, Regulation of the formation and external transport of secretory immunoglobulins. Crit Rev Immunol, 1999. 19(5-6): p. 481-508.
103. Kaetzel, C.S., The polymeric immunoglobulin receptor: bridging innate and adaptive immune responses at mucosal surfaces. Immunol Rev, 2005. 206: p. 83-99.
104. Jaffar, Z., *et al.*, Cutting edge: lung mucosal Th17-mediated responses induce polymeric Ig receptor expression by the airway epithelium and elevate secretory IgA levels. J Immunol, 2009. 182(8): p. 4507-11.
105. van der Ark, A.A., *et al.*, Resurgence of pertussis calls for re-evaluation of pertussis animal models. Expert Rev Vaccines, 2012. 11(9): p. 1121-37.
106. Mielcarek, N., *et al.*, Live attenuated B. pertussis as a single-dose nasal vaccine against whooping cough. PLoS Pathog, 2006. 2(7): p. e65.
107. Bart, M.J., *et al.*, Comparative genomics of prevaccination and modern *Bordetella pertussis* strains. BMC Genomics, 2010. 11: p. 627.
108. Verwey, W.F., E.H. Thiele, and *et al.*, A simplified liquid culture medium for the growth of Hemophilus pertussis. J Bacteriol, 1949. 58(2): p. 127-34.
109. Pennings, J.L., *et al.*, Gene expression profiling in a mouse model identifies fetal liver- and placenta-derived potential biomarkers for Down Syndrome screening. PLoS One, 2011. 6(4): p. e18866.

110. Benjamini, Y. and Y. Hochberg, Controlling the false discovery rate: a practical and powerful approach to multiple testing. Journal of the Royal Statistical Society, 1995. 57(1): p. 289–300.
111. Huang da, W., B.T. Sherman, and R.A. Lempicki, Systematic and integrative analysis of large gene lists using DAVID bioinformatics resources. Nat Protoc, 2009. 4(1): p. 44-57.
112. Wu, C., *et al.*, BioGPS: an extensible and customizable portal for querying and organizing gene annotation resources. Genome Biol, 2009. 10(11): p. R130.
113. Lattin, J.E., *et al.*, Expression analysis of G Protein-Coupled Receptors in mouse macrophages. Immunome Res, 2008. 4: p. 5.
114. Zollinger, W.D., *et al.*, Design and evaluation in mice of a broadly protective meningococcal group B native outer membrane vesicle vaccine. Vaccine, 2010.
115. Stenger, R.M., *et al.*, Fast, antigen-saving multiplex immunoassay to determine levels and avidity of mouse serum antibodies to pertussis, diphtheria, and tetanus antigens. Clin Vaccine Immunol, 2011. 18(4): p. 595-603.
116. Hijnen, M., *et al.*, The *Bordetella pertussis* virulence factor P.69 pertactin retains its immunological properties after overproduction in *Escherichia coli*. Protein Expr Purif, 2005. 41(1): p. 106-12.
117. Raychaudhuri, S., J.M. Stuart, and R.B. Altman, Principal components analysis to summarize microarray experiments: application to sporulation time series. Pac Symp Biocomput, 2000: p. 455-66.

Supplementary information

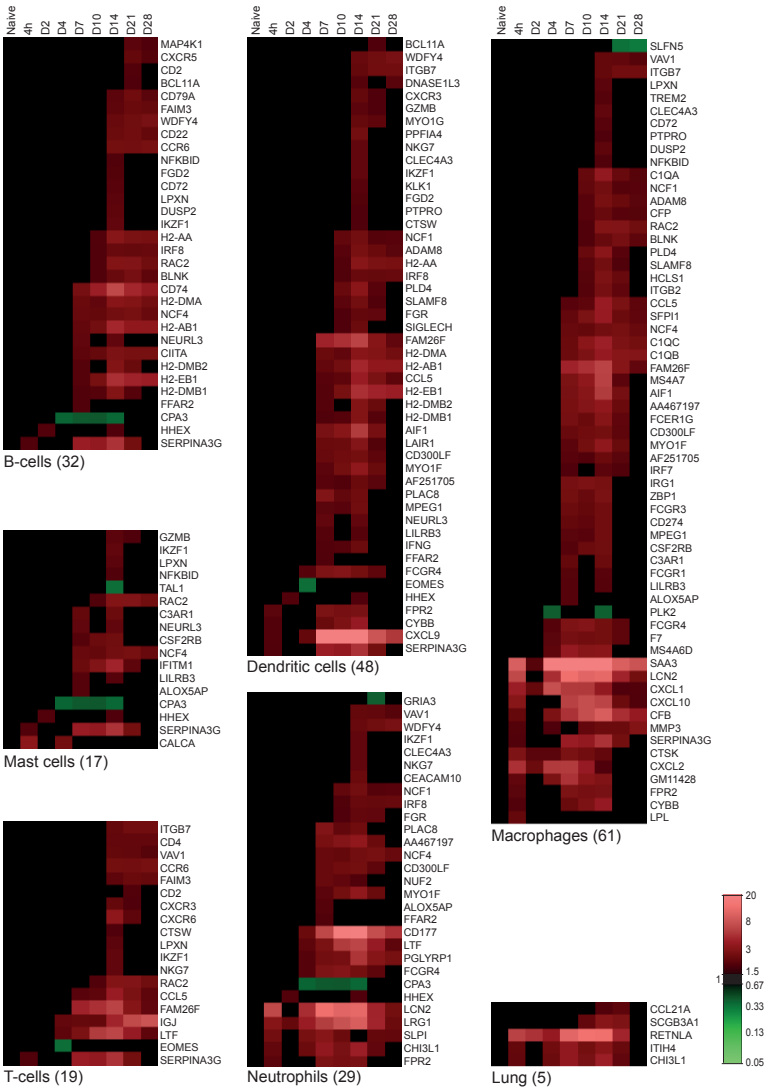

Figure S1 - Cell type comparison analysis for lung gene expression. Data (mean of n = 3) represent gene profiles in the lung per cell type or tissue extracted from BioGPS. Results from B-cells, mast cells, T-cells, dendritic cells, neutrophils, and lung-specific genes are depicted.

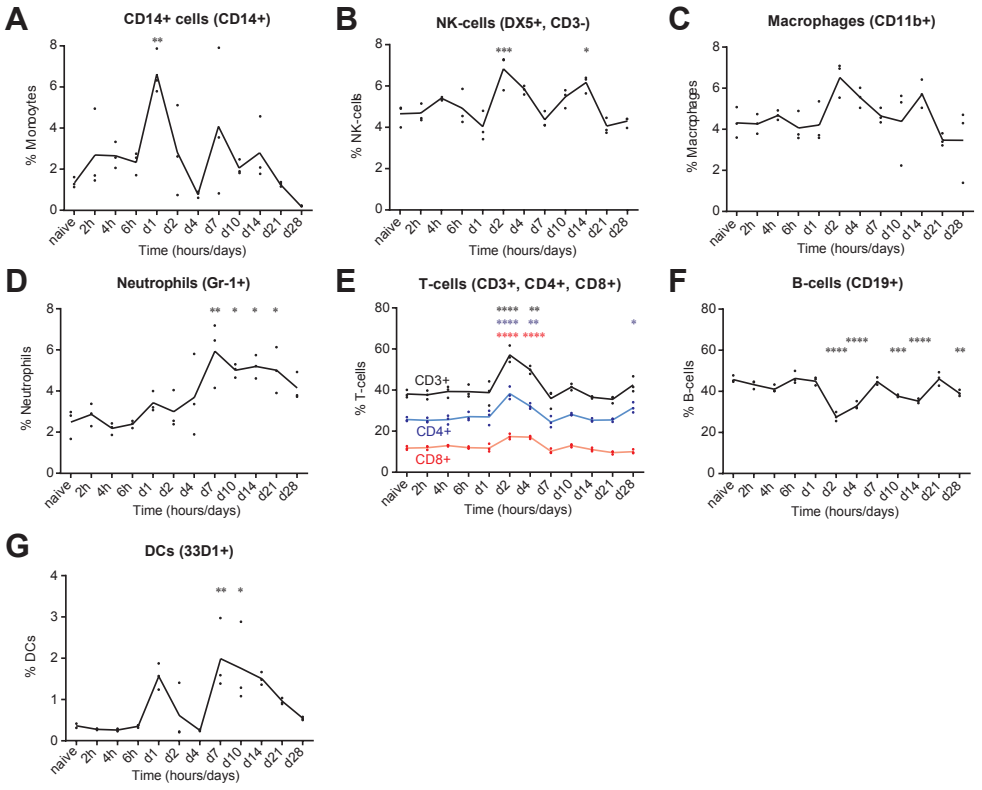

Figure S2 - Cellular composition of the spleen as function of time after *B. pertussis* infection. The percentage of **(A)** $CD14^+$ cells ($CD14^+$), **(B)** NK cells ($DX5^+$), **(C)** macrophages ($CD11b^+$), **(D)** neutrophils ($Gr\text{-}1^+$), **(E)** T-cells ($CD3^+$, $CD4^+CD8^-$, and $CD8^+CD4^-$), **(F)** B-cells ($CD19^+$), and **(G)** dendritic cells ($33D1^+$) in splenocytes were analyzed over time. *p*-values were determined by one-way ANOVA with multiple comparison compared to naive mice, * $p \leq 0.05$, ** $p \leq 0.01$, *** $p \leq 0.001$, and **** $p \leq 0.0001$ (mean of n = 3). An increased percentage of $CD14^+$ cells (monocytes, DCs and macrophages) was found 1 day p.i., followed by natural killer (NK) cells and macrophages at 2 days p.i. There was a gradual increase in the percentage of neutrophils in the spleen until 7 days p.i. Furthermore, an increased percentage of T-cells, distinguished by the CD3 marker, was found 2 and 4 days p.i. A similar increase was observed for both $CD4^+CD8^-$ and $CD8^+CD4^-$ T-cell subsets, indicating that this increase was not specific for either T helper or cytotoxic T-cells. The $CD4^+$ cells increased significantly 21 days p.i. and remained constant until at least 28 days p.i. B-cells decreased during two periods: 2-4 and 10-14 days p.i. Finally, a significant increase in percentage of DCs ($33D1^+$) was detected 7 days p.i.

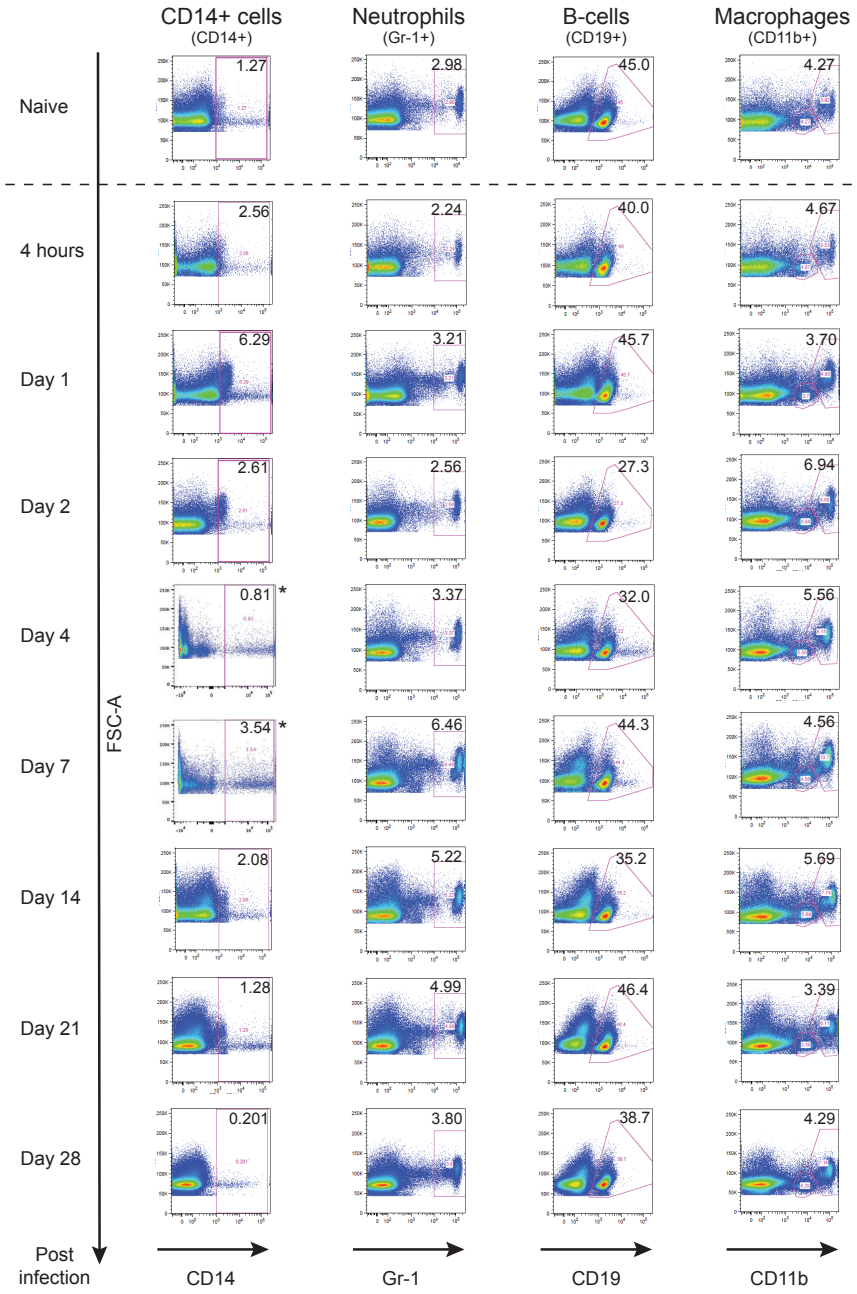

Figure S3 - Flow cytometric-gating strategy for CD14⁺, Gr-1⁺, CD19⁺, and CD11b⁺ cell population analysis in splenocytes. Each FACS plot shows results from one mouse of the group. Per cell type, the change in numbers of cells is visible over time for CD14⁺, Gr-1⁺, CD19⁺, and CD11b⁺ cell populations. Time points 2 hours, 6 hours and 10 days p.i. were excluded in this figure. (*) FACS plot for CD14⁺ cells at day 4 and day 7 p.i. were manually adapted by BiExponential transformation in FlowJo for better visualization without influencing the gating.

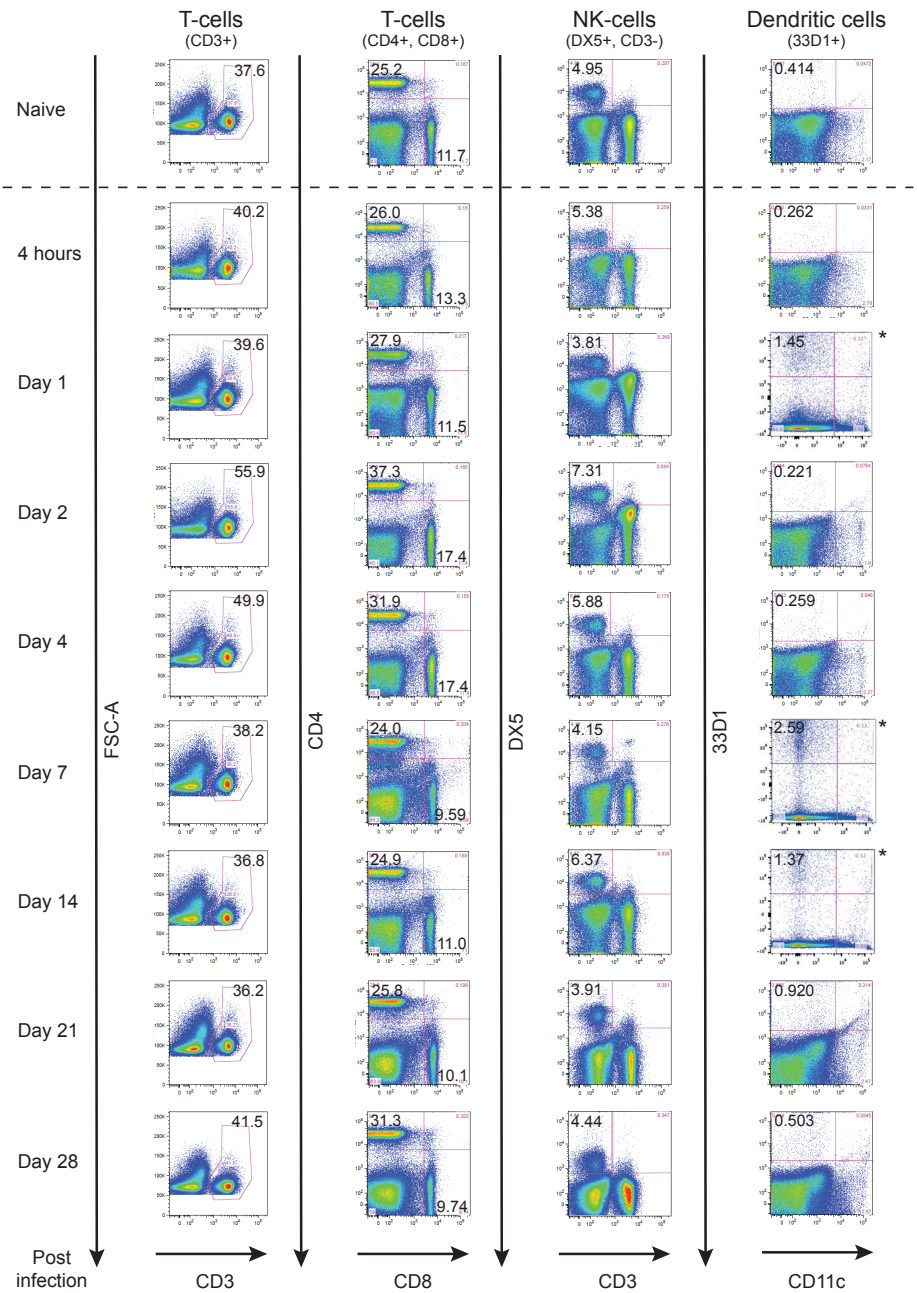

Figure S4 - Flow cytometric-gating strategy for CD3⁺, CD4⁺, CD8⁺, DX5⁺ and 33D1⁺ cell population analysis in splenocytes. Each FACS plot shows results from one mouse of the group. Per cell type, the change in numbers of cells is visible over time for CD3⁺, CD4⁺, CD8⁺, DX5⁺, and 33D1⁺ cell populations. Time points 2 hours, 6 hours, and 10 days p.i. were excluded in this figure. (*) FACS plot for 33D1⁺ cells at day 1, day 7, and day 14 p.i. were manually adapted by BiExponential transformation in FlowJo for better visualization without influencing the gating.

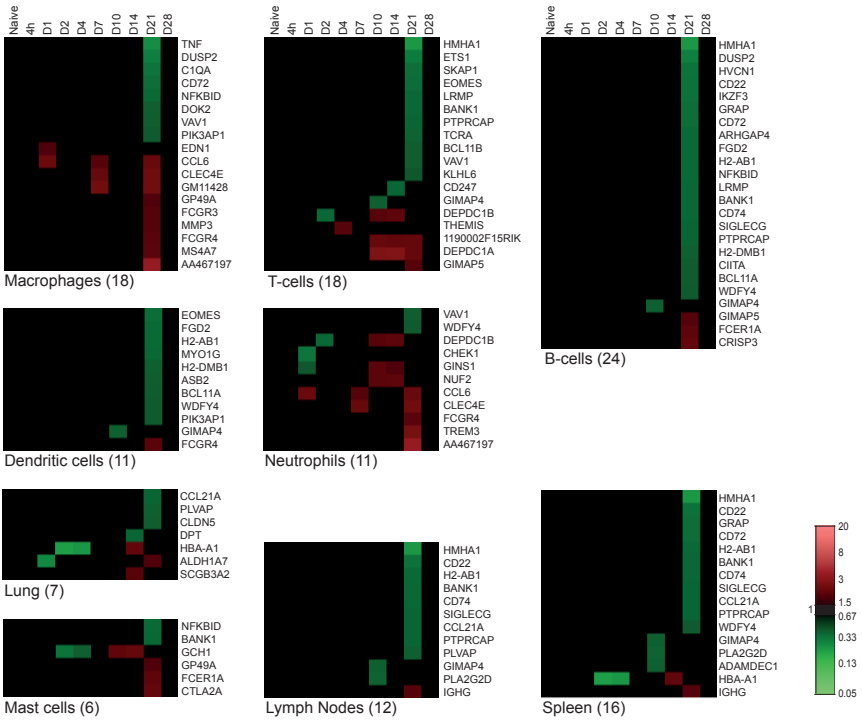

Figure S5 - Splenic gene expression profiles of cell types and tissues extracted from BioGPS databases. Data (mean of n = 3) represent gene profiles of the following cell types or tissues: B-cells, neutrophils, mast cells, T-cells, macrophages, dendritic cells (DCs), lung, lymph nodes, and spleen.

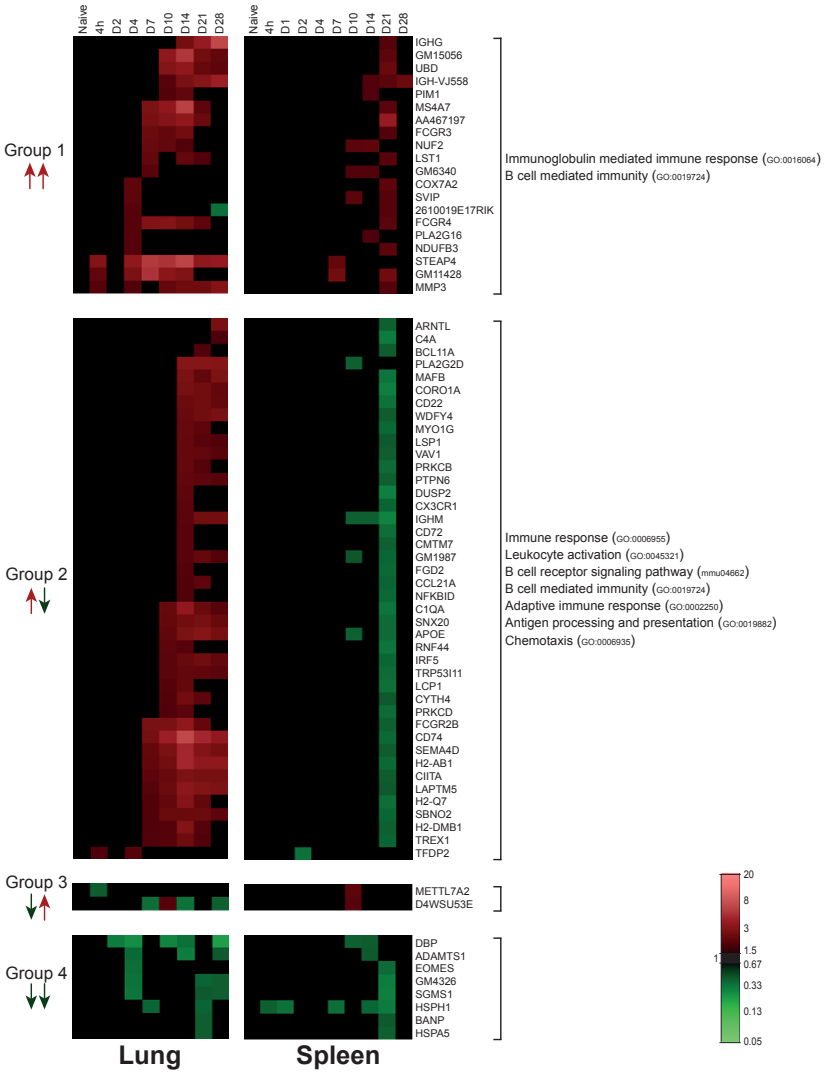

Figure S6 - Genes differentially regulated in both lung and spleen. Comparison of transcriptomic data in lung and spleen (mean of n = 3) revealed an overlap of 72 genes differentially regulated in both tissues. Genes divided in 4 groups based on expression pattern. Functional annotation showed that genes in group 2 were mostly involved in immunological processes.

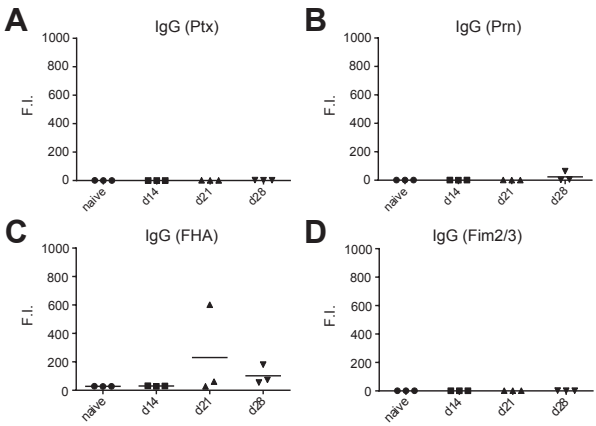

Figure S7 - IgG antibody response in serum against Ptx, Prn, FHA, and Fim2/3 after *B. pertussis* infection. IgG antibody titers against four purified *B. pertussis* antigens; **(A)** pertussis toxin (Ptx), **(B)** pertactin (Prn), **(C)** filamentous hemagglutinin (FHA), and **(D)** Fimbriae 2 and 3 (Fim2/3) were determined using a multiplex immunoassay (mean of n = 3). The antibody titers were determined in mouse sera 14, 21, and 28 days after an intranasal infection with *B. pertussis*. No antibodies were detected for Ptx, Prn, and Fim2/3. For FHA, 1 out of 3 mice showed induced titers antibody titers at 21 days p.i.

Table S1 - Full list of genes expressed in the lungs. This supplementary table can be found in the online version at http://journals.plos.org/plosone/article?id=10.1371/journal.pone.0104548. This table contains the full list of significantly expressed genes obtained by microarray analysis of the lungs, which can be used for additional in-depth information for each gene. In total 558 genes were significantly altered compared to naive mice. The expression pattern for each gene is given including the fold changes at each time point. In addition to the official gene symbol (obtained from the Nimblegen array), the full gene name, synonyms and gene ID are given. Synonyms are not given for all genes but only for genes that were included in detail in the manuscript. Gene ID is a linked to gene information on the NCBI website. Subsequently, there are three columns with gene information obtained in databases; (i) BioGPS, (ii) Gene Ontology - Biological Processes (GO-BP), (iii) KEGG pathways. Pull-down menus can be used to search for specific information in the full gene list. For BioGPS, information about cell and tissue specific gene expression is given for the following databases; B-cells (B), dendritic cells (DC), lung (Lu), lymph node (LN), mast cells (MC), macrophages (MF), neutrophils (N), spleen (Sp) and T-cells (T). For GO-BP the following biological processes were included; 'acute inflammatory response', 'acute-phase response', 'antigen processing and presentation', 'cell activation', 'chemotaxis', 'defense response', 'immune response', 'inflammatory response', 'intracellular signaling cascade', 'phagocytosis', 'regulation of apoptosis', 'response to bacterium', and 'transcription'. For KEGG the following pathways were included; 'Antigen processing and presentation', 'Apoptosis', 'B-cell receptor signaling pathway', 'Cell adhesion molecules (CAMs)', 'Chemokine signaling pathway', 'Complement and coagulation cascades', 'Cytokine-cytokine receptor interaction', 'Endocytosis', 'Leukocyte transendothelial migration', 'MAPK signaling pathway', 'NOD-like receptor signaling pathway', and 'Toll-like receptor signaling pathway'.

Table S2 - Full list of genes expressed in the spleen. This supplementary table can be found in the online version at http://journals.plos.org/plosone/article?id=10.1371/journal.pone.0104548. This table contains the full list of significantly expressed genes obtained by microarray analysis of the spleen, which can be used for additional in-depth information for each gene. In total, 798 genes were significantly altered compared to naive mice. The expression pattern for each gene is given including the fold changes at each time point. In addition to the official gene symbol (obtained from the Nimblegen array), the full gene name, synonyms and gene ID are given. Synonyms are not given for all genes but only for genes that were included in detail in the manuscript. Gene ID is a linked to gene information on the NCBI website. Subsequently, there are three columns with gene information obtained in databases; (i) BioGPS, (ii) Gene Ontology – Biological Processes (GO-BP), (iii) KEGG pathways. Pull-down menus can be used to search for specific information in the full gene list. For BioGPS, information about cell and tissue specific gene expression is given for the following databases; B-cells (B), dendritic cells (DC), lung (Lu), lymph node (LN), mast cells (MC), macrophages (MF), neutrophils (N), spleen (Sp) and T-cells (T). For GO-BP the following biological processes were included; 'acute inflammatory response', 'antigen processing and presentation', 'cell activation', 'chemotaxis', 'chromatin assembly', 'defense response', 'hemopoiesis', 'immune response', 'inflammatory response', 'intracellular signaling cascade', 'regulation of apoptosis', 'response to bacterium' and 'transcription'. For KEGG the following pathways were included; 'Antigen processing and presentation', 'Apoptosis', 'B-cell receptor signaling pathway', 'Cell adhesion molecules (CAMs)', 'Chemokine signaling pathway', 'Complement and coagulation cascades', 'Cytokine-cytokine receptor interaction', 'Endocytosis', 'Leukocyte transendothelial migration', 'MAPK signaling pathway', 'NOD-like receptor signaling pathway' and 'Toll-like receptor signaling pathway'.

About the cover: Ha Long Bay ("Descending dragon bay"). Located in Vietnam with approximately 2,000 limestone islands and part of the UNESCO World Heritage list.

CHAPTER 3

Immunological signatures after *Bordetella pertussis* infection demonstrate importance of pulmonary innate immune cells

René H.M. Raeven[1,2], Jolanda Brummelman[3], Larissa van der Maas[1], Wichard Tilstra[1], Jeroen L.A. Pennings[4], Wanda G.H. Han[3], Cécile A.C.M. van Els[3], Elly van Riet[1], Gideon F.A. Kersten[1,2], Bernard Metz[1]

[1]Intravacc, Bilthoven, The Netherlands
[2]Division of Drug Delivery Technology, Leiden Academic Centre for Drug Research, Leiden, The Netherlands
[3]Centre for Infectious Disease Control, National Institute for Public Health and the Environment (RIVM), Bilthoven, The Netherlands
[4]Centre for Health Protection (GZB), National Institute for Public Health and the Environment (RIVM), Bilthoven, The Netherlands

Submitted for publication

Abstract

Effective immunity against *Bordetella pertussis* is currently under discussion following the stacking evidence of pertussis resurgence in the vaccinated population. Natural immunity is more effective than vaccine-induced immunity. This indicates that much is still to be learnt from infection-induced immune memory and the mechanisms at work during the control of challenge inoculum to improve vaccination strategies. We applied a systems biology approach comprising microarray, flow cytometry and multiplex immunoassays to unravel the molecular and cellular signatures in unprotected mice and protected mice with infection-induced immunity, around a *B. pertussis* challenge. Pre-existing systemic memory Th1/Th17 cells, memory B-cells, and mucosal IgA specific for Ptx, Vag8, Fim2/3 were detected in the protected mice 56 days after an experimental infection. In addition, pre-existing high activity and reactivation of pulmonary innate cells such as alveolar macrophages, M-cells and goblet cells was detected. The pro-inflammatory responses in the lungs and serum, and neutrophil recruitment in the spleen upon an infectious challenge of unprotected mice were absent in protected mice. Instead, fast pulmonary immune responses in protected mice led to efficient bacterial clearance and harbored potential new gene markers that contribute to immunity against *B. pertussis*. These responses comprised of innate makers, such as *Clca3, Retlna, Glycam1, Gp2,* and *Umod*, next to adaptive markers, such as CCR6^{+} B-cells, CCR6^{+} Th17 cells and CXCR6^{+} T-cells as demonstrated by transcriptome analysis. In conclusion, besides effective Th1/Th17 and mucosal IgA responses, the primary infection-induced immunity benefits from activation of pulmonary resident innate immune cells, achieved by local pathogen-recognition. These molecular signatures of primary infection-induced immunity provided potential markers to improve vaccine-induced immunity against *B. pertussis*.

Introduction

The resurgence of pertussis in the vaccinated population prompts the necessity of more knowledge on effective immunity against *Bordetella pertussis* [1, 2]. This global health problem occurs after vaccination with acellular pertussis vaccines (aPV) and whole-cell pertussis vaccines (wPV) as recent data point out [3]. aPV-vaccinated individuals face waning immunity early after vaccination, since the vaccine-induced immunity lasts for only 4-12 years [4, 5] despite multiple booster vaccinations [6]. Moreover, research in baboons revealed that aPV-vaccinated animals are protected against disease, but still harbor viable bacteria resulting in continuation of pathogen transmission [7]. These findings indicate that even aPV-vaccinated individuals may act as an important resource for the transmission of *B. pertussis* [8, 9]. Hence, the present situation necessitates the reevaluation of pertussis immunity and vaccination strategies.

The immunity induced by a *B. pertussis* infection may provide crucial information for improving vaccine-induced immunity, since it provides important advantages compared to immunity induced by aPV or wPV. Infection-induced immunity continues for a longer period [4, 5] and it leads to sterilizing immunity in mice and baboons [7, 10]. Infection as well as aPV and wPV vaccination induces strong systemic responses, but infection induces a mucosal immune response at the site of pathogen entry in addition. As others and we recently showed, this immunity includes pulmonary IgA, systemic IgG [10] and specific Th1/Th17 responses [10-12]. The lungs are naturally exposed to pathogens and therefore equipped with a large number of immune cells and an epithelial layer. The lung epithelial cells offer a first line of defense by secretion of anti-microbial peptides and pathogen recognition, but also by interaction with the local innate immune cells [13]. These innate immune cells include mucin-secreting goblet cells [14], alveolar macrophages [15] and the upper layer of the bronchus-associated lymphoid tissue (BALT) [16], that act in the same way as microfold (M)-cells [17], harbor functions, such as pathogen recognition and antigen-uptake. These pulmonary innate cells orchestrate the specific adaptive immune responses, such as mucosal IgA production and activation of tissue-resident B-cells and T-cells in the BALT [16].

In this study, we further explored the molecular and cellular events underlying infection-induced protective immune responses. To this end, pulmonary transcriptomic profiles were characterized around the challenge of mice protected by primary infection-induced immunity, in comparison to events in unprotected counterparts. Additionally, pulmonary and systemic cytokine profiles as well as cellular and antibody mediated immune responses against *B. pertussis* were studied. Markers for pulmonary immunity included both trained innate and adaptive signatures. M-cells, alveolar macrophages and epithelial cells characterized the former, and $CCR6^+$ B-cells, $CCR6^+$ Th17 cells, $CXCR6^+$ T-cells and mucosal IgA the latter. These

extensive insights into the signatures of infection-induced immunity involving important pulmonary components may be used for the development of improved pertussis vaccines with long lasting immunity.

Results

Pre-existing immunological signatures in protected mice before *B. pertussis* challenge.

Recovery from a *B. pertussis* infection in BALB/c mice is associated with sterilizing immunity. A challenge with *B. pertussis* bacteria showed that the lungs were cleared within two days in these protected mice, whereas this takes approximately 28 days in unprotected mice [10]. To understand infection-induced protection in more detail we designed a systems biology approach to study pre- and post-challenge immune responses in unprotected and

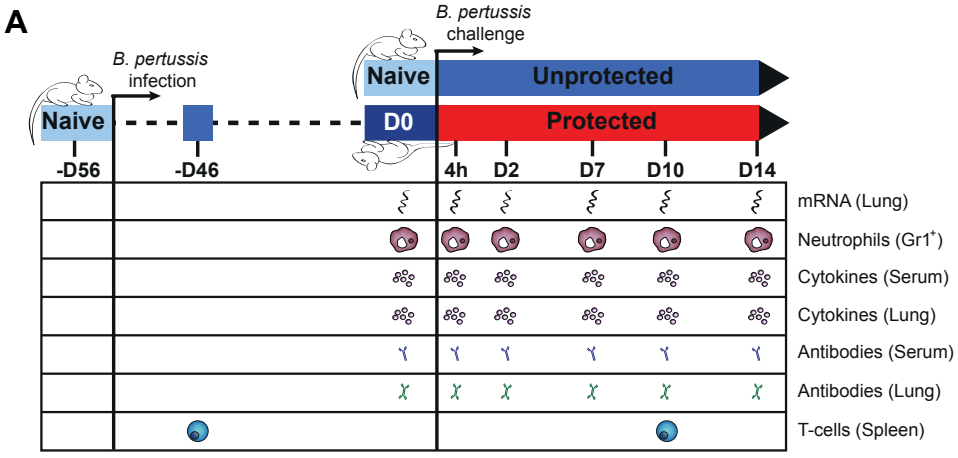

B

Study parameter	Unprotected	Protected	Source
Lung clearance	≥ 28 days	≤ 2 days	Raeven *et al.* 2014
Systemic Th subset	-	Th1/Th17	Raeven *et al.* 2014 Figure 8
Serum IgG	-	++	Figure 7
Mucosal IgA	-	++	Figure 7
Pulmonary transcriptomics	basal	320 genes	Figure 2

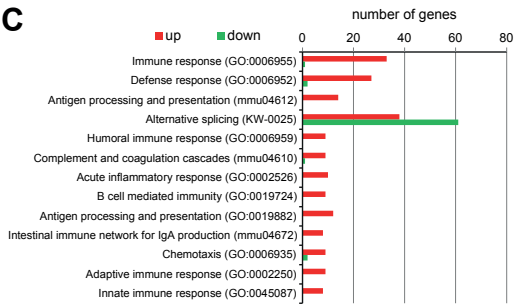

Figure 1 - Design and baseline parameters of a *B. pertussis* challenge model in protected and naive unprotected mice. **(A)** Schematic diagram of animal pre-treatment, sacrifice, sampling and systems analysis on 4 hours and 2, 7, 10 and 14 days p.c. in a *B. pertussis* challenge model in protected and unprotected BALB/c mice. Pulmonary transcriptomic profile, percentage of splenic $Gr1^+$ cells (neutrophils), serum and lung cytokine profiles, serum and lung antibody profiles, and specific splenic $CD4^+CD44^+$ T-cells were assessed at the given time points in protected and unprotected mice. **(B)** Study parameters at baseline (D0) of naive unprotected mice and protected mice, 56 days after primary infection, including time frames of lung clearance, systemic T-helper subsets, serum IgG profile, mucosal IgA, and pulmonary transcriptomic profile as obtained from data in the current study and data adapted from our previous study [10]. 320 genes are differential expressed in protected mice compared to naive (D0 unprotected) mice. **(C)** An overrepresentation analysis was performed using DAVID for Keywords, KEGG-pathways, and gene ontology biological pathways (GO-BP) to determine the function of the 320 genes. For each term, the number of upregulated (red) and downregulated (green) genes are depicted.

protected mice, recovered from a primary infection received 56 days before (**Figure 1A**). Before the receiving the challenge inoculum (D0), protected mice showed enhanced levels of *B. pertussis*-specific serum IgG, mucosal IgA in the lungs, and Th1/Th17 cells in the spleen, which were absent in naive (D0 unprotected) mice (**Figure 1B**). When comparing levels of pulmonary gene expression, 320 genes were still differentially expressed, mostly upregulated, in the lungs of protected compared to naive (D0 unprotected) mice. An overrepresentation analysis (ORA) was performed using DAVID [18] to ascribe the functional group to which the 320 corresponding proteins belong (**Figure 1C**). The data analysis indicated that the pulmonary gene expression of protected mice was enriched with 33 and 27 genes involved in immune response and defense response, respectively. Upregulated genes were further involved in antigen processing, the innate response and several terms indicating B-cell mediated immunity. Notably, a large number of both downregulated and upregulated genes were related to alternative splicing. In conclusion, these results indicated that the protected mice with infection-induced immunity contain a large variety of adaptive and additionally still some innate markers to resist a new *B. pertussis* challenge as compared to their unprotected naive counterparts.

Pulmonary transcriptome of protected and unprotected mice receiving a *B. pertussis* challenge.

To gain more insight into gene transcription patterns associated with fast clearance of *B. pertussis* and protection, we subsequently assessed the pulmonary transcriptome over a period of 14 days post challenge (p.c.) in protected and post infection (p.i.) in unprotected mice in comparison to naive non-challenged mice (unprotected D0) (**Figure 2A**). In total, 786 genes were differentially regulated (p-value ≤ 0.001, fold ratio (FR) ≥ 1.5). These genes were divided in six clusters (I - VI) based on differential expression in unprotected and protected mice (**Figure 2**). Cluster I: differential expression in unprotected mice, absent in protected mice; cluster II: differential expression in both unprotected mice and protected mice; cluster III: differential expression in unprotected mice and in protected mice pre- or post-challenge; cluster IV: differential expression in unprotected mice and additional differential expression post-challenge in protected mice; cluster V: absent in unprotected mice but differential expression in protected mice; cluster VI: absent in unprotected mice but differential expression pre- and post-challenge in protected mice.

The individual fold ratios (FR) of 786 differentially expressed genes were plotted for each time point after being analyzed in protected and unprotected mice (**Figure S1A**). Before the challenge (D0), already 320 genes were differentially regulated in the protected mice if compared to the unprotected mice. Furthermore, this analysis revealed that on 2 days p.c. the largest number of genes was differentially expressed between both groups, namely 212 genes of which 108 genes were upregulated and 104 were downregulated. Since the sterilizing immunity of protected mice resulted in *B. pertussis* clearance within 2 days p.c.

[10], signatures underlying this immunity could be detected on 2 days p.c. in protected mice. Therefore, the transcriptomic profiles of the 786 genes were investigated in detail on 2 days p.c. (Figure 2B). Subsequent to the comparison of both datasets to naive mice, the fold ratios of each gene was calculated between the datasets of unprotected versus protected mice obtained 2 days p.c. (FR ≥ 1.5 or ≤ 0.67, red triangles) (Figure 2B). The scatter plot was divided

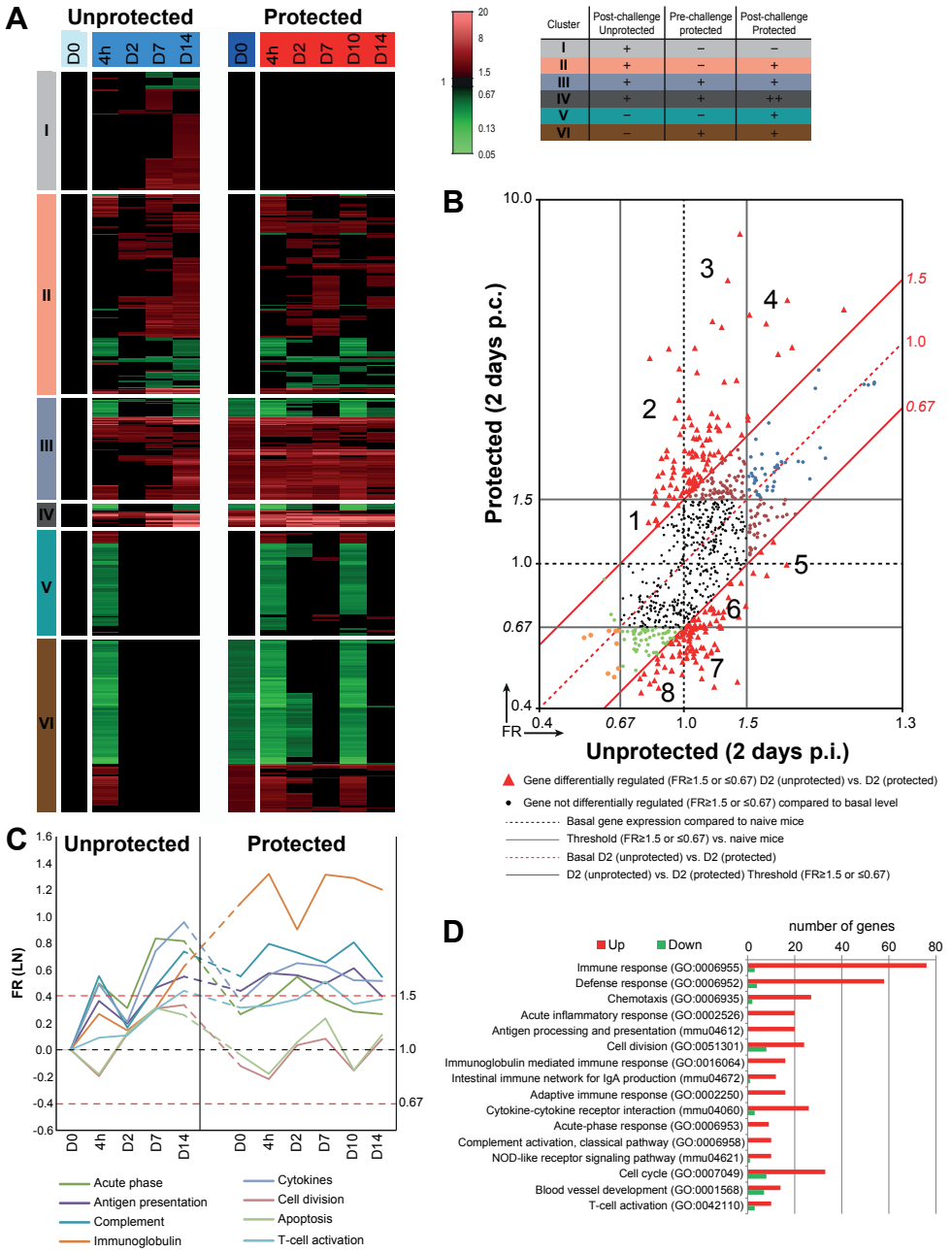

in eight different fractions that were significantly upregulated (1-4) or downregulated (5-8) in protected mice compared to unprotected mice 2 days p.c. The genes of these fractions were shown as heatmaps (**Figure S1B**). Many genes are involved in innate (e.g. *A2m, Saa3, C3, Reg3g, Umod*) and adaptive (e.g. *Cd4, Ighg, Cxcr6, Ccr6, Cd22*) immune responses were upregulated in protected mice.

An ORA for KEGG pathways and GO-BP terms was performed on all 786 genes. In total, 97 terms were enriched (Benjamini ≤ 0.05). The number of upregulated and downregulated genes and the kinetics for a subset of these terms was determined (**Figure 2C-D**). Enriched terms contained genes involved in immune response (79 genes) including innate immune functions such as acute phase (9 genes), antigen presentation (20 genes), chemotaxis (29 genes), and pathogen recognition through the NOD-like receptor (11 genes). Moreover, terms incorporated in the adaptive immune response (16 genes) involved antibody response (16 genes), IgA responses (13 genes) and T-cell activation (13 genes) (**Figure 2D**). The expression kinetics were determined by averaging the FR for each time point for a selection of these enriched terms (**Figure 2C**). This analysis showed that post-challenge in protected mice the immunoglobulin-mediated immune response remained high (4h-D14). The complement response, antigen-presentation, and T-cell activation were still moderately enhanced in protected mice. Furthermore, genes belonging to acute phase, cytokine responses, apoptosis and cell division were expressed to a lesser extent upon challenge in protected mice than in unprotected mice.

Figure 2 (Left) - Pulmonary gene expression profiles in protected and unprotected mice following a *B. pertussis* challenge. **(A)** Fold changes in gene expression of both unprotected and protected mice were calculated compared to naive mice (D0 unprotected). The expression results (FR ≥ 1.5, *p*-value ≤ 0.001) are visualized as heatmap (mean of n = 3). Genes not exceeding a fold change of 1.5 are depicted as basal level (black) at this time point. In total, 786 genes were found to be differentially regulated. Genes were divided in six clusters (I-VI) based on their expression profiles (color coding for these clusters is depicted in an additional table): cluster I (Differential expression in unprotected mice, absent in protected mice), Cluster II (Differential expression in unprotected mice and protected mice), Cluster III (Differential expression in unprotected mice and in protected mice before and after challenge), Cluster IV (Differential expression in unprotected mice and additional differential expression as result of challenge in protected mice), Cluster V (Absent in unprotected mice but differential expression in protected mice) and Cluster VI (absent in unprotected mice but differential expression pre- and post-challenge in protected mice). **(B)** Transcriptomic profiles obtained on 2 days p.i. in unprotected and 2 days p.c. protected mice were compared by plotting all 786 genes in a scatter plot and divide the genes in different fractions based on co-expression. The black solid lines are the thresholds for the significant FR (FR ≥ 1.5 or ≤ 0.67) compared to naive mice (D0 unprotected) for both unprotected and protected mice. Black dots represent genes that are not significantly regulated compared to naive mice (D0 unprotected) in both groups. The red solid lines represent the threshold for the significant FR (FR ≥ 1.5 or ≤ 0.67) of both unprotected 2 days p.i. and protected mice 2 days p.c. All red triangles represent genes that show significant differential expression (FR ≥ 1.5 or ≤ 0.67) between unprotected 2 days p.i. and protected mice 2 days p.c. In total, 212 genes were differentially expressed between both groups of which 108 genes were upregulated and 104 were downregulated. These genes were divided in eight fractions that are significantly up-regulated (1-4) or downregulated (5-8) in protected mice compared to unprotected mice and are further specified as heatmaps in **Figure S1B**. Dots with other colors (orange, green, brown, and blue) represent genes that are significantly regulated in unprotected and/or protected mice compared to naive mice (D0 unprotected) but these genes are not differentially regulated between unprotected 2 days p.i. and protected mice 2 days p.c. **(C-D)** A selection of eight terms (KEGG-pathways and GO-BP terms) found enriched in the ORA of the 786 genes and the kinetics over time of indicated terms is depicted. **(C)** Kinetics was determined by averaging the FR for each term at each time point and is expressed on LN-scale. **(D)** For each enriched term, the Benjamini score and the number of upregulated (red) and downregulated (green) genes in the protected mice and unprotected mice is shown.

While the ORA gave an insight in several functions involved upon challenge of protected as well as unprotected mice, a large number of genes that were differentially regulated in our dataset were not annotated. To obtain in depth information on the function of these genes, we performed additional text mining on all individual genes using BioGPS, GeneRifs, and the literature (Pubmed). Based on this information, selected genes could be grouped according to function such as T-cell-related responses, B-cell-related responses, membrane receptors and secreted proteins, as is described in more detail hereafter.

Gene expression of membrane receptors and secreted proteins

The gene expression profiles of membrane receptors and secreted proteins indicated the involvement of specific cell types and biological processes. Therefore, the expression of all genes encoding for membrane proteins and secreted proteins was further investigated (**Figure 3**) and divided in four groups (Group A-D), based on their involvement during the first two days following challenge.

Genes in group A were mainly upregulated in unprotected mice 7-14 days p.i., but unaltered in protected mice. Therefore, this gene expression is essential for a first encounter with *B. pertussis*, but it is not required for protected mice. In group A, membrane marker genes were in general related to myeloid cells (*Cd300lf, Fcgr4, Gp49a, Cd200r1, Cd302, Lair1, Sirpb1a*). Other membrane marker genes are specific, for example for neutrophils (*Cxcr2, Fpr1, Fpr2*) or for macrophages, such as *Il1rn*, killer-cell lectin-like receptors (*Klra2, Klra17*), C-type lectins (*Clec4a2, Clec4a3, Clec4b1, Clec4d*) and membrane-spanning four-domains, subfamily A (*Ms4a6c, Ms4a6d, Ms4a4a, Ms4a4c*). Moreover, the expression of *Cd1d1* and *Cd1d2*, involved in MHC Class I antigen presentation, *C3ar1* (APCs, Macrophages, T-cell activation), *Clmp* (cell-cell adhesion molecule), and *Chl1* was only upregulated in unprotected mice. In addition, expression of some T-cell-related genes (*Art2b, Cd48*) were found. *Art2b* is constitutively expressed on T-cells, whereas *Cd48* is expressed on multiple immune cells playing a major role in T-cell activation. Finally, podoplanin (*Pdpn*) which is a lung injury marker and serves as a $CD4^+$ effector T-cell inhibitor [19], was only expressed in unprotected mice. Among the genes encoding secreted proteins, expression of a number of acute inflammatory genes was altered in unprotected mice (*Cp, Fn1, Il1a, Il1b, Il6, Ptx3, Saa1, S100a9, S100a8*), but not in protected mice. Some genes are involved in blood vessel formation (*Fn1, Vegfc, Vegfd*) or LPS-binding (*Crispld2*). Furthermore, the genes of a Th17-specific cytokine (*Il17f*), and mucosal chemokines attracting IgA plasmablasts (*Ccl28*) and $CCR7^+$ lymphocytes (*Ccl21b*) were only upregulated in unprotected mice.

The genes in group B were not expressed until 7 days p.i. in unprotected mice. However, in protected mice, these genes were already upregulated between 4 hours and 2 days p.c. Here, higher activity of microfold cells (M-cells) was suggested by enhanced gene expression of *Gp2* and *Umod*. Moreover, macrophage-related genes (*Basp1, Mpeg1, Ms4a7*), innate-specific receptors such as Fc-receptors (*Fcgr2b, Fcer1g, Fcgr3*) and genes important for function

of multiple innate cells (*Fnbp1, Parm1, Cdhr1*) were expressed earlier in protected mice. Additionally, gene expression of membrane markers (*Vcam1, Cd22, Cd72, Cd4, Cd3g, Cxcr6, Ccr6, Art2a-ps*) demonstrated earlier adhesion of immune cells in the lungs of protected mice. It indicated early presence of adaptive immune cells such as B-cells (*Cd22, Cd72, Ccr6*) and T-cells (*Cd4, Cd3g, Cxcr6, Ccr6, Art2a-ps*). In total, 16 genes encoding secreted proteins were still upregulated in protected mice before challenge, whereas seven genes were reactivated following the challenge. These genes included many chemoattractants (*Ccl8, Cxcl9, Cxcl12, Cxcl13, Ccl19, Glycam1, Gm12407, Gm2023, Gm1987*). Some genes are associated with attracting specific cells, such as B-cells (*Cxcl13*), $CXCR4^+$ lymphocytes (*Cxcl12*), $CCR7^+$ lymphocytes (*Ccl19*), $CD62l^+$ lymphocytes (*Glycam1*), $CXCR3^+$ T-cells (*Cxcl9*), and $CCR5^+$ cells (*Ccl8*). In addition, upregulation was detected for genes associated with antibodies (*Ighg*), complement (*C1qa, C1qb, C1qc*), activated macrophages (*Aif1*), Peyer's patches (*Pglyrp1*), matrix metalloproteinases (*Mmp3, Mmp12*) and an MMP inhibitor (*Timp4*), increased mucus production by goblet cells (*Agr2, Clca1, Clca3, Clca4*) and genes related to lipid metabolism (*Apod, Pla2g2d*). Expression of *Pla2g2d* in DCs and macrophages is related to induction of anti-inflammatory lipid mediators [20].

Most genes in group C were upregulated early (4 hours) after challenge in protected and unprotected mice. Analyzing the membrane markers, the expression of 12 genes was still upregulated prior to the challenge of protected mice, while the other 13 genes were reactivated post-challenge. The membrane marker genes in group C included a neutrophil specific marker (*Cd177*), for which the expression was earlier and more intense in protected mice. A similar observation was found for *Pigr*, which traffics IgA across the epithelial barrier. The C-type lectins (*Clec4e, Clec4n*), found on DCs, were detected in unprotected mice till 7 days p.i., but were only expressed in protected mice 4 hours p.c. The early expression of *Cd14* suggests LPS binding in both protected and unprotected mice, whereas *Tlr2* is involved in pathogen recognition. Additionally, markers for antigen presentation (*Cd74, H2-d1*), macrophages (*Msr1*), regulation of anti-inflammatory activities in murine airways (*Adam8*) [21], epithelial cells (*Pigr, Rab11b, Retnla*), DCs (*Cd209f*), and the endothelial marker *Plvap*, which enables lymphocytes to enter the lungs [22], were detected in this group of genes. Among the genes encoding secreted proteins, a selection of acute phase genes (*Saa3, Reg3g, Lcn2*) were highly upregulated in protected and unprotected mice. However, the expression went down after 2 days p.c. whereas this continued in unprotected mice. In protected mice, *Cxcl5* remained highly upregulated while *Cxcl1*, *Cxcl2*, and *Cxcl3* were expressed for a limited amount of time. The chemokines encoded by *Cxcl1*, *Cxcl2*, *Cxcl3* and *Cxcl5* are involved in $CXCR2^+$ leukocyte recruitment. Expression of *Ccl20*, the chemokine attracting $CCR6^+$ cells, was increased more intensely in protected mice than in unprotected mice. In addition, genes involved in the complement system (*Cfb, C3, C4b*), cytokine expression (*Ccl2, Ccl7, Ccl17, Cxcl17*), mucosal tissue repair (*Tff2*), epithelial cells (*Cyr61*), and mast cells (*5730469M10RIK / Fam213a*) were observed in both groups.

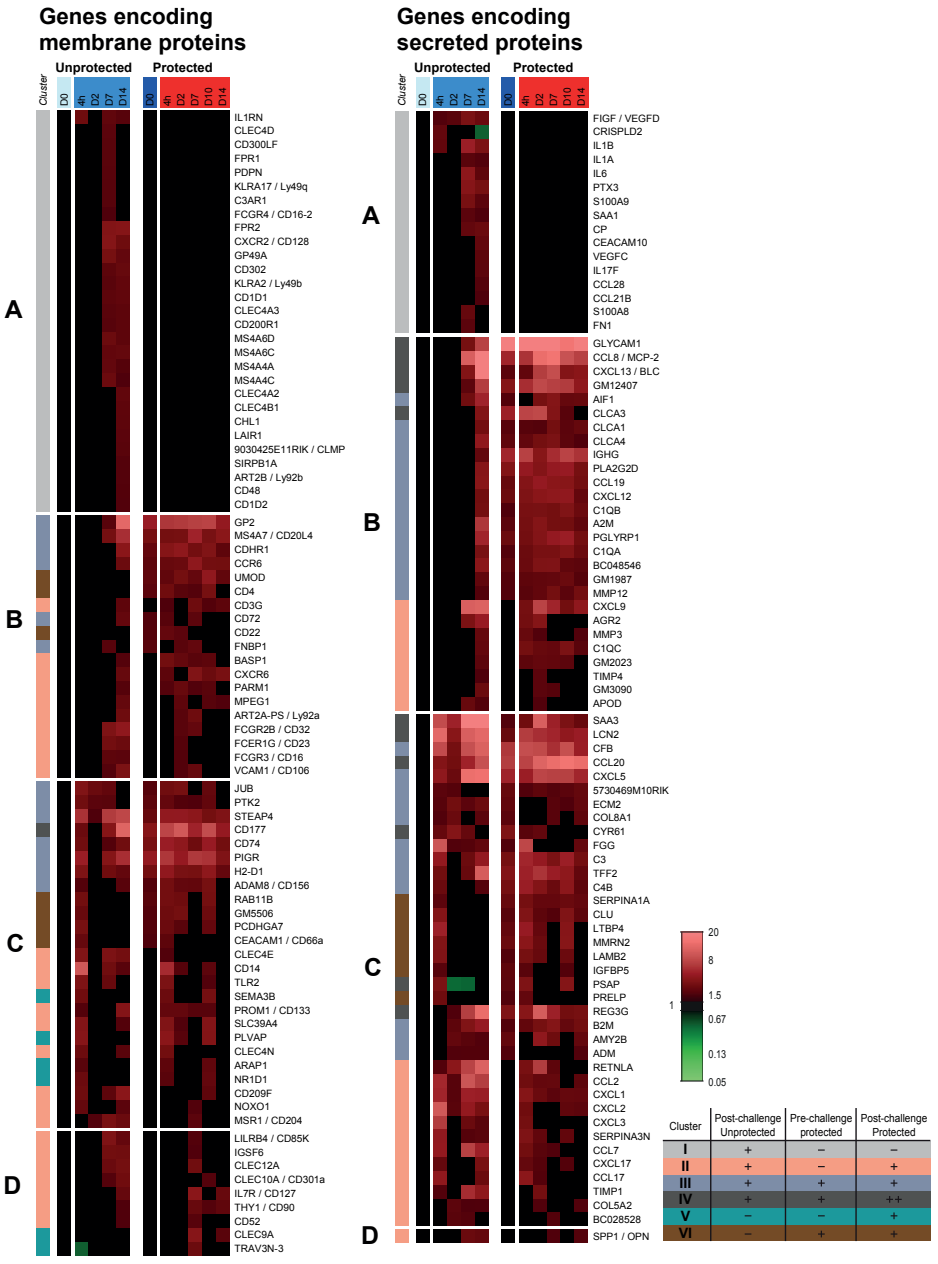

Figure 3 - Pulmonary gene expression profiles of membrane proteins and secreted proteins in protected and unprotected mice following *B. pertussis* challenge. Expression profiles of genes in the lungs encoding membrane proteins (left panel) and secreted proteins (right panel) were selected according to GO-BP terms, KEGG pathways and text mining. Each list is divided in four groups (A-D) based on their expression profile on 4 hours and 2 days p.c. Group A contains genes that are significantly upregulated in unprotected mice, but unaltered in protected mice. Group B covers genes that are not upregulated on 4 hours and 2 days p.i. in unprotected mice, but are directly activated in protected mice. Group C comprehends genes that are upregulated on 4 hours and/or 2 days p.c. in both protected and unprotected mice. Group D includes genes that are significantly regulated from 7 days p.c. in both protected and unprotected mice. In addition, the color codes of the six clusters from **Figure 2** are added.

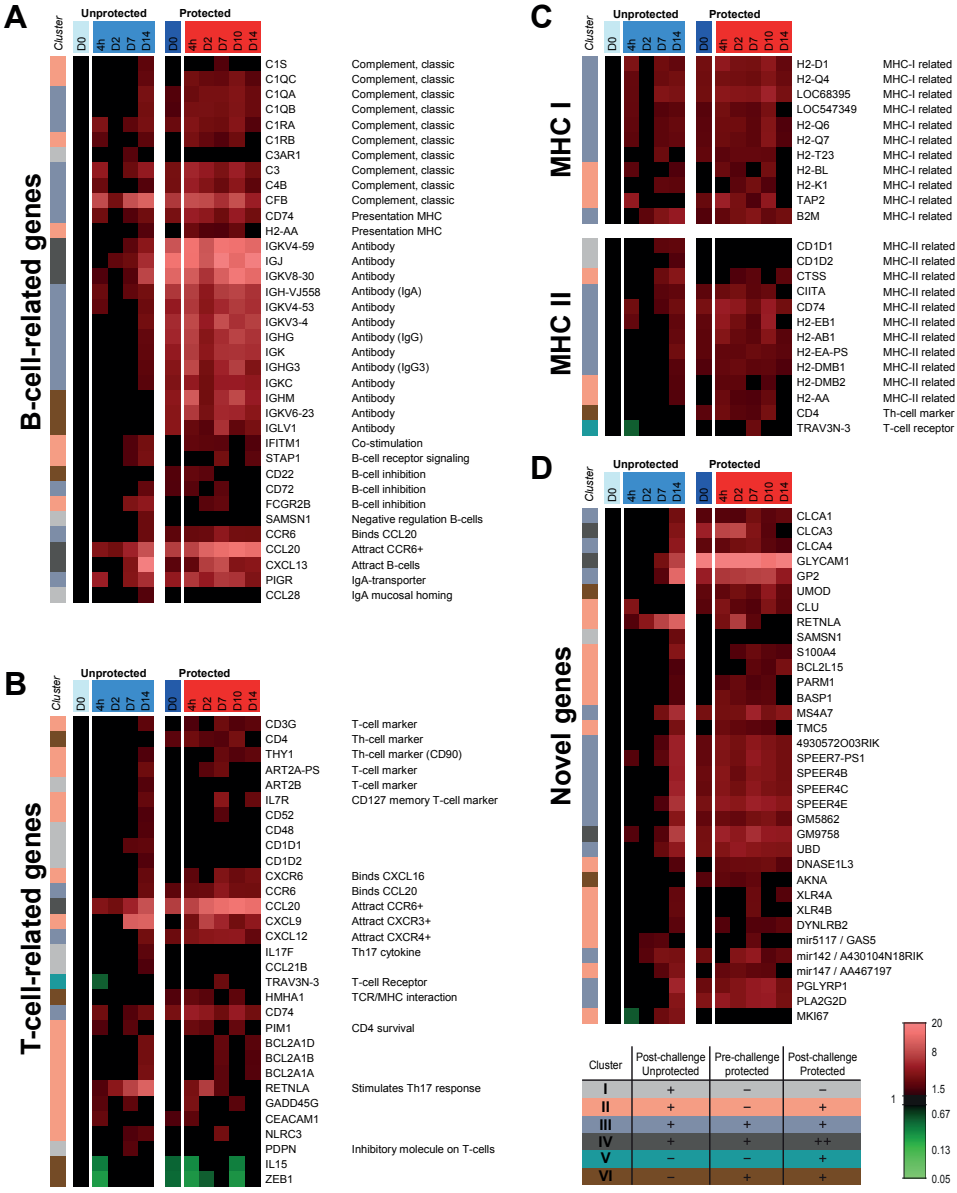

Figure 4 - Pulmonary gene expression profiles of genes related to T-cells, B-cells, MHC-I and II and novel genes in protected and unprotected mice following *B. pertussis* challenge. Expression profiles of genes in the lungs related to **(A)** T-cells, **(B)** B-cells, **(C)** and antigen presentation by MHC-I and MHC-II were selected according to GO-BP terms, KEGG pathways and text mining. In addition, genes with unknown or poorly understood function that showed interesting gene expression profiles in protected mice were listed as **(D)** novel genes. Additionally, the color codes of the six clusters from **Figure 2** are added.

Genes in group D were mainly up-regulated in protected and unprotected mice between 7 and 14 days p.c. The expression of these genes returned faster to basal level in protected mice than in unprotected mice. Based on the membrane-related genes in group D, this phase indicates innate and adaptive immune cells interacting with each other (*Clec9a, Clec10a, Clec12a, Il7r, Thy1, Trav3n-3*). For example, genes were detected related to T-cells (*Il7r, Thy1, Trav3n-3*), DCs (*Clec9a, Clec10a, Clec12a*), leukocytes (*Lilrb4*), macrophages (*Igsf6*) and lymphocytes or myeloid cells (*Cd52*). Group D also contained the upregulated gene *Spp1*. The corresponding protein of *Spp1* is also known as osteopontin (OPN), which is produced by many different immune cells and possesses many immunological functions [23]. However, the expression of this gene was not different between protected and unprotected mice.

B-cell and antibody-related signatures

The enhanced gene expression for the B-cell chemoattractant *Cxcl13*, detected 7 days p.i., suggested recruitment of B-cells towards the lungs of unprotected mice (**Figure 4A**). In protected mice, the expression of *Cxcl13* had raised earlier at 2 days p.c. Increased expression of antibody-related genes indicated B-cell recruitment to the lungs 14 days p.i. in unprotected mice. Higher and earlier expression of the immunoglobulin-related genes (i.e. *Igj, Igk, Ighm, Igkc*) was observed in protected mice than in unprotected mice (**Figure 4A**). These immunoglobulin-related genes indicated the formation of IgM, IgG and IgA by these B-cells in the lung. Notably, a small decrease in expression of antibody-related genes occurred 2 days p.c. in protected mice. Furthermore, genes of the classic complement pathway were co-expressed with the immunoglobulin-related genes. Genes of B-cell inhibitory receptors (*Cd22, Cd72, Fcgr2b*) were expressed slightly earlier in protected mice compared to unprotected mice. Moreover, the co-stimulatory receptor *Ifitm1* was earlier and more constant in protected mice. The upregulation of *Ccl28* in unprotected mice 14 days p.i. indicated homing of IgA producing B-cells to the mucosa. However, the expression of *Ccl28* was absent in protected mice. The upregulation of *Pigr*, the IgA transporter on epithelial cells, suggested an increase of IgA in the mucosa of protected and unprotected mice.

T-cell-related signatures

Gene expression of T-cell-related markers (*Cd3g, Cd4*) indicated the presence of T-cells, most likely T-helper (Th) cells, in the lungs of unprotected mice around 14 days p.i. (**Figure 4B**). The upregulation of *Cd3g* and *Cd4* is still present in protected mice prior to the challenge. The enhanced RNA levels remain high during challenge of these mice. In addition, multiple T-cell-related genes (*Il7r, Cxcr6, Thy1*) were upregulated 14 days p.i. in unprotected mice. The expression in protected mice was observed earlier at 7 days p.c., indicating a faster recall of memory T-cell responses. Expression of the IL-7 receptor gene (*Il7rl*) indicated the presence of memory T-cells. The Th17 specific cytokine gene (*Il17f*) was significantly upregulated in unprotected mice, but unaffected in protected mice. Resistin-like alpha (*Retnla*) was earlier expressed by epithelial

cells in protected mice, and the expression was already diminished 7 days p.c. Resistin-like alpha stimulates Th17 responses [24].

Antigen presentation

Genes related to MHC class I and II were upregulated in unprotected mice following the challenge (**Figure 4C**). Whereas enhanced MHC-I expression was observed during the whole course of the challenge, MHC-II expression was found upregulated 7-14 days p.i. In protected mice, genes related to both antigen-presenting pathways were expressed at every time point and decreased 14 days p.c.

Genes not previously described in the context of immunity against *B. pertussis*

Some genes showed increased expression in response to *B. pertussis* challenge, but limited or no information is available about their function (**Figure 4D**). The expression of most of these genes was induced during the adaptive phase in unprotected mice and persisted in protected mice after challenge. Therefore, these genes may play an important role in immunity against *B. pertussis*. These genes include members of the SPEER-family (*4930572003rik, Speer7-ps1, Speer4b, Speer4c, Speer4e, Gm5862, Gm9758*), chloride channel calcium activated channels (*Clca1, Clca3, Clca4*), microRNAs (*Mir142, Mir147, Mir5117*), a transcription factor (*Akna*), and X-linked lymphocyte-regulated genes (*Xlr4a, Xlr4b*). Significant expression of cell proliferation marker *Ki-67* was found in unprotected mice, but unaffected in protected mice. Moreover, the expression of M-cell specific genes (*Gp2, Umod*), an effector protein of $CD4^+CD25^+$ regulatory T-cells (*Pla2g2d*) [25], and of *Glycam1*, *Pglyrp1*, and *Retnla* were expressed earlier or to a stronger extent in protected mice compared to unprotected mice yet their involvement is not previously described in the context of immunity against *B. pertussis*.

Modulated cytokine levels in lung tissue extract

The protein concentrations of 32 cytokines in the lungs were analyzed. The concentrations of thirteen cytokines significantly changed following a *B. pertussis* challenge in protected and unprotected mice (**Figure 5**). CCL4 was decreased in protected mice 10 days p.c. (**Figure 5A**). CCL11 decreased in unprotected mice until 14 days p.i. and in protected mice until 2 days p.i. (**Figure 5B**). Moreover, a significant decrease occurred for VEGF in unprotected mice between 2-7 days p.i., which was less dramatic in protected mice (**Figure 5C**). In unprotected mice, G-CSF concentrations were elevated 7 days p.i. In protected mice, higher concentrations of G-CSF were found already at 4 hours and 2 days p.c. (**Figure 5D**). Both CXCL1 and CXCL2 were enhanced in unprotected mice, whereas only CXCL1 was significantly increased 4 hours p.c. in protected mice (**Figure 5E-F**). CXCL5 was significantly induced in unprotected mice and remained elevated until 7 days p.i. (**Figure 5G**). CXCL9, CXCL10 and IL-17A were elicited 14 days p.i. in unprotected mice, but they were absent in protected mice (**Figure 5H-J**). IL-5, TNFα and M-CSF were produced in the lungs of protected mice 4 hours p.c., but not in unprotected mice (**Figure 5K-M**).

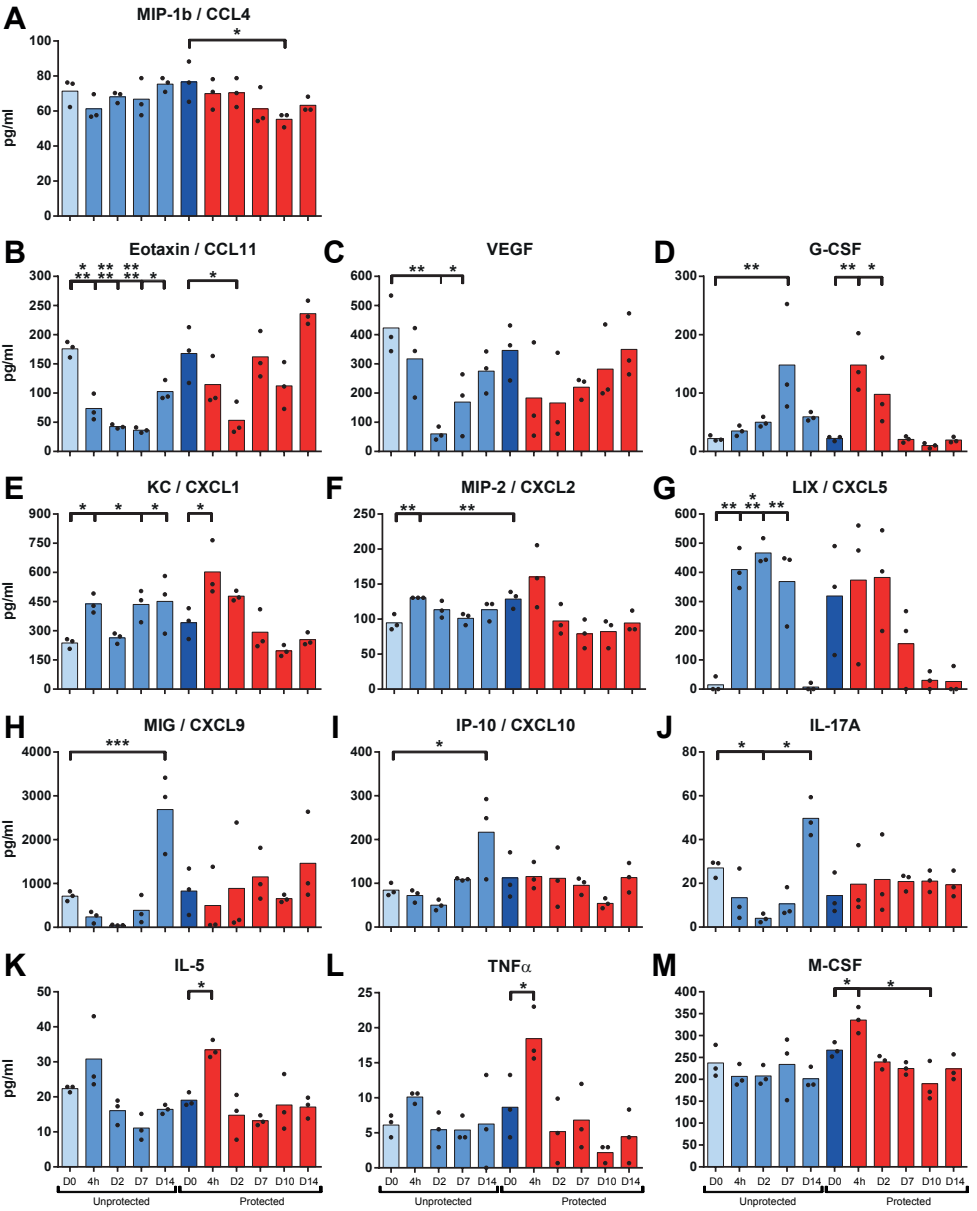

Figure 5 - Cytokine profiles in the lungs following *B. pertussis* challenge in unprotected and protected mice. Pulmonary concentrations of **(A)** CCL4, **(B)** CCL11, **(C)** VEGF, **(D)** G-CSF, **(E)** CXCL1, **(F)** CXCL2, **(G)** CXCL5, **(H)** CXCL9, **(I)** CXCL10, **(J)** IL-17A, **(K)** IL-5, **(L)** TNFα and **(M)** M-CSF were analyzed before and after a *B. pertussis* challenge in unprotected (lighter blue bars) and protected (dark blue and red bars) mice, as indicated. Data represented as mean concentrations of individual values (n = 3). Significant values were calculated by one-way ANOVA with multiple comparison compared to the pre-challenge level (D0) of unprotected mice or protected mice (* = $p \leq 0.05$, ** = $p \leq 0.01$, and *** = $p \leq 0.001$, **** = $p \leq 0.0001$).

Enhanced cytokine levels in mouse serum

The concentrations of 33 cytokines were analyzed in serum of protected or unprotected mice before and following the *B. pertussis* challenge. Only for seven of these, significant alterations in their levels were found upon challenge (**Figure 6A**). The concentrations of CXCL1 (KC) and CCL11 (Eotaxin) were increased 4 hours p.i. in unprotected mice. Higher concentrations of both IL-6 and G-CSF were detected 7 days p.i. in unprotected mice. A decrease in both CXCL10 and IL-13 occurred between 7-14 days p.i. in protected mice. B lymphocyte chemoattractant (BLC) CXCL13 was elevated 14 days p.i. in unprotected mice and unaltered in protected mice. Overall, serum cytokines present during infection of unprotected mice are unaltered during the challenge of protected mice. In conclusion, these results indicate that systemic signals for pro-inflammatory cytokines (CXCL1 and IL-6) and recruitment of B-cells (CXCL13), T-cells (CCL11 and CXCL10) and neutrophils (CXCL1, G-CSF) are not required in protected mice during a challenge with *B. pertussis*.

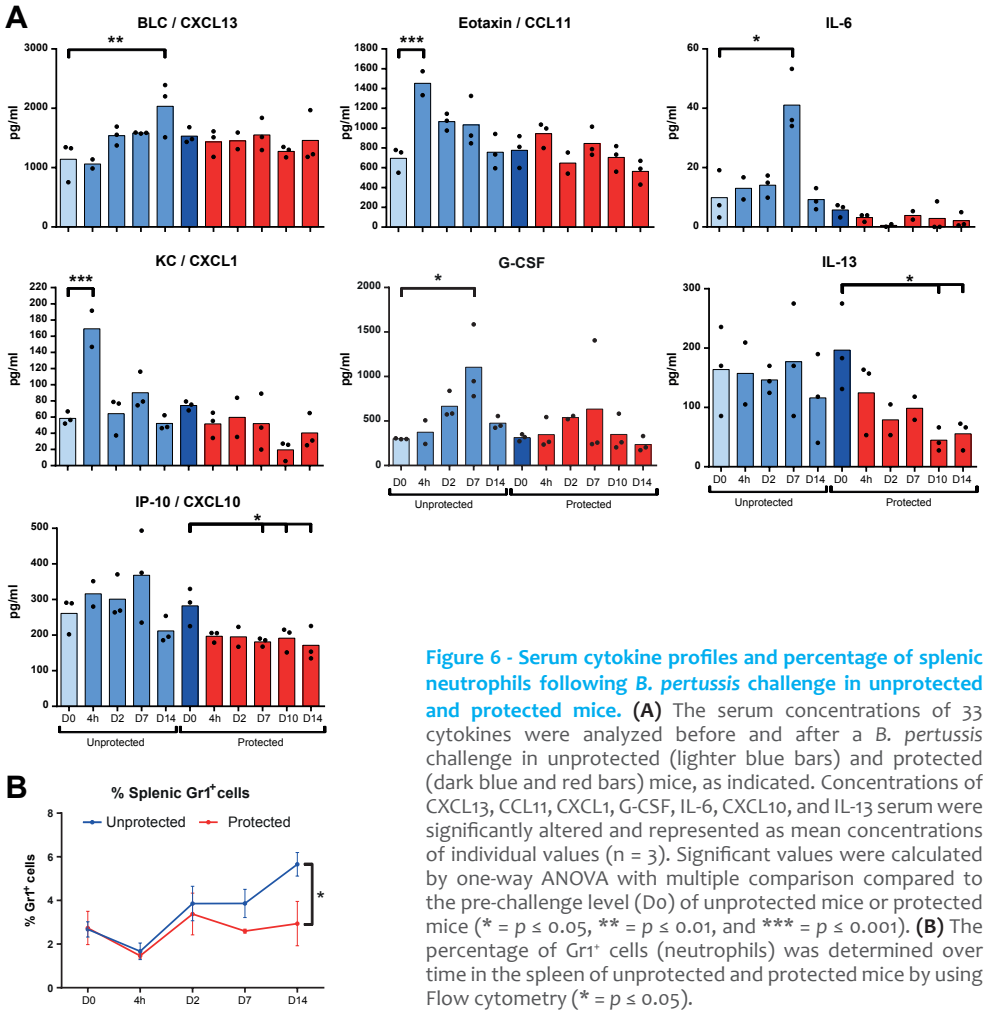

Figure 6 - Serum cytokine profiles and percentage of splenic neutrophils following *B. pertussis* challenge in unprotected and protected mice. **(A)** The serum concentrations of 33 cytokines were analyzed before and after a *B. pertussis* challenge in unprotected (lighter blue bars) and protected (dark blue and red bars) mice, as indicated. Concentrations of CXCL13, CCL11, CXCL1, G-CSF, IL-6, CXCL10, and IL-13 serum were significantly altered and represented as mean concentrations of individual values (n = 3). Significant values were calculated by one-way ANOVA with multiple comparison compared to the pre-challenge level (D0) of unprotected mice or protected mice (* = $p \leq 0.05$, ** = $p \leq 0.01$, and *** = $p \leq 0.001$). **(B)** The percentage of Gr1$^+$ cells (neutrophils) was determined over time in the spleen of unprotected and protected mice by using Flow cytometry (* = $p \leq 0.05$).

Cellular composition spleen

In unprotected mice, neutrophils ($Gr1^+$) play an important role in the clearance of bacteria from the lungs and are often used as marker of disease. This process is characterized by a gradually increased percentage of neutrophils in the spleen between 4 and 21 days p.i. [10]. Analysis of the percentage $Gr1^+$ cells in the spleen following challenge in protected mice indicated that this recruitment of granulocytes did not occur 14 days p.c. whereas the drastic increase of granulocytes in unprotected mice was again observed (**Figure 6B**). Together, these results show that recruitment of circulating granulocytes/neutrophils occurs only in unprotected mice after a challenge.

B. pertussis-specific antibody responses in serum and lung tissue extract

Levels of IgA, IgG, and IgG subclasses were determined just before and after 14 days challenge in sera of unprotected and protected mice (**Figure 7A-E**) *B. pertussis* outer membrane vesicles (OMV) and purified antigens (Prn, Ptx, FHA, and Fim2/3) were used as coating antigen. Only anti-OMV antibodies were induced in unprotected mice 14 days p.i., while antibodies against purified antigens could not be detected. Antibodies specific for all five purified antigens were observed in protected mice before challenge (D0).

After the challenge, anti-Ptx IgG and IgA levels dropped in protected mice, whereas the anti-OMV and anti-FHA IgG levels remained high. Moreover, the anti-Prn IgG1 and IgA levels decreased, while IgG2a and IgG2b levels increased. Notably, serum IgA levels against Fim2/3 were only detected in protected mice 14 days p.c. In addition to systemic antibody levels, the local formation of IgA antibodies was determined in lung lysates (**Figure 7F**). Challenge in unprotected mice elicited mainly anti-OMV IgA, which was detected 14 days p.i.

In protected mice, anti-OMV IgA antibodies were present before challenge (D0) and were further increased 14 days p.c. Anti-Prn and anti-Fim2/3 IgA remained elevated, while anti-Ptx IgA decreased. Combined data of all time points showed a gradual increase of pulmonary anti-OMV IgA levels post-challenge in protected mice (**Figure 7G**). Western blotting and mass spectrometry was used to determine the antigen specificity of the anti-OMV IgA antibodies in protected mice before (D0) and after the challenge (D14) (**Figure 7H**). The IgA antibodies on D0 were solely directed against Vag8. Notably, challenge of protected mice led to strong anti-LPS IgA antibody formation, whereas the level of anti-Vag8 antibodies remained unaltered (**Figure 7H**).

Specific $CD4^+$ T-cell response in the spleen

After challenge, the presence and type of *B. pertussis* antigen-specific memory $CD4^+CD44^+$ T-cells in the spleen were determined. The cytokine production of $CD4^+$ T-cells was analyzed according to the study design depicted in **Figure 8A** on single cell level and in culture supernatants after stimulation of splenocytes with Ptx, FHA, or Prn. The $CD4^+$ T-cell response was determined after primary infection of unprotected mice 10 days and 66 days p.i. (-D46

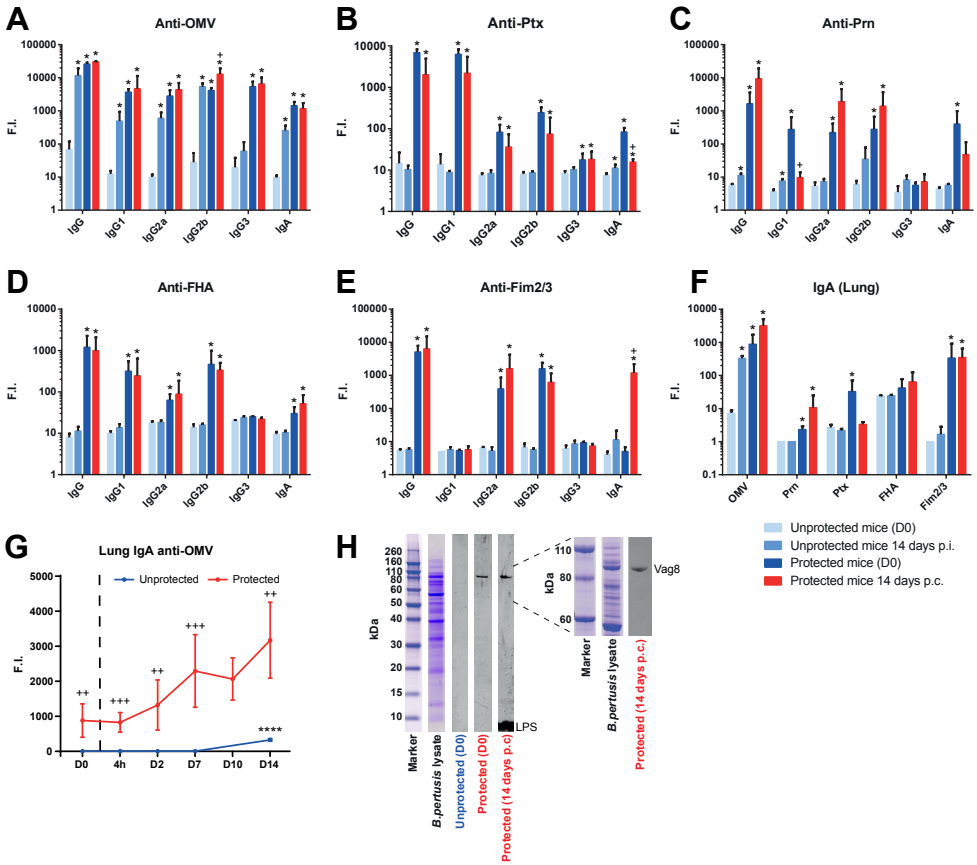

Figure 7 - Serum and pulmonary antibody profiles in unprotected and protected mice following *B. pertussis* challenge. Serum IgA, IgG, and IgG subclass responses specific for **(A)** OMV, **(B)** Ptx, **(C)** Prn, **(D)** FHA, and **(E)** Fim2/3 were determined by using a MIA. Data were obtained in naive mice and protected mice prior to challenge (D0) and 14 days post infection (p.i.) or 14 days post-challenge (p.c.) (n = 3 / time point). **(F)** Pulmonary IgA responses against these antigens were determined on the same time points. * = $p \leq 0.05$ experimental group versus unprotected group (D0), + = $p \leq 0.05$ protected group (D0) versus protected group (14 days p.c.). **(G)** The kinetics of the anti-OMV IgA antibody formation in lung lysates were analyzed at more time points (n=3/time point) and expressed in fluorescence intensity (F.I.). **** = $p \leq 0.0001$, challenged unprotected or protected group versus unprotected or protected group (day 0), ++ and +++ = $p \leq 0.01$ and $p \leq 0.001$ unprotected group versus protected group (for each time point). **(H)** Western blot on separated *B. pertussis* B1917 proteins was performed with pooled lung lysates (1:50) of unprotected and protected mice prior to challenge (D0), and of protected mice 14 days p.c. with IR800-labeled secondary antibody. Left panel shows whole protein range (260kDa-<10kDa) of *B. pertussis* lysate. Right panel shows more detailed separation of the 110-60kDa protein range. Antigen identification for Vag8 and LPS is depicted.

and D10, respectively). Primary infection led to increased percentages of IFNγ- and IL-17A-producing Prn-specific $CD4^+$ T-cells on 10 days p.i. (-D46), which percentages significantly increased 66 days p.i. (D10). In addition, IFNγ- and IL-17A-producing FHA-specific $CD4^+CD44^+$ T-cells could be detected on this time point (**Figure 8B**). Protected mice received an intranasal *B. pertussis* challenge 56 days after the primary infection (D0) and showed increased percentages of IFNγ- and IL-17A-producing Prn-specific $CD4^+CD44^+$ T-cells on 10 days p.c.

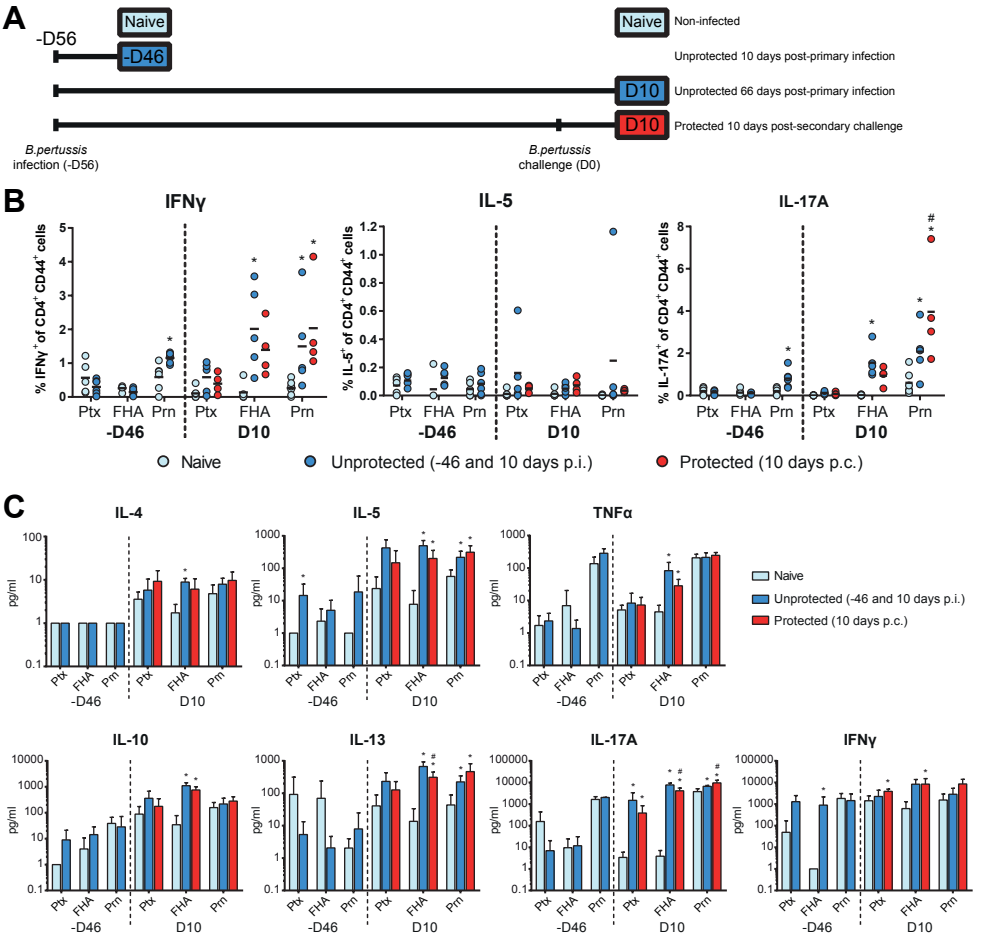

Figure 8 - Systemic T-cell responses in unprotected and protected mice. **(A)** Study design is depicted for the collection of splenocytes in two different experiments (-D46 and D10). The first experiment (-D46) included unprotected mice 10 days p.i. and naive mice. The second experiment (D10) included unprotected mice 66 days p.i., protected mice 10 days post-secondary challenge, and naive mice. Splenocytes were *in vitro* restimulated with Prn, FHA or Ptx for 8 days. **(B)** The percentages of IFNγ-, IL-5-, and IL-17A-producing $CD4^+CD44^+$ T-cells were determined using ICS (n = 6). **(C)** Cytokine levels of IL-4, IL-5, IL-10, IL-13, IL-17A, IFNγ, and TNFα in supernatant after 7 days of stimulation were determined by using a MIA. Results (mean of n = 6) are corrected for the background level in the presence of medium as control. Statistical differences between the groups were detected for the ICS with a non-parametric Mann-Whitney test and for the MIA with a Student t-test on the log-transformed data. * = $p \leq 0.05$ experimental group versus naive group, # = $p \leq 0.05$ protected group (D10) versus unprotected group (D10).

compared to the percentage in naive mice. Notably, the percentage IL-17A-producing Prn-specific $CD4^+CD44^+$ T-cells in these challenged protected mice 10 days p.c. was increased compared to the percentage in the unprotected mice on that time point (**Figure 8B**).
Cytokine levels in culture supernatant revealed that 10 days p.i. (-D46) splenocytes showed a moderate production of IL-5 and IFNγ after stimulation with Ptx and FHA, respectively (**Figure 8C**). In unprotected mice that were sacrificed 66 days p.i. (D10), Prn-stimulation resulted in enhanced production of IL-5, IL-13, and IL-17A while production of IL-17A was also observed after Ptx stimulation. FHA stimulation caused production of IL-4, IL-5, IL-13, TNFα, IL-17A, and IL-10. Data obtained in protected mice 10 days p.c. revealed the induction of IL-5, IL-13 and IL-17A after Prn-stimulation, increase in IFNγ- and IL-17A after Ptx-stimulation, and production of IL-5, IL-13, IFNγ, TNFα, IL-17A and IL-10 after FHA-stimulation. In conclusion, infection-induced T-cell responses were Th1 and Th17 mediated. Additionally, challenge of protected mice did not result in a dramatic booster of the $CD4^+$ T-cell response, since only a higher percentage of IL-17A-producing $CD4^+CD44^+$ was observed in protected compared to unprotected mice

Discussion

A *Bordetella pertussis* infection in mice or baboons causes sterilizing immunity [7, 10]. There are strong indications that the Th1/Th17 responses and mucosal IgA are major contributors to this superior protection [10-12]. Nevertheless, many immunological responses caused upon a *B. pertussis* infection are still not discovered. In the current study, protected and unprotected mice were challenged intranasally with *B. pertussis* after which innate and adaptive immunological signatures were identified associated with the infection-induced and excellent immunity in mice.

Protected mice had high levels of *B. pertussis*-specific serum IgG, mucosal IgA in the lungs and Th1/Th17 cells in the spleen, whereas unprotected mice have not. In addition, pulmonary molecular signatures in the protected mice revealed unique markers of B-cells, T-cells, and immunoglobulins, implying the presence of tissue-resident adaptive immune cells in the lungs. Moreover, molecular signatures of myeloid and mucosal-specific cells, such as mast cells and goblet cells were present. Interestingly, 320 genes were still differentially expressed before the challenge in protected mice as result of the first infection, as compared to unprotected mice before challenge. Since bacteria were cleared from the lungs 28 days after primary infection [10], the question was raised what is the source responsible for this upregulation. Possibly, a change in the cellular composition of the lungs due to residence of new innate and adaptive immune cells result an aberrant gene expression profiles. Importantly, the overall transcriptomics data indicate not only a relatively persistent and broadly altered adaptive pulmonary immune status but also maintained innate changes in protected mice in comparison to their naive counterparts.

Pathogenesis of pertussis in non-vaccinated individuals is characterized by prolonged bacterial presence and severe lung tissue distress and damage [26]. It is hypothesized that immune evasion strategies of *B. pertussis* [27] extend residence time. Ideally, pre-existing immunity induced by vaccination should provide fast clearance of pertussis bacteria and long-lasting immunity to avert bacterial transmission [7] and limit respiratory tissue damage. The absence of pro-inflammatory responses and neutrophil circulation may be signs of less severe disease. Protected mice, in contrast to unprotected mice, had reduced systemic serum cytokine secretion, including the pro-inflammatory cytokine IL-6 and neutrophil attractants (CXCL1 and G-CSF), and no induction of neutrophils in the spleens. Additionally, selective innate molecular signatures were absent in the lungs of protected mice following the *B. pertussis* challenge. This included genes encoding pro-inflammatory cytokines such as *Il1a, Il1b, Il6* and *Saa1* as part of the acute phase response. Moreover, enhanced gene expression of the KLR and CLEC-family, was not detected in protected mice. KLR and CLEC genes may harbor similar functions [28], which are specifically found on myeloid cells [29] and play an

important role in tissue infiltration of neutrophils following inflammation [30]. This lack of expression in protected mice implies that myeloid cells expressing these membrane markers are not required for the sterilizing immunity. Finally, the enhanced cell proliferation in the lungs of unprotected mice, based on the high expression of *Ki-67*, was absent in protected mice. Overall, the altered transcriptomes in the lungs of protected mice suggest that these mice are able to control the challenge locally without alarming systemic pro-inflammatory signals.

The acquired immune status of the protected mice enables an alternative solution for fast bacterial clearance with limited systemic recruitment of immune cells from the circulation. Specific markers (IL-5, TNFα and M-CSF) were exclusively present in the protected mice, which may contribute to the sterilizing immunity. Secretion of IL-5 indicates the presence of antigen specific Th2-cells in the lungs. However, no *B. pertussis*-specific Th2-cell formation was detected in the spleen of protected mice. Therefore, IL-5 could be produced by innate lymphoid cells (ILCs). The presence of ILCs is indicated by gene expression of *Thy1* and *Il7r* [31]. While pulmonary innate immune cells still play a role during the challenge of protected mice, some of these cells signatures (i.e. *Gp2, Umod, Pglyrp1, Clca3*) were also highly active prior to the challenge. The pulmonary expression of *Gp2* and *Umod* was increased in protected mice prior and post-challenge. Glycoprotein 2 (GP2) and uromodulin (Umod) are expressed on microfold cells (M-cells) [32]. M-cells facilitate the uptake of antigens at the mucosal site and the subsequent transportation across the epithelial barrier. GP2 serves as a receptor for mucosal antigen and binds adhesins on Fim^+ bacteria [33], such as *B. pertussis*. Simultaneously, expression of peptidoglycan recognition protein 1 (*Pglyrp1*) was detected, which at the intestinal mucosal site is found in Peyer's patches co-localized with M-cells [34]. This indicates that the M-cells are either increased in number or more active in protected mice prior and post-challenge. At the pulmonary site, M-cells are commonly found in the Bronchus-Associated Lymphoid Tissue (BALT) [35] gathered with tissue-resident adaptive cells, such as B-cells and T-cells, facilitating a more efficient antigen presentation. This suggests that the local pulmonary immunity induced by a primary *B. pertussis* challenge is a result of not only the induction of acquired immunological memory, but also increased innate activity and subsequent interplay between of innate and acquired immune cells in the BALT. Enhanced expression of genes specific for goblet cells (mucus-producing cells), such as chloride channel calcium activated channels (*Clca1, Clca3* and *Clca4*) and anterior gradient 2 (*Agr2*) [36] suggests that these cells are more active during the challenge in protected mice. Goblet cells can also orchestrate local immune responses. For instance, IL-17 and CXCL1 induction in the lungs and leukocyte recruitment are modulated by CLCA3 in mucus cells [37].
Myeloid cells play an important role in clearance of *B. pertussis*. For instance, a large neutrophil influx into the lungs occurs during the challenge of unprotected mice [10, 38]. Neutrophils are essential for phagocytosis and may serve as a marker for disease like white

blood cell counts for baboons and young infants [39, 40]. Myeloid cells expressing membrane markers of the KLRs, CLECs and the MS4A family [28, 29, 41] were absent in the protected mice after the challenge. However, the enhanced gene expression of the neutrophil-specific *Cd177* and macrophage-specific *Mpeg1* suggests involvement of other subsets of myeloid cells during the challenge in protected mice. The expression of CD177 on neutrophils is enhanced in the presence of G-CSF [42] which was also detected in the lungs of protected mice. These signatures could be related to changes in the pulmonary cell composition as a result of the first infection. For example, opsonization of bacteria by pre-existing specific antibodies and the subsequent phagocytosis by different myeloid cells enables an enhanced clearance of bacteria. In addition, the outgrowth of bacteria is absent in protected mice after challenge. Hence, the total number of phagocytes required for removal of bacteria is expected to be lower. Finally, the infection-induced immunity might result in signatures of airway specific cells, such as was detected for alveolar macrophages. Both GC-CSF and M-CSF play an important role in proliferation and differentiation of alveolar macrophages [43]. In addition, pulmonary secretion of M-CSF was detected exclusively in protected mice 4 hours p.c. This change in lung environment enables formation of specific alveolar macrophages with a very high antigen-presenting capacity [44]. The contribution of alveolar macrophages [45] and mast-cells [46] with respect to immunity against *B. pertussis* has previously been demonstrated.
Together these findings demonstrate that the infection-primed immunity resulted in the enhanced activity of pulmonary innate cells, such as alveolar macrophages, M-cells, and ILCs. This may indicate that these innate cells have trained innate immunity [47] that provides an altered pulmonary innate homeostasis [48]. This different status of innate cells may contribute to the local immunity in protected mice. Therefore, pulmonary innate cells are interesting targets for optimizing pertussis vaccination strategies, e.g. by pulmonary vaccination.

Infection-induced immunity comprised of a Th1/Th17-mediated response, as was demonstrated by the systemic analysis of *B. pertussis*-specific T-cells in the spleen. After the challenge, these responses were recalled fast in the protected mice. Despite the upregulated pulmonary gene expression of *Cxcl9*, protein secretion of CXCL9 and CXCL10 was not detectable in lung lysates and serum of protected mice, indicating reduced recruitment of $CXCR3^+$ T-cells. However, gene expression showed that molecular signatures of T-cells (i.e. *Cd3g, Cd4, Thy1*) were further enhanced in protected mice post-challenge. This indicates the presence of tissue-resident memory $CD4^+$ T-cells. This assumption is emphasized by the enhanced expression of the memory T-cell marker *Il7r* (*Cd127*). Moreover, gene expression of the chemokines *Ccl20* and *Cxcl12* and their corresponding receptors *Cxcr6* and *Ccr6* implied recruitment of different types of T-cells, such as $CCR6^+$ Th17-cells [49] and $CXCR6^+$ T-cells [50] in the lungs. Lee *et al.* showed that the presence of pulmonary $CXCR6^+$ T-cells correlated with local protective immunity against *Mycobacterium tuberculosis* [50]. Furthermore, CCR6 is

an important mediator of mucosal immunity [51], indicating a potential role for pulmonary CXCR6$^+$ and CCR6$^+$ T-cells in immunity against *B. pertussis*. Strong *B. pertussis*-specific Th17 responses occur during infection in unprotected mice, which remain present for a long period [10]. Moreover, the Resistin like alpha (*Retnla*) was found to stimulate Th17 responses [24]. However, the secretion of IL-17A and expression of *Il17f* in the lungs was absent after the challenge of protected mice. This indicates either that we missed this expression due to a change in expression kinetics or that the effector function of the Th17 cells had changed.

Protected mice had high levels of *B. pertussis*-specific IgG in the serum. In addition, protected mice expressed genes encoding for B-cell markers and antibody production in their lungs. This was confirmed by the presence of mucosal IgA in the lungs. We demonstrated that this pulmonary IgA in protected mice is directed against Ptx, Fim2/3, and Vag8. The inclusion of Fim2 or Vag8 in pertussis vaccines may improve efficacy. IgA plays an important role in protection against *B. pertussis* [52]. Therefore, the induction of mucosal IgA by mucosal vaccination might be a big advantage, especially because IgA induction is completely absent after immunization with current pertussis vaccines [53]. Induction of B-cell-related gene expression after a challenge of protected mice shows a recall response leading to increased antibody production. Here, CCR6 expression may be important for memory B-cells to mount a recall response [54]. The antibody-related gene expression showed co-expression with components of the classical complement pathway and seven genes of the SPEER-family with unknown function, suggesting the expression of these genes occurring in the B-cells. Overall, these findings demonstrate the presence of both systemic and pulmonary humoral responses primarily directed against Ptx, Fim2/3 and Vag8. This is where the results obtained in this study may contribute to understanding and optimizing immunity against *B. pertussis*. Pertussis vaccines, such as the acellular (aPV), whole-cell (wPV) and outer membrane vesicle (omvPV) vaccines, substantially different T-helper cell polarization [11, 55] and humoral immunity based on subclass responses and antigen specificity [53]. All vaccines provide enhanced bacterial clearance in mice as compared to non-vaccinated mice, indicating that multiple types of immunity can achieve protection against pertussis. Nonetheless, sterilizing immunity in the lungs that is seen for infection induced-immunity [7, 10] is not provided by subcutaneous vaccination [7].

In conclusion, the comprehensive comparison of responses between protected mice and unprotected mice resulted in detailed insight in characteristics of protective immune responses against pertussis. The unprotected mice are largely depending on recruitment of phagocytic cells into the lungs to remove the bacteria, whereas the acquired immunity in the protected mice enables fast recognition and neutralization of the bacteria. The presence of memory Th1/Th17 cells, memory B-cells, and mucosal IgA characterized this effective immunity against *B. pertussis*. Here, CCR6$^+$ B-cells, Th17 cells and CXCR6$^+$ T-cells play an important role

in the *B. pertussis* infection-induced pulmonary immunity. Moreover, high activity of 'trained' pulmonary innate immune cells, such as alveolar macrophages, M-cells and goblet cells, was observed in the lungs of protected mice. Hence, induction of pulmonary immunity e.g. achieved by local immunization will improve the efficacy of pertussis vaccines, perhaps also on the long term. A single dose of intranasally administered live-attenuated pertussis vaccine shows that such an approach induces good protection in mice [56] with longer lasting immunity [57] and also through a Th1/Th17-mediated response [58]. In conclusion, the present study showed that the use of a systems approach enables to unravel infection-induced responses in more detail, including the interplay between innate and acquired immune responses.

Methods

Ethics Statement

An independent ethical committee for animal experimentations (DEC) of Intravacc reviewed the animal experiments according to the guidelines provided by the Dutch Animal Protection Act. The committee approved documents with the identification number 'DPA201100348'.

B. pertussis challenge culture

Cultivation of *Bordetella pertussis* B1917 and preparation of the challenge culture was performed as previously described [10].

Animal experiments

Thirty female, 8-weeks-old, BALB/c mice (Harlan, The Netherlands) were divided in ten groups of three animals and housed in cages (macrolon III including filter top). Six groups of naive mice (n = 3 mice/group) were intranasally infected under anesthesia (isoflurane/oxygen), with $2x10^5$ CFU *B. pertussis* B1917 in 40µl Verweij medium and left 56 days to recover. 56 days p.i. (D0), five groups of these protected mice with infection-induced immunity and five groups of naive (D0 unprotected) mice (n = 3) of the same age were challenged intranasally as described above for the primary infection and euthanized at 4 hours, and 2, 7, 10 and 14 days after challenge, according to the study design in **Figure 1**. Additionally, 30 mice were included for two individual experiments analyzing $CD4^+$ T-cell responses (Experiment design in **Figure 8A**). On 10 days p.i. (-D46), six primary-infected and six complete naive mice were euthanized. On day 10 p.c., six mice that had encountered two infectious doses (-D56 and D0), six primary-infected mice (66 days p.i.), and six complete naive mice were euthanized. Mice from all groups were bled under anesthesia (isoflurane/oxygen) by orbital bleeding and euthanized by cervical dislocation. Collection of whole blood, lungs and spleen were performed as described before [10].

Microarray analysis

RNA isolation from lung tissue, determination of RNA concentrations, and RNA integrity was executed as described before [10]. Amplification, labeling and hybridization of RNA samples to microarray chips was carried out at the Microarray Department of the University of Amsterdam, The Netherlands, as described previously [59]. Complete raw and normalized microarray data and their MIAME compliant metadata from this publication have been submitted to the GEO database (www.ncbi.nlm.nih.gov/geo) and assigned the identifier GSE75438.

Data analysis of gene expression

Statistical analysis of gene expression data was done in R according to methods described before [10]. Further functional interpretation, was performed using resources such as DAVID [18], Gene Ontology, KEGG, and BioGPS. Data visualization was done in R as well as GeneMaths XT software (Applied Maths, Sint-Martens-Latem, Belgium).

Antibody levels in serum and lung lysate

Levels of pulmonary total IgA and serum total IgA, IgG and IgG subclass (IgG1, IgG2a, IgG2b and IgG3) specific for *B. pertussis* antigens P.69 pertactin (P.69 Prn), filamentous hemagglutinin (FHA), pertussis toxin (Ptx), combined fimbria type 2 and 3 antigens (Fim2/3) and outer membrane vesicles B1917 (OMV B1917) were determined using a multiplex immunoassay (MIA) as described previously [10].

Western Blotting using IgA from lung lysate

Infrared labeling (IR800) of goat-anti-mouse IgA (Southern Biotech), protein separation by SDS-PAGE, and immunoproteomic profiling by Western blot (1:50 dilution) and MS-MS were performed as described previously [53]. For improved separation of the 80kD-110kD range, a 4-12% Bis-Tris protein gel (NuPAGE Novex, 1.0mm 10wells, Invitrogen) was used.

Splenic Gr-1$^+$ cell analysis

Determination of the percentage Gr-1$^+$ cells in isolated splenocytes was carried out as described before [10].

Stimulation of *B. pertussis*-specific T-cell from spleens

Splenocytes were isolated and stimulated with 1 µg/ml Prn, Ptx or FHA in IMDM complete medium (IMDM medium (Gibco) supplemented with 8% FCS, 100 units penicillin, 100 units streptomycin, 2.92 mg/ml L-glutamine, and 20 µM β-mercaptoethanol (Sigma)), or only medium, as described previously [10]. Supernatants were collected after 7 days for cytokine analysis. After overnight stimulation with the same conditions, intracellular cytokine staining was executed splenocytes that were stimulated for 8 days to identify CD4$^+$CD44$^+$ T-cells producing IL-5, IFNγ or IL-17A.

Multiplex immunoassay (MIA) for cytokines

A mouse cytokine 7-plex luminex kit (Milliplex; Merck KGaA, Darmstadt, Germany) was used to determine concentrations (pg/ml) of IL-4, IL-5, IL-10, IL-13, IL-17A, TNFα, and IFNγ in culture supernatants of 7 days stimulated splenocytes of individual mice in a MIA.

A mouse cytokine/chemokine 32-plex luminex kit (Milliplex MAP Mouse Cytokine/Chemokine - Premixed 32 Plex; Merck KGaA, Darmstadt, Germany) was used to determine concentrations (pg/ml) of Eotaxin, G-CSF, GM-CSF, IFNγ, IL-10, IL-12 (p40), IL-12 (p70), IL-13, IL-15, IL-17A,

IL-1α, IL-1β, IL-2, IL-3, IL-4, IL-5, IL-6, IL-7, IL-9, IP-10, KC, LIF, LIX, M-CSF, MCP-1, MIG, MIP-1α, MIP-1β, MIP-2, RANTES, TNF-α, and VEGF, in serum and lung lysates in a MIA (according to the manufacturer's instructions and as described previously [10]). Measurements and data analysis were performed with Bio-Plex 200, using Bio-Plex Manager software (version 5.0, Bio-Rad Laboratories).

BLC (CXCL13) cytokine ELISA

Serum concentration of B lymphocyte chemoattractant (BLC/CXCL13) was determined by ELISA (Mouse BLC ELISA kit, RAB0046, Sigma-Aldrich, Germany) according to the manufacturer's manual. In short, serum (50 µl) was diluted in assay buffer A (1/1; v/v) and incubated in an antibody-coated ELISA plate (overnight, 4°C, gentle shaking). After washing four times with 300 µl wash buffer, wells were incubated with 100 µl biotinylated antibody (1 hour, room temperature, gentle shaking). After washing four times with 300 µl wash buffer, wells were incubated with 100 µl streptavidin solution (45 min., room temperature, gentle shaking). After washing four times, wells were incubated with 100 µl TMB one-step substrate reagent (30 min., RT) and reaction stopped with 50 µl stop solution. Finally, the absorbance was recorded at 450 nm with a plate reader (BioTek reader EL808, Bio-Tek) and converted to BLC concentration by using a dilution series of a standard (1.37 – 1,000 pg/ml) and Gentech 5 software (BioTek).

Statistical analysis

Serum and pulmonary cytokines levels were analyzed by using a one-way ANOVA with multiple comparisons compared to the pre-challenge level (D0) of unprotected mice or protected mice followed by a Dunnett t-test. ICS data was analyzed by using a Mann-Whitney t-test. For cytokine profiling after re-stimulation of splenocytes, cellular composition of spleen, and antibody levels, data was first log-transformed before t-test analysis. In all corresponding figures, *p*-values are represented as * = $p \leq 0.05$, ** = $p \leq 0.01$, *** = $p \leq 0.001$ and **** = $p \leq 0.0001$.

Acknowledgements

The authors thank the employees of the Animal Research Centre (ARC) of Intravacc, for the performance of animal experiments and the Microarray Department (MAD) of the University of Amsterdam for the performance of the microarray analyses.

References

1. Cherry, J.D., Epidemic pertussis in 2012--the resurgence of a vaccine-preventable disease. N Engl J Med, 2012. 367(9): p. 785-7.
2. Jackson, D.W. and P. Rohani, Perplexities of pertussis: recent global epidemiological trends and their potential causes. Epidemiol Infect, 2014. 142(4): p. 672-84.
3. Tan, T., *et al.*, Pertussis Across the Globe: Recent Epidemiologic Trends From 2000-2013. Pediatr Infect Dis J, 2015. 34(9): p. e222-32.
4. Wendelboe, A.M., *et al.*, Duration of immunity against pertussis after natural infection or vaccination. Pediatr Infect Dis J, 2005. 24(5 Suppl): p. S58-61.
5. Campbell, P.T., *et al.*, Defining long-term drivers of pertussis resurgence, and optimal vaccine control strategies. Vaccine, 2015. 33(43): p. 5794-800.
6. Klein, N.P., *et al.*, Waning protection after fifth dose of acellular pertussis vaccine in children. N Engl J Med, 2012. 367(11): p. 1012-9.
7. Warfel, J.M., L.I. Zimmerman, and T.J. Merkel, Acellular pertussis vaccines protect against disease but fail to prevent infection and transmission in a nonhuman primate model. Proc Natl Acad Sci U S A, 2014. 111(2): p. 787-92.
8. Bertilone, C., T. Wallace, and L.A. Selvey, Finding the 'who' in whooping cough: vaccinated siblings are important pertussis sources in infants 6 months of age and under. Commun Dis Intell Q Rep, 2014. 38(3): p. E195-200.
9. Wendelboe, A.M., *et al.*, Transmission of *Bordetella pertussis* to young infants. Pediatr Infect Dis J, 2007. 26(4): p. 293-9.
10. Raeven, R.H.M., *et al.*, Molecular Signatures of the Evolving Immune Response in Mice following a *Bordetella pertussis* Infection. PLoS One, 2014. 9(8): p. e104548.
11. Ross, P.J., *et al.*, Relative contribution of Th1 and Th17 cells in adaptive immunity to *Bordetella pertussis*: towards the rational design of an improved acellular pertussis vaccine. PLoS Pathog, 2013. 9(4): p. e1003264.
12. Warfel, J.M. and T.J. Merkel, *Bordetella pertussis* infection induces a mucosal IL-17 response and long-lived Th17 and Th1 immune memory cells in nonhuman primates. Mucosal Immunol, 2013. 6(4): p. 787-96.
13. Whitsett, J.A. and T. Alenghat, Respiratory epithelial cells orchestrate pulmonary innate immunity. Nat Immunol, 2015. 16(1): p. 27-35.
14. Rogers, D.F., Airway goblet cells: responsive and adaptable front-line defenders. Eur Respir J, 1994. 7(9): p. 1690-706.
15. Lambrecht, B.N., Alveolar macrophage in the driver's seat. Immunity, 2006. 24(4): p. 366-8.
16. Foo, S.Y. and S. Phipps, Regulation of inducible BALT formation and contribution to immunity and pathology. Mucosal Immunol, 2010. 3(6): p. 537-44.
17. Corr, S.C., C.C. Gahan, and C. Hill, M-cells: origin, morphology and role in mucosal immunity and microbial pathogenesis. FEMS Immunol Med Microbiol, 2008. 52(1): p. 2-12.
18. Huang da, W., B.T. Sherman, and R.A. Lempicki, Systematic and integrative analysis of large gene lists using DAVID bioinformatics resources. Nat Protoc, 2009. 4(1): p. 44-57.
19. Peters, A., *et al.*, Podoplanin negatively regulates CD4+ effector T cell responses. J Clin Invest, 2015. 125(1): p. 129-40.
20. Miki, Y., *et al.*, Lymphoid tissue phospholipase A2 group IID resolves contact hypersensitivity by driving antiinflammatory lipid mediators. J Exp Med, 2013. 210(6): p. 1217-34.
21. Knolle, M.D., *et al.*, Adam8 limits the development of allergic airway inflammation in mice. J Immunol, 2013. 190(12): p. 6434-49.
22. Rantakari, P., *et al.*, The endothelial protein PLVAP in lymphatics controls the entry of lymphocytes and antigens into lymph nodes. Nat Immunol, 2015. 16(4): p. 386-96.
23. O'Regan, A., The role of osteopontin in lung disease. Cytokine Growth Factor Rev, 2003. 14(6): p. 479-88.
24. Chen, G., *et al.*, Polarizing the T helper 17 response in Citrobacter rodentium infection via expression of resistin-like molecule alpha. Gut Microbes, 2014. 5(3): p. 363-8.
25. von Allmen, C.E., *et al.*, Secretory phospholipase A2-IID is an effector molecule of CD4+CD25+ regulatory T cells. Proc Natl Acad Sci U S A, 2009. 106(28): p. 11673-8.
26. Mattoo, S. and J.D. Cherry, Molecular pathogenesis, epidemiology, and clinical manifestations of respiratory infections due to *Bordetella pertussis* and other Bordetella subspecies. Clin Microbiol Rev, 2005. 18(2): p. 326-82.
27. de Gouw, D., *et al.*, Pertussis: a matter of immune modulation. FEMS Microbiol Rev, 2011. 35(3): p. 441-74.
28. Flornes, L.M., *et al.*, Identification of lectin-like receptors expressed by antigen presenting cells and neutrophils and their mapping to a novel gene complex. Immunogenetics, 2004. 56(7): p. 506-17.
29. Rahim, M.M., *et al.*, Ly49 receptors: innate and adaptive immune paradigms. Front Immunol, 2014. 5: p. 145.
30. Sasawatari, S., *et al.*, The Ly49Q receptor plays a crucial role in neutrophil polarization and migration by regulating raft trafficking. Immunity, 2010. 32(2): p. 200-13.
31. Monticelli, L.A., *et al.*, Innate lymphoid cells promote lung-tissue homeostasis after infection with influenza virus. Nat Immunol, 2011. 12(11): p. 1045-54.
32. Sato, S., *et al.*, Transcription factor Spi-B-dependent and -independent pathways for the development of Peyer's patch M cells. Mucosal Immunol, 2013. 6(4): p. 838-46.
33. Hase, K., *et al.*, Uptake through glycoprotein 2 of FimH(+) bacteria by M cells initiates mucosal immune response. Nature, 2009. 462(7270): p. 226-30.
34. Lo, D., *et al.*, Peptidoglycan recognition protein expression in mouse Peyer's Patch follicle associated epithelium suggests functional specialization. Cell Immunol, 2003. 224(1): p. 8-16.
35. Pabst, R. and T. Tschernig, Bronchus-associated lymphoid tissue: an entry site for antigens for successful mucosal vaccinations? Am J Respir Cell Mol Biol, 2010. 43(2): p. 137-41.
36. Pelaseyed, T., *et al.*, The mucus and mucins of the goblet cells and enterocytes provide the first defense line of the gastrointestinal tract and interact with the immune system. Immunol Rev, 2014. 260(1): p. 8-20.

37. Dietert, K., *et al.*, mCLCA3 modulates IL-17 and CXCL-1 induction and leukocyte recruitment in murine Staphylococcus aureus pneumonia. PLoS One, 2014. 9(7): p. e102606.
38. 38. Carbonetti, N.H., *et al.*, Pertussis toxin plays an early role in respiratory tract colonization by *Bordetella pertussis*. Infect Immun, 2003. 71(11): p. 6358-66.
39. Warfel, J.M., *et al.*, Nonhuman primate model of pertussis. Infect Immun, 2012. 80(4): p. 1530-6.
40. Wirsing von Konig, C.H., Pertussis diagnostics: overview and impact of immunization. Expert Rev Vaccines, 2014. 13(10): p. 1167-74.
41. Eon Kuek, L., *et al.*, The MS4A family: counting past 1, 2 and 3. Immunol Cell Biol, 2015.
42. Stroncek, D.F., *et al.*, Expression of neutrophil antigens after 10 days of granulocyte-colony-stimulating factor. Transfusion, 1998. 38(7): p. 663-8.
43. Chen, B.D., M. Mueller, and T.H. Chou, Role of granulocyte/macrophage colony-stimulating factor in the regulation of murine alveolar macrophage proliferation and differentiation. J Immunol, 1988. 141(1): p. 139-44.
44. Guth, A.M., *et al.*, Lung environment determines unique phenotype of alveolar macrophages. Am J Physiol Lung Cell Mol Physiol, 2009. 296(6): p. L936-46.
45. Bernard, N.J., *et al.*, A critical role for the TLR signaling adapter Mal in alveolar macrophage-mediated protection against *Bordetella pertussis*. Mucosal Immunol, 2015. 8(5): p. 982-92.
46. Vukman, K.V., *et al.*, Mannose receptor and macrophage galactose-type lectin are involved in *Bordetella pertussis* mast cell interaction. J Leukoc Biol, 2013. 94(3): p. 439-48.
47. Netea, M.G., J. Quintin, and J.W. van der Meer, Trained immunity: a memory for innate host defense. Cell Host Microbe, 2011. 9(5): p. 355-61.
48. Netea, M.G., Training innate immunity: the changing concept of immunological memory in innate host defence. Eur J Clin Invest, 2013. 43(8): p. 881-4.
49. Hirota, K., *et al.*, Preferential recruitment of CCR6-expressing Th17 cells to inflamed joints via CCL20 in rheumatoid arthritis and its animal model. J Exp Med, 2007. 204(12): p. 2803-12.
50. Lee, L.N., *et al.*, CXCR6 is a marker for protective antigen-specific cells in the lungs after intranasal immunization against *Mycobacterium tuberculosis*. Infect Immun, 2011. 79(8): p. 3328-37.
51. Ito, T., *et al.*, CCR6 as a mediator of immunity in the lung and gut. Exp Cell Res, 2011. 317(5): p. 613-9.
52. Hellwig, S.M., *et al.*, Immunoglobulin A-mediated protection against *Bordetella pertussis* infection. Infect Immun, 2001. 69(8): p. 4846-50.
53. Raeven, R.H.M., *et al.*, Immunoproteomic Profiling of *Bordetella pertussis* Outer Membrane Vesicle Vaccine Reveals Broad and Balanced Humoral Immunogenicity. J Proteome Res, 2015. 14(7): p. 2929-42.
54. Elgueta, R., *et al.*, CCR6-dependent positioning of memory B cells is essential for their ability to mount a recall response to antigen. J Immunol, 2015. 194(2): p. 505-13.
55. Mascart, F., *et al.*, Modulation of the infant immune responses by the first pertussis vaccine administrations. Vaccine, 2007. 25(2): p. 391-8.
56. Mielcarek, N., *et al.*, Live attenuated *B. pertussis* as a single-dose nasal vaccine against whooping cough. PLoS Pathog, 2006. 2(7): p. e65.
57. Feunou, P.F., *et al.*, Long-term immunity against pertussis induced by a single nasal administration of live attenuated *B. pertussis* BPZE1. Vaccine, 2010. 28(43): p. 7047-53.
58. Fedele, G., *et al.*, Attenuated *Bordetella pertussis* vaccine candidate BPZE1 promotes human dendritic cell CCL21-induced migration and drives a Th1/Th17 response. J Immunol, 2011. 186(9): p. 5388-96.
59. Pennings, J.L., *et al.*, Gene expression profiling in a mouse model identifies fetal liver- and placenta-derived potential biomarkers for Down Syndrome screening. PLoS One, 2011. 6(4): p. e18866.

Supplementary information

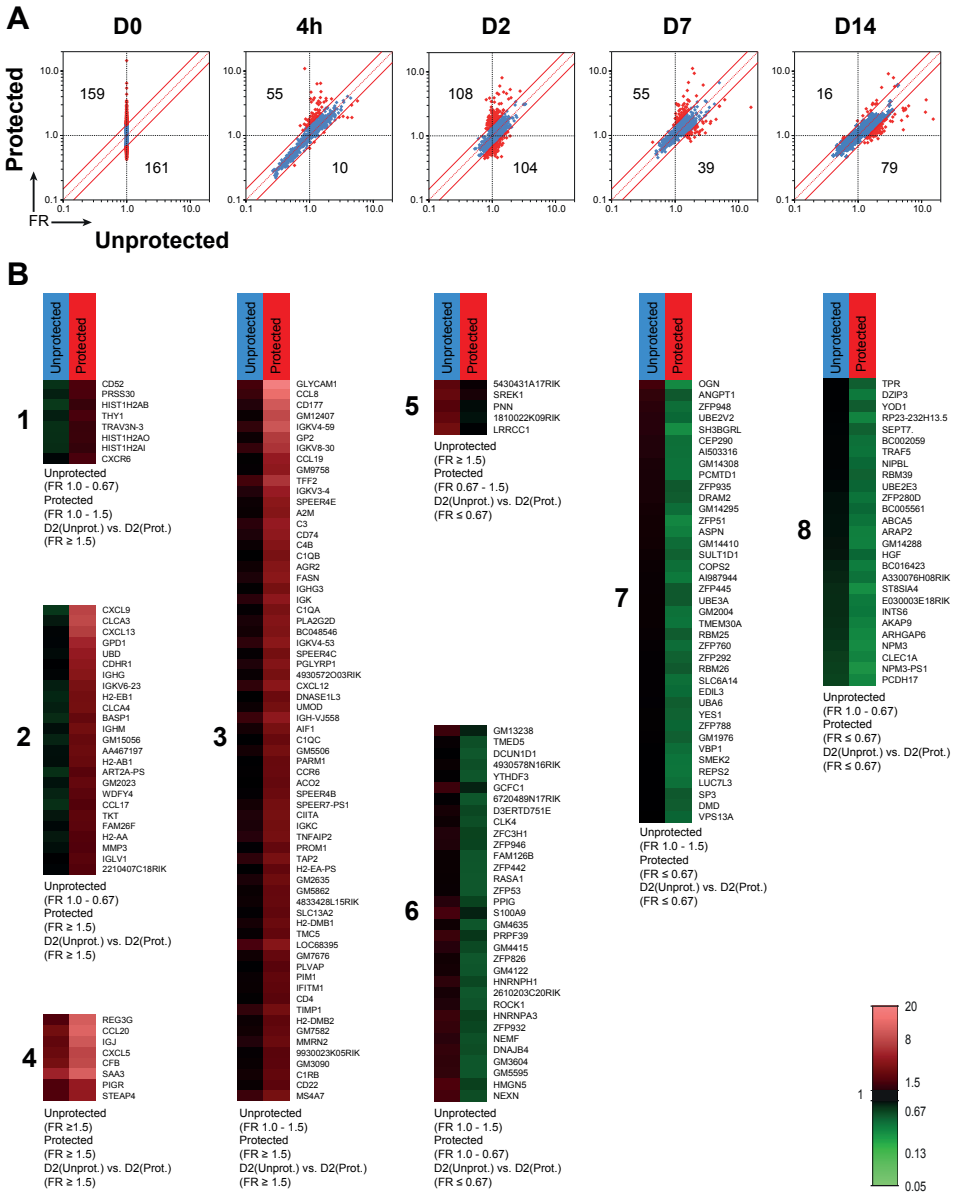

Figure S1 - Comparison of pulmonary transcriptomic profiles between unprotected and protected mice per time point. **(A)** The fold ratios (FR) of all 786 differentially regulated genes compared to non-infected naive mice for both unprotected and protected mice were portrayed as scatter plot at all five time points. At each time point, for each gene, the FR was calculated between unprotected and unprotected mice. All genes that were differently expressed (FR ≥ 1.5 or ≤ 0.67) were depicted in red. The number of upregulated and downregulated genes is given for each comparison. **(B)** The 212 genes that were found differently expressed (FR ≥ 1.5 or ≤ 0.67) between unprotected and protected mice 2 days p.c. in **Figure 2D** were divided in in eight fractions based on upregulation (1-4) or downregulation (5-8). These genes are depicted as heatmap per fraction with additional information on the FR of these genes in unprotected mice and protected mice compared to non-infected naive mice.

About the cover: Dried surface of Salar de Uyuni in Bolivia. The world's largest salt flat located on the Altiplano at 3,656 metres above sea level.

CHAPTER 4

Immunoproteomic profiling of *Bordetella pertussis* outer membrane vesicle vaccine reveals broad and balanced humoral immunogenicity

René H.M. Raeven[1,2], Larissa van der Maas[1], Wichard Tilstra[1], Joost P. Uittenbogaard[1], Tim H.E. Bindels[1], Betsy Kuipers[3], Arno van der Ark[1], Jeroen L.A. Pennings[4], Elly van Riet[1], Wim Jiskoot[2], Gideon F.A. Kersten[1,2], Bernard Metz[1]

[1]Institute for Translational Vaccinology (Intravacc), Bilthoven, The Netherlands
[2]Division of Drug Delivery Technology, Leiden Academic Centre for Drug Research, Leiden, The Netherlands
[3]Centre for Infectious Disease Control, National Institute for Public Health and the Environment (RIVM), Bilthoven, The Netherlands
[4]Centre for Health Protection (GZB), National Institute for Public Health and the Environment (RIVM), Bilthoven, The Netherlands

Journal of Proteome Research. 2015 14(7):2929-42.

Abstract

The current resurgence of whooping cough is alarming and improved pertussis vaccines are thought to offer a solution. Outer membrane vesicle vaccines (omvPV) are potential vaccine candidates, but omvPV-induced humoral responses have not yet been characterized in detail. The purpose of this study was to determine the antigen composition of omvPV and to elucidate the immunogenicity of the individual antigens. Quantitative proteome analysis revealed the complex composition of omvPV. The omvPV immunogenicity profile in mice was compared to those of classic whole-cell vaccine (wPV), acellular vaccine (aPV) and pertussis infection. Pertussis-specific antibody levels, antibody isotypes, IgG subclasses, and antigen specificity were determined after vaccination or infection by using a combination of multiplex immunoassays, 2-dimensional immunoblotting and mass spectrometry. The vaccines and infection raised strong antibody responses, but large quantitative and qualitative differences were measured. The highest antibody levels were obtained by omvPV. All IgG subclasses (IgG1/IgG2a/IgG2b/IgG3) were elicited by omvPV and in a lower magnitude by wPV, but not by aPV (IgG1) or infection (IgG2a/b). The majority of omvPV-induced antibodies were directed against Vag8, BrkA and LPS. The broad and balanced humoral response makes omvPV a promising pertussis vaccine candidate.

Study design

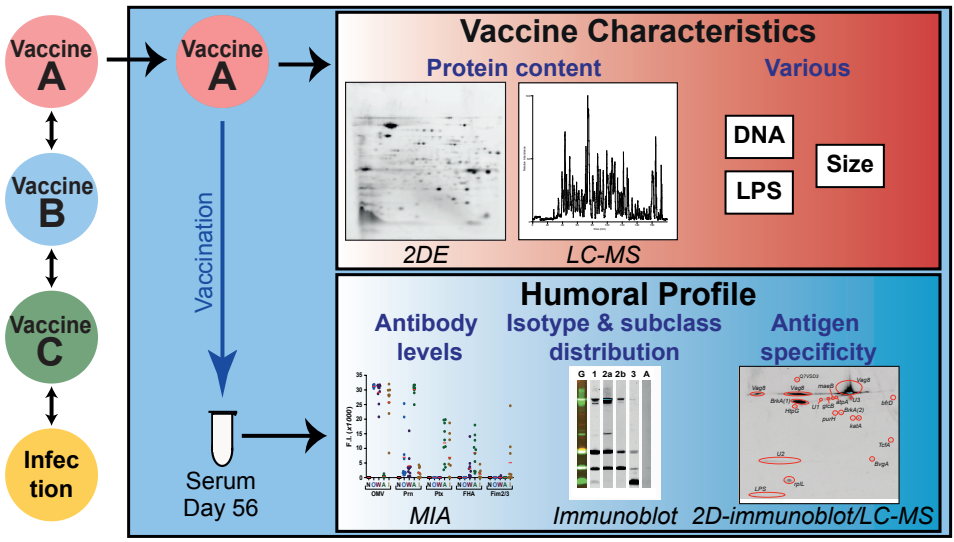

Introduction

The resurgence of whooping cough in the vaccinated population [1-4] demands improved pertussis vaccines. Two types of pertussis vaccines are marketed: whole-cell (wPV) and acellular vaccines (aPV). Other types are under development, such as live attenuated and outer membrane vesicle pertussis vaccines (omvPV) [5, 6]. These vaccines differ largely in their composition. The first marketed vaccines were wPVs, which are inactivated bacteria that are naturally adjuvated with bacterial components, such as lipopolysaccharide (LPS) [6-8]. Despite an acceptable vaccine efficacy, wPVs were found to be reactogenic due to the presence of endotoxins. This lead to the development of alum-adjuvated aPVs containing one to five purified pertussis antigens: pertussis toxoid (Ptd), filamentous hemagglutinin (FHA), pertactin (Prn), and fimbriae types 2 and 3 (Fim2 and Fim3). Despite low reactogenicity of aPVs, waning immunity [9, 10] and persistent transmission of *Bordetella pertussis* [11] call for reevaluation of aPVs. To retain high vaccine compliance, the target product profile of an improved pertussis vaccine should include better efficacy compared to aPV while maintaining a low reactogenicity.

Currently, antibodies are used as correlates of vaccine-induced immunity for most commercial vaccines [12], including pertussis vaccines [13, 14]. The protective role of pertussis antibodies was supported by passive immunization studies in naive mice [15, 16], though cellular responses may also contribute to protection, at least during infection [17, 18]. Antibody responses can be characterized by several parameters, including (i) antigen specificity, (ii) titer, (iii) isotype and subclasses, and (iv) avidity. The IgG antibody subclass profile reflects the T-helper (Th) cell environment [19, 20]. For instance, vaccination with aPV results in the formation of IgG1 antibodies and Th2 cells [21, 22]. Contrarily, vaccination with wPV generates a Th1/Th17 response [23] which is thought to be important for protection against *B. pertussis* [17, 18, 23]. The functionality of the antibodies is determined by antigen specificity, avidity and antibody subclass. This determines the ability of antiserum to kill bacteria directly or by opsonophagocytic killing through activation of Fc-receptors (FcRs) on phagocytes, with an important role for FcγRs in the clearance of *B. pertussis* [24, 25]. For aPV vaccines, antibodies against pertussis toxin (Ptx) and Prn are considered to be protective against a *B. pertussis* infection [13, 26, 27]. For wPV, many immunogenic proteins have been identified by 2D-electrophoresis and western blotting [8, 28, 29]. The humoral immune response generated by omvPV is not well defined, although some major antigens were identified [30] and long-lasting immunity observed [31].

In this study, the systemic humoral response after immunization of mice with an experimental omvPV was compared with the response elicited by classic vaccines, aPV and wPV. Multiplex immunoassays, gel electrophoresis, immunoblotting and mass spectrometry were used to

identify the immunogenic antigens and the subclass profiles they induced. Because mice develop sterilizing immunity after a pertussis infection [18], antisera from *B. pertussis*-infected mice were included for comparison.

Materials and Methods

Vaccines

B. pertussis B1917 was heat-inactivated (30 min, 56°C) in PBS to produce wPV. Outer membrane vesicles from *B. pertussis* B1917 (omvPV) were produced as previously described [32] with minor changes. Both wPV and omvPV were diluted in PBS to a final concentration of 4 µg total protein per vaccine dose (300 µl). One human dose of a tetanus-diphtheria-3-component (25 µg pertussis toxoid, 25 µg filamentous hemagglutinin, and 8 µg pertactin) acellular pertussis vaccine (TDaP, Infanrix, GSK) was diluted in PBS (aPV) to a final concentration of 0.25 µg Ptd, 0.25 µg FHA, and 0.08 µg Prn per vaccine dose (300 µl).

Dynamic Light Scattering (DLS)

Particle size was determined by analyzing 0.5 ml of vaccine stock solutions diluted in PBS (1:100) at 25°C using a Zetasizer Nano-ZS (Malvern Instruments). For each sample, three records of 12 scans were obtained. The Z-average particle size and polydispersity index (PdI) were calculated using DTS Nano software (Malvern Instruments).

Double stranded (ds) DNA quantitation

Samples were diluted in Tris EDTA (TE) buffer (Invitrogen). Salmon sperm ds-DNA (Invitrogen) was used as standard (0 – 2500 ng/ml). In a V-bottom (black) 96-wells plate, 50 µl of each sample or standard was incubated with 50 µl of PicoGreen reagent solution (Invitrogen). Fluorescence intensity (excitation 480 nm, emission 520 nm) was measured by using a SynergyMx (BioTek Instruments, USA). Concentration of dsDNA was calculated based on the standard curve.

LPS analysis

LPS concentration was determined by analyzing fatty acid composition with a modified gas chromatography method [33]. The peak height of C14:0-3OH was used to quantify LPS, while C12:0-2OH was used as the internal standard. The molecular weight (4057 g/mol [34]) of *B. pertussis* LPS was used to calculate the LPS-concentrations.

Challenge culture

A stock suspension of *B. pertussis* strain B1917 was diluted with Verweij medium (BBio, Bilthoven, The Netherlands) to a final concentration of $5x10^6$ colony-forming units (cfu)/ml. The cfu concentration was confirmed by plating 100 µL of the bacterial suspension (after 2000-fold dilution in Verweij medium) on Bordet-Gengou agar plates (Cat. no. 254400, BD, The Netherlands). Plates were incubated for 4 days at 35°C and the number of colonies was counted by using a ProtoCOL colony counter (Synbiosis, Cambridge, United Kingdom).

Animal experiment

An independent ethical committee for animal experimentations of the Institute for Translational Vaccinology (Intravacc) approved the animal experiment. Female BALB/c mice (Harlan, The Netherlands), 8-week-old, were divided in five groups of ten animals and housed in cages (macrolon III including filter top). Group 1 remained naive. Groups 2, 3 and 4 were vaccinated twice with 300 µl omvPV (4 µg total protein), 300 µl wPV (4 µg total protein) and 300 µl aPV (1:100 HD in PBS), respectively, on day 0 and day 28. Vaccinations with omvPV, wPV, and aPV were administered subcutaneously in the left groin for primary vaccination, followed by booster vaccination in the right groin. Group 5 was intranasally infected under anesthesia (isoflurane/oxygen), with $2x10^5$ CFU *B. pertussis* B1917 in 40 µl Verweij medium on day 0. Mice in all groups were bled, under anesthesia (isoflurane/oxygen), by orbital bleeding and euthanized by cervical dislocation on day 56. Whole blood was collected in blood collection tubes (MiniCollect 0.8ml Z Serum Sep GOLD, Greiner Bio-One, Austria). After coagulation (10 min. at room temperature (RT)), sera were collected by centrifugation (10 min., 3000 g) and stored at -80°C for further use.

Multiplex immunoassay

Serum total IgA, IgG, and IgG subclasses (IgG1, IgG2a, IgG2b and IgG3) levels against pertactin (Prn), filamentous hemagglutinin (FHA), pertussis toxin (Ptx), combined fimbriae type 2 and 3 antigens (Fim2/3), and outer membrane vesicles B1917 (OMV B1917) were determined using a multiplex immunoassay (MIA). Conjugation of OMVs and purified antigens to beads was performed as described previously [35]. Serum was diluted 100-fold or 1250-fold in PBS containing 0.1% Tween 20 and 3% bovine serum albumin and mixed 1:1 (v/v) with 25 µl conjugated beads (4,000 beads/region/well). After incubation with *R*-Phycoerythrin (RPE)-conjugated anti-mouse IgA (1:100), IgG (1:200), IgG1 (1:200), IgG2a (1:40), IgG2b (1:200) and IgG3 (1:200) (Southern Biotech), samples were analyzed by using a Bio-Plex system (Bio-Plex 200, BioRad). Results for antibody levels were illustrated with GraphPad Prism 6.04 (GraphPad Software Inc., USA), and presented in fluorescent intensity (F.I.).

Protein digestion by proteinase K treatment

For protein digestion, 5 µg *B. pertussis* B1917 was incubated (Overnight (ON), 56°C) with 5 µl (20 mg/ml) proteinase K (Proteinase K, recombinant, PCR Grade, Roche). Incubation was terminated by heating the sample for 5 minutes at 100°C.

Sample preparation

Protein concentrations were determined using a bicinchoninic acid (BCA) assay (Pierce). For SDS-PAGE, *B. pertussis* B1917 (100 µg) was denatured in a total volume of 100 µl 8 M urea (GE Healthcare) in 500 mM bicarbonate (Merck) solution (pH 8.5, 1 h, RT). For 2DE, *B. pertussis* B1917 (100 µg) was centrifuged (1 min., 16200 g) and the pellet was dissolved and denatured in 100 µl DeStreak Rehydration Solution (GE Healthcare) (1h, RT).

Infrared labeling

IR680 label (15 µg) (Pierce) and IR800 label (100 µg) (Licor) were reconstituted in 100 µl and 25 µl water, respectively. For conjugation of IR800 label to secondary antibodies, 100 µl goat-anti-mouse IgG, IgG1, IgG2a, IgG2b, IgG3 or IgA (Southern Biotech) was mixed with 1 µl (4 µg) IR800 label. For IR680 labeling of *B. pertussis* proteins, 100 µg denatured proteins were mixed with 10 µl IR680 label with optimized concentrations. For 1DE gels and corresponding western blots, a 1:10 and 1:100 dilution of IR-680 stock (0.15 µg/ml) were used, respectively. For 2DE, an undiluted and 1:20 dilution of IR-680 stock (0.15 µg/ml) were used for gels and western blot, respectively. All samples were incubated for 1 hour (RT, in the dark). Subsequently, unbound IR label was removed from samples by using a ZEBA spin desalting column (Pierce) (2 min, 1500 g).

Isoelectric focusing (IEF)

After sample preparation and IR-labeling, samples for 2DE (25 µg *B. pertussis* proteins) were incubated (60 min., RT) in a total volume of 115 µl DeStreak Rehydration Solution plus 10 µl 250 mM DTT and 0.62 µl (0.5%) IPG Buffer pH 3-10NL (GE Healthcare). Immobiline DryStrip pH 3-10NL, 7 cm (GE Healthcare) were rehydrated (ON, RT) with protein sample in an IPGbox (GE Healthcare). Isoelectric focusing (IEF) was performed in an Ettan IPGphor 3 IEF system (GE Healthcare) according to the following conditions: 0.5 h at 300 V, 0.5 h at 1000 V, 1 h at 2000 V, 1 h at 3000 V, 1 h at 4000 V, and 1 h at 5000 V. After IEF, strips were equilibrated in 3 ml equilibration buffer (75 mM Tris-HCl pH 8.8, 6 M urea, 30% glycerol, 2% SDS, and bromophenol blue) with DTT (65 mM) for 15 min. at RT, followed by 3 ml equilibration buffer with iodoacetamide (54 mM) for 15 min. at RT.

Gel electrophoresis

For SDS-PAGE, 10 µg *B. pertussis* (B1917) lysate, 1 µg of Prn P.69 (in house prepared [36]), Ptx (Kaketsuken, Japan), FHA (Kaketsuken, Japan), or Fim2/3 (Sanofi) were incubated (10 min., 100°C) with 3.3 µl reducing sample buffer (250 mM Tris, 8% SDS, 400 mM DTT, 40% Glycerol, 0.04% bromophenol blue) and loaded on a 10% NuPAGE bis tris 1.0-mm precast gel (Invitrogen). For 2DE, the equilibrated strip was placed on a 4-12% NuPAGE Novex bis-tris ZOOM gel (Invitrogen) and sealed with agarose sealing buffer (Bio-rad). Proteins were separated (SDS-PAGE, 45 min., 200 V) (2DE, 50 min., 200 V) with MES running buffer (Invitrogen) in a Xcell surelock minicell electrophoresis system (Invitrogen). Gels were washed in water and either stained with Coomassie (Imperial protein stain, Thermo Scientific), used for western blot or scanned using an Odyssey infrared imager (Westburg).

Western blotting

Nitro-cellulose membrane (Biorad), filters (Biorad) and gel were equilibrated in transfer buffer (48 mM Tris, 39 mM glycine, 20% methanol in 1 liter water). Subsequently, proteins were transferred (60 min., 60 mA) (TE77 semidry pwr transfer unit, Amersham Biosciences) from

the acrylamide gel to the nitro-cellulose membrane. Blot was blocked in block buffer (0.5% protifar in TBS-T, 20 mM Tris, 150 mM NaCl, 0.5% Tween-20 in 1 liter water) (ON, 4°C). Blot was incubated (2 h, RT) with pooled murine sera (100-fold diluted in block buffer) or a monoclonal anti-LPS antibody (Mab 88F3) (1:200) followed by frequent washing with TBS-T. Subsequently, secondary antibody incubation (1 h, RT) was performed using goat-anti-mouse IgG, IgG1, IgG2a, IgG2b, IgG3 or IgA (Southern Biotech) labeled with IR800 (Licor) (1:5000 diluted in block buffer), which was followed by frequent washing with TBS-T. Blots were scanned using an Odyssey infrared imager.

Delta2D analysis

Image warping and spot detection on 2DE gels and western blots were done by using Delta2D software (Version 4.5) (Decodon, Germany). Images of 2DEWB using five distinct sera (omvPV, wPV, aPV, infection and control) were merged by using the Delta2D group warping strategy for IgA, IgG and IgG subclasses individually. Subsequently, spot detection was performed and the intensities were measured in grey values.

In-gel protein digestion for LC-MS/MS analysis

Spots were manually excised from the acrylamide gel. In-gel digestion was performed according to a protocol based on Yan *et. al* [37]. Briefly, individual gel spots were cut in pieces of about 1 mm3 and washed three times with water, followed by washings with 50% acetonitrile and 100% acetonitrile for dehydration. Trypsin (Promega) digestion (pH 8.5, ON, 37°C) was performed in 50 mM triethyl ammonium bicarbonate. Peptides were extracted with three sequential steps of 5% formic acid solution and extracts were dried in a vacuum concentrator. Peptides were dissolved in formic acid/dimethyl sulfoxide (DMSO)/water (0.1/5/94.9% v/v) for LC-MS/MS analysis.

Protein digestion for LC-MS/MS analysis

Samples (omvPV or wPV) were diluted in a denaturation buffer containing 1 M guanidine hydrochloride (Gnd-HCl) and 50 mM triethyl ammonium bicarbonate, pH 8.5, to a final concentration of 0.5 mg/ml protein. For digestion, 100 µg of protein was digested with 2 µl of 0.25 µg/µl endoproteinase Lys-C (Roche) followed by incubation (4h, 37°C). Subsequently, digests were incubated (ON, 37°C) with 2 µl of 0.5 µg/µl trypsin (Promega). The samples were stored at –20 °C before dimethyl labeling. A common reference was prepared by mixing equal volumes of both omvPV and wPV digests. The samples and common reference were dimethylated by treatment with formaldehyde (CH_2O) and d2-formaldehyde (CD_2O) and sodium cyanoborohydride, respectively, and subsequently pooled in a 1:1 w/w ratio [38]. Solid-phase extraction was performed to remove excess reagents using C18 Sep-pack cartridges according to the manufacturer's protocol. Peptides were dried in a vacuum concentrator. Peptides were dissolved in formic acid/DMSO/water (0.1/5/94.9% v/v) for LC-MS/MS analysis.

Peptide identification by LC-MS/MS analysis

Samples were analyzed by nano-scale reversed-phase liquid chromatography electrospray mass spectrometry, according to the method by Meiring *et al.* [39]. The analysis was performed on LTQ-Orbitrap XL mass spectrometer (Thermo Fisher Scientific, Germany). Analytes were loaded on a trapping column (Reprosil-Pur C18-AQ 5 µm (Dr. Maish, Germany); 23 mm long x 100 µm inner diameter) with solvent A (0.1% (v/v) formic acid in water) in 10 min. at 5 µl/min. The analytes were separated by reversed-phase chromatography on an analytical column (Reprosil-Pur C18-AQ 3 µm (Dr. Maish, Germany); 36.2 cm long x 50 µm inner diameter) at a flow rate of 100-150 nl/min. A gradient was started with solvent B (0.1% (v/v) formic acid in acetonitrile): 6% to 28% in 130 min, 28% to 38% in 10 min and 90% for 10 min. After the gradient, the columns were equilibrated in 100% solvent A for 20 min at 100-150 nl/min. The peptides were measured by data-dependent scanning; comprising a MS-scan (m/z 300 – 1500) in the orbitrap with a resolution of 60,000 (FWHM), followed by collision-induced dissociation (LTQ) of the ten most abundant ions of the MS spectrum. The threshold value for these precursor ions was set at 1000 counts. The normalized collision energy was set at 35% and isolation width at 2.0 Da, activation Q to 0.250 and activation time to 30 ms. The maximum ion time (dwell time) for MS scans was set to 250 ms and for MS/MS scans to 1000 ms. Precursor ions with unknown and +1 charge states were excluded for MS/MS analysis. Dynamic exclusion was enabled (exclusion list with 500 entries) with repeat set to 1 and an exclusion duration of 15s. The background ion at 391.28428 was used as lock mass for internal calibration.

Data handling for total vaccine protein digests

Proteome Discoverer software (version 1.4.1.14, Thermo) was used for peak area determination, identification and relative quantification of the LC-MS/MS raw data. Identification of peptides was performed by searching MS/MS spectra against the protein database of *B. pertussis* Tohama (NCBI 257313) (3261 entries) and *B. pertussis* B1917 (3513 entries) [40] using the SEQUEST HT mode. Asparagine deamidation and methionine oxidation were set as variable modifications and lysine dimethylation (light) as a fixed modification. The data were searched with full trypsin cleavage specificity, allowing 2 miscleavages. Precursor ion and MS/MS tolerances were set to 5 ppm and 0.6 Da, respectively. Peptides were filtered to 1% FDR using Perculator (Proteome Discoverer, Thermo). Relative protein concentrations were calculated using the quantification module of Proteome Discoverer using default settings (light: 28.013 Da, heavy 32.055 Da). The molar concentration of proteins was estimated according to Silva *et. al.* [41], except that the peptides were dimethyl-labeled in our method. The molar concentrations were converted to mass concentrations by multiplying with the molecular masses of the proteins. The percentage of protein abundance for each individual protein relative to the total sum of all identified proteins was used to determine an estimated protein amount in one vaccine dose (4 µg total protein) of wPV and omvPV.

Data handling for in-gel protein digests

Proteome Discoverer software was used for identification of the LC-MS/MS raw data for in-gel digested proteins almost in a similar way as described in data handling for total vaccine protein digests. Asparagine deamidation and methionine oxidation were set as variable modification. The data were searched with full trypsin cleavage specificity, allowing 2 miscleavages. Precursor ion and MS/MS tolerances were set to 5 ppm and 0.6 Da, respectively. Peptides were filtered to 1% FDR using Perculator.

Bioinformatics

Functional enrichment with an over-representation analysis (ORA) of the detected *B. pertussis* proteins was carried out by using DAVID [42] based on Gene Ontology Biological Processes (GO-BP), Molecular Function (GO-MF) and Cellular Component (GO-CC).

Results

Characteristics and composition of pertussis vaccines

The outer membrane vesicle vaccine (omvPV), heat-inactivated whole-cell vaccine (wPV), and acellular vaccine (aPV) were characterized with respect to particle size, DNA content, LPS concentration and protein composition (Table 1). OMVs were about ten times smaller in diameter (114 nm) than the inactivated bacteria in the wPV (1156 nm). Further, the omvPV contained a small amount of DNA per vaccine dose (0.2 µg) when compared to wPV (1.2 µg), whereas aPV contained undetectable levels of DNA. In addition, the LPS concentration was slightly lower in omvPV compared to wPV.

Table 1. Characteristics of the vaccines studied.

Characteristic	omvPV	wPV	aPV
Dose	4 µg B. *pertussis* proteins	4 µg *B. pertussis* proteins	0.25 µg FHA, 0.25 µg Ptx, 0.08 µg Prn
Z-average particle size (d.nm ± SD)	114 ± 1	1156 ± 37	N/M[1]
Polydispersity Index (PdI)	0.22	0.19	N/M
DNA[2] (µg ± SD)	0.18 ± 0.02	1.19 ± 0.15	0
LPS[2,3] (µg)	1.0	1.5	N/M
Number of proteins	268	332	3
Additional Adjuvant	-	-	$Al(OH)_3$

[1] N/M = Not measured.
[2] Based on the vaccine dose of 4 µg total protein for omvPV and wPV.
[3] Analysis n = 1 (All other analysis n = 3)

LC-MS analysis was performed to characterize total vaccine protein composition of omvPV and wPV. In total, 268 and 332 proteins were identified and quantified in omvPV and wPV, respectively (Table S1). Obviously, these numbers do not cover the identification of all proteins present in both vaccines, as *B. pertussis* has more than 3500 genes. However, this LC-MS method identified and quantified the most abundant proteins present in the vaccines. The quantity of different proteins differed remarkably between omvPV and wPV. For both vaccine formulations, the top 25 of most abundant proteins is shown in Figure 1A. The 25 proteins that are most abundant in omvPV cover 86% of the total protein content in omvPV. Autotransporters Vag8 (34%) and BrkA (24%) are the major antigens. The other proteins of the top 25 contributed each less than 5% of the total protein amount. For wPV, the top 25 of proteins of this vaccine covered 67% of the total protein content. GroEL (17%) and FHA (11%) were the most abundant proteins in wPV.

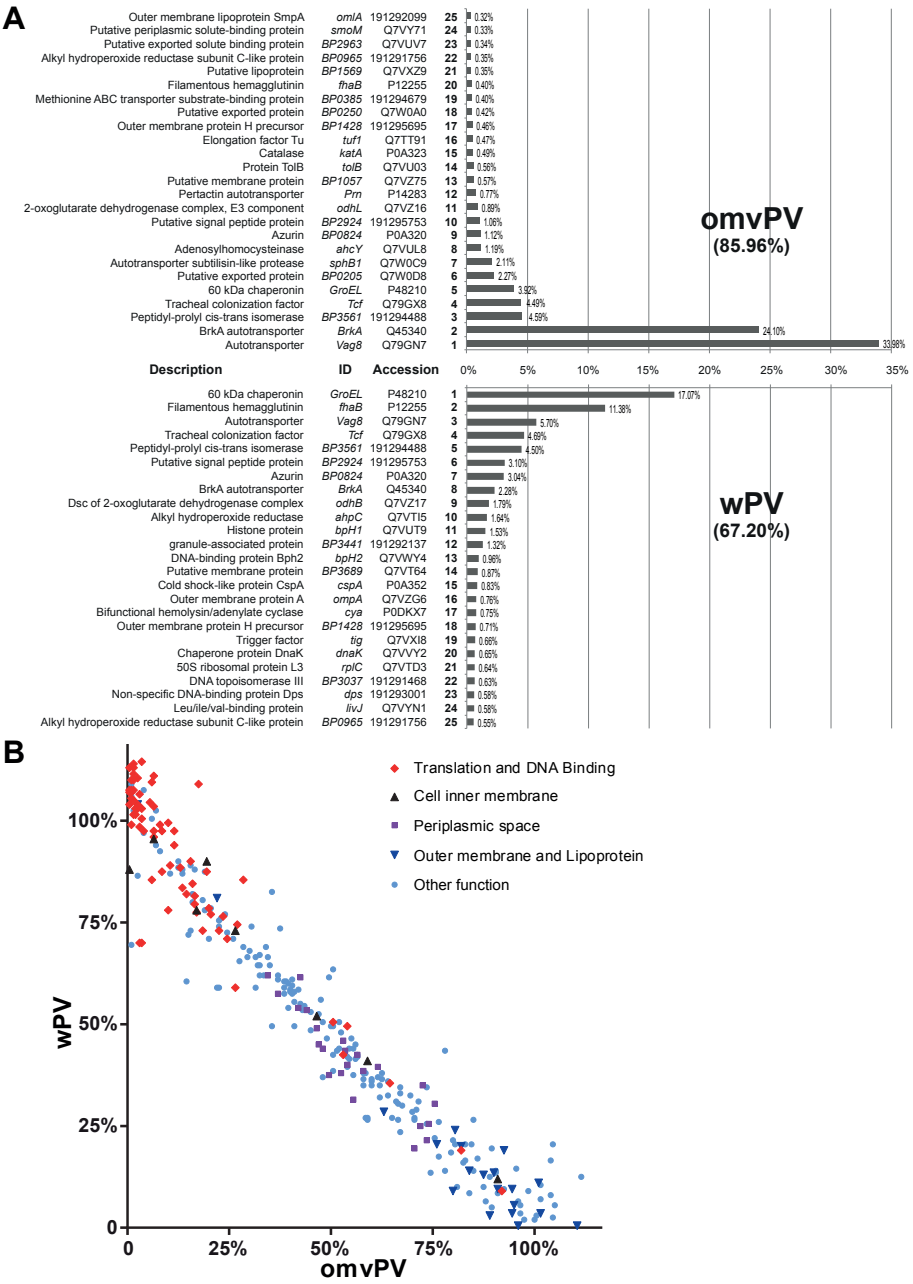

Figure 1 - Protein composition wPV and omvPV. **(A)** Proteins in omvPV and wPV were determined by quantitative LC-MS-analysis. Protein abundance is expressed as percentage of total detected protein content. The top 25 proteins cover 86.0% of the total protein content in the omvPV, compared to 67.2% in wPV. **(B)** For each individual protein, the amount in wPV was compared to omvPV and expressed as percentage as shown in the scatter plot. For instance, 50% - 50% indicate equal presence of a protein in both vaccines. Sum of percentages in omvPV and wPV is in principle 100%. Functional analysis indicates enrichment of proteins involved in translation, DNA binding and the cell inner membrane in wPV, while the outer membrane proteins and lipoproteins are enriched in the omvPV. Three technical replicates of both vaccines were characterized.

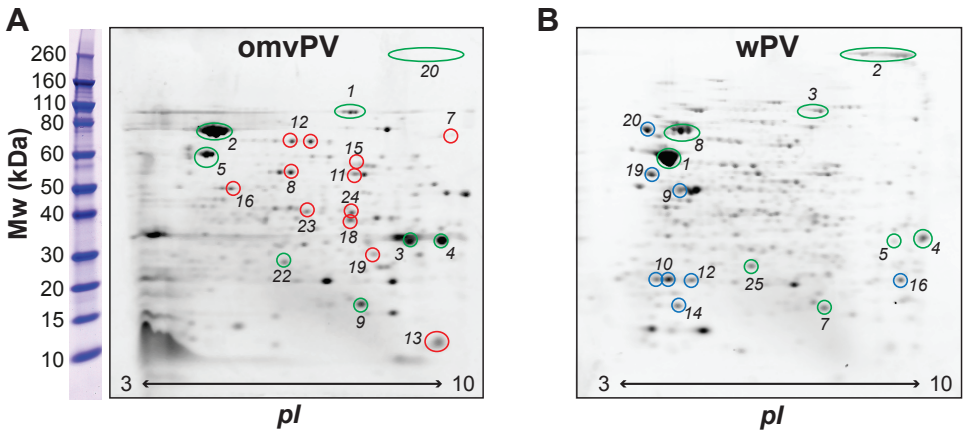

Figure 2 - Protein fingerprint of wPV and omvPV by 2-dimensional gel electrophoresis. Total protein lysates (25 µg total protein) of omvPV **(A)** and wPV **(B)** were separated by 2-dimensional gel electrophoresis. Gels were Coomassie stained and scanned on an Odyssey infrared imager (680 nm, Int. 5.0). Numbers in the gels correspond with the 25 most abundant proteins identified by LC-MS/MS analysis in either omvPV or wPV. Different colors correspond with proteins that are present in both vaccines (green), only present in omvPV (red), and only present in wPV (blue), respectively. For each vaccine, three technical replicates were characterized and one representative gel is presented.

Next, the relative amounts of each individual protein present in omvPV and wPV were compared between both vaccines (**Figure 1B**). In addition, functional analysis using DAVID [42] revealed that nuclear, cytoplasmic and inner membrane proteins were more abundant in wPV, whereas omvPV was enriched for outer membrane proteins and lipoproteins. Periplasmic proteins were present in similar amounts in both vaccines. The protein composition of aPV was not investigated, since it is specified by the manufacturer (one human dose contains 25 µg FHA, 25 µg Ptx and 8 µg Prn).

By using 2-dimensional electrophoresis (2DE), 182 spots were visualized in omvPV and 270 in wPV (**Figure 2A and 2B**, respectively). The most intense spots were isolated and the proteins present identified by LC-MS after in-gel protein digestion. The 25 most abundant proteins in omvPV as determined by total vaccine protein LC-MS analysis could also be recovered from the 2DE gels. For wPV, five proteins (bpH1, bpH2, cspA, rplC, BP3037) (see **Figure 1**) were not found by 2DE, presumably because their isoelectric point (pI) was outside the range (3-10) of the IPG-strip.

Serum levels and subclass distribution of antibodies against antigens in OMVs and aPV.

Serum IgG levels against purified antigens (Prn, Ptx, FHA and Fim2/3) as well as *B. pertussis* OMVs were determined in mice vaccinated subcutaneously with omvPV, wPV or aPV at day 0 and day 28. In addition, a group of mice was intranasally infected with *B. pertussis* at day 0. Vaccination with omvPV induced the highest concentration of anti-OMV IgG, followed by wPV and intranasal infection, whereas anti-OMV IgG was absent after aPV vaccination (**Figure 3A**

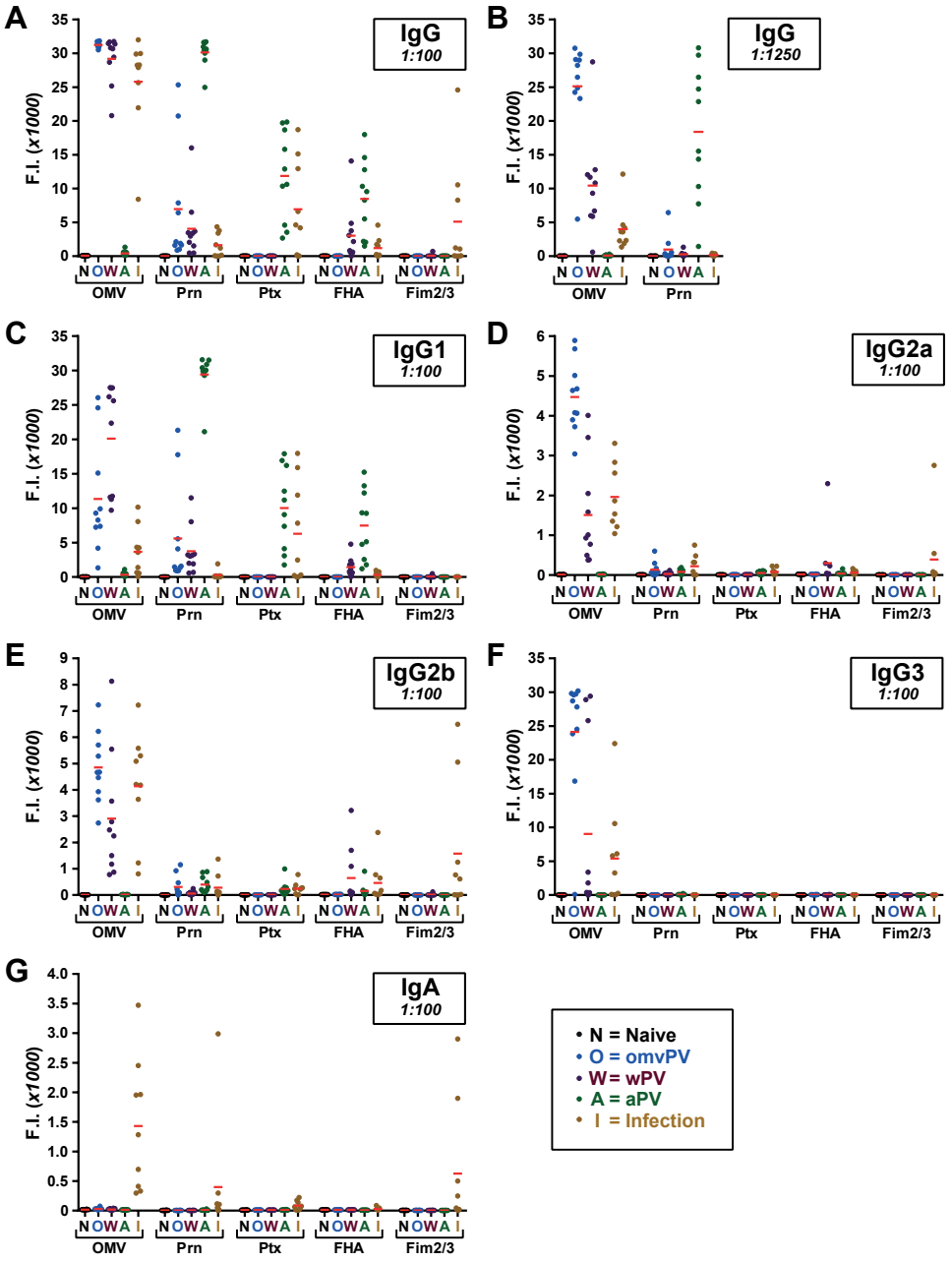

Figure 3 - Immunoproteomic profiling by multiplex immunoassay of different pertussis vaccines. **(A-G)** Antibody profiles against OMV, Prn, Ptx, FHA and Fim2/3 antigens (indicated at x-axes) were analyzed in serum of mice (n = 10). Each group of mice was either untreated (naive), received a different pertussis vaccine (omvPV, wPV, aPV), or underwent an intranasal infection. The intensity of all antibody concentrations is expressed in fluorescence intensity (F.I.). **(A)** The antibody levels were determined in 1:100 diluted sera. **(B)** Samples exceeding the detection limit were further analyzed by using a 1:1250 serum dilution. In addition, the antibody concentrations of IgG-subclasses **(C)** IgG1, **(D)** IgG2a, **(E)** IgG2b and **(F)** IgG3, as well as **(G)** IgA antibodies were determined in 1:100 diluted serum samples.

and 3B). As expected, vaccination with aPV induced antibodies against all components present in the vaccine: Prn, Ptx and FHA. Anti-Prn IgG antibodies were also detected upon omvPV and wPV vaccination. Anti-FHA IgG was measured after immunization with wPV, but not after vaccination with omvPV. *B. pertussis* infection resulted in high anti-Ptx IgG and moderate IgG levels against Prn and FHA. In addition, upon infection antibodies against Fim2/3, antigens that are present in certain other aPVs, were present in serum (Figure 3A).

Subsequently, IgG subclass (IgG1, IgG2a, IgG2b and IgG3) and IgA serum levels were determined (Figure 3C-G). Vaccination with omvPV and wPV generated antibodies of all IgG subclasses (IgG1, IgG2a, IgG2b and IgG3). However, the magnitude of the responses was lower in case

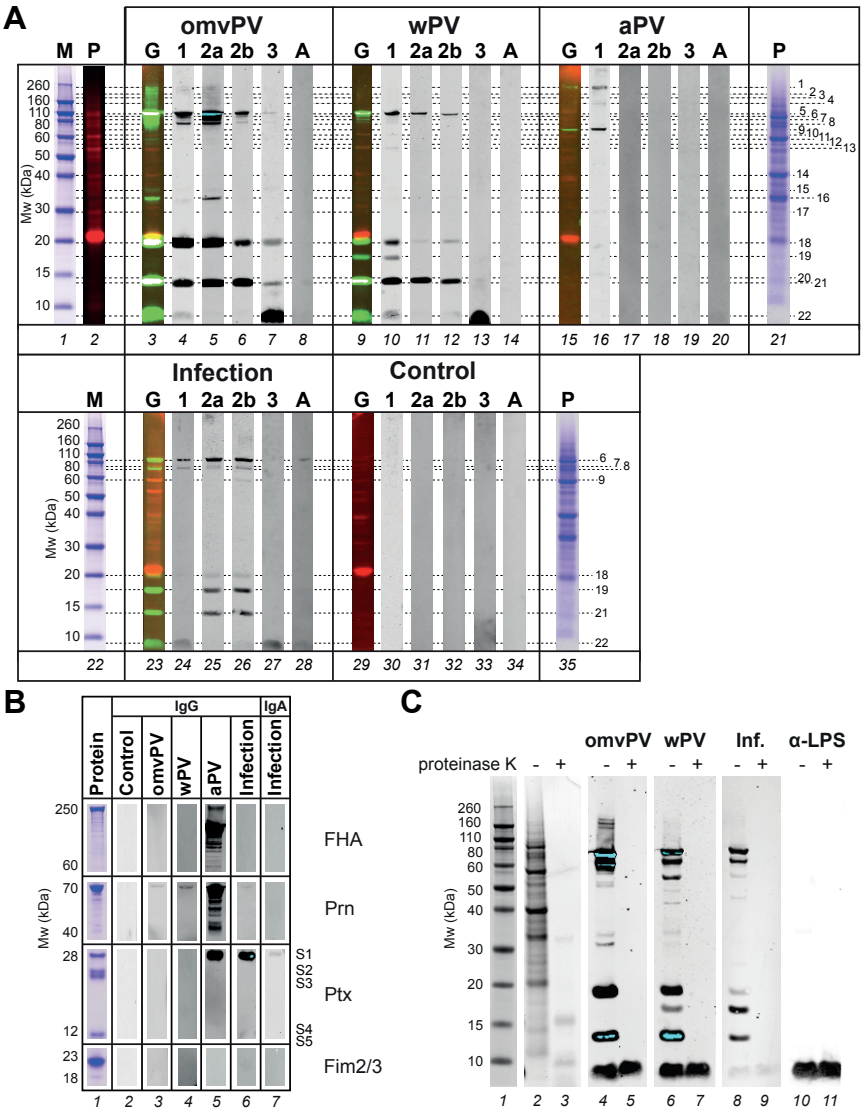

of wPV vaccination with the exception of IgG1. Vaccination with aPV induced antibodies solely of the IgG1 subclass. An intranasal infection induced predominantly IgG2a and IgG2b antibodies and was the only condition inducing measurable serum IgA antibodies (**Figure 3G**). After the infection of mice, high levels of serum IgA antibodies were detected binding to pertussis OMVs. In addition, IgA against Fim2/3, Prn or Ptx could be measured in some mice. No pertussis-specific antibodies were measured in serum of naive mice (**Figure 3A-G**).

Heterogeneity of antigen specificity and anti-LPS antibodies identified by using immunoblotting

A combination of 1-dimensional gel electrophoresis and western blotting (1DEWB) was used in order to identify the antigen-specificity of the antibody isotypes or subclasses elicited by the different vaccines (**Figure 4**). 1DEWB unraveled staining against 22 bands in a *B. pertussis* lysate, as marked in lane 21 and 35 (**Figure 4A**). The most intense staining was obtained with sera from omvPV-vaccinated mice. In addition, it was observed that antibody subclass formation is antigen specific in some cases. For instance, antibodies against band 16 were only formed upon omvPV vaccination and were exclusively of the IgG2a subclass. A broad subclass induction was observed in these sera for the other antigens (**Figure 4A, lane 3-8**). These results for IgG subclasses are in line with those of the MIA measurements, as are the results found for wPV (**Figure 4A, lane 9-14**), aPV (**Figure 4A, lane 15-20**), and infection (**Figure 4A, lane 23-28**). Untreated mice showed no staining on the Western blots (**Figure 4A, lane 29-34**).

Figure 4 (Left) - 1-Dimensional immunoproteomic profiles of pertussis vaccines. **(A)** *B. pertussis* B1917 proteins labeled with IR-680 were separated by SDS-PAGE (lane 2, P) (680 nm, Int. 5.0). Subsequently, blots were incubated with pooled serum of ten mice either vaccinated with omvPV (lane 3-8), wPV (lane 9-14), or aPV (lane 15-20), mice that underwent an intranasal infection (lane 23-28) or untreated mice (lane 29-34). Immunostaining was performed with six different IR-800-labeled goat-anti-mouse secondary antibodies (IgG, IgG1, IgG2a, IgG2b, IgG3 or IgA). Results for total IgG (G) are shown as dual staining (680 nm, Int. 5.0, 800 nm, Int. 8.0) with *B. pertussis* proteins in red and IgG antibodies in green. Blots with IgG subclasses and IgA display single staining for antibodies in grey/black. The 22 unique bands detected on one or more blots are marked on a Coomassie stained gel with *B. pertussis* B1917 proteins (P, lane 21 & 35). **(B)** Purified pertussis antigens (FHA, Prn, Ptx, Fim2/3) (1 µg) were individually separated on SDS-PAGE (Lane 1). Blots were incubated with serum of naive mice (lane 2), mice vaccinated either with omvPV (lane 3), wPV (lane 4), or aPV (lane 5) or mice that underwent an intranasal infection (lane 6-7). Subsequent IR800-labeled goat anti-mouse IgG incubation (1:5000) indicated IgG formation against FHA, Prn and Ptx in aPV vaccinated mice. In addition, anti-Prn was detected in omvPV and wPV vaccinated mice as well as infected mice. Both IgG (Lane 6) and IgA (lane 7) formation against Ptx was observed in serum upon intranasal infection. No antibody formation was observed against Fim2/3. **(C)** Coomassie stained *B. pertussis* B1917 proteins were untreated (-) (lane 2) or digested (+) (lane 3) with proteinase K. Western blot was performed with both treated and untreated *B. pertussis* by incubation with serum (1:100) of mice vaccinated either with omvPV (lane 4-5) or wPV (lane 6-7), or mice that underwent an intranasal infection (lane 8-9). Treatment with IR800-labeled anti-IgG (1:5000) (800 nm, Int. 7.0) showed that proteinase K treatment leads to diminished immunostaining in all sera except for the band at approximately 7kD. Anti-LPS incubation (1:200) showed a similar band (lane 10-11) (800 nm, Int. 4.0). Blue color in lanes 4 and 6 indicates saturation of signal obtained by the Odyssey scanner. For each condition, experiments were performed three times with pooled serum of 10 mice resulting in similar outcomes, and one representative blot is presented.

Since concentrations of Ptx, Prn, and Fim2/3 were low in the *B. pertussis* B1917 lysate used on the blot, the pools of serum of vaccinated mice were analyzed on blotted purified antigens (i.e. Ptx, Prn, Fim2/3 and FHA) (Figure 4B). This analysis revealed that the anti-Ptx antibodies detected upon both aPV vaccination (IgG) and infection with *B. pertussis* (IgG and IgA) were only directed against Ptx subunit 1 (Ptx S1) (Figure 4B). In addition, results revealed high anti-Prn, anti-FHA and anti-Ptx antibody formation after aPV vaccination, whereas these antibodies were not detectable or low in serum of mice vaccinated with omvPV or wPV. These results are in line with the observations made by MIA.

Since western blot analysis was performed on both untreated *B. pertussis* proteins and proteins digested with proteinase K, one non-proteinaceous band could be identified as LPS by using an anti-LPS monoclonal antibody (Figure 4C). Thus, a substantial fraction of the IgG

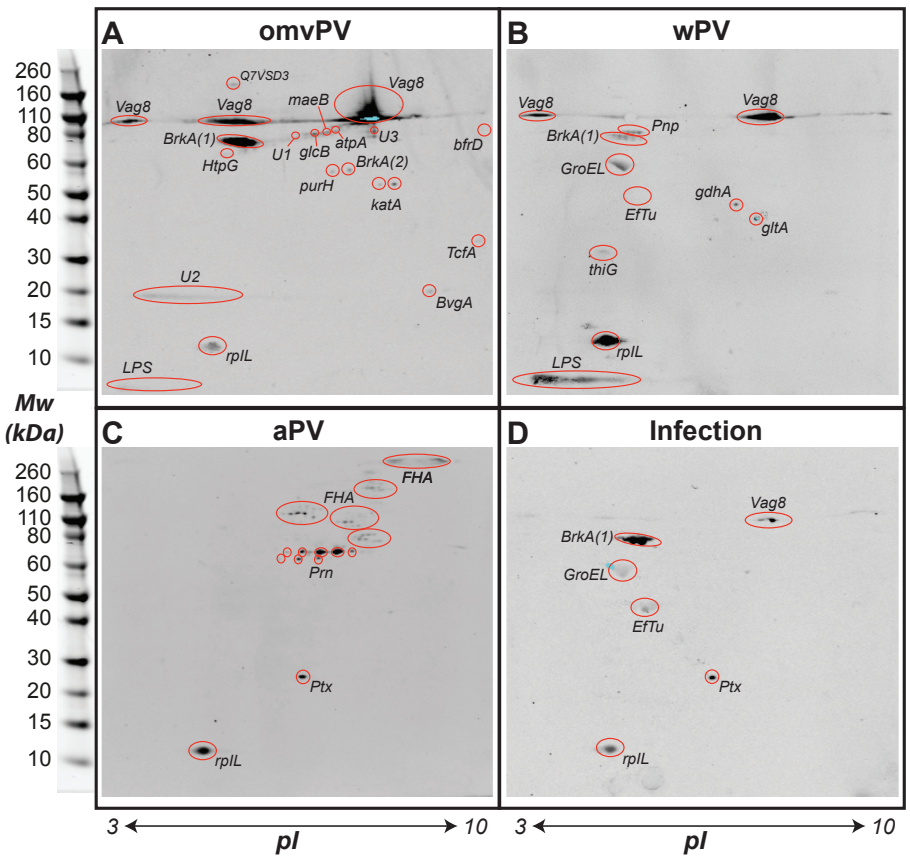

Figure 5 - 2-Dimensional immunoproteomic profiling. *B. pertussis* B1917 proteins were separated by 2-dimensional gel electrophoresis followed by western blot analysis with serum of mice that underwent vaccination with **(A)** omvPV, **(B)** wPV, or **(C)** aPV, or **(D)** a *B. pertussis* infection. Immunogenic proteins were detected (800 nm, Int. 8.0) with IR800-labeled anti-IgG and identified by LC-MS-analysis. For each condition, experiments were performed three times with pooled serum of 10 mice resulting in similar outcomes. One representative total IgG blot is presented.

elicited by omvPV and wPV was directed against LPS (Figure 4C). Antibodies against LPS were mainly of the IgG3 subclass (Figure 4A, lane 7, 13 and 27), but were also of the IgG1 subclass (Figure 4A, lane 4, 10 and 24). After a *B. pertussis* infection, less anti-LPS IgG antibodies were found but in addition IgA antibodies were formed against LPS (Figure 4A, lane 28).

Identification of the antibody-inducing antigens

A combination of 2-dimensional gel electrophoresis, western blot analysis (2DEWB) and LC-MS was performed on a *B. pertussis* lysate (Figure 2B) to identify the immunogenic proteins and the subclass specificity of the serum antibodies from vaccinated or infected mice (Figure 5A-D). We detected 16, 9, 3, and 5 antibody-inducing proteins in serum from omvPV, wPV and aPV-vaccinated mice, or infected mice, respectively. The immunogenic proteins were identified and quantified by LC-MS (Table 2). Highest staining intensities for IgG after omvPV vaccination were found directed against Vag8 and BrkA. Moderate antibody binding was measured against atpA, bfrD, BvgA, glcB, HtpG, katA, maeB, purH, Tcf and three unidentified proteins (U1-3). Anti-Tcf antibodies were only detected upon omvPV vaccination (Figure 5A), although similar concentrations of Tcf are present in wPV (Figure 6). The humoral response induced by wPV was mainly characterized by antibodies against BrkA, GroEL and Vag8 (Figure 5B). In addition, immunostaining of EfTu, gdhA, gltA, Pnp, and thiG was observed. It was confirmed that vaccination with aPV induced antibodies directed against FHA, Prn and Ptx (Figure 5C). Anti-Ptx antibodies were directed against a single spot, whereas anti-Prn and anti-FHA were detected as multiple spots, most likely indicating degradation (change in size), deamination or post-translational modifications (change in pI). Although FHA was present in both wPV and omvPV, only aPV elicited detectable anti-FHA antibodies. *B. pertussis* infection resulted in moderate antibody levels against BrkA, EfTu, GroEL, Ptx and Vag8 (Figure 5D). Western blot analysis of serum of naive mice revealed the presence of antibodies against the 50S ribosomal protein L7/L12 (Q7W0S0) (Figure 6).

The results of 2DEWB analyses are summarized in heatmaps (Figure 6). Vaccination with omvPV induced antibodies of all IgG subclasses against Vag8 and BrkA. The formation of IgG3 against Vag8 and BrkA and IgG2a against Tcf was only detected upon omvPV vaccination. All vaccines generated IgG1 against multiple antigens. However, the staining intensities were the strongest upon aPV and wPV vaccination. The aPV elicited only antibodies of the IgG1 subclass against FHA, Prn, and Ptx. The wPV-induced antibodies against BrkA, Pnp and EfTu were only of the IgG1 subclass, while antibodies against Vag8 consisted of both IgG1 and IgG2a subclasses. Western blots revealed that anti-GroEL antibodies formed upon wPV vaccination and after pertussis infection were predominantly IgG1 and to a lesser extent IgG2b. The infection induced IgG2a and IgG2b antibodies against Vag8 and BrkA. However, the highest staining intensities of BrkA were found to be IgG1. Finally, serum IgA was exclusively measured after infection and was directed against Vag8 and BrkA.

Table 2. Immunogenic proteins determined by LC/MS of excised spots found by immunoblotting on 2DE gels.

Protein Description[1]	Accession number[2]	ID[2]	Mw (kDa)[3]	pI[3]	Coverage (%)[4]	Number of peptides assigned with high confidence	Estimated amount in omvPV (µg)[5]	Estimated amount in wPV (µg)[5]
50S ribosomal protein L7/L12	Q7W0S0	rplI	12.8	4.9	68	5	0.001	0.006
60 kDa chaperonin	P48210	GroEL	57.4	5.2	80	45	0.2	0.7
Autotransporter	Q79GN7	Vag8	94.8	6.8	42	26	1.4	0.2
Bifunctional purine biosynthesis protein PurH	Q7VTU1	purH	55.8	6.3	46	16	N/D	N/D
BrkA (1)	Q45340	BrkA	103.3	7.1	41	25	1.0	0.1
BrkA (2)	Q45340	BrkA	103.3	7.1	18	11	1.0	0.1
Catalase	P0A323	katA	54.5	7.1	66	23	0.02	0.004
Chaperone protein HtpG	Q7W0M8	htpG	71.1	5.2	55	33	0.001	0.01
Citrate synthase	Q7VWA4	gltA	48.4	6.4	40	14	N/D	N/D
Elongation factor Tu	Q7TT91	tuf1	42.9	5.5	78	22	0.02	0.02
Filamentous hemagglutinin	P12255	fhaB	367.3	8.8	41	93	0.02	0.5
Glutamate dehydrogenase	Q7VXC5	gdhA	46.3	6.4	31	10	N/D	0.003
Malate synthase G	Q7VT71	glcB	78.5	6.3	40	22	0.002	N/D
NADH-ubiquinone oxidoreductase, 75 kDa subunit	Q7VU46	atpA	81.1	6.3	25	16	0.002	0.01
NADP-dependent malic enzyme	Q7VZ22	maeB	82.2	6.1	37	22	N/D	0.002
Pertussis toxin subunit 1	P04977	ptxA	30.0	7.5	47	11	N/D	N/D
Polyribonucleotide nucleotidyltransferase	Q7VZU0	pnp	77.3	5.4	56	26	N/D	0.002
Probable TonB-dependent receptor BfrD	P81549	bfrD	81.5	9.2	59	48	0.004	N/D
Putative uncharacterized protein	Q7VSD3	BP0500	68.6	5.3	49	21	0.002	0.01
Thiazole synthase	Q7VTE5	thiG	28.1	5.0	31	7	0.001	N/D
Tracheal colonization factor	Q79GX8	Tcf	66.3	6.0	35	22	0.2	0.2
Virulence factors putative positive transcription regulator BvgA	P0A4H2	bvga	22.9	8.4	77	14	N/D	0.02

[1] Proteins in excised gel spots identified by LC-MS analysis
[2] Accession numbers of proteins and corresponding ID provided by uniprot (http://www.uniprot.org)
[3] Molecular weight (Mw) and iso-electric point (pI) are calculated based on protein sequence
[4] Percentage of a protein sequence covered by identified peptides from the corresponding protein
[5] Estimated amount (µg) of protein present in omvPV and wPV based on the vaccine dose of 4 µg total protein (N/D = Not detected).

Figure 6 - Immunoproteomic profiles elicited by pertussis vaccines and pertussis infection. In total, against 26 immunogenic proteins antibodies were detected that were induced by one or more vaccination schemes. For each protein, the estimated amount (0 – 1.4 µg) present in one vaccination dose of omvPV, wPV (vaccine dose is 4 µg total protein) (analyzed by LC-MS) and aPV (0.25 µg Ptx, 0.25 µg FHA, and 0.08 µg Prn) is listed. The staining intensities of the immunogenic spots were determined and are presented as a heatmap for total IgG (average of 3 blots with pooled serum of 10 mice), IgG subclasses (IgG1, IgG2a, IgG2b and IgG3) and IgA (1 blot with pooled serum of 10 mice). For immunogenic proteins that were detected in multiple spots (i.e. Vag8), the signal of these spots were averaged and summarized as one antigen in the heatmap.

Discussion

This study demonstrates that vaccination with three different pertussis vaccines (omvPV, wPV or aPV) elicited distinct differences in humoral responses, not only with respect to antigen–specificity and antibody levels, but also with respect to antibody isotypes and IgG subclasses. Characterization of complex vaccines by immunoproteomic profiling enabled us to identify and quantify immunogenic proteins in omvPV and wPV. Vaccine protein composition was determined by quantitative proteomics using LC-MS. The immunogenic proteins of the *B. pertussis* B1917 proteome were identified by 2-dimensional immunoblotting and subsequent LC-MS analysis.

To our best knowledge, this is the first time that immunoproteomic profiles of different pertussis vaccines were extensively compared. This study will be useful for understanding host-pathogen interaction and for vaccine design, since complete subclass profiling, especially regarding IgG2b and IgG3, is often absent [15, 43]. Distinct variances in IgG subclass response were seen in mice receiving different pertussis vaccines or *B. pertussis* infection (**Figure 3, 4 and 6**). Vaccination with omvPV and wPV resulted in antibodies of all IgG subclasses, although the wPV elicited a subclass response that was dominated by IgG1. Vaccination with aPV solely induced IgG1 antibodies, while a *B. pertussis* infection led to the formation of mainly IgG2a and IgG2b antibodies. The formation of antibody-producing B-cells can occur either through a T-cell dependent or independent way. In the case of T-cell involvement, the type of cytokines secreted, e.g. IFNγ, IL-4, IL-5, and IL-17, determines the IgG subclass production by B-cells [19, 20, 44]. In mice, Th1 type responses promote the production of IgG2a, whereas Th2 responses stimulate the formation of IgG1 [19, 44]. In addition, production of IgG2b seems to be linked to a Th17 type response [20]. Whereas all types of T-cell help stimulate the secretion of IgG3 [19, 44], the highest IgG3 formation is achieved by T-cell independent antibody responses by B-cells, i.e. against LPS [45].

The differences in IgG subclass responses observed in the mice upon vaccination with different pertussis vaccines are likely influenced by the vaccine characteristics, such as (i) particle size, (ii) vaccine composition or (iii) presence of adjuvants, along with (iv) the route of administration. For instance, OMVs are ten times smaller in diameter than whole bacteria. This may increase the exposure to different cell types because there are more particles present in the omvPV or affect the uptake by different cell types with respect to efficiency in uptake and routing within the cells [46]. In addition, OMVs may reach immune cells deeper in the tissue, which are less accessible for the whole bacteria or the large alum particles [47], or drain faster (unprocessed) to the lymph nodes [46], thereby affecting the immune responses induced.

Further, the presence of natural immune potentiators or co-administered adjuvants is known to influence the type of immune response. No adjuvants were added to the omvPV and wPV vaccines. However, these vaccine formulations do contain LPS and bacterial DNA, which are agonists for TLR4 and TLR9, respectively [48]. Activation of these pathogen recognition receptors stimulates and directs the humoral immune response in a T-cell dependent or independent way [49]. The higher concentrations of LPS and especially DNA detected in wPV, when compared to omvPV, might partly explain the different subclass responses. In addition, LPS-recognition by TLR4 in synergy with the B-cell receptor may also lead to direct T-cell independent anti-LPS antibody formation, especially IgG3, by B-cells [45]. In the case of aPV, the presence of aluminum hydroxide leads to a Th2 biased response [50] and subsequently the formation of IgG1 against purified pertussis antigens [22], as was also found in this study. Interestingly, it was shown that this Th2 response caused by aluminum-containing vaccines could be steered towards a Th1 response by addition of TLR ligands that induce strong Th1 responses, such as an LPS derivate (TLR4 ligand) [51] or CpG (TLR9-agonist) [52]. This indicates that the sum of all interactions within and between activated pathways determines the environmental conditions in which the B-cells reside, and consequently the outcome of the humoral response.

The intranasal infection resulted in production of IgG2a and IgG2b, which is thought to be related to a Th1/Th17 response [18, 20]. An enhanced IgG2a antibody formation, relative to IgG1, was also found upon intranasal administration of live attenuated pertussis vaccine [5]. A bacterial infection results in colonization and protein secretion of the bacteria leading to prolonged antigen exposure [18] when compared to vaccination. The intranasal route of administration of the infection, compared to subcutaneous vaccination with omvPV, wPV or aPV, at least partly explains the exclusive presence of serum IgA antibodies in infected mice [18].

Antibody subclasses determine the functionality of antibodies, since IgG subclasses may have a different bactericidal and opsonophagocytic activity [53]. Recently, it was suggested that for *B. pertussis*, antibodies with opsonophagocytic killing functionality might be more important compared to direct serum bactericidal killing [54]. For *B. pertussis*, Fc-receptors play an important role in opsonophagocytic killing in the respiratory tract in mice [24, 25]. IgG subclasses have a different affinity and selectivity towards FcRs [55]. In mice, IgG1 predominantly targets FcγRIII (CD16) [56]. FcγRIV (CD16-2) exclusively binds IgG2a and IgG2b that both have the highest affinity for this receptor but are able to bind all FcRs [57]. Finally, murine IgG3 has a high affinity for FcRn and low affinity for FcγRI (CD64). Fc-receptors are present on several cell types such as B-cells and NK-cells, but predominantly on phagocytes, such as neutrophils and macrophages [55]. The neutrophils seem essential to protect against *B. pertussis*, since neutrophil depletion resulted in impaired lung clearance, especially in

immunized mice [58]. Because multiple immune cells, such as neutrophils, B-cells and macrophages, express different FcγRs [55], a certain IgG subclass cannot predict the involved type of FcγR-expressing cells. However, the humoral response with multiple antibody subclasses after omvPV vaccination might result in the involvement of different FcγR-expressing cells resulting in a broad immune response. In contrast, selective IgG1 induction by aPV suggests mainly involvement of FcγRIII-expressing cells. A broad subclass distribution against surface exposed antigens, such as Vag8, BrkA, Prn and FHA should therefore lead to addressing a variety of FcγR-containing cells. The involvement of multiple FcγR-containing cells might result in increased phagocytosis. Antibodies against secreted antigens, such as Ptx, are less involved in direct phagocytosis of the bacteria. However, Ptx inhibits neutrophil recruitment [59]. Therefore, antibody-mediated neutralization of Ptx might prevent the impaired recruitment of neutrophils, increasing phagocytosis of bacteria in the respiratory tract.

The present study showed the essence of characterization of complex vaccines for understanding antibody profiles. In another study describing the antigenic composition of an omvPV, Ptx and Fim2 were reported to be present in that vaccine [30]. However, this was not observed in our study using a different omvPV. The differences in vaccine composition might be explained by the use of different *B. pertussis* strains, culture conditions, OMV extraction methods [38], vaccine dose, and methods of analysis. Though some antigens that were most abundant induced the highest antibody responses (such as Vag8 and BrkA in omvPV), other abundant proteins (such as FHA and Prn in omvPV and wPV) did not induce that high antibody responses, whereas some less abundant proteins (Pnp, BvgA) induced higher responses than expected based on the quantity present. In addition, some proteins present in equal amounts in omvPV and wPV (Tcf, EfTu) induced different antibody levels.
While many immunogenic proteins are present in omvPV and wPV, little is known about their protective capacity. Some indications have been reported, for example, using a mouse intracerebral protection assay it was shown that in combination with non-protective levels of anti-Ptx, Vag8 induced protective activity [60]. In addition, when administered as a single component vaccine, recombinant Vag8 could induce a protective response in the lung [16]. For another autotransporter, BrkA, human antibodies against this protein were shown to have bactericidal activity [61]. In addition, a three-component acellular vaccine with BrkA, Ptx and FHA was shown to induce a protective immune response in mice [62]. However, vaccination with recombinant BrkA as a single component did not protect against *B. pertussis* infection [62]. The tracheal colonization factor (Tcf) is a virulence factor and aerosol challenge of mice with a Tcf-deficient *B. pertussis* strain resulted in a 10-fold decrease in trachea colonization compared to a WT strain, indicating an important role for Tcf during colonization [63]. This might suggest a protective function for anti-Tcf antibodies in the respiratory tract. Indeed, intranasal administration of Tcf, carried by an attenuated strain of *Vibrio cholerae*,

resulted in clearance of *B. pertussis* in the trachea, but not in the lungs of vaccinated mice [64]. The GroEL protein is a conserved protein, found in many species of bacteria as well as in humans and therefore probably less suitable as a vaccine antigen [65]. In this study, anti-GroEL antibody formation was found upon wPV vaccination and *B. pertussis* infection. Active immunization with GroEL induced only little protection against a *B. pertussis* infection [65]. In the present study, anti-LPS antibodies were detected at high levels in mice vaccinated with omvPV or wPV and to a lesser extent in infected mice. Others have demonstrated that anti-LPS antibodies in mice [66], rats [67], and humans [68] have bactericidal activity and reduce bacterial colonization in the respiratory tract. In addition, anti-LPS antibodies might lead to diminished pro-inflammatory cytokine production by binding LPS, leading to reduced endotoxic effects of an infection. Immunization with LPS-based oligosaccharide conjugates induced bactericidal antibodies, indicating the potential for improving immunity by implementing pertussis LPS in a vaccine [69].

The question remains whether omvPV provides protective immunity by eliciting a humoral immune response. Based on the protective capacity of antibody induction against antigens, such as BrkA, LPS, Tcf and Vag8 described in literature [61, 64, 69, 70], the omvPV antibody profile in our study suggests potential induction of protective humoral immunity in mice. Other studies have shown that omvPV confers protection similar to aPV when studying the short-term responses [6, 31]. More importantly, it was shown that omvPV could also provide long-lasting immunity. This was also achieved by a commercial aPV but only at a high dose (1/10 Human Dose) in mice [31]. In addition, omvPV protects against different strains [31]. The broader response against multiple relevant antigens by omvPV, instead of selective antigens by aPV, may prevent impaired immunity due to strain adaptation. Future studies should demonstrate the relationship between the immunoproteomic profiles determined for different pertussis vaccines and the presence of long lasting-immunity. These studies should provide us with important new insights into the role of the humoral response and protection.

In order to maintain high vaccine compliance after introducing an improved pertussis vaccine, first a better efficacy but not more reactogenicity of omvPV compared to aPV should be established.

In conclusion, the humoral immune response elicited by omvPV is distinct from that induced by classic pertussis vaccines, such as wPV and aPV. The omvPV elicits high serum antibody levels that consist of a broad subclass response in mice against multiple antigens. The study supports wider exploration of omvPV as an improved pertussis vaccine.

Acknowledgement

The authors thank employees of the Animal Research Centre (ARC) of Intravacc for the performance of animal experiments.

Supplementary information

Supplementary Table 1 - Protein composition of omvPV and wPV determined by LC-MS. This table is available at http://pubs.acs.org/doi/abs/10.1021/acs.jproteome.5b00258.

References

1. Cherry, J.D., Epidemic pertussis in 2012--the resurgence of a vaccine-preventable disease. N Engl J Med, 2012. 367(9): p. 785-7.
2. Baxter, R., *et al.*, Effectiveness of pertussis vaccines for adolescents and adults: case-control study. BMJ, 2013. 347: p. f4249.
3. Celentano, L.P., *et al.*, Resurgence of pertussis in Europe. Pediatr Infect Dis J, 2005. 24(9): p. 761-5.
4. Kretzschmar, M., P.F. Teunis, and R.G. Pebody, Incidence and reproduction numbers of pertussis: estimates from serological and social contact data in five European countries. PLoS Med, 2010. 7(6): p. e1000291.
5. Mielcarek, N., *et al.*, Live attenuated *B. pertussis* as a single-dose nasal vaccine against whooping cough. PLoS Pathog, 2006. 2(7): p. e65.
6. Roberts, R., *et al.*, Outer membrane vesicles as acellular vaccine against pertussis. Vaccine, 2008. 26(36): p. 4639-46.
7. Bottero, D., *et al.*, Pulsed-field gel electrophoresis, pertactin, pertussis toxin S1 subunit polymorphisms, and surfaceome analysis of vaccine and clinical *Bordetella pertussis* strains. Clin Vaccine Immunol, 2007. 14(11): p. 1490-8.
8. Altindis, E., *et al.*, Immunoproteomic analysis of *Bordetella pertussis* and identification of new immunogenic proteins. Vaccine, 2009. 27(4): p. 542-8.
9. Misegades, L.K., *et al.*, Association of childhood pertussis with receipt of 5 doses of pertussis vaccine by time since last vaccine dose, California, 2010. JAMA, 2012. 308(20): p. 2126-32.
10. Mooi, F.R., N.A.T. van der Maas, and H.E. De Melker, Pertussis resurgence: waning immunity and pathogen adaptation - two sides of the same coin. Epidemiol Infect, 2013: p. 1-10.
11. Warfel, J.M., L.I. Zimmerman, and T.J. Merkel, Acellular pertussis vaccines protect against disease but fail to prevent infection and transmission in a nonhuman primate model. Proc Natl Acad Sci U S A, 2014. 111(2): p. 787-92.
12. Plotkin, S.A., Correlates of protection induced by vaccination. Clin Vaccine Immunol, 2010. 17(7): p. 1055-65.
13. Storsaeter, J., *et al.*, Levels of anti-pertussis antibodies related to protection after household exposure to *Bordetella pertussis*. Vaccine, 1998. 16(20): p. 1907-16.
14. van den Berg, B.M., *et al.*, Protection and humoral immune responses against *Bordetella pertussis* infection in mice immunized with acellular or cellular pertussis immunogens. Vaccine, 2000. 19(9-10): p. 1118-28.
15. Mills, K.H., *et al.*, A murine model in which protection correlates with pertussis vaccine efficacy in children reveals complementary roles for humoral and cell-mediated immunity in protection against *Bordetella pertussis*. Infect Immun, 1998. 66(2): p. 594-602.
16. Gouw, D., *et al.*, Proteomics-Identified Bvg-Activated Autotransporters Protect against *Bordetella pertussis* in a Mouse Model. PLoS One, 2014. 9(8): p. e105011.
17. Warfel, J.M. and T.J. Merkel, *Bordetella pertussis* infection induces a mucosal IL-17 response and long-lived Th17 and Th1 immune memory cells in nonhuman primates. Mucosal Immunol, 2013. 6(4): p. 787-96.
18. Raeven, R.H.M., *et al.*, Molecular Signatures of the Evolving Immune Response in Mice following a *Bordetella pertussis* Infection. PLoS One, 2014. 9(8): p. e104548.
19. Stevens, T.L., *et al.*, Regulation of antibody isotype secretion by subsets of antigen-specific helper T cells. Nature, 1988. 334(6179): p. 255-8.
20. Mitsdoerffer, M., *et al.*, Proinflammatory T helper type 17 cells are effective B-cell helpers. Proc Natl Acad Sci U S A, 2010. 107(32): p. 14292-7.
21. Redhead, K., *et al.*, Effective immunization against *Bordetella pertussis* respiratory infection in mice is dependent on induction of cell-mediated immunity. Infect Immun, 1993. 61(8): p. 3190-8.
22. Rowe, J., *et al.*, Antigen-specific responses to diphtheria-tetanus-acellular pertussis vaccine in human infants are initially Th2 polarized. Infect Immun, 2000. 68(7): p. 3873-7.
23. Ross, P.J., *et al.*, Relative contribution of Th1 and Th17 cells in adaptive immunity to *Bordetella pertussis*: towards the rational design of an improved acellular pertussis vaccine. PLoS Pathog, 2013. 9(4): p. e1003264.
24. Hellwig, S.M., *et al.*, Targeting to Fcgamma receptors, but not CR3 (CD11b/CD18), increases clearance of *Bordetella pertussis*. J Infect Dis, 2001. 183(6): p. 871-9.
25. Rodriguez, M.E., *et al.*, Fc receptor-mediated immunity against *Bordetella pertussis*. J Immunol, 2001. 167(11): p. 6545-51.
26. Hellwig, S.M., *et al.*, Crucial role of antibodies to pertactin in *Bordetella pertussis* immunity. J Infect Dis, 2003. 188(5): p. 738-42.
27. Taranger, J., *et al.*, Correlation between pertussis toxin IgG antibodies in postvaccination sera and subsequent protection against pertussis. J Infect Dis, 2000. 181(3): p. 1010-3.
28. Zhu, Y.Z., *et al.*, Immunoproteomic analysis of human serological antibody responses to vaccination with whole-cell pertussis vaccine (WCV). PLoS One, 2010. 5(11): p. e13915.
29. Tefon, B.E., *et al.*, A comprehensive analysis of *Bordetella pertussis* surface proteome and identification of new immunogenic proteins. Vaccine, 2011. 29(19): p. 3583-95.
30. Ormazabal, M., *et al.*, Characterization of the key antigenic components of pertussis vaccine based on outer membrane vesicles. Vaccine, 2014. 32(46): p. 6084-90.
31. Gaillard, M.E., *et al.*, Acellular pertussis vaccine based on outer membrane vesicles capable of conferring both long-lasting immunity and protection against different strain genotypes. Vaccine, 2014. 32(8): p. 931-7.
32. Zollinger, W.D., *et al.*, Design and evaluation in mice of a broadly protective meningococcal group B native outer membrane vesicle vaccine. Vaccine, 2010. 28(31): p. 5057-67.
33. Welch, D.F., Applications of cellular fatty acid analysis. Clin Microbiol Rev, 1991. 4(4): p. 422-38.
34. Caroff, M., *et al.*, Structure of the *Bordetella pertussis* 1414 endotoxin. FEBS Lett, 2000. 477(1-2): p. 8-14.
35. Stenger, R.M., *et al.*, Fast, antigen-saving multiplex immunoassay to determine levels and avidity of mouse serum antibodies to pertussis, diphtheria, and tetanus antigens. Clin Vaccine Immunol, 2011. 18(4): p. 595-603.

36. Hijnen, M., *et al.*, The *Bordetella pertussis* virulence factor P.69 pertactin retains its immunological properties after overproduction in *Escherichia coli*. Protein Expr Purif, 2005. 41(1): p. 106-12.
37. Yan, J.X., *et al.*, A modified silver staining protocol for visualization of proteins compatible with matrix-assisted laser desorption/ionization and electrospray ionization-mass spectrometry. Electrophoresis, 2000. 21(17): p. 3666-72.
38. van de Waterbeemd, B., *et al.*, Quantitative proteomics reveals distinct differences in the protein content of outer membrane vesicle vaccines. J Proteome Res, 2013. 12(4): p. 1898-908.
39. Meiring, H.D., Van Der Heeft, E., Ten Hove, G.J., De Jong, A.P.J.M., Nanoscale LC-MS(n): Technical design and applications to peptide and protein analysis. Journal of Separation Science, 2002. Volume 25(Issue 9): p. Pages 557-568.
40. Bart, M.J., *et al.*, Comparative genomics of prevaccination and modern *Bordetella pertussis* strains. BMC Genomics, 2010. 11: p. 627.
41. Silva, J.C., *et al.*, Absolute quantification of proteins by LCMSE: a virtue of parallel MS acquisition. Mol Cell Proteomics, 2006. 5(1): p. 144-56.
42. Huang da, W., B.T. Sherman, and R.A. Lempicki, Systematic and integrative analysis of large gene lists using DAVID bioinformatics resources. Nat Protoc, 2009. 4(1): p. 44-57.
43. Canthaboo, C., *et al.*, Investigation of cellular and humoral immune responses to whole cell and acellular pertussis vaccines. Vaccine, 2000. 19(6): p. 637-43.
44. Germann, T., *et al.*, Interleukin-12 profoundly up-regulates the synthesis of antigen-specific complement-fixing IgG2a, IgG2b and IgG3 antibody subclasses in vivo. Eur J Immunol, 1995. 25(3): p. 823-9.
45. Quintana, F.J., *et al.*, Induction of IgG3 to LPS via Toll-like receptor 4 co-stimulation. PLoS One, 2008. 3(10): p. e3509.
46. Bachmann, M.F. and G.T. Jennings, Vaccine delivery: a matter of size, geometry, kinetics and molecular patterns. Nat Rev Immunol, 2010. 10(11): p. 787-96.
47. Kuehn, M.J. and N.C. Kesty, Bacterial outer membrane vesicles and the host-pathogen interaction. Genes Dev, 2005. 19(22): p. 2645-55.
48. Akira, S. and K. Takeda, Toll-like receptor signalling. Nat Rev Immunol, 2004. 4(7): p. 499-511.
49. Bekeredjian-Ding, I. and G. Jego, Toll-like receptors--sentries in the B-cell response. Immunology, 2009. 128(3): p. 311-23.
50. Hogenesch, H., Mechanism of immunopotentiation and safety of aluminum adjuvants. Front Immunol, 2012. 3: p. 406.
51. Brummelman, J., *et al.*, Modulation of the CD4 T cell response after acellular pertussis vaccination in the presence of TLR4 ligation. Vaccine, 2015. 33(12): p. 1483-91.
52. Gracia, A., *et al.*, Antibody responses in adult and neonatal BALB/c mice to immunization with novel *Bordetella pertussis* vaccine formulations. Vaccine, 2011. 29(8): p. 1595-604.
53. Michaelsen, T.E., *et al.*, The four mouse IgG isotypes differ extensively in bactericidal and opsonophagocytic activity when reacting with the P1.16 epitope on the outer membrane PorA protein of *Neisseria meningitidis*. Scand J Immunol, 2004. 59(1): p. 34-9.
54. Geurtsen, J., K.C. Fae, and G.P. van den Dobbelsteen, Importance of (antibody-dependent) complement-mediated serum killing in protection against *Bordetella pertussis*. Expert Rev Vaccines, 2014: p. 1-12.
55. Bruhns, P., Properties of mouse and human IgG receptors and their contribution to disease models. Blood, 2012. 119(24): p. 5640-9.
56. Hazenbos, W.L., *et al.*, Murine IgG1 complexes trigger immune effector functions predominantly via Fc gamma RIII (CD16). J Immunol, 1998. 161(6): p. 3026-32.
57. Nimmerjahn, F., *et al.*, FcgammaRIV: a novel FcR with distinct IgG subclass specificity. Immunity, 2005. 23(1): p. 41-51.
58. Andreasen, C. and N.H. Carbonetti, Role of neutrophils in response to *Bordetella pertussis* infection in mice. Infect Immun, 2009. 77(3): p. 1182-8.
59. Kirimanjeswara, G.S., *et al.*, Pertussis toxin inhibits neutrophil recruitment to delay antibody-mediated clearance of *Bordetella pertussis*. J Clin Invest, 2005. 115(12): p. 3594-601.
60. Hamstra, H.J., *et al.*, The purification and protective capacity of *Bordetella pertussis* outer membrane proteins. Vaccine, 1995. 13(8): p. 747-52.
61. Oliver, D.C. and R.C. Fernandez, Antibodies to BrkA augment killing of *Bordetella pertussis*. Vaccine, 2001. 20(1-2): p. 235-41.
62. Marr, N., *et al.*, Protective activity of the *Bordetella pertussis* BrkA autotransporter in the murine lung colonization model. Vaccine, 2008. 26(34): p. 4306-11.
63. Finn, T.M. and L.A. Stevens, Tracheal colonization factor: a *Bordetella pertussis* secreted virulence determinant. Mol Microbiol, 1995. 16(4): p. 625-34.
64. Chen, I., *et al.*, A recombinant live attenuated strain of *Vibrio cholerae* induces immunity against tetanus toxin and *Bordetella pertussis* tracheal colonization factor. Infect Immun, 1998. 66(4): p. 1648-53.
65. Burns, D.L., *et al.*, Purification and immunological characterization of a GroEL-like protein from *Bordetella pertussis*. Infect Immun, 1991. 59(4): p. 1417-22.
66. Mountzouros, K.T., A. Kimura, and J.L. Cowell, A bactericidal monoclonal antibody specific for the lipooligosaccharide of *Bordetella pertussis* reduces colonization of the respiratory tract of mice after aerosol infection with *B. pertussis*. Infect Immun, 1992. 60(12): p. 5316-8.
67. Gotto, J., *et al.*, Protective effect of *Bordetella pertussis* lipopolysaccharide in the rat intratracheal challenge model of pertussis. Abstracts Of The General Meeting Of The American Society For Microbiology, 1992. Abstr. 92nd(abstr. E-15): p. p. 146.
68. Weiss, A.A., *et al.*, Characterization of human bactericidal antibodies to *Bordetella pertussis*. Infect Immun, 1999. 67(3): p. 1424-31.
69. Kubler-Kielb, J., *et al.*, Oligosaccharide conjugates of *Bordetella pertussis* and bronchiseptica induce bactericidal antibodies, an addition to pertussis vaccine. Proc Natl Acad Sci U S A, 2011. 108(10): p. 4087-92.
70. Finn, T.M. and D.F. Amsbaugh, Vag8, a *Bordetella pertussis* bvg-regulated protein. Infect Immun, 1998. 66(8): p. 3985-9.

About the cover: Temples and pagodas of the ancient city of Bagan in Myanmar. Capital of the kingdom of Pagan between the 9th and 13th century. Today, the remains of approximately 2,200 temples and pagodas are still present. Part of the UNESCO World Heritage list.

CHAPTER 5

Bordetella pertussis outer membrane vesicle vaccine confers equal efficacy in mice with a lower inflammatory response compared to a classic whole-cell vaccine

René H. M. Raeven[1,2], Jolanda Brummelman[3], Jeroen L. A. Pennings[4], Larissa van der Maas[1], Wichard Tilstra[1], Kina Helm[3], Elly van Riet[1], Wim Jiskoot[2], Cécile A. C. M. van Els[3], Wanda G. H. Han[3], Gideon F. A. Kersten[1,2], Bernard Metz[1]

[1]Institute for Translational Vaccinology (Intravacc), Bilthoven, The Netherlands,
[2]Division of Drug Delivery Technology, Leiden Academic Centre for Drug Research, Leiden, The Netherlands,
[3]Centre for Infectious Disease Control, National Institute for Public Health and the Environment (RIVM), Bilthoven, The Netherlands,
[4]Centre for Health Protection (GZB), National Institute for Public Health and the Environment (RIVM), Bilthoven, The Netherlands

Submitted for publication

Abstract

Resurgence of whooping cough demands better understanding of the mode of action of pertussis vaccines. A systems biology approach was applied to investigate the immunogenicity, potency, and potential adverse effects in mice of a candidate outer membrane vesicles pertussis vaccine (omvPV) and a whole-cell pertussis vaccine (wPV) as comparator. To this end, responses were compared after (i) subcutaneous immunization and (ii) an intranasal *Bordetella pertussis* challenge. Both vaccines stimulated a mixed systemic response of Th1/Th2/Th17 cells. Remarkably, omvPV, as compared to wPV, evoked higher serum IgG levels, lower systemic pro-inflammatory cytokine responses, higher numbers of splenic neutrophils, and enhanced gene expression in the spleen. The transcriptome comprised gene signatures of the IFN-signaling pathway, anti-inflammatory signatures that attenuate LPS responses, anti-inflammatory metabolic signatures, IgG responses, and confirmed the presence of neutrophils. Upon intranasal challenge, mice immunized with omvPV or wPV were equally efficient in clearing *B. pertussis* from the lungs. Both immunized groups evoked diminished pulmonary and splenic gene transcription and pulmonary cytokine secretion as compared to challenged non-immunized mice. In conclusion, omvPV and wPV provide equal protection to bacterial colonization and induce a similar mixed Th1/Th2/Th17 response, while omvPV induced higher IgG levels. Moreover, omvPV elicited less pro-inflammatory cytokines, but more anti-inflammatory signatures. Therefore, milder inflammatory responses are observed in mice upon immunization with omvPV compared to wPV. These results emphasize the potential of omvPV as a third-generation pertussis vaccine.

Introduction

The efficacy of the pertussis vaccines on the market, whole-cell pertussis vaccine (wPV) and acellular pertussis vaccine (aPV), is under scrutiny because of the resurgence of whooping cough, despite high vaccination coverage [1, 2]. The current view on immunity to *B. pertussis* is that T-helper 1 and T-helper 17 (Th1/Th17) responses [3, 4] and specific antibody responses are preferred for protection. wPV induce a predominant Th1/Th17 response [4-6] and a broad systemic antibody repertoire [7], but wPV is associated with mild adverse effects [8, 9]. The suspected correlation between wPV and serious acute neurological illness in children [10, 11] has finally led to the call for safer pertussis vaccines. This resulted in the introduction of better-defined aPVs in many countries. The aPVs evoke high IgG1 antibody titers and mainly a Th2 response, which provides protection against disease, however, with a relatively short duration. Recent findings for aPV suggest waning immunity in children [12] and impaired prevention of transmission in baboons [13]. It is thought that the breadth of the antibody response [7] and the type of T-cell response induced by aPVs are suboptimal [14]. This situation calls for improved pertussis vaccines.

Outer membrane vesicles from *B. pertussis* are a potential vaccine candidate (omvPV). The protection in mice induced by omvPV is comparable to that of aPV, based on lung colonization data after *B. pertussis* challenge [15, 16]. Nevertheless, the omvPV elicits a broader humoral immunity compared to aPV [7]. To match the high short-term efficacy and good safety profile of current aPVs, a more comprehensive insight into omvPV-induced responses is required to unravel the type of immunity and assist in future vaccine registration. For this, an unbiased and detailed systems biology approach may be suitable. The application of systems biology in vaccine research has provided a better understanding of immune mechanisms and has been useful for the prediction of vaccine efficacy based on correlating biomarkers both for yellow fever and influenza [17-19]. Moreover, systems biology can be applied for comparing molecular signatures induced by distinct vaccines [20, 21] and for gaining insight into vaccine safety [22]. Previously we used a systems approach in mice to study *B. pertussis* infection-induced responses [23].

Here, a systems vaccinology approach is implemented to investigate the potency of omvPV in mice. In addition, wPV is included in the study as a benchmark. Furthermore, markers for vaccine safety are measured with respect to pro- and anti-inflammatory cytokine secretion and splenic transcriptome. Finally, immunized mice were subjected to a *B. pertussis* challenge to compare the induced immune responses to those in non-immunized mice.

Results

OmvPV provides slightly better protection than wPV against *B. pertussis* challenge

The composition of both omvPV and wPV, in terms of proteins, DNA, and LPS as well as particle size [7], was determined before mice were immunized twice with a four-week interval as illustrated in **Figure 1**. Vaccine efficacy was assessed by determining lung colonization in omvPV-immunized mice (omvPV-mice) compared to wPV- and non-immunized mice (wPV-mice and N.I.-mice, respectively) upon an intranasal challenge with *B. pertussis* (**Figure 2A**). As observed before [23], N.I.-mice showed extensive colonization and lungs were not cleared at day 77, the end of the observation time (21 days post challenge). The lungs of immunized mice were cleared faster. The lungs of omvPV-mice were cleared as fast as those of wPV-mice. Though omvPV-mice seemed to be even faster, no significant differences were found. In conclusion, this indicates that omvPV provides slightly better protection than wPV against *B. pertussis* challenge.

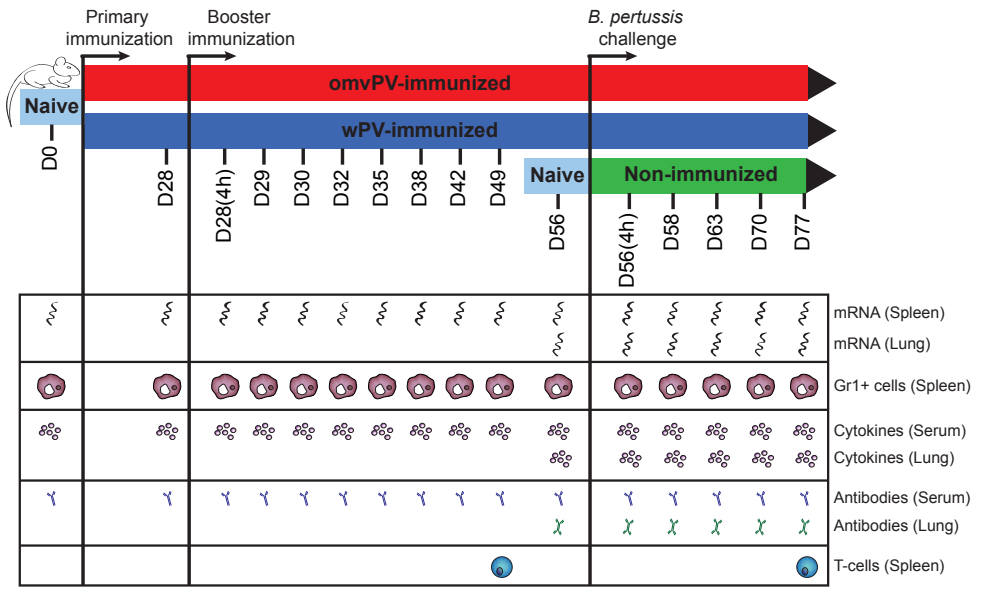

Figure 1 - Study design of the systems approach on omvPV- and wPV-induced responses. BALB/c mice were subcutaneously immunized with 4 µg omvPV (red) or wPV (blue) on day 0 and day 28. Subsequently, the vaccine-induced responses of both vaccines were characterized over a period of 56 days at 10 different time points. Additionally, an intranasal *B. pertussis* challenge ($2x10^5$ cfu/mouse) was performed on day 56 in immunized groups and in non-immunized mice (green). Both vaccine- and infection-induced responses were characterized at a transcriptomic, proteomic and cellular level on given time points, as depicted.

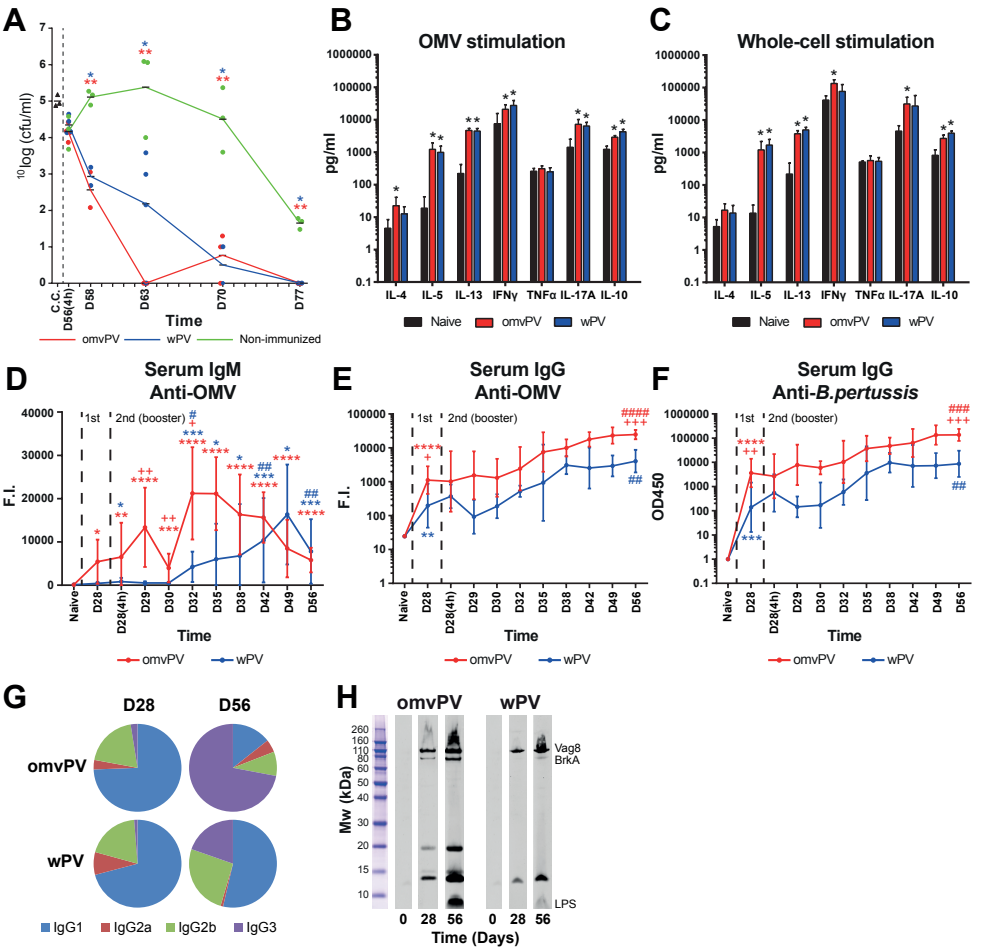

Figure 2 - Lung colonization and vaccine-induced adaptive responses in omvPV- and wPV-immunized mice. **(A)** Non-immunized, omvPV-immunized, and wPV-immunized mice were intranasally challenged with 2x10^5/40 µl cfu *B. pertussis*. The number of cfu in 1 ml challenge culture (c.c.) was confirmed before challenge. Subsequently, the cfu/ml in the lungs of mice was determined 4 hours and 2, 7, 14, and 21 days after challenge (day 56(4h)-77). * and ** = $p \leq 0.05$ and $p \leq 0.01$ for immunized group vs. non-immunized group. **(B-C)** Splenocytes were obtained post booster immunization (day 49) of mice that were naive (black), omvPV-immunized (red), or wPV-immunized (blue). Concentrations of IL-4, IL-5, IL-13, IFNγ, TNFα, IL-17A and IL-10 were determined in the culture supernatants after 7 days of stimulation with **(B)** 5 µg/ml OMVs or **(C)** 5 µg/ml *B. pertussis* whole-cells. Results for each mouse are corrected for medium stimulation. Data presented as mean ± SD (n = 4). * = $p \leq 0.05$ for immunized group vs. naive group. **(D-H)** The kinetics of serum **(D)** anti-OMV IgM, **(E)** anti-OMV IgG and **(F)** anti-*B. pertussis* IgG formation was determined for a period of 56 days after omvPV and wPV immunization. Data are presented as mean ± SD (n = 4). For **(D)**, *, **, *** and **** = $p \leq 0.05$, $p \leq 0.01$, $p \leq 0.001$ and $p \leq 0.0001$ for day 28-56 vs. naive, # and ## = $p \leq 0.05$ and $p \leq 0.01$, for day 28(4h)-56 vs. day 28, + and ++ = $p \leq 0.05$ and $p \leq 0.01$ for omvPV-mice vs. wPV-mice. For **(E-F)**, *, **, *** and **** = $p \leq 0.05$, $p \leq 0.01$, $p \leq 0.001$ and $p \leq 0.0001$ for naive vs. day 28, #, ##, ### and #### = $p \leq 0.05$, $p \leq 0.01$, $p \leq 0.001$ and $p \leq 0.0001$ for day 28 vs. day 56, + and ++ = $p \leq 0.05$ and $p \leq 0.01$ for omvPV-mice vs. wPV-mice. The significance in **(E)** and **(F)** between day 28(4h)-49 is not depicted. **(G)** Subclass distribution was determined at day 56 in serum of mice immunized with omvPV or wPV by calculating the ratio of the level for each subclass from the sum of the levels all subclasses. **(H)** To determine antigen-specificity, the immunoproteomic profiles of serum antibodies (pooled sera, n = 4) following primary immunization (day 28) and booster immunization (day 56) were obtained. The band positions of Vag8, BrkA and LPS antigens, identified previously [7], are indicated.

OmvPV and wPV induce a mixed Th1/Th2/Th17 response

To investigate the vaccine-induced systemic T-cell responses, the levels of seven cytokines related to Th-responses were determined in culture supernatants from stimulated splenocytes harvested three weeks after the second immunization (**Figure 2B-C**). Stimulation with *B. pertussis* OMVs or whole-cells resulted in enhanced production of Th1 (IFNγ), Th2 (IL-5 and IL-13), and Th17 (IL-17A) cytokines and IL-10 in omvPV-mice and wPV-mice, compared to naive mice. TNFα was not observed, while IL-4 (Th2) was only detected after OMV stimulation of splenocytes from omvPV-mice. Upon stimulation of splenocytes with purified antigens, pertussis toxin (Ptx), filamentous hemagglutinin (FHA), and pertactin (Prn), hardly any cytokines were produced, with the exception of IL-17A after FHA stimulation of splenocytes from wPV-mice and IL-5 after Prn stimulation of splenocytes from omvPV-mice (**Figure S3A-C, left panels**). In conclusion, the cytokine profiles indicate that immunization of mice with omvPV and wPV generated a mixed repertoire of Th1/Th2/Th17 cells.

OmvPV induces higher serum IgG antibody responses

The IgG and IgM levels in mouse sera were monitored for 56 days (**Figure 2D-F**). omvPV induced IgM specific for OMV proteins and reached highest IgM levels on day 32 (**Figure 2D**). wPV also stimulated IgM production specific for OMV proteins, but at a slower rate and with a maximum level on day 49 (**Figure 2D**). Moderate IgG levels were detected 28 days after the primary immunization with either omvPV or wPV, detected by both a multiplex immunoassay (MIA) against OMVs and a whole-cell ELISA (**Figure 2E-F**). Booster immunization resulted in a strong increase of IgG production, with omvPV-mice developing higher IgG levels than wPV-mice. No IgG or IgM antibodies were found directed against purified antigens (Ptx, FHA, Prn, and Fimbriae 2 and 3 (Fim2/3)) (data not shown). The subclass distribution and immunoproteomic profiles of serum IgG antibodies were compared for both vaccines on day 28 and 56 (**Figure 2G-H**). The subclass distribution on day 28 was dominated by IgG1 for both omvPV and wPV (**Figure 2G**). However, booster immunizations with wPV and to a much larger extent with omvPV, stimulated production of IgG3 antibodies on day 56 (**Figure 2G**). As described previously, most of the IgG3 antibodies induced by omvPV and wPV immunization were shown to be specific for LPS [7]. Confirmed here, higher levels of anti-LPS IgG antibodies were detected after omvPV immunization compared to wPV immunization (**Figure 2H**). Moreover, these anti-LPS IgG antibodies were observed solely on day 56, indicating that these antibodies were elicited by the booster immunization. Additionally, both vaccines mainly induced antibodies specific for Vag8 and BrkA (**Figure 2H**).

Less pro-inflammatory cytokine induction in serum by omvPV compared to wPV

A MIA was performed on mouse sera to measure the vaccine-induced cytokine responses elicited by immunization with omvPV or wPV (**Figure 3**). Cytokine levels were mainly affected 4 hours after booster immunization (day 28(4h)), when the concentrations of CXCL10, G-CSF,

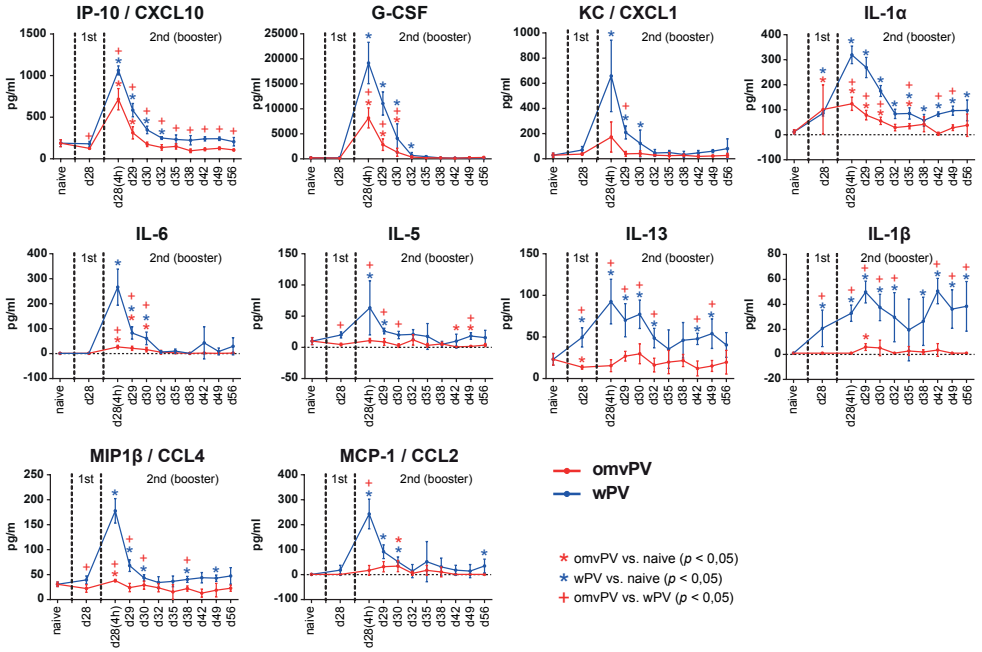

Figure 3 - Serum cytokine secretion following omvPV or wPV immunization. Concentrations of 32 cytokines were determined in serum at multiple time points after immunization with omvPV or wPV. Levels of CXCL10, G-CSF, CXCL1, IL-1α, IL-6, IL-5, IL-13, IL-1β, CCL4, and CCL2 were significantly altered and are depicted here. The different stages of primary immunization and booster immunization are depicted in the panels. Data represent mean ± SD (n = 4). * = $p \leq 0.05$ for immunized group vs. naive, + = $p \leq 0.05$ for omvPV group vs. wPV group.

IL-1α, IL-6 and CCL4 were significantly enhanced in omvPV-mice and wPV-mice compared to pre-immunization levels. In omvPV-mice, all these cytokine concentrations were significantly lower than in wPV-mice. Moreover, concentrations of CXCL1, CCL2, IL-1β, IL-5, and IL-13 were only significantly elicited by the wPV booster immunization. These results indicate that the induction of pro-inflammatory cytokine levels is less intense after booster immunization with omvPV compared to wPV.

Transcriptomic profiles in the spleen induced by immunization with omvPV or wPV

Gene expression profiles were obtained in the spleen over a period of 28 days (day 28-56) to reveal the effects of immunization with omvPV or wPV. In total, 423 and 185 genes were identified that were differentially regulated compared to naive mice (day 0) (p-value ≤ 0.001, Fold Ratio (FR) ≥ 1.5) in omvPV-mice and wPV-mice, respectively (**Figure 4A**). Of these genes, 160 (132 upregulated, 28 downregulated) overlapped between both immunized groups. Additionally, differential expression of 263 genes (180 upregulated, 83 downregulated) was exclusively detected in omvPV-mice, whereas 25 genes (21 upregulated, 4 downregulated) were only differentially regulated in wPV-mice (**Figure 4A**).

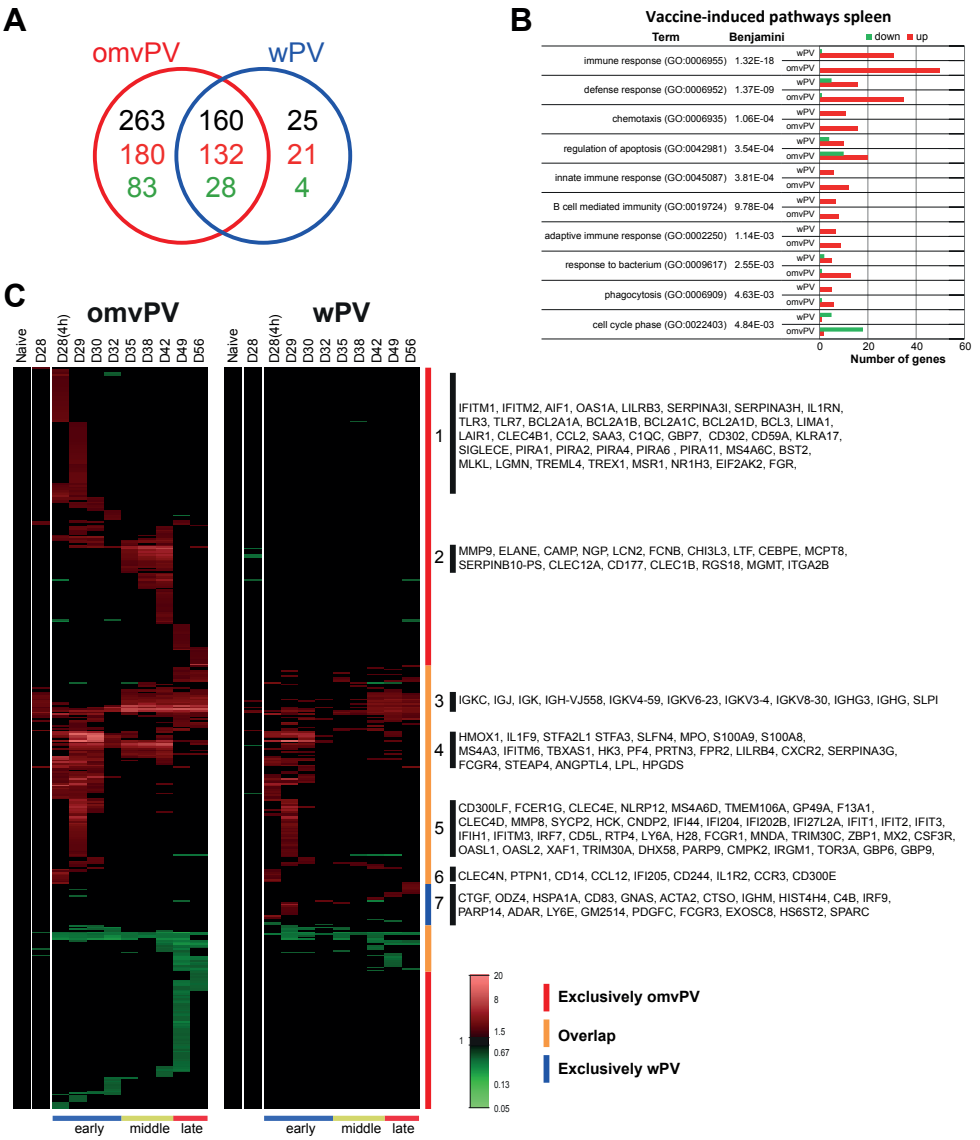

Figure 4 - Transcriptomic profiles in the spleen following omvPV and wPV booster immunization. **(A)** Fold changes of differentially expressed genes were calculated compared to naive mice (FR ≥ 1.5, *p*-value ≤ 0.001). In total, 448 differentially expressed genes were found divided over both vaccine responses, as depicted in a Venn-diagram with total number of genes (black) and both upregulated (red) and downregulated genes (green). **(B)** Overrepresentation analysis on all 448 genes revealed the involvement of specific GO-BP terms and KEGG pathways with corresponding upregulated (red) and downregulated (green) genes. **(C)** All differentially upregulated (red) and downregulated (green) genes are portrayed as heatmap (mean of n=4). Genes not surpassing a FR of 1.5 are shown as basal level (black) at this time point. Gene clustering is based on up/downregulation, time of involvement, and presence in the immunization group. The overlap and the exclusive presence of differentially expressed genes in either the omvPV or wPV groups are further depicted next to the heatmap. Booster immunization-induced responses were divided in three phases: early phase (day 28(4h)-32), middle phase (day 35-42) and late phase (day 49-56) as calculated in **Figure S1A**. Selections of genes co-expressed in seven (1-7) areas of the heatmap are shown.

To gain insight into the molecular pathways regulated by immunization, an overrepresentation analysis (ORA) was performed using DAVID. This analysis revealed enrichment of 77 gene ontology biological pathways (GO-BP) terms and 2 KEGG pathways (Benjamini ≤ 0.05) in the dataset of omvPV-mice and/or wPV-mice. The pathways related to immunity are shown in **Figure 4B**. The terms Immune response, Defense response, and Cell cycle contained more genes upregulated in omvPV-mice than in wPV-mice. Both groups have an equal number of genes related to Phagocytosis and B-cell mediated immunity (**Figure 4B**).
Genes were clustered based on (i) co-expression over time and (ii) overlap between both immunized groups (**Figure 4C**). Additionally, based on hierarchical clustering (**Figure S1A**), the time points in the vaccine-induced response could be divided in three phases; early phase (day 28(4h)-32), middle phase (day 35-42) and late phase (day 49-56) (**Figure 4C**). Based on the clustering of genes, 7 groups were identified that were further investigated in-depth using text mining and are described below.

Group 1 consists of genes that were detected exclusively in the early phase of the omvPV-induced response. This group comprised genes related to pathogen recognition, such as formyl peptide receptor 1 (*Fpr1*) and genes involved Toll-like receptor (TLR) 3 (*Tlr3, Mlkl*) and TLR7 (*Tlr7, Treml4, Lgmn, Trex1*) mediated signaling. Trex1 limits the pro-inflammatory signals following TLR7 activation in macrophages [24], whereas Siglece represses TLR-signaling in general [25]. Moreover, members of the Bcl family, (*Bcl2a1a, Bcl2a1b, Bcl2a1c, Bcl2a1d, Bcl3*), paired-Ig-like receptors (*Pira1, Pira2, Pira4, Pira6, Pira11, Lilrb3*), IFN-induced transmembrane proteins 1 and 2 (*Ifitm1, Ifitm2*) and IL-1 receptor antagonist (*Il1rn*) were detected. In addition, enhanced expression was detected of the liver X receptor (*Nr1h3*), which is involved in lipid metabolism and an important mediator of inflammation in macrophages. Genes related to processing of LPS included *Bst2*, the macrophage scavenger receptor 1 (*Msr1*) that inhibits LPS-stimulated IL-6 secretion [26], and PKR (*Eif2ak2*), which is essential for LPS-induced iNOS production [27]. Finally, neutrophil-related genes (*Pram1, Fgr*), the C-type lectin receptor DCIR (*Clec4a2*), and two cytokines (*Ccl2, Saa3*) were found.
Group 2 genes were exclusively upregulated in the middle phase of the omvPV-induced response. This group contained genes related to myeloid cells (*Mcpt8, Clec12a, Chi3l3*) and more specifically neutrophil markers, including late stage neutrophil differentiation marker [28], lactotransferrin (*Ltf*), a neutrophil activation marker (*Clec1b*), *Cd177*, *Ngp*, and *Cebpe*. Moreover, the neutrophil-secreted lipocalin 2 (*Lcn2*), elastase (*Elane*), matrix metalloproteinase-9 (*Mmp9*), cathelicidin antimicrobial peptide (*Camp*), and ficolin B (*Fcnb*) were detected. Similar gene expression profiles were observed for *Rgs18*, *Mgmt*, and integrin alpha 2 (*Itga2b*).
Group 3 includes antibody-related genes, such as *Igkc, Igj, Igk*, and *Ighg*, which showed higher expression in omvPV-mice than in wPV-mice (**Figure 5A**), in line with the increased antibody levels (**Figure 2D-F**).

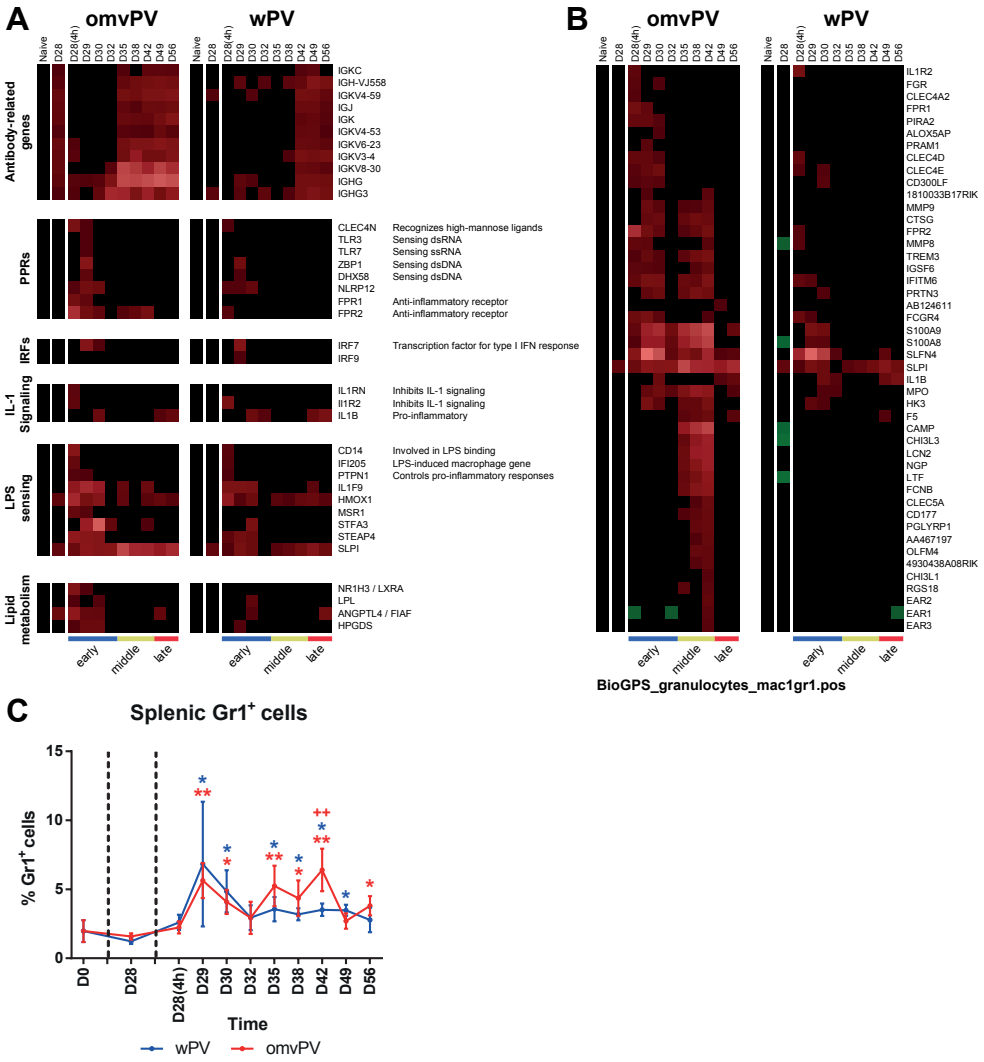

Figure 5 - Selected splenic transcriptome profiles and the involvement of Gr1⁺ cells following omvPV and wPV booster immunization. **(A)** The splenic transcriptome profiles of genes related to antibodies, pathogen recognition receptors (PRRs), interferon regulatory factors (IRFs), IL-1 signaling, LPS sensing, and lipid metabolism are depicted. **(B)** Transcriptomic profiles from spleen tissue of omvPV-mice and wPV-mice were compared with BioGPS databases. In total, 46 genes found following immunization showed overlap with the Mac⁺Gr1⁺ granulocytes dataset, which are depicted as heatmap. **(C)** Flow cytometry was subsequently used to determine the percentage of Gr1⁺ cells in the spleen following omvPV and wPV immunization. Data presented as mean ± SD (n = 4). * and ** = $p \leq 0.05$ and $p < 0.01$ for immunized mice vs. naive mice (day 0), ++ = $p \leq 0.01$ for omvPV-mice vs. wPV-mice.

Group 4 genes were upregulated in the early phase of immunization in omvPV-mice, but were not or hardly upregulated in wPV-mice. In addition, most of these genes were differentially expressed in omvPV-mice during the middle phase, while the expression in wPV-mice was unaltered. This group contained the anti-inflammatory formyl-peptide receptor (*Fpr2*) [29]

and Steap4 that decreases the inflammatory effect by repressing IL-6 production [30]. Moreover, genes involved in LPS responsiveness were upregulated, such as the secretory leukocyte peptidase inhibitor (*Slpi*) that suppresses responses to LPS [31], heme oxygenase 1 (*Hmox1*), *Stfa3* with a member of the same family *Stfa2l1*, and angiopoietin-like 4 (*Angptl4*) that is induced by LPS in the acute phase response [32]. Notably, *Angptl4* has multiple functions, e.g. inflammation and lipid metabolism [33]. Genes involved in metabolism (*Hk3, Tbxas1*) and more specifically the lipid metabolism (*Angptl4, Lpl, Hpgds*) were found in this group. Furthermore, this group comprised *Pf4/Cxcl4* that induces phagocytosis [34], myeloid cell specific genes (*Lilrb4, Ms4a3, Serpina3g*), danger-associated molecular patterns (DAMPs) (*S100a9, S100a8*), IFN-induced genes *Slfn4* and *Ifitm6*, and *Fcgr4* that binds IgG2a and IgG2b. Moreover, genes were detected encoding proteins expressed on or secreted by neutrophils, such as myeloperoxidase (*Mpo*), proteinase 3 (*Prtn3*), a chemoattractant receptor (*Cxcr2*), and *Il1f9* [35]. IL-1F9 promotes Th1 formation by binding IL-36R on T-cells [36].

Group 5 genes were increased on day 29 by both vaccines. Some of these genes are involved in the type I IFN-signaling pathway. This included *Irf7* as well as *Oasl1* that inhibits IRF7 [37], in addition to other IFN-induced proteins (*Ifi44, Ifi204, Ifi202b, Ifi27l2a, Ifit1, Ifit2, Ifit3, Ifih1, Ifitm3, Irgm1, H28, Mnda, Oasl2, Tor3a, Lgals3bp, Mx2*). Moreover, two genes were detected that encode PRRs which involved in sensing cytosolic DNA: DAI (*Zbp1*) [38] and LPG2 (*Dhx58*) [39]. Furthermore, genes encoding Fc receptors (*Fcgr1, Fcer1g*), a NOD-like receptor (*Nlrp12*), which is a neutrophil migration marker [40], C-type lectins (*Clec4d, Clec4e*), and other membrane markers (*Ly6a, Ms4a6d, Cd300lf, Gp49a*) were identified. Moreover, differential gene expression was detected for matrix metalloproteinase-8 (*Mmp8*), hemopoietic cell kinase (*Hck*), LPS-induced gene (*Cmpk2*), the colony stimulating factor 3 receptor (*Csf3r*), genes involved in apoptosis (*Cd5l, Xaf1*), two members of the guanylate-binding protein gene family (*Gbp6, Gbp9*) that assist in protection against bacterial infection [41], and two genes encoding tripartite-motif proteins (*Trim30a, Trim30c*) of which TRIM30α inhibits TLR4-mediated NF-kappaB activation [42].

Group 6 genes were upregulated on day 28(4h) by both vaccines. This group included an LPS-induced macrophage gene (*Ifi205*), the inflammatory chemokine Ccl12, the interleukin 1 receptor, type II (*Il1r2*), and protein tyrosine phosphatase 1B (*Ptpn1*) that controls pro-inflammatory responses after LPS exposure [43]. Moreover, upregulated genes encoding membrane markers were detected that are mainly myeloid-restricted (*Cd300e*) of which some are related to pathogen-recognition, such as dectin-2 (*Clec4n*) that recognizes high-mannose ligands, *Cd14* commonly expressed on monocytes and involved in LPS binding, and other membrane markers (*Cd244, Ccr3*).

Group 7 genes were merely differentially expressed in the wPV-mice in the early phase after immunization. This group included increased gene expression of PDGFC (*Pdgfc*), IFN regulatory factor 9 (*Irf9*), complement component 4B (*C4b*), lymphocyte membrane marker (*Ly6e*), an Fc-receptor (*Fcgr3*), adenosine deaminase (*Adar*) that represses the effect after

bacterial DNA sensing, and PARP-14 (*Parp14*) that promotes Th2 and Th17 cell formation and steers the antibody subclass distribution [44, 45]. In the late phase after wPV immunization, ten genes were exclusively expressed including an IgM gene (*Ighm*), *Cd83* an important activation marker on B-cell, T-cell, and dendritic cell populations [46], and others (*Gnas, Ctso, Hspa1a, Acta2, Ctgf,* and *Odz4*).

Based on this text mining, sets of genes involved in antibody formation, pathogen recognition receptors (PRRs), interferon regulatory factors (IRFs), IL-1 signaling, LPS sensing and lipid metabolism were found (**Figure 5A**). For further investigation of genes related to IFN-signaling, the transcriptome of the spleen was matched with the Interferome database to identify which vaccine-induced genes were involved in the type I and type II IFN-signaling pathways (**Figure S2**). In total, 91 genes were related to type I IFN, 22 to type II IFN, and 60 genes to both pathways. The omvPV induced the majority of IFN-related genes of both type I and II, whereas only 13 of such genes were found exclusively in wPV-mice. Moreover, the type II IFN-signaling pathway was mainly involved in the early phase of the immune responses after omvPV and wPV immunization. Genes of the type I IFN-signaling pathway were also mainly found in the early phase, but also partly in later phases (**Figure S2**).

Together, comparison of the splenic transcriptomes after omvPV and wPV immunization demonstrated that omvPV conferred a more diverse and more intense gene expression compared to wPV. Moreover, omvPV activated genes are involved in pathogen-recognition, dampening of LPS-responses, IFN-related genes, lipid metabolism, neutrophils, and antibody production.

Higher neutrophil responses elicited by omvPV compared to wPV

Gene expression profiles were compared with BioGPS databases to identify which cell types were involved in vaccine-induced immune responses (**Figure S1B**). According to this analysis, 46 genes were associated with $MAC^{+}GR1^{+}$ granulocytes (neutrophils). All 46 genes were detected in omvPV-mice and were mainly activated during the early and middle phase of the vaccine-induced response (**Figure 5B**). In contrast, only 16 of these 46 genes were upregulated in the wPV-mice. Flow cytometry confirmed that the percentage of $Gr1^{+}$ cells in the spleen was significantly increased by omvPV and wPV immunization between days 29-42 (**Figure 5C**). In line with the enhanced gene expression, the omvPV-induced response was characterized by a significant increase in $Gr1^{+}$ cells in the middle phase on day 42 compared to the wPV-induced response.

Reduced serum and pulmonary cytokine responses in immunized mice following *B. pertussis* challenge

Subsequent to the investigation of vaccine-induced responses, we examined the immune responses in omvPV-mice, wPV-mice, and N.I.-mice after *B. pertussis* challenge by measuring gene expression profiles, cytokine profiles, splenic neutrophils, antibody levels, and T-cell responses (Figure 1).

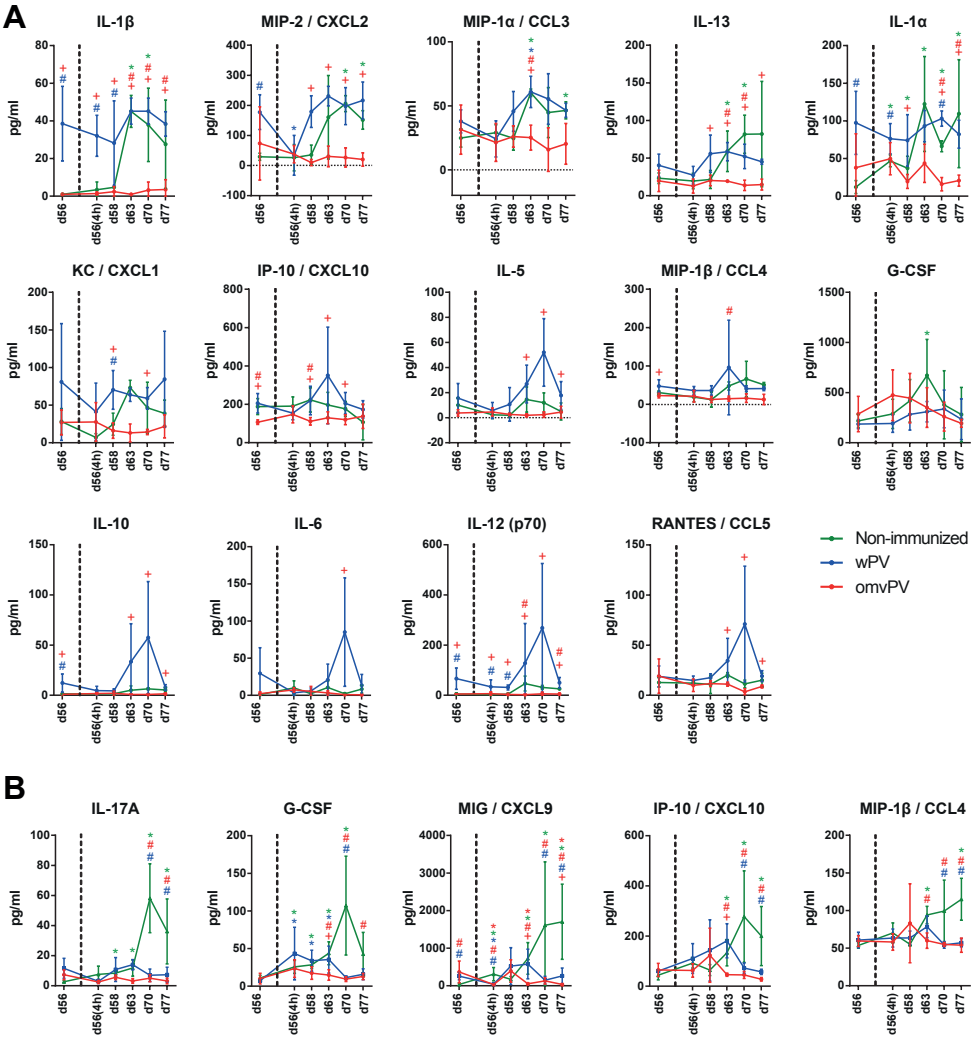

Figure 6 - Serum and pulmonary cytokine secretion following *B. pertussis* challenge in mice immunized with omvPV or wPV and non-immunized mice. **(A-B)** The concentrations of 32 cytokines were determined prior to and at multiple time points post challenge with *B. pertussis* in non-immunized mice (green) or mice immunized with omvPV (red) or wPV (blue). Only cytokines that were significantly altered in **(A)** serum and **(B)** lung lysate are depicted. Data are presented as mean ± SD for immunized groups (n = 4) and non-immunized groups (n = 3). * = $p \leq 0.05$ for challenged groups vs. day 56, # = $p \leq 0.05$ for immunized groups vs. non-immunized group, + = $p \leq 0.05$ for omvPV group vs. wPV group.

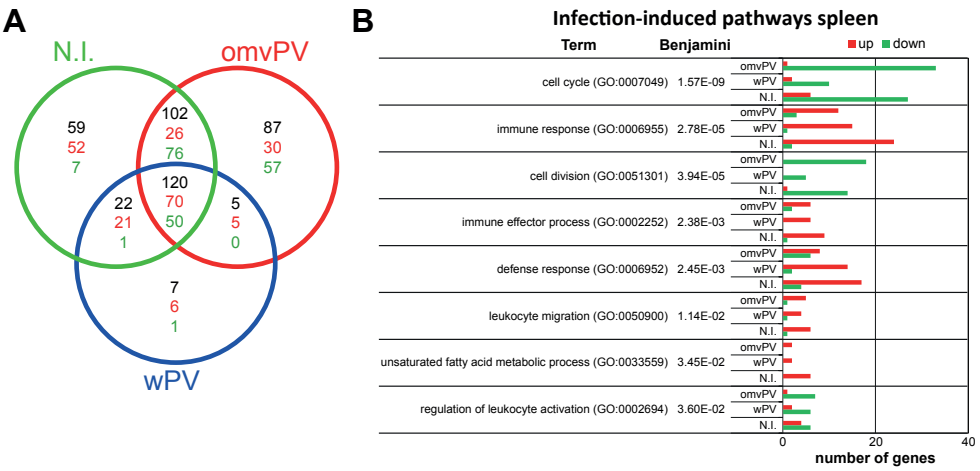
A
N.I.
omvPV
wPV
59
52
7
102
26
76
87
30
57
120
70
50
22
21
1
5
5
0
7
6
1
B
Infection-induced pathways spleen
Term
Benjamini
up
down
cell cycle (GO:0007049) 1.57E-09
immune response (GO:0006955) 2.78E-05
cell division (GO:0051301) 3.94E-05
immune effector process (GO:0002252) 2.38E-03
defense response (GO:0006952) 2.45E-03
leukocyte migration (GO:0050900) 1.14E-02
unsaturated fatty acid metabolic process (GO:0033559) 3.45E-02
regulation of leukocyte activation (GO:0002694) 3.60E-02
omvPV
wPV
N.I.
0
20
40
number of genes

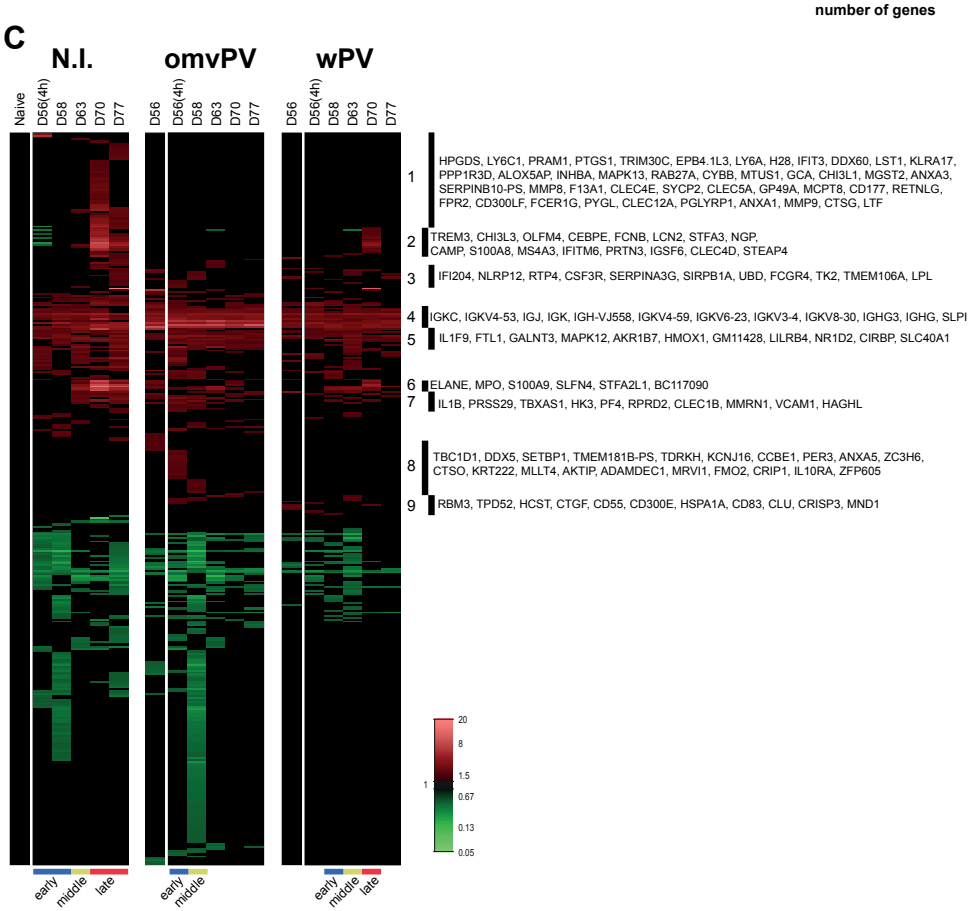
C
N.I.
omvPV
wPV
Naive
D56(4h)
D58
D63
D70
D77
D56
early
middle
late
1 HPGDS, LY6C1, PRAM1, PTGS1, TRIM30C, EPB4.1L3, LY6A, H28, IFIT3, DDX60, LST1, KLRA17, PPP1R3D, ALOX5AP, INHBA, MAPK13, RAB27A, CYBB, MTUS1, GCA, CHI3L1, MGST2, ANXA3, SERPINB10-PS, MMP8, F13A1, CLEC4E, SYCP2, CLEC5A, GP49A, MCPT8, CD177, RETNLG, FPR2, CD300LF, FCER1G, PYGL, CLEC12A, PGLYRP1, ANXA1, MMP9, CTSG, LTF
2 TREM3, CHI3L3, OLFM4, CEBPE, FCNB, LCN2, STFA3, NGP, CAMP, S100A8, MS4A3, IFITM6, PRTN3, IGSF6, CLEC4D, STEAP4
3 IFI204, NLRP12, RTP4, CSF3R, SERPINA3G, SIRPB1A, UBD, FCGR4, TK2, TMEM106A, LPL
4 IGKC, IGKV4-53, IGJ, IGK, IGH-VJ558, IGKV4-59, IGKV6-23, IGKV3-4, IGKV8-30, IGHG3, IGHG, SLPI
5 IL1F9, FTL1, GALNT3, MAPK12, AKR1B7, HMOX1, GM11428, LILRB4, NR1D2, CIRBP, SLC40A1
6 ELANE, MPO, S100A9, SLFN4, STFA2L1, BC117090
7 IL1B, PRSS29, TBXAS1, HK3, PF4, RPRD2, CLEC1B, MMRN1, VCAM1, HAGHL
8 TBC1D1, DDX5, SETBP1, TMEM181B-PS, TDRKH, KCNJ16, CCBE1, PER3, ANXA5, ZC3H6, CTSO, KRT222, MLLT4, AKTIP, ADAMDEC1, MRVI1, FMO2, CRIP1, IL10RA, ZFP605
9 RBM3, TPD52, HCST, CTGF, CD55, CD300E, HSPA1A, CD83, CLU, CRISP3, MND1
20
8
1.5
1
0.67
0.13
0.05

Figure 7 (Left) - Transcriptomic profiles in the spleen following *B. pertussis* challenge in omvPV-, wPV-, and non-immunized mice. **(A)** Fold changes in expression and significant gene expression were calculated compared to naive mice (FR ≥ 1.5, *p*-value ≤ 0.001). In total, 402 differentially expressed genes were found divided over the three groups in a Venn-diagram with total number of genes (black), upregulated genes (red), and downregulated genes (green). **(B)** Overrepresentation analysis on all 402 genes revealed the involvement of specific GO-BP terms and KEGG pathways with corresponding upregulated (red) and downregulated (green) genes. **(C)** All differentially upregulated (red) and downregulated (green) genes are portrayed as heatmap (mean of n = 3 for immunized groups, n = 1 (pool of 3 mice for non-immunized group)). Genes not surpassing a FR of 1.5 are shown as basal level (black). Gene clustering is based on up/downregulation, time of involvement, and presence in different groups. Infection-induced responses were divided in phases according to the hierarchical clustering calculated in **Figure S1C**. Selections of genes in nine (1-9) areas of the heatmap are shown.

First, concentrations of 32 cytokines were determined in serum and lung lysate (**Figure 6A-B**). In sera of N.I.-mice, IL-1α, IL-1β, CXCL2, CCL3, IL-13, and G-CSF were significantly increased mainly between days 63-77. Notably, no significant cytokine secretion was observed in sera of omvPV-mice (Figure 6A). The concentrations of IL-1α, IL-1β, IL-5, IL-6, IL-10, IL-12(p70), IL-13, CCL3, CCL4, CCL5, CXCL1, CXCL2, and CXCL10 were significantly higher in the sera of wPV-mice compared to omvPV-mice, mainly on day 63. However, the cytokine levels of wPV-mice were not induced upon challenge, as no significant differences were found after challenge compared to day 56, except for CCL3 (**Figure 6A**). Analysis of the pulmonary cytokine profiles demonstrated that IL-17A, G-CSF, CXCL9, CCL4, and CXCL10 were significantly increased in lung tissue of N.I.-mice, between day 63-77 (**Figure 6B**). These cytokines were not elevated in either of the immunized groups, except for G-CSF in wPV-mice between day 56(4h)-63. These results demonstrate that both omvPV and wPV immunization prevented pulmonary cytokine secretion following a *B. pertussis* challenge. However, the systemic cytokine responses in wPV-mice appeared more like those in N.I.-mice, but different in omvPV-mice.

Transcriptomic profiles in the spleen following *B. pertussis* challenge

Splenic transcriptomes of immunized mice were compared to those of N.I.-mice at 5 timepoints after an intranasal challenge. In total, 402 genes were differentially expressed in the spleen of immunized mice or N.I.-mice (*p*-value ≤ 0.001, FR ≥ 1.5) (**Figure 7A**). Differential expression of 87, 7, and 59 genes was exclusively detected in the challenged omvPV-mice, wPV-mice, and N.I.-mice, respectively. 120 genes (70 upregulated, 50 downregulated) were found in all three groups (**Figure 7A**). The ORA on infection-induced responses in the spleen revealed enrichment of 24 gene ontology biological pathways (GO-BP) terms and 2 KEGG pathways (Benjamini ≤ 0.05) in omvPV-mice, wPV-mice, and N.I.-mice (**Figure 7B**). In omvPV-mice, several of the downregulated genes are involved in Cell cycle (33 genes) and Cell division (18 genes). The terms Immune response and Defense response comprised a small number of genes that were differentially regulated in omvPV-mice, but in higher numbers in wPV-mice and N.I.-mice. Genes were clustered based on (i) co-expression over time and (ii) overlap between both experimental groups (**Figure 7C**). Hierarchical clustering on the three challenged groups indicated that the infection-induced response was distinct in immunized mice compared to the

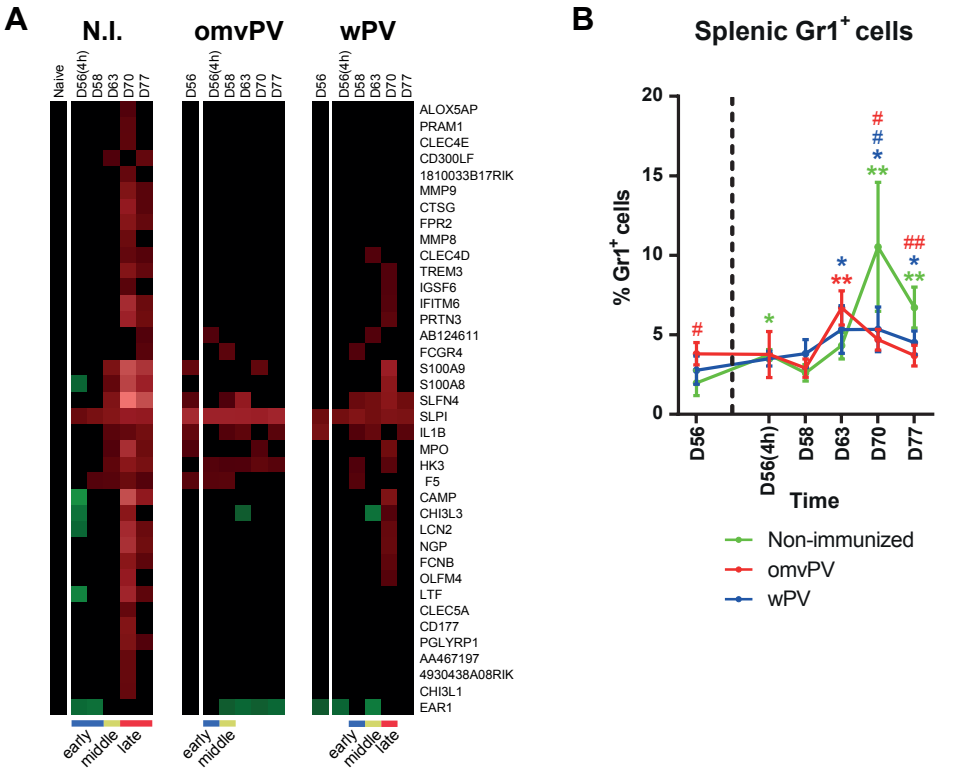

Figure 8 - Cell specific transcriptomic profiles and the involvement of Gr1⁺ cells after challenge of omvPV-, wPV-, and non-immunized mice. **(A)** Transcriptomic profiles from spleen tissue of omvPV-, wPV-, and non-immunized mice following a *B. pertussis* challenge were compared with BioGPS databases. In total, 38 differentially regulated genes matched with the Mac⁺Gr1⁺ granulocytes dataset and are depicted as heatmap. **(B)** Flow cytometry was used to determine the percentage of Gr1⁺ cells in the spleen after challenge of immunized and non-immunized mice. Data are presented as mean ± SD (n = 3). * and ** = $p \leq 0.05$ and $p \leq 0.01$ for challenged groups vs. day 56, # and ## = $p \leq 0.05$ and $p \leq 0.01$ for immunized groups vs. non-immunized group.

challenged N.I.-mice (Figure S1C). The infection-induced response of N.I.-mice was divided in three phases: early phase (day 56(4h)-58), middle phase (day 63), and late phase (day 70-77). In omvPV-mice, a faster response was observed compared to N.I.-mice and was divided in two phases: early phase (day 56(4h)) and middle phase (day 58). The later time points (day 63-77) were similar to the expression levels prior to challenge (day 56). In wPV-mice, a slightly slower response compared to omvPV was seen and could be divided in an early phase (day 58), middle phase (day 63), and late phase (day 70) (Figure 7C and S1C). A selection of genes in nine (1-9) areas in the heatmap is depicted. BioGPS analysis revealed induction of 38 genes in challenged N.I.-mice that are usually expressed in MAC⁺GR1⁺ granulocytes (Figure 8A). In immunized mice, neutrophil involvement after challenge was much less pronounced as only 10 and 22 genes were found in omvPV-mice and wPV-mice, respectively. Additional flow cytometry analysis on splenocytes revealed that the number of Gr1⁺ cells, indicative for

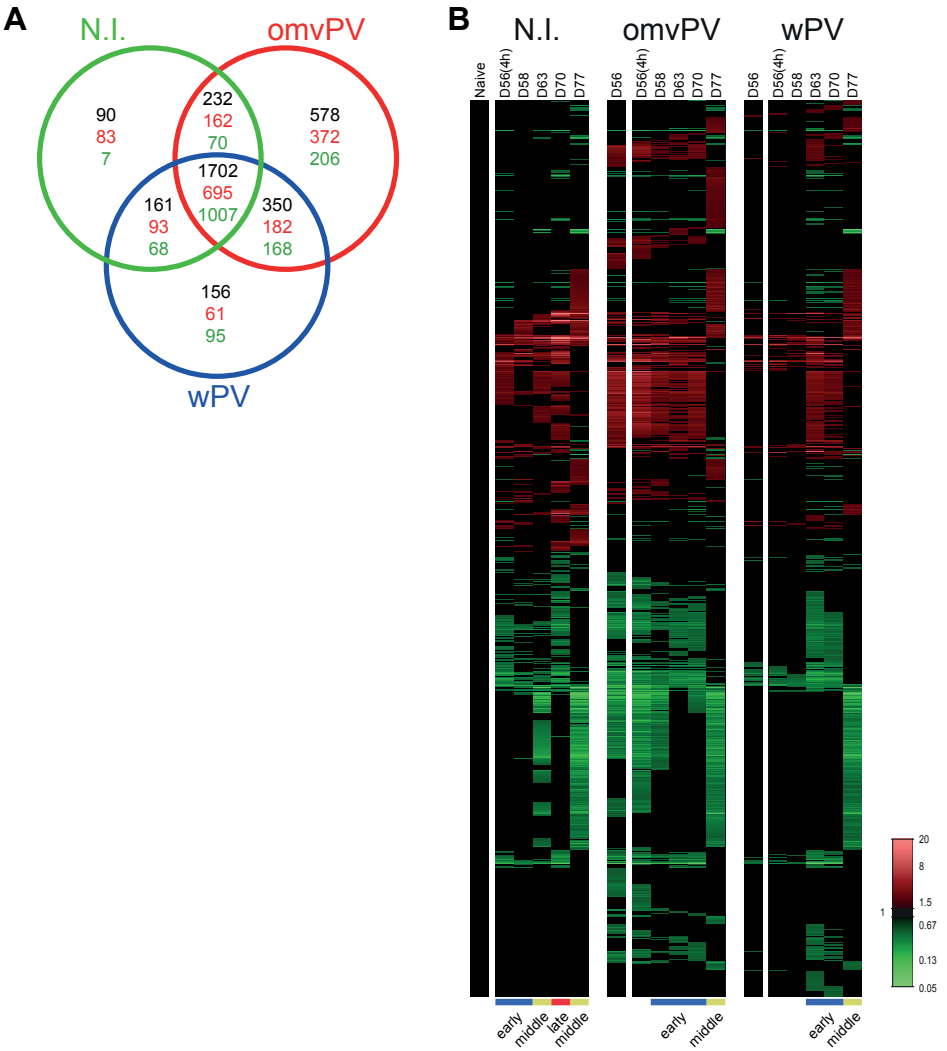

Figure 9 - Pulmonary transcriptomic profiles following *B. pertussis* challenge in omvPV- and wPV-and non-immunized mice. **(A)** Fold changes in expression and significant gene expression were calculated compared to naive mice (FR ≥ 1.5, *p*-value ≤ 0.001). In total, 3269 differentially expressed genes were found divided over the three groups in a Venn-diagram with total number of genes (black), upregulated genes (red), and downregulated genes (green). **(B)** All differentially upregulated (red) and downregulated (green) genes are portrayed as heatmap (mean of n = 3 for immunized groups, n = 1 (pool of 3 mice for non-immunized group)). Genes not surpassing a FR of 1.5 are shown as basal level (black). Gene clustering is based on up/downregulation, time of involvement, and presence in the different groups. Infection-induced responses were divided in phases according to the hierarchical clustering calculated in **Figure S1D**.

neutrophils, was significantly increased in N.I.-mice on day 70 (**Figure 8B**). In contrast, the fraction of Gr1$^+$ cells in omvPV-mice and wPV-mice was enhanced on day 63 and day 63-77, respectively. The Gr1$^+$ cell fraction in immunized mice was significantly lower between days 70-77 compared to N.I.-mice. Altogether, splenic transcriptome analysis after a challenge with

B. pertussis demonstrated less intense gene expression profiles in omvPV-mice and wPV-mice than in N.I.-mice. These responses were even lower in omvPV-mice than in wPV-mice.

Pulmonary transcriptomic profiles following *B. pertussis* challenge

To determine the effect of immunization on the murine host response in the lung following *B. pertussis* challenge, pulmonary transcriptomic profiles of challenged immunized mice were compared to those of challenged N.I.-mice. In total, 3269 genes were differentially expressed in lungs of immunized mice or N.I.-mice (p-value ≤ 0.001, FR ≥ 1.5) (**Figure 9A**). Exclusive differential expression of 578, 156, and 90 genes was detected in challenged omvPV-mice, wPV-mice, and N.I.-mice, respectively. In total, 1702 genes (695 upregulated, 1007 downregulated) were found in all three groups (**Figure 9A**). Genes were clustered based on (i) co-expression over time and (ii) overlap between both experimental groups (**Figure 9B**). Hierarchical clustering on the pulmonary transcriptome of the three challenged groups demonstrated a distinct infection-induced response in immunized mice compared to challenged N.I.-mice (**Figure S1D**). The infection-induced response of N.I.-mice was divided in three phases: early phase (day 56(4h)-58), middle phase (day 63 and day 77) and late phase (day 70), as seen before [23]. In omvPV-mice, the response was less diverse compared to day 56 and was divided in two phases; early phase (day 56(4h)) and middle phase (day 70). In wPV-mice, the response compared to day 56 was more diverse and developed slower than in omvPV-mice with an early phase (day 63-70) and middle phase (day 77) (**Figure 9B and S1D**). The pulmonary transcriptome in omvPV-mice on day 56 prior to challenge differs a lot from the naive basal gene expression level. Moreover, omvPV-mice show less change in pulmonary gene expression as compared to wPV-mice and N.I.-mice after challenge. Together, these results demonstrate that a *B. pertussis* challenge evokes fewer effects on gene expression levels in omvPV-mice than wPV-mice and N.I.-mice.

Adaptive recall responses in omvPV-mice and wPV-mice following *B. pertussis* challenge

Prior to the challenge (day 56), no vaccine-induced anti-OMV IgA could be detected in the lungs of omvPV-mice and wPV-mice (**Figure 10A**). However, after intranasal *B. pertussis* challenge, anti-OMV IgA antibodies were detected in a similar amount in wPV-mice and N.I.-mice on day 63-77, yet not in omvPV-mice. Serum IgG levels specific for pertussis OMV or whole-cells were unaltered in wPV-mice and were slightly decreased in omvPV-mice after the intranasal challenge, whereas IgG levels in N.I.-mice were rising between day 63-77 (**Figure 10B-C**). The specificity of IgG antibodies, as determined by immunoblot, did not change in omvPV-mice after a challenge, except for the disappearance of the band at 15 kDa (**Figure 10D**). The challenge of wPV-mice led to the formation of additional antibodies directed against GroEL (60 kDa) and an unknown antigen of 20 kDa.

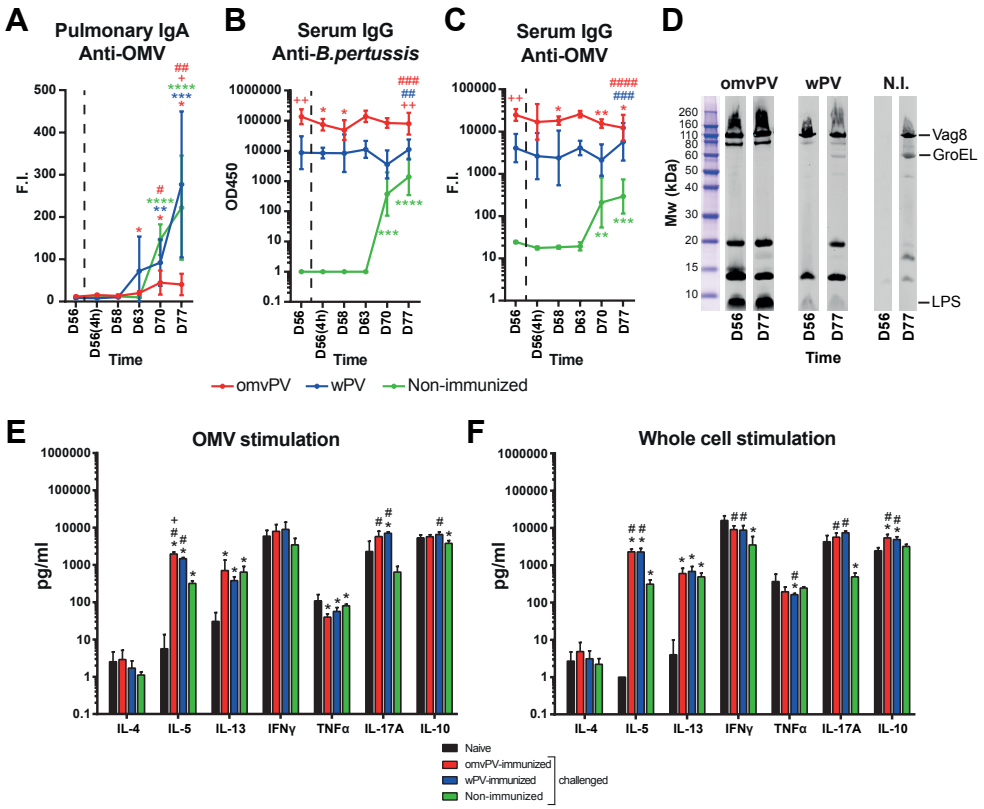

Figure 10 - Humoral and cellular adaptive recall responses following *B. pertussis* challenge in omvPV- and wPV-immunized mice as compared to control mice before and after challenge. **(A-C)** Kinetics of **(A)** pulmonary anti-OMV IgA, **(B)** serum anti-*B. pertussis* IgG, and **(C)** serum anti-OMV IgG levels were determined for a period of 21 days following intranasal challenge in immunized mice (n = 4) and non-immunized mice (N.I.) (n = 3). Data are presented as mean ± SD. Statistical significance of differences in **(A)**, **(B)** and **(C)**: *, **, *** and **** = $p \leq 0.05$, $p \leq 0.01$, $p \leq 0.001$ and $p \leq 0.0001$ for vs. day 56 per group, + and ++ = $p \leq 0.05$ and $p \leq 0.01$ for omvPV vs. wPV, #, ##, ### and #### = $p \leq 0.05$, $p \leq 0.01$, $p \leq 0.001$ and $p \leq 0.0001$ for immunized groups vs. non-immunized group. **(D)** Immunoproteomic profiles of serum IgG antibodies (pooled sera, n = 4) before (day 56) and 21 days post challenge (day 77) were obtained on a *B. pertussis* lysate. **(E-F)** Concentrations of IL-4, IL-5, IL-13, IFNγ, TNFα, IL-17A and IL-10 were determined in the culture supernatants after 7 day stimulation with **(E)** 5 µg/ml OMVs, or **(F)** 5 µg/ml *B. pertussis* whole-cells. Splenocytes were obtained from naive mice (black) and post-challenge (day 77) of mice that were omvPV- (red), wPV- (blue) or non-immunized (green). Results for each mouse are corrected for medium stimulation. Data in **(E)** and **(F)** presented as mean ± SD (n = 4). Statistical significance of differences in **(E)** and **(F)**: * = $p \leq 0.05$ for challenged groups vs. naive, + = $p \leq 0.05$ for omvPV group vs. wPV group, # = $p \leq 0.05$ for immunized group vs. non-immunized group.

Th-responses were determined post challenge, by analyzing the levels of seven cytokines in culture supernatants after antigen-specific stimulation of splenocytes from challenged omvPV-mice, wPV-mice, and N.I.-mice, with those of non-challenged naive mice as control, harvested on day 77 (Figure 10E-F and S3). After stimulation with OMVs, Th1 (TNFα), Th2 (IL-5 and IL-13), and Th17 (IL-17A) cytokines were altered in challenged omvPV-mice, wPV-mice, and N.I.-mice compared to naive mice. IL-5 and IL-17A levels were higher in immunized mice compared to N.I.-mice (Figure 10E). Stimulation with *B. pertussis* whole-cells led to altered levels of Th1

(IFNγ), Th2 (IL-5 and IL-13) and Th17 (IL-17A) cytokines in omvPV-mice, wPV-mice, and N.I.-mice compared to naive mice. The levels of these cytokines were overall higher in immunized mice compared to N.I.-mice. Moreover, production of IL-10 was only observed in immunized mice (**Figure 10F**). IFNγ and TNFα were both high in naive control mice after stimulation with *B. pertussis* OMVs and whole-cells, most likely caused by LPS. Nevertheless, omvPV-mice and wPV-mice showed a similar result post challenge on day 77 as after immunization on day 49. Stimulation with Prn resulted in increased concentrations of IL-13 and IL-17A in challenged immunized and N.I.-mice compared to the non-challenged naive group (**Figure S3A, right panel**). These IL-17A levels were significantly higher in both immunized groups compared to the N.I.-mice. Furthermore, significantly higher IL-5 production was observed in omvPV-mice and N.I.-mice than in wPV-mice. After Ptx stimulation, IL-17A production was exclusively observed in wPV-mice (**Figure S3B, right panel**). IL-5, IL-13 and IL-17A production was evoked by FHA stimulation in immunized and N.I.-mice. Moreover, enhancement of IFNγ, TNFα, and IL-10 was detected in wPV-mice (**Figure S3C, right panel**). In conclusion, the cytokine profiles showed enhanced Th1/Th2/Th17 *ex vivo* recall responses in challenged omvPV-mice and wPV-mice compared to challenged N.I.-mice.

Discussion

Introduction of an improved third generation pertussis vaccine requires in-depth knowledge on vaccine-induced responses in comparison to current pertussis vaccines especially in terms of efficacy and safety profile. To that end, we applied a systems biology approach to compare comprehensive immune responses in a murine model induced by an OMV-based pertussis vaccine (omvPV) or a classical whole-cell pertussis vaccine (wPV).

Parenteral injection of wPV has been related to adverse effects [8, 9] and suspected correlation with serious acute neurological illness in children [10, 11] mainly as a result of circulating pro-inflammatory cytokines such as IL-1β, TNFα, and IL-6 [11, 47]. This has been a key reason for the development of aPVs that are safer and better defined. Our *in vivo* study demonstrated that omvPV in comparison to wPV, with an equal total protein dose, elicited reduced concentrations of serum pro-inflammatory cytokines (IL-1α, IL-1β, and IL-6), chemokines (CXCL1 and CXCL10), and G-CSF. Especially, the reduced IL-1β secretion by omvPV may be beneficial given its involvement in the suspected acute neurological illness [11]. Activation of Toll-like receptors (TLRs) [48] by pathogen-associated molecular patterns (PAMPs), like lipopolysaccharide (LPS) and bacterial DNA, result in the secretion of these cytokines. Previously we showed that the omvPV contains less TLR activating LPS and DNA per amount protein than wPV [7]. An additional hypothesis might be that omvPV contains mostly membrane-associated LPS and less free LPS compared to wPV thus resulting in lower cytokine induction. Less pro-inflammatory cytokine production was also seen when LPS is adsorbed to alum [49], which demonstrates that free LPS might be more pyrogenic than bound LPS. On the other hand, LPS in omvPV seems more immunogenic than LPS in wPV (**Figure 2H**). The lower concentrations of LPS and DNA in omvPV may therefore lead to less activation of TLR4 and TLR9 and contribute to the attenuated pro-inflammatory cytokine response by omvPV compared to wPV.

The splenic transcriptome measured after booster omvPV and wPV immunization demonstrated that omvPV induced a larger number of genes than wPV. This was an unexpected observation in light of the attenuated pro-inflammatory cytokine signatures. The triggering of anti-inflammatory responses, diminished PRR responses, and expression of modifiers that dampen inflammatory LPS responses in omvPV-mice may explain why omvPV elicited low amounts of pro-inflammatory cytokines. OmvPVs activated genes encoding anti-inflammatory formyl peptide receptors FPR1 and FPR2. These PRRs bind many different signal peptides of bacteria [50] which are important for rapid neutrophil recruitment [51]. Furthermore, the response induced by omvPV may repress pro-inflammatory responses following LPS recognition due to enhanced gene expression of FPR2, SPLI, STEAP4, PTPN1, and MSR1, which correspond to proteins that are attenuators of LPS responses [26, 29-31, 43].

Finally, omvPV stimulated genes encoding proteins with a dual function in lipid metabolism and anti-inflammatory responses, namely ANGPTL4 [32, 33], HPGD2S [52], and LXRα. These metabolic signatures may have been activated by lipid mediators induced by omvPV and may subsequently contribute to the anti-inflammatory response that is less prominent in the wPV-induced response. Despite the lower content of genomic DNA in omvPV [7], two genes encoding PRRs sensing cytosolic DNA, DAI [38], and LPG2 [39], were upregulated by both vaccines. Interestingly, only omvPV immunization led to enhanced gene expression of TLR3 and TLR7, intracellular sensors for viral and bacterial nucleotides. Activation of TLRs leads to induction of IFN-signaling pathways. For instance, we found induction of transcription factor IRF7, a factor downstream of TLR7, by both vaccines. IRF7 is an important mediator of type I IFN-signaling [53]. Overall, a large number of genes of the type I IFN-signaling pathway were induced by omvPV and wPV, which were more profound in the omvPV response. Type I IFN-signaling can affect a broad range of immune mediators, including both innate and adaptive immune cells [54]. With respect to CD4 T-cells, the pathway is important for the regulation of Th1 and Th17 responses [55]. Additionally, both vaccines induced many genes involved in the type II IFN-signaling pathway. IFNγ is the only member of the type II IFN family, for which upregulation of associated genes was again more profound in the omvPV response. Therefore, induction of both types of IFN-signaling pathways by omvPV and wPV seems to contribute to Th1/Th17 responses that are thought to be important for protection [3, 4, 23].
TLR4 activation by LPS is one of the pathways that can direct the cellular responses towards Th1 and Th17 responses [5, 6]. Thus, it is important to evaluate whether the reduced TLR4-signaling by omvPV does not affect the ability of omvPV to induce *B. pertussis*-specific Th1 and Th17 responses. Cytokine profiles of stimulated splenocytes revealed that omvPV and wPV both induce mixed systemic Th1/Th2/Th17 responses, in contrast to the Th2-biased aPV-induced response [4, 14]. This indicates that despite lower LPS concentration and TLR4-signaling, the omvPV still induced a similar Th response as wPV. This may suggest that the LPS concentration in omvPV is sufficient for the induction of Th1/Th17 responses or that other signaling, such as TLR2 [56], promote Th17 responses.
The concentrations of aPV components (Prn, FHA, and Ptx) are low in the omvPV and wPV used in this study, except for FHA in wPV [7]. Therefore, it was not surprising that antibody and T-cell responses specific for these antigens were low following immunization with omvPV and wPV. However, high levels of antibodies against other *B. pertussis*-specific antigens were detected that were more strongly induced by omvPV when compared to wPV. Especially the booster immunization induced a strong antibody response that was mainly directed against BrkA, Vag8 and LPS, in line with our previous study [7]. This broad humoral response conferred by both omvPV and wPV might limit the risk of driving *B. pertussis* adaptation as a result of vaccine-induced selection pressure. As Prn-deficient *B. pertussis* strains are increasingly circulating, especially in aPV-immunized populations, it has been hypothesized that this might be the result of pathogen adaptation [57, 58]. Since omvPV contains more BrkA and Vag8 [7],

higher antibody levels were induced against these antigens. Remarkably, despite the lower LPS concentrations measured in omvPV, the omvPV booster immunization induced higher anti-LPS IgG3 antibody levels than wPV. This indicates that the LPS in omvPV was processed in a different way by the immune system during the first immunization compared to booster immunization. Since anti-LPS IgG3 antibodies are mostly produced in a T-cell independent manner [59], this may indicate that omvPV evokes a more efficient T-cell independent B-cell response than wPV. Furthermore, mucosal *B. pertussis*-specific IgA induction in the lungs was absent after immunization with omvPV and wPV, as expected. Mucosal IgA is produced after natural infection [23, 60] and contributes most likely to a faster lung clearance during *B. pertussis* challenge. Presumably, direct involvement of the respiratory tract through intranasal or pulmonary vaccine administration may result in more effective immunity.

Mice immunized with omvPV or wPV showed rapid clearance of *B. pertussis* from the lungs after challenge when compared to N.I.-mice. Whereas no significant differences were observed between both immunized groups, lungs of omvPV-mice tended to be cleared slightly faster perhaps because of the higher serum IgG levels. Previously, intraperitoneal immunization with alum-adjuvated omvPV and wPV derived from a *B. pertussis* Tohama strain also demonstrated equal protection [15]. The *B. pertussis* challenge was utilized to elucidate the pre-existing immunity in omvPV-mice and wPV-mice. The immune responses of challenged immunized mice were characterized by (i) adaptive recall responses, (ii) a change in pulmonary environment by reduced cytokine secretion and transcriptome expression, (iii) altered systemic cytokine responses, and (iv) reduced splenic transcriptome expression in comparison to challenged N.I.-mice. The presence of high serum IgG levels and the strong recall of Th1/Th2/Th17 responses enabled a rapid clearance in both immunized groups. In contrast to the vaccine-induced responses, the responses after challenge of immunized and N.I.-mice were characterized by detectable Th cytokines after stimulation with purified proteins, which indicates significant specific T-cell activation as a result of prolonged exposure to these antigens after *B. pertussis* challenge [23]. Furthermore, immunized mice responded less vigorous on an infection with respect to the splenic and pulmonary transcriptome, pulmonary and serum cytokine responses, and number of splenic neutrophils. The N.I.-mice showed the largest changes in gene expression in the lungs 14 days after challenge, which is in line with our previous study [23]. These responses were overall lower in omvPV-mice than wPV-mice. Finally, no IL-17A was secreted after *ex vivo* Ptx stimulation of splenocytes, and no antigen-specific IgA was detected in the lungs of challenged omvPV-mice, while these were present in both wPV-mice and N.I.-mice. This Ptx exposure occurred during *B. pertussis* colonization, as Ptx is absent in both omvPV and wPV used in this study [7]. Since the responses after *B. pertussis* challenge of wPV-mice and N.I.-mice show more similarities compared to those of omvPV-mice, this may indicate that omvPV-mice controlled the *B. pertussis* challenge more effectively than wPV-mice.

In summary, we demonstrated that in comparison to wPV, omvPV confers equal protection with higher IgG levels and a comparable Th1/Th2/Th17 response. Additionally, the systems approach provided detailed insight into the molecular signatures of the vaccine as well as challenge-induced responses. The inflammatory responses elicited by omvPV were milder, as reflected by reduced levels of pro-inflammatory cytokines. Probably, inflammatory responses are attenuated by the enhanced anti-inflammatory responses, i.e. ANGPTL4, FPR2, PTPN1, SPLI, and STEAP4. Therefore, it is tempting to speculate that the decreased inflammatory responses induced by omvPV reflect a better safety profile. In conclusion, our collective findings emphasize the potential of omvPV as a third-generation pertussis vaccine.

Methods

Vaccines and challenge culture

OmvPV from *B. pertussis* B1917 were produced as previously described [61]. For production of wPV, *B. pertussis* B1917 was heat-inactivated (30 min, 56°C) in PBS. Both omvPV and wPV were diluted in PBS to a final concentration of 4 µg total protein per immunization dose (300 µl). Vaccine characterization included particle size, protein composition, and LPS and DNA content [7]. For the challenge culture, stock suspension of *B. pertussis* strain B1917 was diluted with Verweij medium (BBio, Bilthoven, The Netherlands) to a final concentration of $5x10^6$ colony-forming units (cfu)/ml.

Animal experiment

An independent ethical committee of the Institute for Translational Vaccinology (Intravacc) approved the animal experiment with identifier 201200073. 8 week old female BALB/c mice (Harlan, The Netherlands) were subcutaneously immunized with 4 µg total protein in 300 µl of either omvPV or wPV on day 0 (left groin) and day 28 (right groin). Mice were challenged intranasally under anesthesia (isoflurane/oxygen), with 2×10^5 cfu of *B. pertussis* B1917 in 40 µL of Verweij medium on day 56. Non-immunized (N.I.) mice were used as a control.

For the determination of gene expression in spleen, cytokine responses and antibody responses, mice (n = 4) were sacrificed on day 28 after primary immunization. In addition, mice (n = 4) were euthanized after booster immunization on day 28 + 4 hours (day 28(4h)), and day 29, 30, 32, 35, 38, 42, 49 and 56. Finally, mice (n = 4 per group) were sacrificed 4 hours after challenge and on day 58, 63, 70, and 77 to measure bacterial load in the respiratory tract, antibody responses and cytokine responses. For the investigation of Th subsets, mice (n = 4) were sacrificed on day 49 and 84. Naive mice (n = 4) were included as additional control group on each time point. Mice were bled under anesthesia (isoflurane/oxygen) by orbital bleeding and sacrificed by cervical dislocation for further sample collection. An overview of the study design is depicted in **Figure 1A**.

Sample collection and preparation

For investigation of cytokine and antibody responses in serum, whole blood from each mouse was collected in a blood collection tube (MiniCollect 0.8 ml Z Serum Sep GOLD, Greiner Bio-One, Austria). After coagulation (10 min. at room temperature) and centrifugation (10 min., 3000 g), sera were taken and stored at -80°C. For the colonization assay, the right lung lobe was placed in 900 ml Verweij medium at room temperature. To determine pulmonary cytokine and antibody responses, the lung lysates used for colonization assays were filtered (Millex GV Filter unit 0.22 µm, Millipore) and stored at -80°C. For characterization of pulmonary gene expression, the left lung lobe was placed in 1 ml RNAlater (Qiagen), incubated overnight at 4°C, and stored at -80°C. In addition, the spleen was excised and divided in two equal parts.

For gene expression analysis, one piece was placed in 1 ml RNAlater (Qiagen), incubated overnight at 4°C and stored at -80°C. For detection of $Gr1^+$ cells, the other piece was placed in in 5 ml RPMI-1640 medium (Gibco) supplemented with 10% FCS (Hyclone), 100 units penicillin, 100 units streptomycin, and 2.92 mg/ml L-glutamine (Invitrogen), hereafter called RPMI complete medium, and kept on ice. For the analysis of Th responses, the whole spleen was placed in 5 ml of RPMI medium and kept on ice. Splenocytes were isolated by homogenization of spleens using a 70-µm cell strainer (BD Falcon, BD Biosciences) in RPMI complete medium.

Colonization assay

The numbers of cfu in lung tissue were determined as previously described [23].

RNA isolation and microarray analysis

Isolation and determination of concentration and integrity of RNA obtained from lung and spleen tissue were performed as described before [23]. For spleen tissue of both omvPV-mice and wPV-mice, individual RNA concentrates of individual mice (n = 3) were analyzed for all 16 time points (naive, and day 28, 28(4h), 29, 30, 31, 32, 35, 42, 49, 56, 56(4h), 58, 63, 70, and 77 post primary immunization). For lung tissue, samples of individual mice were analyzed for the following time points: day 56(4h), 58, 63, 70, and 77 post primary immunization. For the non-immunized mice after challenge, samples of lung and spleen tissue were pooled (n = 3). Amplification, labeling and hybridization of RNA samples for either lung or spleen tissue to microarray chips (NimbleGen 126135 k Mus musculus, Roche, Germany) was carried out at the Microarray Department of the University of Amsterdam, The Netherlands, as described previously [23].

Data analysis of gene expression

Quality control and normalization of raw microarray data was performed as described before [23]. To identify differentially expressed genes between experimental groups (naive and various time points post immunization or challenge) an ANOVA was applied. The induction or repression of individual genes was expressed as fold ratio (FR) by comparing mean gene expression levels of experimental groups to the naive mice. Average normalized gene expression levels contain data of three mice per immunized group. The data of challenged non-immunized mice are individual samples of pooled RNA of three mice. The dataset of challenged non-immunized mice (n = 3) of our previous study [23] was incorporated in the analysis to increase the statistical power. Probes were considered differentially expressed if they met the following two criteria: (i) a *p*-value < 0.001 (ANOVA), which corresponds to a Benjamini-Hochberg False discovery rate (FDR) [62] of < 5%; and (ii) an absolute FR ≥ 1.5 (experimental groups compared to naive mice) for at least one time point. If multiple probes corresponding to the same gene were differentially expressed, their data were averaged to remove redundancy for further analysis. GeneMaths XT (Applied Maths, St-Martens-Latem,

Belgium) was used to visualize differences in gene expression in heatmaps and perform the hierarchical clustering using Euclidean distance (linear scaling) with UPGMA clustering. Genes were arranged according to similar expression patterns in time at which genes exceeded the FR cut-off of 1.5. To facilitate visual interpretation of heatmaps, only induction (red) and repression (green) of gene expression levels with fold ratios ≥ 1.5 are visualized, therefore presenting fold ratios ≤ 1.5 as naive level (black). Functional enrichment with an over-representation analysis (ORA) based on Gene Ontology Biological Processes (GO-BP) and Kyoto Encyclopedia of Genes and Genomes (KEGG) by using DAVID and the detection of cell-specific or tissue-specific gene expression based on BioGPS datasets was performed as described previously [23]. Involvement of type I and II IFN-signaling pathway was performed by using the Interferome database (http://www.interferome.org/interferome/home.jspx) [63]. Additional text mining on gene function was performed in PubMed.

Multiplex immunoassay (MIA) and ELISA for antibody response

Levels of pulmonary IgA and serum IgM, IgA, total IgG and IgG subclasses (IgG1, IgG2a, IgG2b and IgG3) specific for *B. pertussis* antigens Prn, FHA, Ptx, combined fimbria type 2 and 3 antigens (Fim2/3) and outer membrane vesicles B1917 (OMV B1917) were determined as described previously [23] and are presented as fluorescent intensity (F.I.). Whole-cell *B. pertussis* ELISA for total serum IgG was performed as described before [23].

Immunoproteomic profiling of serum IgG antibodies

Antigen specificity of *B. pertussis*-specific serum IgG antibody responses were determined by SDS-PAGE and subsequent Western blotting as described before [7].

$Gr1^+$ cells in the spleen

After treatment with erythrocyte lysis buffer (8.3 g/L NH_4CL, 1 g/L $NaHCO_3$, 5000 IE/L Heparin in dH_20; pH 7.4), the percentage of $Gr1^+$ cells in the spleen was determined with flow cytometry as described before [23].

Isolation and *in vitro* restimulation of splenocytes

After treatment with erythrocyte lysis buffer, splenocytes were cultured in 24-well plates at 6×10^6 cells/well for 7 days at 37°C in a humidified atmosphere containing 5% CO_2 in IMDM medium (Gibco) supplemented with 8% FCS, 100 units penicillin, 100 units streptomycin, 2.92 mg/ml L-glutamine, and 20 µM β-mercaptoethanol (Sigma). The cells were either left unstimulated (medium control) or stimulated with 1 µg/ml, 1 µg/ml Ptx, 1 µg/ml FHA, 5 µg/ml OMV, or 5 µg/ml heat-killed *B. pertussis*. *B. pertussis* antigens Ptx and FHA were obtained from Kaketsuken (Japan), Prn and Fim2/3 were kindly provided by Betsy Kuipers (National Institute for Public Health and the Environment, Bilthoven, the Netherlands). On day 7, supernatant was collected for cytokine analysis.

Cytokine profiling using multiplex technology

Concentrations (pg/ml) of 32 cytokines (Eotaxin, G-CSF, GM-CSF, IFNγ, IL-10, IL-12 (p40), IL-12 (p70), IL-13, IL-15, IL-17A, IL- 1α, IL-1β, IL-2, IL-3, IL-4, IL-5, IL-6, IL-7, IL-9, IP-10, KC, LIF, LIX, M-CSF, MCP-1, MIG, MIP-1α, MIP-1β, MIP-2, RANTES, TNFα, VEGF) present in serum and lung lysates were determined by using a MIA (Milliplex MAP Mouse Cytokine/ Chemokine - Premixed 32 Plex; Merck KGaA, Darmstadt, Germany) following the manufacturer's protocol.

The concentration of various Th cytokines (IL-4, IL-5, IL-10, IL-13, IL-17A, TNFα, and IFNγ) was determined in culture supernatant using a Milliplex mouse cytokine 7-plex luminex kit (Millipore), according to the manufacturer's protocol. Measurements and data analysis were performed with Bio-Plex 200, using Bio-PlexManager software (version 5.0, Bio-Rad Laboratories). Results were corrected for the background (medium control) per mouse per stimulation per cytokine and calculated in pg/ml.

Statistical analysis

Data of the antibody, cytokine, and colonization assays were log-transformed after which a t-test was performed. *P*-values ≤ 0.05 were considered to indicate significant differences.

Acknowledgments

The authors are grateful to Tim Bindels of Intravacc for the production of the omvPV. The authors thank employees of the Animal Research Centre (ARC) of Intravacc for the performance of animal experiments, and employees of the Microarray Department (MAD) of the University of Amsterdam for the performance of the microarray analyses.

References

1. Cherry, J.D., Epidemic pertussis in 2012--the resurgence of a vaccine-preventable disease. N Engl J Med, 2012. 367(9): p. 785-7.
2. Tan, T., *et al.*, Pertussis Across the Globe: Recent Epidemiologic Trends From 2000-2013. Pediatr Infect Dis J, 2015. 34(9): p. e222-32.
3. Warfel, J.M. and T.J. Merkel, *Bordetella pertussis* infection induces a mucosal IL-17 response and long-lived Th17 and Th1 immune memory cells in nonhuman primates. Mucosal Immunol, 2013. 6(4): p. 787-96.
4. Ross, P.J., *et al.*, Relative contribution of Th1 and Th17 cells in adaptive immunity to *Bordetella pertussis*: towards the rational design of an improved acellular pertussis vaccine. PLoS Pathog, 2013. 9(4): p. e1003264.
5. Higgins, S.C., *et al.*, TLR4 mediates vaccine-induced protective cellular immunity to *Bordetella pertussis*: role of IL-17-producing T cells. J Immunol, 2006. 177(11): p. 7980-9.
6. Banus, S., *et al.*, The role of Toll-like receptor-4 in pertussis vaccine-induced immunity. BMC Immunol, 2008. 9: p. 21.
7. Raeven, R.H.M., *et al.*, Immunoproteomic Profiling of *Bordetella pertussis* Outer Membrane Vesicle Vaccine Reveals Broad and Balanced Humoral Immunogenicity. J Proteome Res, 2015. 14(7): p. 2929-42.
8. Jefferson, T., M. Rudin, and C. DiPietrantonj, Systematic review of the effects of pertussis vaccines in children. Vaccine, 2003. 21(17-18): p. 2003-14.
9. David, S., P.E. Vermeer-de Bondt, and N.A. van der Maas, Reactogenicity of infant whole cell pertussis combination vaccine compared with acellular pertussis vaccines with or without simultaneous pneumococcal vaccine in the Netherlands. Vaccine, 2008. 26(46): p. 5883-7.
10. Miller, D.L., *et al.*, Pertussis immunisation and serious acute neurological illness in children. Br Med J (Clin Res Ed), 1981. 282(6276): p. 1595-9.
11. Armstrong, M.E., *et al.*, IL-1beta-dependent neurological effects of the whole cell pertussis vaccine: a role for IL-1-associated signalling components in vaccine reactogenicity. J Neuroimmunol, 2003. 136(1-2): p. 25-33.
12. Klein, N.P., *et al.*, Waning protection after fifth dose of acellular pertussis vaccine in children. N Engl J Med, 2012. 367(11): p. 1012-9.
13. Warfel, J.M., L.I. Zimmerman, and T.J. Merkel, Acellular pertussis vaccines protect against disease but fail to prevent infection and transmission in a nonhuman primate model. Proc Natl Acad Sci U S A, 2014. 111(2): p. 787-92.
14. Brummelman, J., *et al.*, Modulation of the CD4 T cell response after acellular pertussis vaccination in the presence of TLR4 ligation. Vaccine, 2015. 33(12): p. 1483-91.
15. Roberts, R., *et al.*, Outer membrane vesicles as acellular vaccine against pertussis. Vaccine, 2008. 26(36): p. 4639-46.
16. Gaillard, M.E., *et al.*, Acellular pertussis vaccine based on outer membrane vesicles capable of conferring both long-lasting immunity and protection against different strain genotypes. Vaccine, 2014. 32(8): p. 931-7.
17. Nakaya, H.I., *et al.*, Systems biology of vaccination for seasonal influenza in humans. Nat Immunol, 2011. 12(8): p. 786-95.
18. Furman, D., *et al.*, Apoptosis and other immune biomarkers predict influenza vaccine responsiveness. Mol Syst Biol, 2013. 9: p. 659.
19. Querec, T.D., *et al.*, Systems biology approach predicts immunogenicity of the yellow fever vaccine in humans. Nat Immunol, 2009. 10(1): p. 116-25.
20. Obermoser, G., *et al.*, Systems scale interactive exploration reveals quantitative and qualitative differences in response to influenza and pneumococcal vaccines. Immunity, 2013. 38(4): p. 831-44.
21. Li, S., *et al.*, Molecular signatures of antibody responses derived from a systems biology study of five human vaccines. Nat Immunol, 2014. 15(2): p. 195-204.
22. Mizukami, T., *et al.*, System vaccinology for the evaluation of influenza vaccine safety by multiplex gene detection of novel biomarkers in a preclinical study and batch release test. PLoS One, 2014. 9(7): p. e101835.
23. Raeven, R.H.M., *et al.*, Molecular Signatures of the Evolving Immune Response in Mice following a *Bordetella pertussis* Infection. PLoS One, 2014. 9(8): p. e104548.
24. Pereira-Lopes, S., *et al.*, The exonuclease Trex1 restrains macrophage proinflammatory activation. J Immunol, 2013. 191(12): p. 6128-35.
25. Chen, G.Y., *et al.*, Broad and direct interaction between TLR and Siglec families of pattern recognition receptors and its regulation by Neu1. Elife, 2014. 3: p. e04066.
26. Jozefowski, S., *et al.*, The class A scavenger receptor SR-A/CD204 and the class B scavenger receptor CD36 regulate immune functions of macrophages differently. Innate Immun, 2014. 20(8): p. 826-47.
27. He, Y., L. Franchi, and G. Nunez, The protein kinase PKR is critical for LPS-induced iNOS production but dispensable for inflammasome activation in macrophages. Eur J Immunol, 2013. 43(5): p. 1147-52.
28. Kovacic, B., *et al.*, Lactotransferrin-Cre reporter mice trace neutrophils, monocytes/macrophages and distinct subtypes of dendritic cells. Haematologica, 2014. 99(6): p. 1006-15.
29. Dufton, N., *et al.*, Anti-inflammatory role of the murine formyl-peptide receptor 2: ligand-specific effects on leukocyte responses and experimental inflammation. J Immunol, 2010. 184(5): p. 2611-9.
30. Inoue, A., *et al.*, Murine tumor necrosis factor alpha-induced adipose-related protein (tumor necrosis factor alpha-induced protein 9) deficiency leads to arthritis via interleukin-6 overproduction with enhanced NF-kappaB, STAT-3 signaling, and dysregulated apoptosis of macrophages. Arthritis Rheum, 2012. 64(12): p. 3877-85.
31. Jin, F.Y., *et al.*, Secretory leukocyte protease inhibitor: a macrophage product induced by and antagonistic to bacterial lipopolysaccharide. Cell, 1997. 88(3): p. 417-26.
32. Lu, B., *et al.*, The acute phase response stimulates the expression of angiopoietin like protein 4. Biochem Biophys Res Commun, 2010. 391(4): p. 1737-41.
33. Zhu, P., *et al.*, Angiopoietin-like 4: a decade of research. Biosci Rep, 2012. 32(3): p. 211-9.
34. Pervushina, O., *et al.*, Platelet factor 4/CXCL4 induces phagocytosis and the generation of reactive oxygen metabolites in mononuclear phagocytes independently of Gi protein activation or intracellular calcium transients. J Immunol, 2004. 173(3): p. 2060-7.

35. Bozoyan, L., *et al.*, Interleukin-36gamma is expressed by neutrophils and can activate microglia, but has no role in experimental autoimmune encephalomyelitis. J Neuroinflammation, 2015. 12: p. 173.
36. Vigne, S., *et al.*, IL-36R ligands are potent regulators of dendritic and T cells. Blood, 2011. 118(22): p. 5813-23.
37. Lee, M.S., *et al.*, OASL1 inhibits translation of the type I interferon-regulating transcription factor IRF7. Nat Immunol, 2013. 14(4): p. 346-55.
38. Takaoka, A., *et al.*, DAI (DLM-1/ZBP1) is a cytosolic DNA sensor and an activator of innate immune response. Nature, 2007. 448(7152): p. 501-5.
39. Pollpeter, D., *et al.*, Impaired cellular responses to cytosolic DNA or infection with Listeria monocytogenes and vaccinia virus in the absence of the murine LGP2 protein. PLoS One, 2011. 6(4): p. e18842.
40. Arthur, J.C., *et al.*, Cutting edge: NLRP12 controls dendritic and myeloid cell migration to affect contact hypersensitivity. J Immunol, 2010. 185(8): p. 4515-9.
41. Kim, B.H., *et al.*, A family of IFN-gamma-inducible 65-kD GTPases protects against bacterial infection. Science, 2011. 332(6030): p. 717-21.
42. Shi, M., *et al.*, TRIM30 alpha negatively regulates TLR-mediated NF-kappa B activation by targeting TAB2 and TAB3 for degradation. Nat Immunol, 2008. 9(4): p. 369-77.
43. Traves, P.G., *et al.*, Pivotal role of protein tyrosine phosphatase 1B (PTP1B) in the macrophage response to pro-inflammatory and anti-inflammatory challenge. Cell Death Dis, 2014. 5: p. e1125.
44. Riley, J.P., *et al.*, PARP-14 binds specific DNA sequences to promote Th2 cell gene expression. PLoS One, 2013. 8(12): p. e83127.
45. Cho, S.H., *et al.*, B cell-intrinsic and -extrinsic regulation of antibody responses by PARP14, an intracellular (ADP-ribosyl)transferase. J Immunol, 2013. 191(6): p. 3169-78.
46. Lechmann, M., *et al.*, The CD83 reporter mouse elucidates the activity of the CD83 promoter in B, T, and dendritic cell populations in vivo. Proc Natl Acad Sci U S A, 2008. 105(33): p. 11887-92.
47. Loscher, C.E., *et al.*, Proinflammatory cytokines in the adverse systemic and neurologic effects associated with parenteral injection of a whole cell pertussis vaccine. Ann N Y Acad Sci, 1998. 856: p. 274-7.
48. O'Neill, L.A., How Toll-like receptors signal: what we know and what we don't know. Curr Opin Immunol, 2006. 18(1): p. 3-9.
49. Shi, Y., *et al.*, Detoxification of endotoxin by aluminum hydroxide adjuvant. Vaccine, 2001. 19(13-14): p. 1747-52.
50. Bufe, B., *et al.*, Recognition of bacterial signal peptides by mammalian formyl peptide receptors: a new mechanism for sensing pathogens. J Biol Chem, 2015. 290(12): p. 7369-87.
51. Fu, H., *et al.*, Ligand recognition and activation of formyl peptide receptors in neutrophils. J Leukoc Biol, 2006. 79(2): p. 247-56.
52. Rajakariar, R., *et al.*, Hematopoietic prostaglandin D2 synthase controls the onset and resolution of acute inflammation through PGD2 and 15-deoxyDelta12 14 PGJ2. Proc Natl Acad Sci U S A, 2007. 104(52): p. 20979-84.
53. Sato, M., *et al.*, Positive feedback regulation of type I IFN genes by the IFN-inducible transcription factor IRF-7. FEBS Lett, 1998. 441(1): p. 106-10.
54. McNab, F., *et al.*, Type I interferons in infectious disease. Nat Rev Immunol, 2015. 15(2): p. 87-103.
55. Huber, J.P. and J.D. Farrar, Regulation of effector and memory T-cell functions by type I interferon. Immunology, 2011. 132(4): p. 466-74.
56. Reynolds, J.M., *et al.*, Toll-like receptor 2 signaling in CD4(+) T lymphocytes promotes T helper 17 responses and regulates the pathogenesis of autoimmune disease. Immunity, 2010. 32(5): p. 692-702.
57. Martin, S.W., *et al.*, Pertactin-negative *Bordetella pertussis* strains: evidence for a possible selective advantage. Clin Infect Dis, 2015. 60(2): p. 223-7.
58. Lam, C., *et al.*, Rapid increase in pertactin-deficient *Bordetella pertussis* isolates, Australia. Emerg Infect Dis, 2014. 20(4): p. 626-33.
59. Quintana, F.J., *et al.*, Induction of IgG3 to LPS via Toll-like receptor 4 co-stimulation. PLoS One, 2008. 3(10): p. e3509.
60. Raeven, R.H.M., *et al.*, Immunological signatures after *Bordetella pertussis* infection demonstrate importance of pulmonary innate immune cells. Manuscript submitted.
61. Zollinger, W.D., *et al.*, Design and evaluation in mice of a broadly protective meningococcal group B native outer membrane vesicle vaccine. Vaccine, 2010.
62. Benjamini, Y. and Y. Hochberg, Controlling the false discovery rate: a practical and powerful approach to multiple testing. Journal of the Royal Statistical Society, 1995. 57(1): p. 289–300.
63. Samarajiwa, S.A., *et al.*, INTERFEROME: the database of interferon regulated genes. Nucleic Acids Res, 2009. 37(Database issue): p. D852-7.

Supplementary information

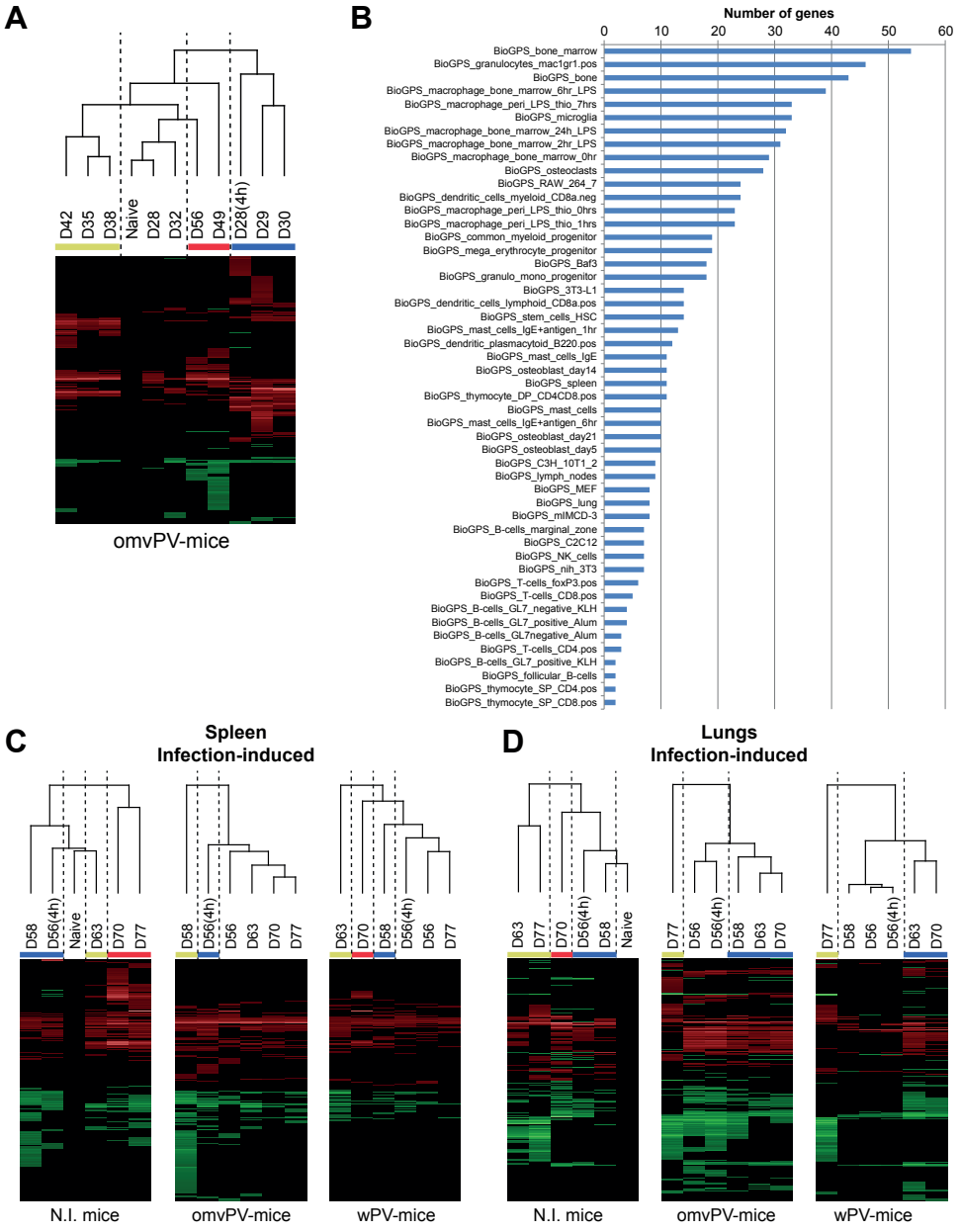

Figure S1 - Hierarchical clustering and BioGPS comparison of splenic transcriptome. **(A)** Hierarchical clustering of the omvPV-induced splenic transcriptome dataset to identify which time points showed a similar response. The response was divided in four parts illustrated by the different colors. **(B)** Transcriptomic profiles from spleen tissue of omvPV-mice and wPV-mice were compared with BioGPS databases. The numbers of genes detected in the different BioGPS databases are listed. **(C-D)** Hierarchical clustering on the **(C)** splenic and **(D)** pulmonary transcriptome datasets of challenged N.I.-mice, omvPV-mice and wPV-mice to identify which time points showed a similar response.

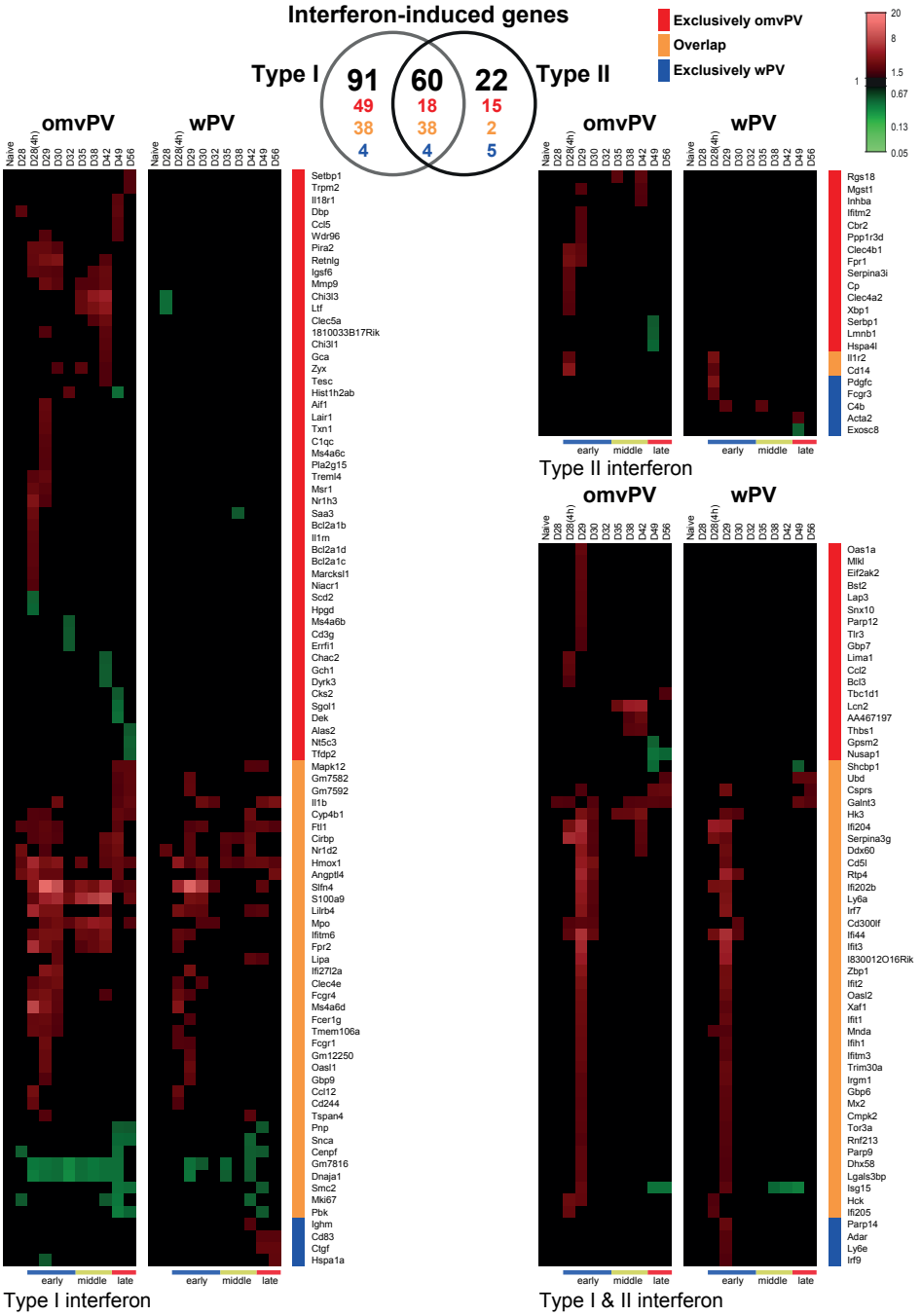

Figure S2 - IFN-induced genes in spleens of omvPV- and wPV-immunized mice. Genes induced by omvPV and wPV in the transcriptome of the spleen were matched with the Interferome database (http://www.interferome.org/interferome/home.jspx). A Venn diagram shows the total number of genes (black) induced by type I IFN, type II IFN, or both. Genes that were found exclusively in the omvPV-mice (red), wPV-mice (blue) or overlapped in both groups (orange) are depicted. The individual genes involved in type I IFN, type II IFN, or both are shown in heatmaps with the corresponding color codes of immunization background.

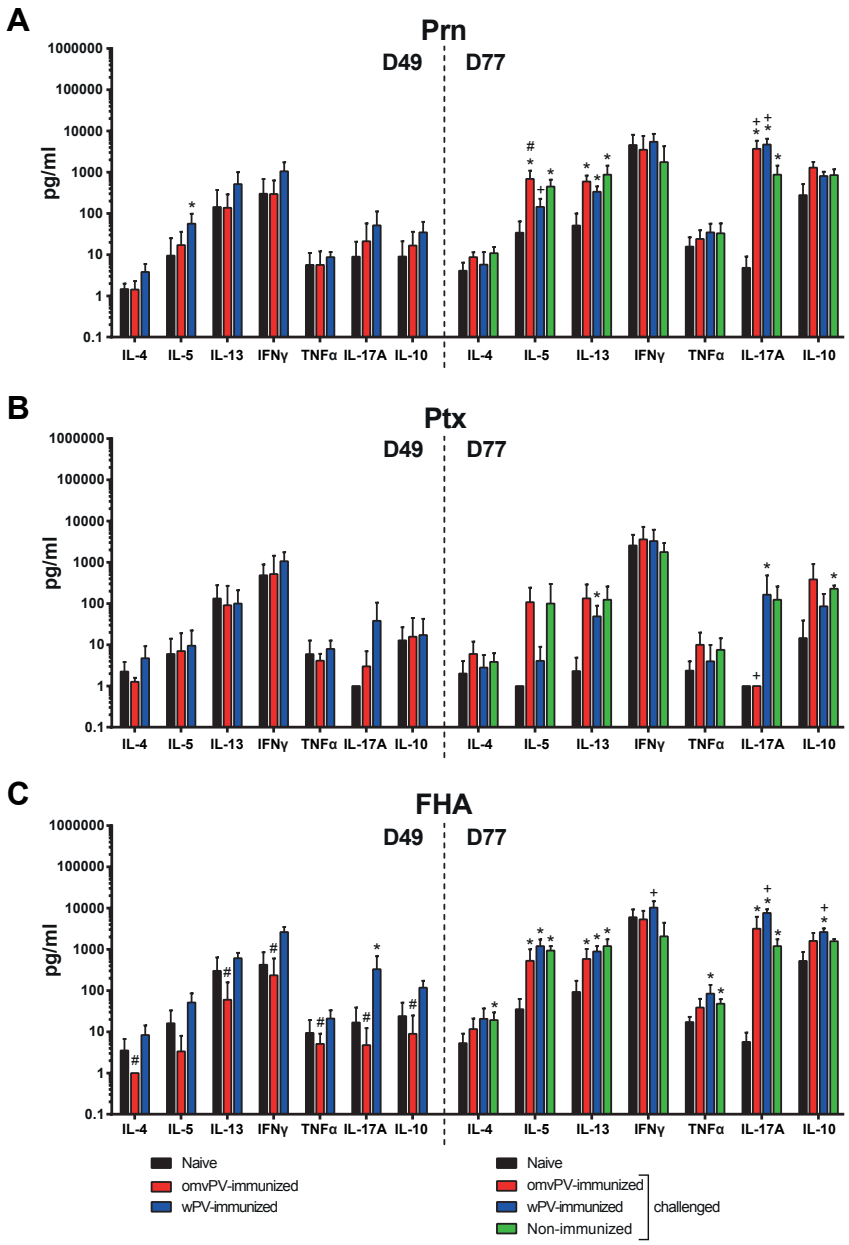

Figure S3 - Splenic cytokine responses after antigen restimulation in omvPV- and wPV-immunized mice before and after challenge as compared to naive control mice before and after challenge. **(A-C)** Concentrations of IL-4, IL-5, IL-13, IFNγ, TNFα, IL-17A and IL-10 were determined in the culture supernatants after 7 day stimulation of splenocytes with 1 µg/ml **(A)** Prn, **(B)** Ptx, or **(C)** FHA. Splenocytes were harvested post booster immunization (day 49, left panel) of mice immunized with omvPV (red) or wPV (blue). Post-challenge (day 77, right panel), same groups were included with an additional group of non-immunized mice that received a challenge (green). In both experiments, complete naive mice (black) were used as control. Results for each mouse are corrected for medium stimulation. * = $p \leq 0.05$ for immunized group and challenged group vs. naive group, # = $p \leq 0.05$ for omvPV group vs. wPV group, + = $p \leq 0.05$ for challenged immunized group vs. challenge non-immunized group.

About the cover: The Devil's Throat of the Iguazu waterfalls seen from the Brazilian side. The world's biggest waterfall system divided over approximately 275 falls stretched over 2.7 km on the border between Brazil and Argentina. Part of the UNESCO World Heritage. In 2013, René attended the Keystone Symposium "*Advancing Vaccines in the Genomics Era*" that was held in Rio de Janeiro, Brazil.

CHAPTER 6

Transcriptome signature for dampened Th2 dominance in acellular pertussis vaccine-induced $CD4^+$ T-cell responses through TLR4 ligation

Jolanda Brummelman[1,4], René H.M. Raeven[2], Kina Helm[1], Jeroen L.A. Pennings[3], Bernard Metz[2], Willem van Eden[4], Cécile A.C.M. van Els[1+], Wanda G.H. Han[1+]

[1]Centre for Infectious Disease Control, National Institute for Public Health and the Environment, Bilthoven, The Netherlands,
[2]Intravacc, Institute for Translational Vaccinology, Bilthoven, The Netherlands,
[3]Centre for Health Protection, National Institute for Public Health and the Environment, Bilthoven, The Netherlands,
[4]Department of Infectious Diseases and Immunology, Utrecht University, The Netherlands
[+]These authors contributed equally

Scientific Reports 2016. 6:25064.

Abstract

Current acellular pertussis (aPV) vaccines promote a T-helper 2 (Th2)-dominated response, while Th1/Th17 cells are protective. As our previous study showed, after adding a non-toxic TLR4 ligand, LpxL1, to the aPV in mice, the *Bordetella pertussis*-specific Th2 response is decreased and Th1/Th17 responses are increased as measured at the cytokine protein level. However, how this shift in Th response by LpxL1 addition is regulated at the gene expression level remains unclear. Transcriptomics analysis was performed on purified $CD4^+$ T-cells of control and vaccinated mice after *in vitro* restimulation with aPV antigens. Multiple key factors in Th differentiation, including transcription factors, cytokines, and receptors, were identified within the differentially expressed genes. Upregulation of Th2- and downregulation of follicular helper T-cell-associated genes were found in the $CD4^+$ T-cells of both aPV- and aPV+LpxL1-vaccinated mice. Genes exclusively upregulated in $CD4^+$ T-cells of aPV+LpxL1-vaccinated mice included Th1 and Th17 signature cytokine genes *Ifng* and *Il17a* respectively. Overall, our study indicates that after addition of LpxL1 to the aPV the Th2 component is not downregulated at the gene expression level. Rather an increase in expression of Th1- and Th17-associated genes caused the shift in Th subset outcome.

Introduction

Pertussis or whooping cough, caused by the gram-negative bacterium *Bordetella pertussis*, remains endemic even in highly vaccinated populations [1-3]. This resurgence has been ascribed to multiple causes, including suboptimal programming of the adaptive immune response by second generation acellular pertussis (aPV) vaccines. This has been supported by several studies in different models, namely mice, baboons, and humans, which have revealed that a mixed T-helper 1 (Th1) and Th17 type of $CD4^+$ T-cell response is induced by *B. pertussis* infection [4-7]. Moreover, these Th subsets have been shown, by both the mice and baboon models, to be crucial in the protection against *B. pertussis* [4, 7]. In contrast, the $CD4^+$ T-cell response induced by current aPV is rather Th2-dominated [4, 8-10].

Th subsets are mainly identified by the production of Th subset signature cytokines, such as IFNγ (Th1), IL-4, IL-5, and IL-13 (Th2), IL-17A (Th17), IL-10 and TGFβ (regulatory T-cells (Treg)), and IL-21 (follicular helper T-cells (Tfh)). $CD4^+$ T-cell differentiation has several underlying processes. After activation through their T-cell receptors, the functional programming of $CD4^+$ T-cells is initiated by differentiation cytokines produced in the priming microenvironment, such as IL-12, interacting with their cognate receptors. This results in the activation of signal transducer and activator of transcription (Stat) proteins [11], which induce the expression of master transcription factors. Each Th subset can be defined by the expression of Stat proteins and master transcription factors, namely Stat4/Stat1/Tbet (Th1), Stat5/Stat6/Gata3 (Th2), Stat3/Rorγt (Th17), Stat5/FoxP3 (Treg), and Stat3/Bcl6 (Tfh) [11-13]. These master transcription factors subsequently induce expression of many Th subset-associated genes and silence genes expressed in other Th subsets. These genes include chemokine and cytokine receptors, which also can be used to discriminate between Th subsets. Th1 cells are characterized by CCR1/CCR5/CXCR3 expression, Th2 cells by CCR3/CCR4/CCR8 expression, Th17 cells by CCR4/CCR6 expression, Treg cells by CD25 expression, and Tfh cells by CXCR5 expression [14].

Recently, the programming of aPV-induced $CD4^+$ memory T-cells was investigated using genome-wide gene expression profiling of human $CD4^+$ T-cells [15]. This approach revealed co-expression of both Th2- and Th1-associated gene modules in reactivated $CD4^+$ memory T-cells generated after aPV vaccination in children. This raised the question of how these in principle antagonistic gene modules can establish a predominantly functional Th2 type of $CD4^+$ T-cell outcome. These gene modules, it was suggested, may exist in a dynamic equilibrium, and depending on ongoing response, the intensity of module components may tip the balance in Th subset outcome towards a Th1 or Th2 response. As several preclinical studies have demonstrated, steering the aPV-induced Th2-dominated response towards a more favorable Th1 and Th17 type of response at the cytokine protein level through the use of adjuvants is feasible, for example through replacement of the currently used adjuvant alum in the aPV

with TLR2 or TLR9 ligands [4, 16]. We recently showed that also adding the TLR4 ligand LpxL1, a non-toxic *Neisseria meningitidis* LPS derivative, to an alum-containing aPV skewed the vaccine-induced CD4+ T-cell response towards a Th1/Th17 type of CD4+ T-cell response at the cytokine level [10]. Yet, how the Th subset outcome in the aPV-induced *B. pertussis*-specific CD4+ T-cell response by LpxL1 as adjuvant is regulated at the level of gene expression remains unclear. This insight is necessary to understand shortcomings and improvement of current aPV vaccination.

Therefore, in the present study we compared, in mice, gene expression profiles of *B. pertussis*-specific CD4+ T-cells induced by aPV or LpxL1-adjuvanted aPV vaccination. Short stimulation of splenocytes of vaccinated mice with *B. pertussis* antigens activated the *B. pertussis*-specific CD4+ T-cells, after which microarray analysis was performed on RNA from isolated CD4+ T-cells. Distinct profiles in CD4+ T-cells were found that are potentially useful in the evaluation of new vaccine candidates and adjuvants.

Results

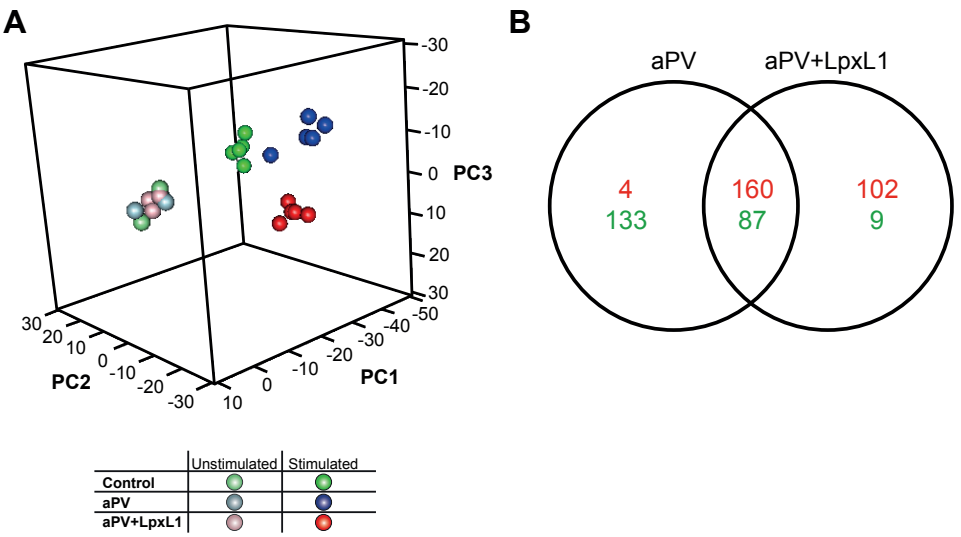

Figure 1 - Visualization of differences in gene expression in CD4⁺ T-cells of control, aPV-, and aPV+LpxL1-vaccinated mice by principle component analysis. **(A)** Principal component analysis, based on the differentially expressed genes, showing (dis)similarities in gene expression in samples stimulated with the Ptx, FHA, and Prn combination (dark colors, n = 5 per group) and medium controls (light colors, n = 3 per group) in all vaccination groups (PBS (blue), aPV (red), aPV+LpxL1 (green)) are shown. **(B)** Venn diagram showing the amount of overlap between up- (red) and downregulated (green) genes in 24 hour *B. pertussis* antigen-stimulated CD4⁺ T-cells of aPV- and aPV+LpxL1-vaccinated mice, as compared to control mice, based on averaged normalized gene expression levels of groups.

B. pertussis-specific CD4⁺ T-cell transcriptome of aPV- or aPV+LpxL1-vaccinated versus control mice

To determine how addition of LpxL1 to the aPV regulates the Th subset outcome of the vaccine-induced *B. pertussis*-specific CD4⁺ T-cells on the molecular level, gene expression profiles of these responding CD4⁺ T-cells were investigated. Splenocytes from control, aPV- and aPV+LpxL1-vaccinated mice were shortly stimulated with *B. pertussis* antigens, Ptx, FHA, and Prn, after which microarray analysis was performed on RNA from isolated CD4⁺ T-cells. The gene expression profiles of unstimulated CD4⁺ T-cells of all groups were taken as a baseline, to establish whether there is an intrinsic difference between the groups. No

Figure 2 (Right) - Gene expression profiles of *B. pertussis*-specific CD4⁺ T-cells of aPV- and aPV+LpxL1-vaccinated mice. The heatmaps depict differential up- (red) or downregulation (green) of genes observed in 24 hour *B. pertussis* antigen-stimulated CD4⁺ T-cells of vaccinated compared to control mice (FR ≥ 1.5). **(A)** 247 genes were differentially expressed in CD4⁺ T-cells of both aPV- and aPV+LpxL1-vaccinated mice. **(B)** 137 genes were differentially expressed in CD4⁺ T-cells of exclusively aPV-vaccinated mice. **(C)** 111 genes were differentially expressed in CD4⁺ T-cells of exclusively aPV+LpxL1-vaccinated mice. Expression data shown are averages from the samples of 5 mice per group.

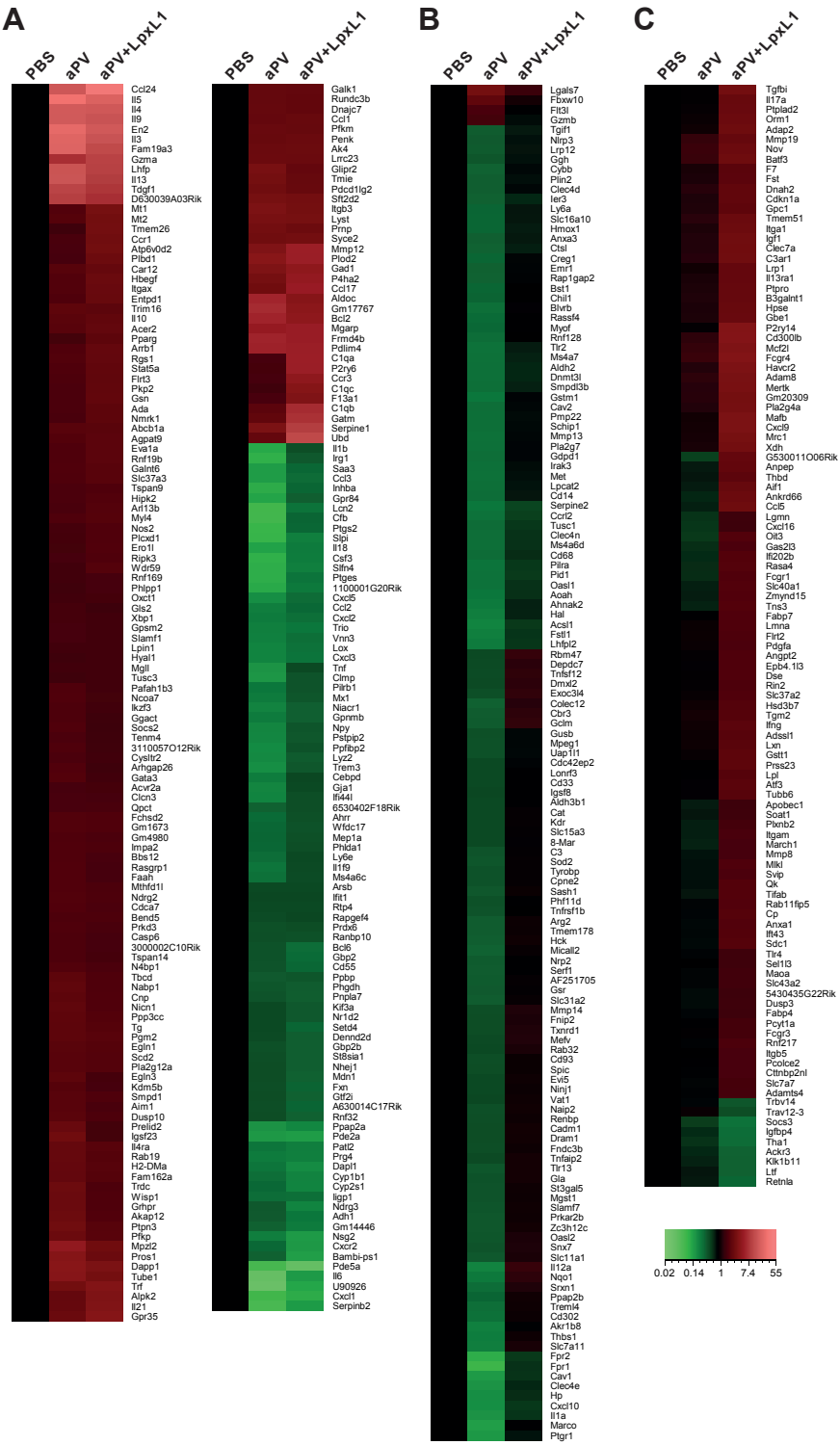
A
PBS
aPV
aPV+LpxL1
Ccl24
Il5
Il4
Il9
En2
Il3
Fam19a3
Gzma
Lhfp
Il13
Tdgf1
D630039A03Rik
Mt1
Mt2
Tmem26
Ccr1
Atp6v0d2
Pltd1
Car12
Hbegf
Itgax
Entpd1
Trim16
Il10
Acer2
Pparg
Arrb1
Rgs1
Stat5a
Flrt3
Pkp2
Gsn
Ada
Nmrk1
Abcb1a
Agpat9
Eva1a
Rnf19b
Galnt6
Slc37a3
Tspan9
Hipk2
Arl13b
Myl4
Nos2
Plcxd1
Ero1l
Ripk3
Wdr59
Rnf169
Phlpp1
Oxct1
Gls2
Xbp1
Gpsm2
Slamf1
Lpin1
Hyal1
Mgll
Tusc3
Pafah1b3
Ncoa7
Ikzf3
Ggact
Socs2
Tenm4
3110057O12Rik
Cysltr2
Arhgap26
Gata3
Acw2a
Clcn3
Qpct
Fchsd2
Gm1673
Gm4980
Impa2
Bbs12
Rasgrp1
Faah
Mthfd1l
Ndrg2
Cdca7
Bend5
Prkd3
Casp6
3000002C10Rik
Tspan14
N4bp1
Tbcd
Nabp1
Cnp
Nicn1
Ppp3cc
Tg
Pgm2
Egln1
Scd2
Pla2g12a
Egln3
Kdm5b
Smpd1
Aim1
Dusp10
Prelid2
Igsf23
Il4ra
Rab19
H2-DMa
Fam162a
Trdc
Wisp1
Grhpr
Akap12
Ptpn3
Pfkp
Mpzl2
Pros1
Dapp1
Tube1
Trf
Alpk2
Il21
Gpr35
B
PBS
aPV
aPV+LpxL1
Lgals7
Fbxw10
Flt3l
Gzmb
Tgif1
Nlrp3
Lrp12
Ggh
Cybb
Plin2
Clec4d
Ier3
Ly6a
Slc16a10
Hmox1
Anxa3
Ctsl
Creg1
Emr1
Rap1gap2
Bst1
Chil1
Blvrb
Rassf4
Myof
Rnf128
Tlr2
Ms4a7
Aldh2
Dnmt3l
Smpdl3b
Gstm1
Cav2
Pmp22
Schip1
Mmp13
Pla2g7
Gdpd1
Irak3
Met
Lpcat2
Cd14
Serpine2
Ccrl2
Tusc1
Clec4n
Ms4a6d
Cd68
Plira
Pid1
Oasl1
Aoah
Ahnak2
Hal
Acsl1
Fstl1
Lhfpl2
Rbm47
Depdc7
Tnfsf12
Dmxl2
Exoc3l4
Colec12
Cbr3
Gclm
Gusb
Mpeg1
Uap1l1
Cdc42ep2
Lonrf3
Cd33
Igsf8
Aldh3b1
Cat
Kdr
Slc15a3
8-Mar
C3
Sod2
Tyrobp
Cpne2
Sash1
Phf11d
Tnfrsf1b
Arg2
Tmem178
Hck
Micall2
Nrp2
Serf1
AF251705
Gsr
Slc31a2
Mmp14
Fnip2
Txnrd1
Mefv
Rab32
Cd93
Spic
Evi5
Ninj1
Vat1
Naip2
Renbp
Cadm1
Dram1
Fndc3b
Tnfaip2
Tlr13
Gla
St3gal5
Mgst1
Slamf7
Prkar2b
Zc3h12c
Oasl2
Snx7
Slc11a1
Il12a
Nqo1
Snx1
Ppap2b
Treml4
Cd302
Akr1b8
Thbs1
Slc7a11
Fpr2
Fpr1
Cav1
Cleo4e
Hp
Cxcl10
Il1a
Marco
Ptgr1
C
PBS
aPV
aPV+LpxL1
Tgfbi
Il17a
Ptplad2
Orm1
Adap2
Mmp19
Nov
Batf3
F7
Fst
Dnah2
Cdkn1a
Gpc1
Tmem51
Itga1
Igf1
Clec7a
C3ar1
Lrp1
Il13ra1
Ptpro
B3galnt1
Hpse
Gbe1
P2ry14
Cd300lb
Mcf2l
Fcgr4
Havcr2
Adam8
Mertk
Gm20309
Pla2g4a
Mafb
Cxcl9
Mrc1
Xdh
G530011O06Rik
Anpep
Thbd
Aif1
Ankrd66
Ccl5
Lgmn
Cxcl16
Oit3
Gas2l3
Ifi202b
Rasa4
Fcgr1
Slc40a1
Zmynd15
Tns3
Fabp7
Lmna
Flrt2
Pdgfa
Angpt2
Epb4.1l3
Dse
Rin2
Slc37a2
Hsd3b7
Tgm2
Ifng
Adssl1
Lxn
Gstt1
Prss23
Lpl
Atf3
Tubb6
Apobec1
Soat1
Pknb2
Itgam
March1
Mmp8
Mlkl
Svip
Qk
Tifab
Rab11fip5
Cp
Anxa1
Ifit3
Sdc1
Tlr4
Sell3
Maoa
Slc43a2
5430435G22Rik
Dusp3
Fabp4
Pcyt1a
Fcgr3
Rnf217
Itgb5
Pcolce2
Ctnnbp2nl
Slc7a7
Adamts4
Trbv14
Trav12-3
Socs3
Igfbp4
Tha1
Ackr3
Klk1b11
Ltf
Retnla
0.02
0.14
1
7.4
55

significant differentially expressed genes could be identified between these unstimulated samples (criteria: *p*-value ≤ 0.001, fold ratio (FR) ≥ 1.5). Nevertheless, to exclude small intrinsic non-significant differences, the expression intensities of the antigen-stimulated samples were corrected for the average expression intensities of unstimulated samples of their corresponding group. In total, 1876 differentially expressed genes (*p*-value ≤ 0.001, FR ≥ 1.5) were identified between averaged unstimulated samples and antigen-stimulated samples of the control, aPV-, or aPV+LpxL1-vaccinated groups. A principal component analysis on these genes showed differences in gene expression profiles between unstimulated and stimulated samples of all groups, including control mice, suggesting an effect of the stimulation on naive $CD4^+$ T-cells (**Figure 1A**). However, distinct gene expression profiles between stimulated samples of all groups were still observed, revealing functionally differently programmed *B. pertussis*-specific $CD4^+$ T-cells (**Figure 1B**). After comparing the *B. pertussis* antigen-stimulated samples of vaccinated mice with those of control mice, differential expression (FR ≥ 1.5) of 384 and 358 genes was identified in the $CD4^+$ T-cells of, respectively, aPV- and aPV+LpxL1-vaccinated mice. Overlap comparison showed that 247 genes were differentially expressed in $CD4^+$ T-cells of both aPV- and aPV+LpxL1-vaccinated mice, 137 genes were exclusively differentially expressed in $CD4^+$ T-cells of aPV-vaccinated mice and 111 genes were exclusively differentially expressed in $CD4^+$ T-cells of aPV+LpxL1-vaccinated mice (**Figures 1 and 2**).

Over-representation of immune- and metabolism-related terms after aPV- and aPV+LpxL1- vaccination

To provide more insight in the differentially expressed genes, functional annotation and over-representation analysis (Benjamini-corrected *p*-value ≤ 0.05) in GO-BP and KEGG databases were performed using DAVID [17]. Analysis of the overlapping 247 differentially expressed genes in $CD4^+$ T-cells from both aPV- and aPV+LpxL1-vaccinated mice showed that 74 GO-BP terms and 8 KEGG pathways were enriched. Based on exclusion of overlapping terms/pathways and their relevance, a selection of these terms/pathways is shown in **Figure 3A**. The enriched terms/pathways are mainly involved in the regulation of the adaptive immune response, as indicated by terms as regulation of lymphocyte activation (GO:0051249), proliferation (GO:0050670), and differentiation (GO:0045597), and cytokine signaling, including chemotaxis (GO:0006935) and Jak-STAT signaling pathway (mmu4630). Moreover, the enrichment of the asthma pathway (mmu05310) indicates the presence of Th2-associated genes. Further, terms involved in metabolic processes are enriched, including positive regulation of macromolecule metabolic process (GO:0010604) and positive regulation of protein metabolic process (GO:0051247).

Functional annotation and over-representation analysis (Benjamini-corrected *p*-value ≤ 0.05) of the 137 genes differentially expressed in $CD4^+$ T-cells of exclusively aPV-vaccinated mice revealed enrichment of 9 GO-BP terms. Five relevant terms are depicted in **Figure 3B**, which includes immune response-related terms, such as immune response (GO:0006955)

and regulation of cytokine production (GO:0001817), and metabolism-related terms such as oxidation-reduction process (GO:0055114) and regulation of nitric oxide biosynthetic process (GO:0045428). Functional annotation and over-representation analysis of the 111 genes solely altered in CD4+ T-cells of aPV+LpxL1-vaccinated mice showed enrichment of 9 GO-terms, including inflammatory response (GO:0006954), chemotaxis (GO:0006935), and phagocytosis (GO:0006909) (Figure 3C).

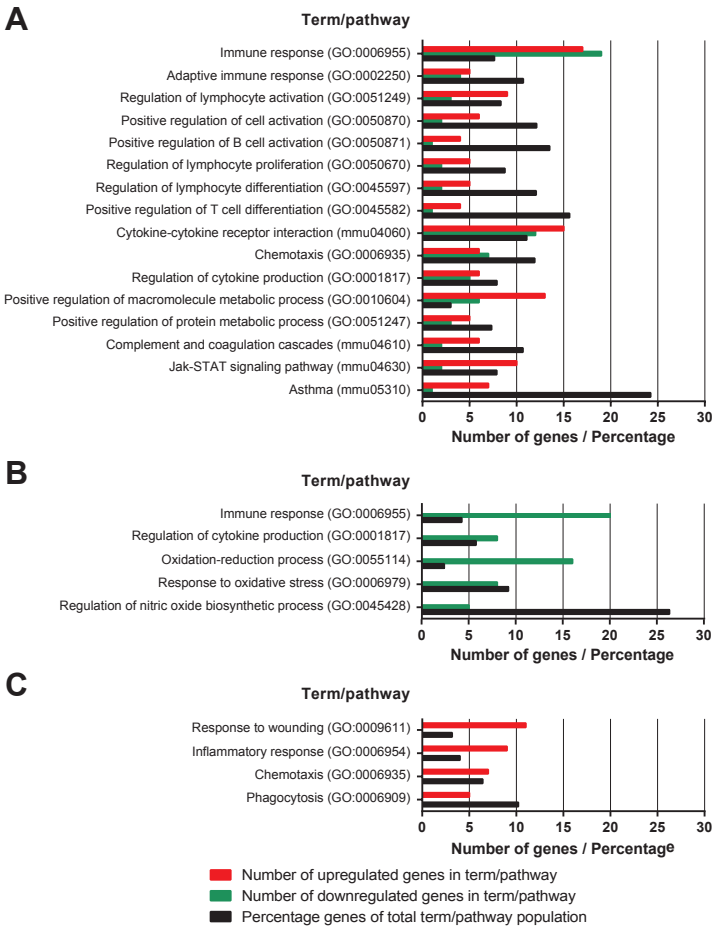

Figure 3 - Functional annotation and pathway enrichment of differentially expressed genes in *B. pertussis*-specific CD4+ T-cells of aPV- and aPV+LpxL1-vaccinated mice. Over-representation analysis (Benjamini-corrected *p*-value ≤ 0.05) in GO-BP and KEGG databases was performed using genes differentially expressed in *B. pertussis* antigen-stimulated CD4+ T-cells of vaccinated compared to control mice. Functional annotation and pathway enrichment are depicted from genes differentially expressed in CD4+ T-cells of both aPV- and aPV+LpxL1 vaccinated mice **(A)**, in CD4+ T-cells of exclusively aPV-vaccinated mice **(B)**, and in CD4+ T-cells of exclusively aPV+LpxL1-vaccinated mice **(C)**. The amount of up- or downregulated genes per term/pathway and the percentage of the genes in the total term/pathway population are shown.

Differential expression of cytokine-encoding genes in vaccine-induced CD4⁺ T-cells

Our previous study investigated the type of CD4⁺ T-cell response at the protein level by determining the percentage of *B. pertussis* antigen-specific IL-5-, IFNγ-, and IL-17A-positive CD4⁺ T-cells using flow cytometry and by supernatant analysis. It showed that addition of LpxL1 to the aPV skews the CD4⁺ T-cell response of a Th2-dominated to a mixed response, dominated by Th1/Th17 [10]. Therefore, we investigated in more detail the expression of cytokine-encoding genes. Some Th subset signature cytokine-encoding genes could be identified which were upregulated in the CD4⁺ T-cells of both aPV- and aPV+LpxL1-vaccinated mice, such as *Il4*, *Il5*, *Il13*, *Il21*, and *Il10* (**Figure 4A**). No signature cytokine-encoding genes were found to be differentially expressed in the CD4⁺ T-cells of solely aPV-vaccinated mice, while both *Ifng* and *Il17a* were found to be upregulated exclusively in those of aPV+LpxL1-vaccinated mice (**Figure 4C**). In addition to the Th subset signature cytokines-encoding genes, other cytokine genes were differentially expressed of which 19 were found in CD4⁺ T-cells of aPV- as well as aPV+LpxL1-vaccinated mice. Genes *Il3*, *Il9*, *Ccl1*, *Ccl17*, and *Ccl24* were upregulated, whereas downregulation was found for genes encoded for chemokines, *Cxcl1, Ccl2, Cxcl2, Cxcl5, Cxcl3, Ccl3,* and *Csf3*, and pro-inflammatory cytokines, *Il1b, Il6, Tnf,* and *Il18* (**Figure 4A**). Five genes encoding other cytokines were detected in the CD4⁺ T-cells of exclusively aPV-vaccinated mice, which included downregulation of *Cxcl10, IL12a, Il1a,* and *Tnfsf12* and upregulation of *Flt3l* (**Figure 4B**). Three upregulated genes were found only in those of aPV+LpxL1-vaccinated mice, namely *Cxcl9, Ccl5,* and *Cxcl16* (**Figure 4C**). Together, these results indicate substantial overlap in the expression of cytokine-encoding genes, including Th2 signature cytokines, after both aPV- and aPV+LpxL1- vaccination, while expression of genes encoding Th1 and Th17 signature cytokines is only induced by aPV+LpxL1 vaccination.

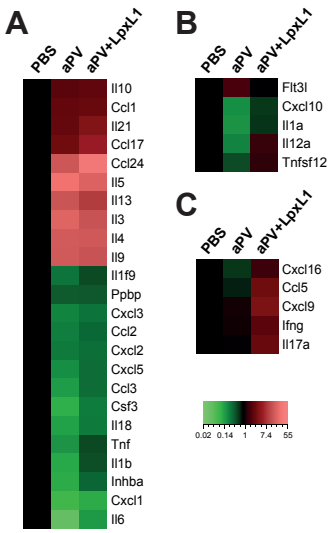

Figure 4 - Gene expression profile of cytokine encoding genes in *B. pertussis*-specific CD4⁺ T-cells of aPV- and aPV+LpxL1-vaccinated mice. Genes encoding cytokines differentially expressed in *B. pertussis* antigen-stimulated CD4⁺ T-cells of both aPV- and aPV+LpxL1-vaccinated mice **(A)**, in CD4⁺ T-cells of exclusively aPV-vaccinated mice **(B)**, and in CD4⁺ T-cells of exclusively aPV+LpxL1-vaccinated mice **(C)**. Expression data shown are averages from the samples of 5 mice per group.

Differential expression of transcription factor-encoding genes in vaccine-induced CD4+ T-cells

Important in the differentiation of CD4+ T-cells to different Th subsets are the master transcription factors, T-bet, Gata3, Rorγt, Bcl6, and FoxP3 [11-13]. Within the CD4+ T-cells of both aPV- and aPV+LpxL1-vaccinated mice, *Gata3*, the gene encoding the Th2 master transcription factor was found upregulated whereas *Bcl6*, the gene encoding the Tfh master transcription factor was found downregulated (**Figure 5A**). Genes encoding other known master transcription factors were not found differentially expressed. The expression of master transcription factors is regulated by different Stat proteins [11]. Upregulation of only one Stat gene, namely *Stat5a*, which is involved in the differentiation of Th2 and Treg cells, was detected within CD4+ T-cells of both aPV- and aPV+LpxL1-vaccinated mice (**Figure 5A**). In addition, five genes encoding other transcription factors were identified as differentially expressed in the CD4+ T-cells of both aPV- and aPV+LpxL1-vaccinated mice, including upregulation of *Pparg*, *Xbp1*, and *Ikzf3* and downregulation of *Nrld2* and *Cebpd* (**Figure 5A**). Transcription factors *Spic* and *Tgif1* were found downregulated only in the CD4+ T-cells of the aPV-vaccinated mice (**Figure 5B**), while transcription factors *Atf3*, *Mafb* and *Batf3* were found upregulated only in the CD4+ T-cells of aPV+LpxL1-vaccinated mice (**Figure 5C**). Based on expression of Th differentiating transcription factors, both aPV and aPV+LpxL1 vaccination induce Th2 and inhibit Tfh differentiation.

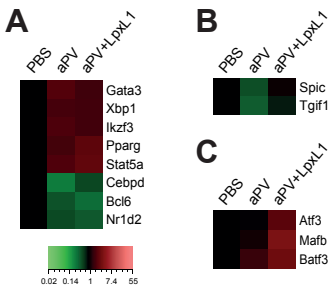

Figure 5 - Gene expression profile of transcription factor encoding genes in *B. pertussis*-specific CD4+ T-cells of aPV- and aPV+LpxL1-vaccinated mice. Genes encoding transcription factors differentially expressed in *B. pertussis* antigen-stimulated CD4+ T-cells from both aPV- and aPV+LpxL1-vaccinated mice **(A)**, in CD4+ T-cells of exclusively aPV-vaccinated mice **(B)**, and in CD4+ T-cells of exclusively aPV+LpxL1-vaccinated mice **(C)**. Expression data shown are averages from the samples of 5 mice per group.

Differential expression of receptor- and cell surface molecule-encoding genes in vaccine-induced CD4+ T-cells

Another way to characterize CD4+ T-cell subsets is by the expression of certain receptors and cell surface markers. Upregulation of markers *Ccr1* and *Ccr3* was detected in the CD4+ T-cells of aPV- and aPV+LpxL1-vaccinated mice (**Figure 6A**). Remarkably, higher expression of the Th2-associated *Ccr3* was seen in aPV+LpxL1 samples than in aPV samples (**Figure 6A**). In addition to the markers used to characterize Th subsets, differential expression was found of genes encoding other receptors and cell surface molecules. Of these genes, 24 were found in CD4+ T-cells of aPV- and aPV+LpxL1-vaccinated mice, and of these, 19 genes were upregulated, including as *Il4ra*, and 5 genes were downregulated, including *Cxcr2* (**Figure 6A**). Within the CD4+ T-cells of aPV-vaccinated mice, 36 receptor- and cell surface marker-encoding genes were

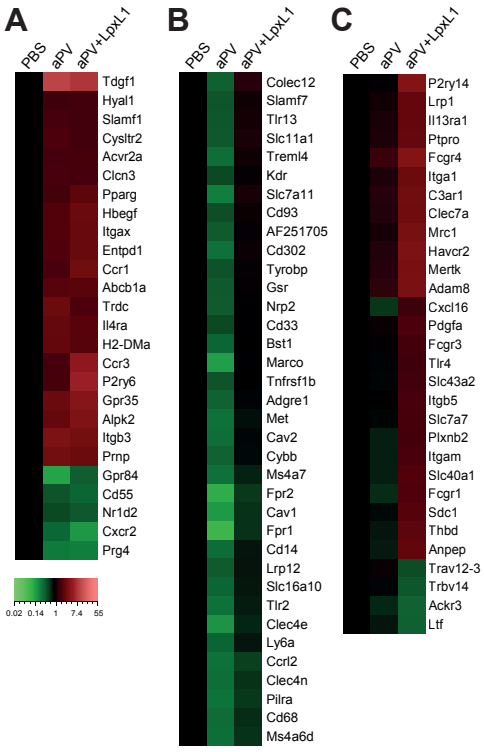

Figure 6 - Gene expression profile of genes encoding receptors and cell surface markers in *B. pertussis*-specific CD4⁺ T-cells of aPV- and aPV+LpxL1-vaccinated mice. Genes encoding receptors and cell surface markers differentially expressed in *B. pertussis* antigen-stimulated CD4⁺ T-cells of both aPV- and aPV+LpxL1-vaccinated mice **(A)**, in CD4⁺ T-cells of exclusively aPV-vaccinated mice **(B)**, and in CD4⁺ T-cells of exclusively aPV+LpxL1-vaccinated mice **(C)**. Expression data shown are averages from the samples of 5 mice per group.

downregulated, including *Ly6a*, and multiple genes encoding for proteins involved in pattern recognition, like *Tlr2, Tlr13, Clec4a, Clec4n,* and *Cd14* (Figure 6B). The 26 upregulated receptor- and cell surface marker-encoding genes in the CD4⁺ T-cells of aPV+LpxL1-vaccinated mice included *Havcr2, Itga1,* and genes encoding proteins involved in the innate immune response, such as *Tlr4, Clec7a, C3ar1, Fcgr1, Fcgr3,* and *Fcgr4* (Figure 6C). The 4 downregulated receptor- and cell surface marker-encoding genes in samples of aPV+LpxL1-vaccinated mice were *Ackr3, Ltf, Trbv14,* and *Trav12-3*. Together, these results suggest that aPV+LpxL1 vaccination induces expression of genes encoding receptors and cell surface markers associated with Th2 (*Ccr3* and *Il4ra*), Th1 (*Havcr2*), and Th17 (*Il13ra1*) subsets, while aPV vaccination only induced genes associated with the Th2 (*Ccr3* and *Il4ra*) subset.

Differential expression of genes encoding proteins involved in metabolism in vaccine-induced CD4⁺ T-cells

Recent studies have revealed that a shift in metabolism from oxidative phosphorylation toward aerobic glycolysis is important in the activation of T-cells [18]. Moreover, the production of IFNy in effector T-cells requires aerobic glycolysis [19]. For this reason, we also analyzed the expression of genes involved in these metabolic pathways. Only one gene encoding a protein involved in the oxidative phosphorylation was found differentially expressed, namely *Fxn*. The *Fxn* gene was downregulated in CD4⁺ T-cells of both aPV- and

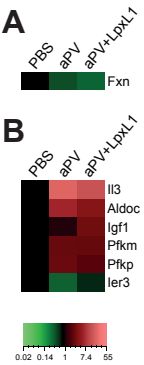

Figure 7 - Gene expression profile of genes encoding proteins involved in metabolism in *B. pertussis*-specific CD4+ T-cells of aPV- and aPV+LpxL1-vaccinated mice. Heatmaps depict genes involved in oxidative phosphorylation **(A)** and glycolytic process **(B)** that are differentially expressed in *B. pertussis* antigen-stimulated CD4+ T-cells of aPV- and aPV+LpxL1-vaccinated mice compared to control mice. Expression data shown are averages from the samples of 5 mice per group.

aPV+LpxL1-vaccinated mice (Figure 7A). Additionally, six genes encoding for proteins with a function in the glycolytic process could be identified in the CD4+ T-cells (Figure 7B). Four genes were found upregulated in both vaccinated groups, namely *Aldoc, Il3, Pfkm,* and *Pfkp*. The *Ier3* gene was downregulated in CD4+ T-cells of aPV-vaccinated mice, while *Igf1* was upregulated in those of aPV+LpxL1-vaccinated mice. In addition, a recent study has shown that regulation of glucose uptake induced by Notch signaling is important in the survival of memory CD4+ T-cells [20]. However, no genes involved in this pathway were found to be differentially expressed in the CD4+ T-cells of aPV- and aPV+LpxL1-vaccinated mice. Overall, these data suggest that there is no difference in the expression of genes involved in metabolic pathways in CD4+ T-cells of aPV- and aPV+LpxL1-vaccinated mice.

Distinct Th subset-associated gene modules expressed after aPV and aPV+LpxL1 vaccination

Based on literature from human and murine studies, a network analysis was performed to visualize the expression patterns of genes associated with different Th subsets that were observed in the CD4+ T-cells of aPV- and aPV+LpxL1-vaccinated mice (Figure 8). In addition to genes encoding the previously mentioned master transcription factors, signature cytokines, and surface markers, other differentially expressed genes associated with the main Th subsets were found. Mainly Th2-associated genes, such as the Th2 subset signature cytokines (*Il4, Il5,* and *Il13*), *Gata3*, *Il3*, *Nabp1*, and *Slc37a3*, were found upregulated in the CD4+ T-cells of both aPV- and aPV+LpxL1-vaccinated mice. Interestingly, another Th2-associated gene, *Socs3*, was downregulated in the CD4+ T-cells of exclusively aPV+LpxL1-vaccinated mice. Th1-associated genes were upregulated in CD4+ T-cells of aPV+LpxL1-vaccinated mice, including *Havcr2* and chemokines *Cxcl9* and *Ccl5*, while downregulation of Th1-associated genes *Scl11a1* and *Il12a* is observed in those of aPV-vaccinated mice. Further, upregulation of Th17-associated genes *Dse*, *Il13ra1*, and *Il17a* was only observed in the CD4+ T-cells of aPV+LpxL1-vaccinated mice. Differential expression of Treg-associated genes was found in the CD4+ T-cells of aPV- as well as aPV+LpxL1-vaccinated mice, namely *Il10* and *Stat5a*. However, other Treg-associated genes, *Flt3l* and *Gzmb*, were only upregulated in CD4+ T-cells of aPV-vaccinated mice. Only 2

Tfh-associated genes were found in our study, *Bcl6* and *Il21*, which were respectively down- and upregulated in $CD4^+$ T-cells of both the aPV- and aPV+LpxL1-vaccinated mice. Moreover, genes involved in glycolysis were found in $CD4^+$ T-cells of both vaccination groups of which 2 genes are associated with the Th2 subset, namely *Pgkp* and *Il3*. Based on this gene expression network, our results suggest that aPV vaccination induces mainly Th2 and Treg gene modules, while addition of LpxL1 to the aPV induces a shift towards Th1 and Th17 gene modules.

Enrichment of transcription factor-binding sites within the gene set of differentially expressed genes in $CD4^+$ T-cells of aPV- or aPV+LpxL1-vaccinated mice

To further provide insight in the concerted regulation of the differentially expressed genes in $CD4^+$ T-cells of aPV and aPV+LpxL1 mice, a transcription factor-binding site (TFBS) analysis was performed. This analysis revealed enrichment of binding sites for SPIB, RELA, and IRF2 within the promoter regions of upregulated genes in the $CD4^+$ T-cells of aPV-vaccinated mice and ELF5, SPI1, Klf4, SPIB, RELA, REL, ELK1, NF-kappaB, and FEV within the upregulated genes in the $CD4^+$ T-cells of aPV+LpxL1-vaccinated mice, respectively (**Figure S1**). Binding sites for transcription factors within the downregulated genes in the $CD4^+$ T-cells of aPV-vaccinated mice were NF-kappaB and RELA, while no enrichment of TFBS was found within the downregulated genes in the $CD4^+$ T-cells of aPV+LpxL1-vaccinated mice (**Figure S1**). An overview of the top 20 transcription factors from each analyzed gene set is given in **Table S1**. These results suggest the involvement of multiple transcription factors that regulate the distinct of Th subset-related gene expression observed after addition of LpxL1 to the aP vaccine. Whereas SPIB and RELA were found in both groups, SPI1, Klf4, and NF-kappaB were only involved after addition of LpxL1.

Figure 8 (Right) - Network analysis of Th subset-associated genes differentially expressed in *B. pertussis*-specific $CD4^+$ T-cells of aPV- and aPV+LpxL1-vaccinated mice. A gene-function network analysis showing the Th subset-associated genes differentially expressed in *B. pertussis* antigen-stimulated $CD4^+$ T-cells of aPV- and aPV+LpxL1-vaccinated was performed using Cytoscape to visualize the patterns of Th subset-associated genes induced by the different vaccines. Association of genes with the gene modules (blue rectangles) was based on literature from mouse (bold blue lines) and human (thin blue lines) studies. The interactions between genes (grey lines) were determined using the STRING database. The shape of the gene nodes indicate whether genes were differentially expressed in $CD4^+$ T-cells of both vaccination groups (circles), had the highest fold-change in either the $CD4^+$ T-cells of aPV-vaccinated mice (diamonds) or in those of aPV-LpxL1-vaccinated mice (triangles). The color intensity of the gene nodes indicate whether genes were differentially expressed in $CD4^+$ T-cell of both aPV- and aPV+LpxL1-vaccinated mice (light green and red) or in $CD4^+$ T-cells of exclusively aPV-vaccinated mice or in those of exclusively aPV+LpxL1-vaccinated mice (dark green and red).

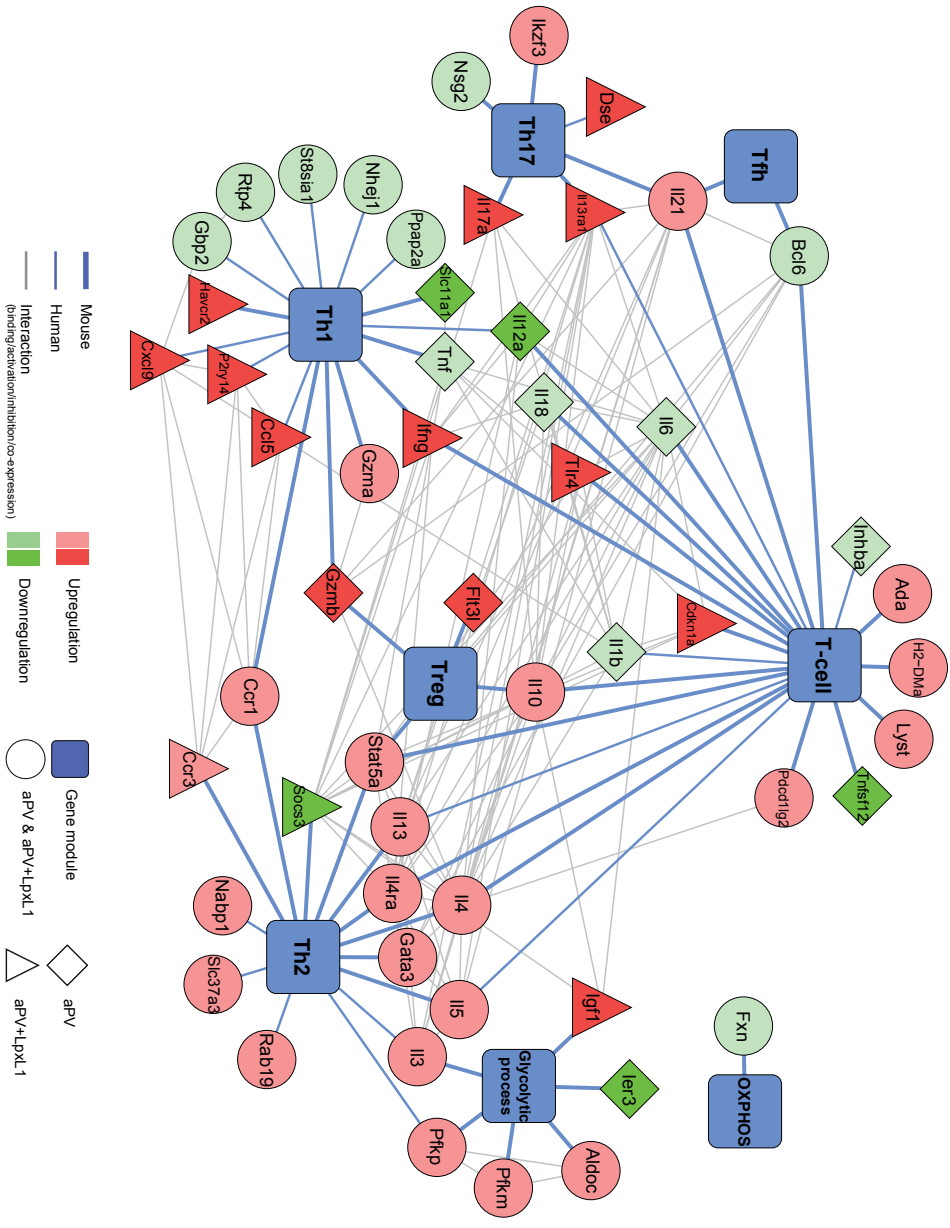
Ikzf3
Nsg2
Dse
Th17
Tfh
Il21
Il13ra1
Il17a
Bcl6
St8sia1
Nhej1
Rtp4
Gbp2
Ppap2a
Slc1a1
Havcr2
Th1
Il12a
Cxcl9
P2ry14
Tnf
Il18
Il6
Ccl5
Ifng
Tlr4
Gzma
Inhba
Ada
H2-DMa
Lyst
Tnfsf12
Pdcd1lg2
Cdkn1a
T-cell
Il1b
Gzmb
Flt3l
Treg
Il10
Ccr1
Ccr3
Stat5a
Socs3
Il13
Il4ra
Il4
Nabp1
Slc37a3
Gata3
Th2
Il5
Rab19
Il3
Igf1
Fxn
OXPHOS
Glycolytic process
Ier3
Pfkp
Pfkm
Aldoc
Mouse
Human
Interaction
(binding/activation/inhibition/co-expression)
Upregulation
Downregulation
Gene module
aPV & aPV+LpxL1
aPV
aPV+LpxL1

Discussion

Addition of the TLR4 ligand LpxL1 to an aPV was found to dampen the Th2 dominance of the antigen-specific CD4$^+$ T-cell response of vaccinated mice and to increase a Th1/Th17 type response, based on cytokine analysis [10]. In the present study, this skewing was investigated in more detail at the gene expression level. Analysis of the expression of Th subset signature cytokine-encoding genes revealed an increased expression of *Ifng* and *Il17a* in CD4$^+$ T-cells of exclusively aPV+LpxL1-vaccinated mice, which is consistent with our previous findings. Most importantly, the Th2 subset signature cytokine genes *Il4*, *Il5*, and *Il13* showed increased expression in the CD4$^+$ T-cells of aPV- as well as aPV+LpxL1-vaccinated mice, suggesting that the Th2 component is not downregulated at the gene expression level of Th subset signature cytokines after addition of LpxL1 to the aPV.

Other Th1-, Th17-, and Th2-associated genes showed the same trend as the genes encoding Th signature cytokines. Genes associated with the Th1 subsets had increased expression in the CD4$^+$ T-cells of exclusively aPV+LpxL1-vaccinated mice, including genes encoding chemokines (*Ccl5* and *Cxcl9*) and cell surface marker Havcr2 (*Tim3*). Both Ccl5 and Cxcl9 are chemoattractants for Th1 cells and are described to be produced by human CD4$^+$ T-cells [21, 22]. Havcr2 is a cell surface marker preferentially expressed on Th1 cells and its expression is induced by Th1 master transcription factor T-bet [23]. Th17-associated genes that showed increased expression solely in the CD4$^+$ T-cells of aPV+LpxL1-vaccinated mice were *Il13ra1* and *Dse*. IL-13Rα1 is a functional receptor found on both murine and human Th17 cells while it is not expressed on Tho, Th1, Th2, and Treg cells [24]. Binding of IL-13 to this receptor attenuates the production of IL-17A [24]. Further, Dse is an intracellular enzyme involved in epitope processing and is preferentially expressed in human Th17 cells [25].

Remarkably, several other Th2-associated genes also showed increased expression in CD4$^+$ T-cells of both aPV- and aPV+LpxL1-vaccinated mice, of which most genes showed the same trend as the expression of the Th2 subset signature cytokine-encoding genes. These other Th2-associated genes include Th2 master transcription factor *Gata3*, Stat protein *Stat5a*, chemokine-receptors *Ccr1* and *Ccr3*, and cytokine-receptor *Il4ra*, and other genes, namely *Rab19, Nabp1, Scl37a3,* and *Pfkp* [15]. Interestingly, downregulation of Th2-associated *Socs3* is observed in the CD4$^+$ T-cells of exclusively aPV+LpxL1-vaccinated mice. Socs3, suppressor of cytokine signaling-3, is preferentially expressed in Th2 cells [26] and inhibits Th1 and Th17 differentiation by suppressing STAT4 and STAT3 activation, respectively [27, 28]. Downregulation of *Socs3* in CD4$^+$ T-cells of aPV+LpxL1-vaccinated mice suggests reduced active suppression of Th1 and Th17 differentiation when LpxL1 is present in the aPV and thereby favors Th1 and Th17 differentiation.

In addition to the involvement of the Th1, Th2, and Th17 subsets, this study in aPV- and aPV+LpxL1-vaccinated mice revealed gene expression modules pointing at the induction or inhibition of other Th subsets, namely Treg and Tfh. Treg cells were induced by both aPV and aPV+LpxL1 vaccination, since increased expression of a Treg subset signature cytokine gene, *Il10*, as well as the Treg-associated Stat gene, *Stat5a*, was detected in CD4+ T-cells of both groups. However, expression of *Gzmb*, encoding Granzyme B, which has cytolytic functions and is expressed in different cells including Tregs [29,30], showed increased expression in the CD4+ T-cells of exclusively aPV-vaccinated mice. Together with the increased expression of *Flt3l*, which is involved in the expansion of Treg cells [31], in only the samples of aPV-vaccinated mice, this suggests that increased numbers of Treg cells were induced after vaccination with the aPV alone. Tfh master transcription factor *Bcl6* showed decreased expression in the CD4+ T-cells of both aPV- and aPV+LpxL1-vaccinated mice, indicating that differentiation towards the Tfh subset was suppressed. This seems contradictory given the increased expression of the Tfh subset signature cytokine gene *Il21*. However, this cytokine can also be produced by Th17 cells [32]. Some induction of Th17 cells by aPV vaccination might explain the increased expression of *Il21*. A study of Ross *et al.* indeed showed that Th17 cells could be detected in mice after aPV vaccination [4]. These results are consistent with the increased expression of *Ikzf3* in CD4+ T-cells of both aPV- and aPV+LpxL1-vaccinated mice, since this gene is specifically expressed in Th17 cells [33].

In addition to Th subset associated genes, genes encoding proteins that are involved in metabolism were investigated, since a shift in metabolism from oxidative phosphorylation toward aerobic glycolysis is important in the activation of T-cells [18]. Only a small number of genes involved in oxidative phosphorylation and glycolysis were differentially expressed in the CD4+ T-cells of aPV- and aPV+LpxL1-vaccinated mice. The genes encoding proteins involved in glycolysis, namely *Il3, Pfkp, Aldoc,* and *Pfkm*, showed increased expression in the samples of both aPV- and aPV+LpxL1-vaccinated mice. Interestingly, *Il3* and *Pfkp* are also associated with Th2 cells [15]. Overall, these results suggest little or no difference in the activation of CD4+ T-cells based on metabolism by the different vaccines.

Within the set of genes differentially expressed in CD4+ T-cells of aPV- and aPV+LpxL1-vaccinated mice, genes were found encoding proteins with a known function in the innate immune system, including cytokines (*Il6, Il1b, Tnf,* and *Il12a*), complement components (*C1qa, C1qb, C1qc, Cd55, Cfb, C3, Cd93, C3ar1, Itgam*), Toll-like receptors (*Tlr2, Tlr13,* and *Tlr4*), C-type lectin receptors (*Clec4a, Clec4d, Clec4n, Clec7a, Cd302*), and Fc-receptors (*Fcgr1, Fcgr3,* and *Fcgr4*). It is unlikely that these innate gene signatures can be fully explained by contamination of innate immune cells within the CD4+ T-cell fraction, since the purity of the samples was >95%. Interestingly, several of these innate immunity genes are known to be expressed in CD4+ T-cells, including complement components such as *Itgam, C3ar1,* and *Cd55* [34-36]. Signaling

through C3a receptor 1, upregulated gene in aPV+LpxL1 samples, by binding a derivative of C3, downregulated gene in aPV samples, has been associated with a Th2 [37] and a Th1 response [38], and with inhibition of Treg function [39]. Moreover, some TLRs, such as TLR2 and TLR4, are also expressed on $CD4^+$ T-cells. Signaling via TLR2, which is downregulated in aPV samples, has been found to induce IFNγ production by Th1 cells [40] and might even inhibit IL-4 production [41]. In addition, TLR2 signaling promotes the differentiation of Tregs into Th17 cells in human [42]. Signaling through TLR4 which gene expression is upregulated in aPV+LpxL1 samples is reported to provide a signal for proliferation and cell survival and seems to regulate persistence of Th lineages [43]. Furthermore, the Fc-gamma receptor *Fcgr3* gene, which was upregulated in aPV+LpxL1 samples, was shown to be expressed on a small proportion of $CD4^+$ T-cells with an effector memory phenotype [44] and activated $CD4^+$ T-cells expressing IFNγ and T-bet [45]. Together these data indicate that the differential expression of innate genes could have a function in $CD4^+$ T-cells.

TFBS analysis indicated enrichment of binding sites for three members of the NF-κB family, REL, RELA, and NF-kappaB, in the gene set from the $CD4^+$ T-cells of aPV+LpxL1-vaccinated mice, while enrichment of binding sites of only one member, RELA, was observed in those of aPV-vaccinated mice. Signaling via multiple receptors, including T-cell receptor, TLRs, including TLR4, and pro-inflammatory cytokine receptors, can lead to the activation of NF-κB [46]. Together with the observed upregulation of Tlr4 in the gene set of $CD4^+$ T-cells of exclusively aPV+LpxL1-vaccinated mice, this suggests that LpxL1 might directly activate these transcription factors via TLR4 signaling. Moreover, there is evidence that and RELA is associated with Th17 differentiation [47] and REL with Th1 [48] and Th17 differentiation [47], although conflicting results are published regarding the association of REL with Th17 differentiation [49]. In addition, enrichment of binding sites of Klf4 was observed in the gene set of $CD4^+$ T-cells of exclusively aPV+LpxL1-vaccinated mice, which is also associated with Th17 differentiation [50]. Binding sites for SPI1 were also enriched within this gene set, which is known to inhibit the expression of Th2 cytokines [51]. Together, the data indicate that LpxL1 activates several transcription factors associated with Th1 and Th17 differentiation, which corroborates our findings of the expression of Th-related genes. Furthermore, the results suggest that LpxL1 might activate these transcription factors via TLR4 signaling.

Within the $CD4^+$ T-cells of aPV+LpxL1-vaccinated mice, increased expression of Th1- and Th17-associated genes, including the signature cytokine genes *Ifng* and *Il17a*, was observed. However, no increased expression of the master transcription factors of Th1 and Th17 cells, *Tbx21* and *Rorc* respectively, was found. An *in vitro* effect of 24-hour stimulation with *B. pertussis* antigens might underlie this effect, since in our previous study IFNγ and IL-17A production by naive $CD4^+$ T-cells was detected after stimulation with the *B. pertussis* antigens [10]. Indeed, in the current study, differently expressed genes found between unstimulated

versus antigen-stimulated CD4+ T-cells of control mice were detected, including the Th1 master transcription factor gene *Tbx21* and Th1 Stat gene *Stat1*. Therefore, we interpret the lack of differential expression of Th1 and Th17 master regulators in the samples of the vaccinated mice compared to those of control mice to be a result of an increased background expression in naive CD4+ T-cells induced by the *in vitro B. pertussis* antigen stimulation. This *in vitro* activation of naive CD4+ T-cells could also explain why only a few genes were found corresponding to proteins involved in metabolism, since the metabolism is altered by activation of CD4+ T-cells [18].

Although addition of LpxL1 to the aPV led to a decreased percentage of Th2 cells and reduced in vitro Th2 cytokine levels in *B. pertussis* antigen-stimulated CD4+ T-cell cultures from vaccinated mice in our previous study [10], no or only a limited decrease in expression of Th2-associated genes was observed in the current study, except for *Socs3*. This might be explained by the duration of in vitro stimulation of the CD4+ T-cells, since in the gene expression analysis the duration was shorter (24 hours) than in the functional read-out study (8 days). In addition, there might be reduced translation of the Th2 cytokine mRNA due to Th1- and Th17-associated miRNA translational repression. Such mechanism was shown for Th1-specific miR-135b [52] repressing Th2-associated genes *Stat6* and *Gata3* mRNA translation to protein [53]. Therefore, we propose that the shift towards a mixed Th1 and Th17 response is likely due to increased expression of Th1- and Th17-associated gene modules rather than downregulation of the Th2-associated gene module. Interestingly, White *et al.* (2012) also found a decisive role for the Th1 gene network module in the outcome of Th responses. In their study, extreme Th2 dominance in atopic allergy was associated with the complete absence of the Th1 gene network module [15]. A limitation of our study is that the differences on gene expression are measured on the total splenic CD4+ T-cell population. Therefore, the question remains whether the shifts in gene modules observed at the population level also occur within the same cell. In future research, investigating the gene expression on single cell level can overcome this limitation, as was described by Chattopadhyay *et al.* [54].

In summary, this study provides a gene expression network model that may explain why aPV vaccination induces Th2 and Treg differentiation of CD4+ T-cells, and why addition of LpxL1 to the aPV leads to the induction of Th1 and Th17 cells. Together with our previous data, showing a shift from a Th2-dominated response to a mixed Th1/Th17 response at the cytokine protein level, this study indicates that only a small change in the balance between the expression of Th1/Th17- and Th2-associated genes results in a shift in Th type. Moreover, this model can be used in the evaluation of the effects of new adjuvants on vaccination-induced T-cell responses, in particular in the context of improving acellular pertussis vaccines.

Materials and Methods

Ethics statement

This study was approved by the Committee on Animal Experimentation of the Netherlands Vaccine Institute (Bilthoven, The Netherlands) under permit number 201200115. Animal handling in this study was carried out in accordance with relevant Dutch national legislation, including the 1997 Dutch Act on Animal Experimentation.

Vaccines and antigens

Pertactin P.69 (Prn) was expressed in *Escherichia coli*, purified as described previously [55] and was tested for *E. coli* LPS impurities using a Limulus Amebocyte Lysate (LAL) test. The endotoxin level was < 0.015 EU/ml. Purified filamentous hemagglutinin (FHA) and pertussis toxin (Ptx) were obtained from Kaketsuken (Japan) and Ptx was heat-inactivated at 95°C for 15 minutes before use. The registered combined pentavalent diphtheria, tetanus, and acellular pertussis vaccine (Infanrix; aPV) was purchased from GlaxoSmithKline and one human dose (HD) contains a minimum of 30 I.E. diphtheria toxoid, a minimum of 40 I.E. tetanus toxoid, 25 µg FHA, 25 µg Ptx, and 8 µg Prn, all absorbed to aluminumhydroxide. LpxL1, a meningococcal LPS derivative, was engineered and obtained as described elsewhere [56].

Mice and immunization

Adult (6-8 weeks old) Balb/c mice (Harlan, The Netherlands) were vaccinated s.c. on day 0 (right flank) and day 28 (left flank) with 0.3 ml of 1/4 HD aPV, 1/4 HD aPV supplemented with 1 µg non-adsorbed LpxL1 (aPV+LpxL1), or as a control with PBS, with 5 mice per group. Mice were sacrificed on day 38, after which spleens were harvested from each mouse.

Isolation and *in vitro* restimulation of splenocytes

From each mouse, homogenized splenocytes were treated with erythrocyte lysis buffer (8.3 g/L NH_4CL, 1 g/L $NaHCO_3$, 5000 IE/L Heparin in dH_20; pH 7.4) and transferred to 24-well plates ($6x10^6$ cells/well). The cells were cultured in IMDM medium (Gibco) supplemented with 8% FCS, 100 units penicillin, 100 units streptomycin, 2.92 mg/ml L-glutamine, and 20 µM β-mercaptoethanol (Sigma) at 37°C in a humidified atmosphere of 5% CO2. The cells were either left unstimulated or stimulated for 24 hours with a combination of Prn, Ptx, and FHA (1 µg/ml each)(2 replicate wells per condition), after which the cells were harvested and pooled per culture condition per mouse.

$CD4^+$ T-cell isolation and purity check

From each cultured splenocyte sample $CD4^+$ T-cells were isolated by positive selection using CD4 magnetic microbeads and a magnetic cell separator (Miltenyi Biotech) according to the manufacturer's instructions. The purity of the $CD4^+$ T-cells was determined using

flowcytometry. Briefly, the isolated cells were stained with Pacific blue-conjugated anti-CD4 (Biolegend) in FACS buffer (PBS (pH 7.2) supplemented with 0.5% BSA (Sigma Aldrich) and 0.5 mM EDTA (ICN Biomedicals). After washing, data were acquired on a FACS Canto II (BD Biosciences) and analyzed using FlowJo software (Tree Star). The purity of the isolated $CD4^+$ T-cells was >95%.

RNA extraction

From each $CD4^+$ T-cell preparation, cells were lysed in Qiazol (Qiagen) and RNA isolation was performed using a miRNeasy Mini Kit with DNAse treatment (Qiagen) according to the manufacturer's protocol. RNA concentrations and quality were determined using respectively UV spectroscopy (Tech3 module, Synergy Mx, BioTek) and electrophoresis (RNA nano 6000 kit, 2100 Bioanalyzer, Agilent Technologies).

Microarray analysis

Amplification, labeling and hybridization of RNA samples to microarray chips (GeneChip HT MG-430 PM Array Plate; Affymetrix) were carried out at the Microarray Department of the University of Amsterdam (The Netherlands) according to Affymetrix protocols. Array plates were scanned with a Genechip HT array plate scanner and analyzed with the Affymetrix HT software suite. Microarray analysis was performed on 3 unstimulated and 5 antigen stimulated samples per group.

Data analysis of gene expression

Quality control and normalization of Affymetrix CEL files were performed using the ArrayAnalysis website (www.arrayanalysis.org) [57], using the Robust Multichip Average (RMA) method [58] and the MBNI custom CDF version 15 [59]. Normalized data consisted of Log2 transformed signal values for 17306 genes. All slides passed quality control. Further analysis of normalized data was performed in R (www.r-project.org) and Microsoft Excel. Genes differentially expressed between the different groups of immunized mice were identified by using ANOVA. Fold ratio induction or repression of individual genes was calculated by comparing mean gene expression levels of the different immunization groups. Probes were considered differentially expressed if they met the following two criteria: (i) a *p*-value ≤ 0.001 (ANOVA), which corresponds to a Benjamini-Hochberg False discovery rate (FDR) of 5%; and (ii) an absolute fold ratio ≥ 1.5. Heatmaps visualizing differently expressed genes were made using GeneMaths XT software (Applied Maths). Hierarchical clustering of the differentially expressed genes was performed in GeneMaths XT software using Euclidean distance (with variances) as a distance metric and UPGMA linkage. Additional data visualization was done by Principal Component Analysis in R. Functional enrichment with an over-representation analysis (ORA) was performed using DAVID [17] based on Gene Ontology biological processes (GO-BP) and Kyoto Encyclopedia of Genes and Genomes (KEGG) databases.

Transcription factor-binding site analysis

For the transcription factor binding site (TFBS) analysis, the platform oPOSSUM3.0 (http://opossum.cisreg.ca/oPOSSUM3) was used. To evaluate whether a TFBS is enriched within the different gene sets, the software detects known transcription factor binding sites in the promoter sequences of the co-expressed genes [60]. Up- and downstream sequences (5000 bp) of up- or downregulated genes in $CD4^+$ T-cells of aPV- or aPV+LpxL1-vaccinated mice were analyzed using the default parameters in oPOSSUM 3.0 Single Site Analysis (SSA). A TFBS was considered enriched when it met the following criteria, Z-score > 10 and Fischer score > 7, which are the recommended criteria at the oPOSSUM site.

Gene network analysis

To construct a gene-function network, genes associated with Th subsets and metabolism were determined using text mining in murine and human studies. Interactions between genes associated with Th subsets and metabolism were determined using the STRING database (http://string.embl.de/) with high confidence (0.700) and using co-occurrence, co-expression, experiments, databases, and text mining as types of evidence. The network visualization was performed using Cytoscape (version 2.8.3).

Acknowledgements

We are grateful to Peter van der Ley of the Institute for Translational Vaccinology, Bilthoven, The Netherlands for supplying the *N. meningitidis* LPS-derivative LpxL1 and to the department Animal Research Center of the Institute for Translational Vaccinology, Bilthoven, The Netherlands, for performing the animal experiments. Further, the authors thank the Microarray Department (MAD) of the University of Amsterdam for performing the microarray analyses. This work was supported by the Dutch Government and carried out in the framework of RIVM Strategic Programme (SPR) (grant S/000193).

References

1. Black, A. J. & McKane, A. J. Stochasticity in staged models of epidemics: quantifying the dynamics of whooping cough. J R Soc Interface 7, 1219-1227, doi:10.1098/rsif.2009.0514 (2010).
2. Cherry, J. D. The present and future control of pertussis. Clin Infect Dis 51, 663-667, doi:10.1086/655826 (2010).
3. Pertussis vaccines: WHO position paper. Wkly Epidemiol Rec 85, 385-400 (2010).
4. Ross, P. J. *et al.* Relative Contribution of Th1 and Th17 Cells in Adaptive Immunity to *Bordetella pertussis*: Towards the Rational Design of an Improved Acellular Pertussis Vaccine. PLoS pathog 9, e1003264, doi:10.1371/journal.ppat.1003264 (2013).
5. Ryan, M. *et al. Bordetella pertussis* respiratory infection in children is associated with preferential activation of type 1 T helper cells. J Infect Dis 175, 1246-1250 (1997).
6. Raeven, R. H. M. *et al.* Molecular signatures of the evolving immune response in mice following a *Bordetella pertussis* infection. PLoS One 9, e104548, doi:10.1371/journal.pone.0104548 (2014).
7. Warfel, J. M. & Merkel, T. J. *Bordetella pertussis* infection induces a mucosal IL-17 response and long-lived Th17 and Th1 immune memory cells in nonhuman primates. Mucosal Immunol 6, 787-796, doi:10.1038/mi.2012.117 (2013).
8. Mascart, F. *et al.* Modulation of the infant immune responses by the first pertussis vaccine administrations. Vaccine 25, 391-398, doi:10.1016/j.vaccine.2006.06.046 (2007).
9. Vermeulen, F. *et al.* Cellular immune responses of preterm infants after vaccination with whole-cell or acellular pertussis vaccines. Clin Vaccine Immunol 17, 258-262, doi: 10.1128/CVI.00328-09 (2010).
10. Brummelman, J. *et al.* Modulation of the CD4(+) T cell response after acellular pertussis vaccination in the presence of TLR4 ligation. Vaccine 33, 1483-1491, doi:10.1016/j.vaccine.2015.01.063 (2015).
11. Christie, D. & Zhu, J. Transcriptional regulatory networks for CD4 T cell differentiation. Curr Top Microbiol Immunol 381, 125-172, doi:10.1007/82_2014_372 (2014).
12. Liu, X. *et al.* Bcl6 expression specifies the T follicular helper cell program *in vivo*. J Exp Med 209, 1841-1852, s1841-1824, doi:10.1084/jem.20120219 (2012).
13. Miyamoto, Y. *et al.* Podoplanin is an inflammatory protein upregulated in Th17 cells in SKG arthritic joints. Mol Immunol 54, 199-207, doi:10.1016/j.molimm.2012.11.013 (2013).
14. Acosta-Rodriguez, E. V. *et al.* Surface phenotype and antigenic specificity of human interleukin 17-producing T helper memory cells. Nat Immunol 8, 639-646, doi:10.1038/ni1467 (2007).
15. White, O. J. *et al.* A genomics-based approach to assessment of vaccine safety and immunogenicity in children. Vaccine 30, 1865-1874, doi:10.1016/j.vaccine.2011.12.118 (2012).
16. Dunne, A. *et al.* A novel TLR2 agonist from *Bordetella pertussis* is a potent adjuvant that promotes protective immunity with an acellular pertussis vaccine. Mucosal Immunol, doi:10.1038/mi.2014.93 (2014).
17. Huang da, W., Sherman, B. T. & Lempicki, R. A. Systematic and integrative analysis of large gene lists using DAVID bioinformatics resources. Nat Protoc 4, 44-57, doi:10.1038/nprot.2008.211 (2009).
18. Palmer, C. S., Ostrowski, M., Balderson, B., Christian, N. & Crowe, S. M. Glucose metabolism regulates T cell activation, differentiation, and functions. Front Immunol 6, 1, doi:10.3389/fimmu.2015.00001 (2015).
19. Chang, C. H. *et al.* Posttranscriptional control of T cell effector function by aerobic glycolysis. Cell 153, 1239-1251, doi:10.1016/j.cell.2013.05.016 (2013).
20. Maekawa, Y. *et al.* Notch controls the survival of memory CD4+ T cells by regulating glucose uptake. Nat Med 21, 55-61, doi:10.1038/nm.3758 (2015).
21. Schrum, S., Probst, P., Fleischer, B. & Zipfel, P. F. Synthesis of the CC-chemokines MIP-1alpha, MIP-1beta, and RANTES is associated with a type 1 immune response. J Immunol 157, 3598-3604 (1996).
22. Liu, W. *et al.* Bortezomib regulates the chemotactic characteristics of T cells through downregulation of CXCR3/CXCL9 expression and induction of apoptosis. Int J Hematol 96, 764-772, doi:10.1007/s12185-012-1195-6 (2012).
23. Anderson, A. C. *et al.* T-bet, a Th1 transcription factor regulates the expression of Tim-3. Eur J Immunol 40, 859-866, doi:10.1002/eji.200939842 (2010).
24. Newcomb, D. C. *et al.* Human TH17 cells express a functional IL-13 receptor and IL-13 attenuates IL-17A production. J Allergy Clin Immunol 127, 1006-1013 e1001-1004, doi:10.1016/j.jaci.2010.11.043 (2011).
25. Zhang, H. *et al.* Profiling of human CD4+ T-cell subsets identifies the TH2-specific noncoding RNA GATA3-AS1. J Allergy Clin Immunol 132, 1005-1008, doi:10.1016/j.jaci.2013.05.033 (2013).
26. Egwuagu, C. E. *et al.* Suppressors of cytokine signaling proteins are differentially expressed in Th1 and Th2 cells: implications for Th cell lineage commitment and maintenance. J Immunol 168, 3181-3187 (2002).
27. Yamamoto, K., Yamaguchi, M., Miyasaka, N. & Miura, O. SOCS-3 inhibits IL-12-induced STAT4 activation by binding through its SH2 domain to the STAT4 docking site in the IL-12 receptor beta2 subunit. Biochem Biophys Res Commun 310, 1188-1193 (2003).
28. Chen, Z. *et al.* Selective regulatory function of Socs3 in the formation of IL-17-secreting T cells. Proc Natl Acad Sci U S A 103, 8137-8142, doi:10.1073/pnas.0600666103 (2006).
29. Gondek, D. C., Lu, L. F., Quezada, S. A., Sakaguchi, S. & Noelle, R. J. Cutting edge: contact-mediated suppression by CD4+CD25+ regulatory cells involves a granzyme B-dependent, perforin-independent mechanism. J Immunol 174, 1783-1786 (2005).
30. Perrella, A. *et al.* CD4+/CD25+ T cells suppress autologous CD4+/CD25- lymphocytes and secrete granzyme B during acute and chronic hepatitis C. Pathog Dis 72, 124-130, doi:10.1111/2049-632x.12190 (2014).
31. Klein, O. *et al.* Flt3 ligand expands CD4+ FoxP3+ regulatory T cells in human subjects. Eur J Immunol 43, 533-539, doi:10.1002/eji.201242603 (2013).
32. Wei, L., Laurence, A., Elias, K. M. & O'Shea, J. J. IL-21 is produced by Th17 cells and drives IL-17 production in a STAT3-dependent manner. J Biol Chem 282, 34605-34610, doi:10.1074/jbc.M705100200 (2007).
33. Quintana, F. J. *et al.* Aiolos promotes TH17 differentiation by directly silencing Il2 expression. Nat Immunol 13, 770-777, doi:10.1038/ni.2363 (2012).

34. Kemper, C. & Atkinson, J. P. T-cell regulation: with complements from innate immunity. Nat Rev Immunol 7, 9-18, doi:10.1038/nri1994 (2007).
35. Wagner, C. *et al.* The complement receptor 3, CR3 (CD11b/CD18), on T lymphocytes: activation-dependent up-regulation and regulatory function. Eur J Immunol 31, 1173-1180, doi: 10.1002/1521-4141(200104)31:4<1173::AID-IMMU1173>3.0.CO;2-9 (2001).
36. Werfel, T. *et al.* Activated human T lymphocytes express a functional C3a receptor. J Immunol 165, 6599-6605 (2000).
37. Wang, F. *et al.* Complement C3a binding to its receptor as a negative modulator of Th2 response in liver injury in trichloroethylene-sensitized mice. Toxicol Lett 229, 229-239, doi:10.1016/j.toxlet.2014.06.841 (2014).
38. Ghannam, A., Fauquert, J. L., Thomas, C., Kemper, C. & Drouet, C. Human complement C3 deficiency: Th1 induction requires T cell-derived complement C3a and CD46 activation. Mol Immunol 58, 98-107, doi:10.1016/j.molimm.2013.11.010 (2014).
39. Kwan, W. H., van der Touw, W., Paz-Artal, E., Li, M. O. & Heeger, P. S. Signaling through C5a receptor and C3a receptor diminishes function of murine natural regulatory T cells. J Exp Med 210, 257-268, doi:10.1084/jem.20121525 (2013).
40. Imanishi, T. *et al.* Cutting edge: TLR2 directly triggers Th1 effector functions. J Immunol 178, 6715-6719 (2007).
41. Watanabe, T. *et al.* Lipid A directly inhibits IL-4 production by murine Th2 cells but does not inhibit IFN-gamma production by Th1 cells. Eur J Immunol 29, 413-418, doi:10.1002/(SICI)1521-4141(199902)29:02<413::AID-IMMU413>3.0.CO;2-Y (1999).
42. Nyirenda, M. H. *et al.* TLR2 stimulation drives human naive and effector regulatory T cells into a Th17-like phenotype with reduced suppressive function. J Immunol 187, 2278-2290, doi:10.4049/jimmunol.1003715 (2011).
43. Reynolds, J. M., Martinez, G. J., Chung, Y. & Dong, C. Toll-like receptor 4 signaling in T cells promotes autoimmune inflammation. Proc Natl Acad Sci U S A 109, 13064-13069, doi:10.1073/pnas.1120585109 (2012).
44. Clemenceau, B. *et al.* Effector memory alphabeta T lymphocytes can express FcgammaRIIIa and mediate antibody-dependent cellular cytotoxicity. J Immunol 180, 5327-5334 (2008).
45. Chauhan, A. K., Chen, C., Moore, T. L. & DiPaolo, R. J. Induced expression of FcgammaRIIIa (CD16a) on CD4+ T cells triggers generation of IFN-gammahigh subset. J Biol Chem 290, 5127-5140, doi:10.1074/jbc.M114.599266 (2015).
46. Bonizzi, G. & Karin, M. The two NF-kappaB activation pathways and their role in innate and adaptive immunity. Trends Immunol 25, 280-288, doi:10.1016/j.it.2004.03.008 (2004).
47. Ruan, Q. *et al.* The Th17 immune response is controlled by the Rel-RORgamma-RORgamma T transcriptional axis. J Exp Med 208, 2321-2333, doi:10.1084/jem.20110462 (2011).
48. Hilliard, B. A. *et al.* Critical roles of c-Rel in autoimmune inflammation and helper T cell differentiation. J Clin Invest 110, 843-850, doi:10.1172/jci15254 (2002).
49. Visekruna, A. *et al.* c-Rel is crucial for the induction of Foxp3(+) regulatory CD4(+) T cells but not T(H)17 cells. Eur J Immunol 40, 671-676, doi:10.1002/eji.200940260 (2010).
50. An, J. *et al.* Kruppel-like factor 4 (KLF4) directly regulates proliferation in thymocyte development and IL-17 expression during Th17 differentiation. FASEB J 25, 3634-3645, doi:10.1096/fj.11-186924 (2011).
51. Chang, H. C. *et al.* PU.1 expression delineates heterogeneity in primary Th2 cells. Immunity 22, 693-703, doi:10.1016/j.immuni.2005.03.016 (2005).
52. Pagani, M. *et al.* Role of microRNAs and long-non-coding RNAs in CD4(+) T-cell differentiation. Immunol Rev 253, 82-96, doi:10.1111/imr.12055 (2013).
53. Matsuyama, H. *et al.* miR-135b mediates NPM-ALK-driven oncogenicity and renders IL-17-producing immunophenotype to anaplastic large cell lymphoma. Blood 118, 6881-6892, doi:10.1182/blood-2011-05-354654 (2011).
54. Chattopadhyay, P. K., Gierahn, T. M., Roederer, M. & Love, J. C. Single-cell technologies for monitoring immune systems. Nat Immunol 15, 128-135, doi:10.1038/ni.2796 (2014).
55. Hijnen, M., van Gageldonk, P. G., Berbers, G. A., van Woerkom, T. & Mooi, F. R. The *Bordetella pertussis* virulence factor P.69 pertactin retains its immunological properties after overproduction in Escherichia coli. Protein Expr Purif 41, 106-112, doi:10.1016/j.pep.2005.01.014 (2005).
56. van der Ley, P. *et al.* Modification of lipid A biosynthesis in *Neisseria meningitidis* lpxL mutants: influence on lipopolysaccharide structure, toxicity, and adjuvant activity. Infect Immun 69, 5981-5990, doi:10.1128/IAI.69.10.5981-5990.2001 (2001).
57. Eijssen, L. M. *et al.* User-friendly solutions for microarray quality control and pre-processing on ArrayAnalysis.org. Nucleic Acids Res 41, W71-76, doi:10.1093/nar/gkt293 (2013).
58. Bolstad, B. M., Irizarry, R. A., Astrand, M. & Speed, T. P. A comparison of normalization methods for high density oligonucleotide array data based on variance and bias. Bioinformatics 19, 185-193 (2003).
59. Dai, M. *et al.* Evolving gene/transcript definitions significantly alter the interpretation of GeneChip data. Nucleic Acids Res 33, e175, doi:10.1093/nar/gni179 (2005).
60. Kwon, A. T., Arenillas, D. J., Worsley Hunt, R. & Wasserman, W. W. oPOSSUM-3: advanced analysis of regulatory motif over-representation across genes or ChIP-Seq datasets. G3 (Bethesda) 2, 987-1002, doi:10.1534/g3.112.003202 (2012).

Supplementary information

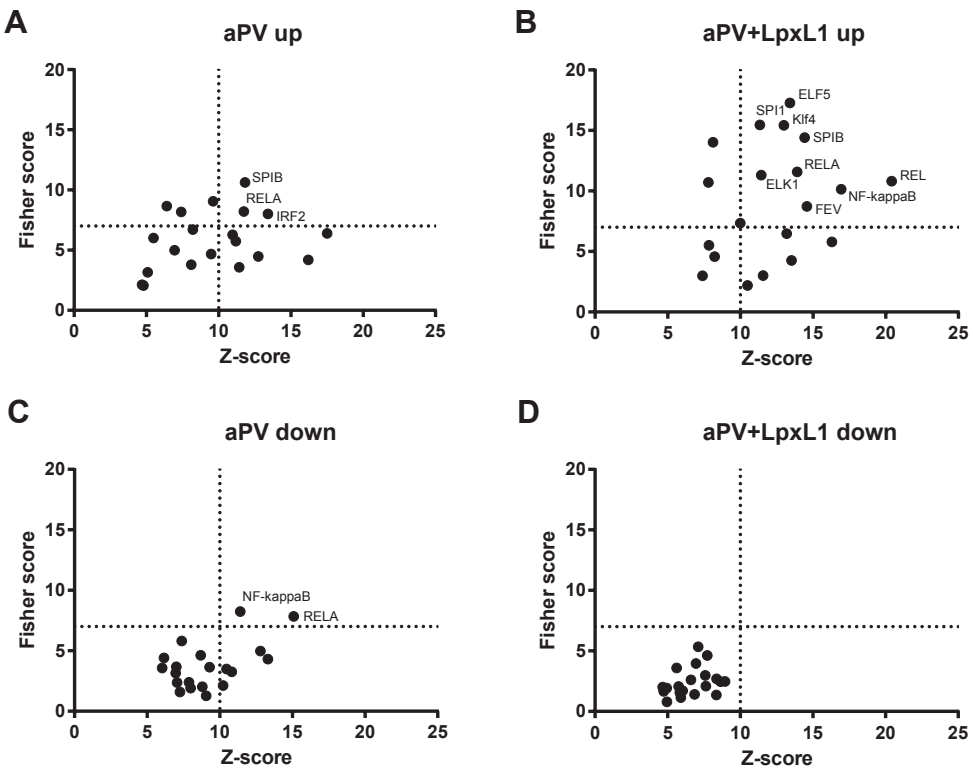

Figure S1 - Over-representation of transcription factor-binding sites. Using the web-based platform oPOSSUM3.0 (http://opossum.cisreg.ca/oPOSSUM3) over-representation of transcription factor binding sites (TBFS) was analyzed within all upregulated genes in $CD4^+$ T-cells of aPV-vaccinated **(A)** or aPV+LpxL1-vaccinated **(B)** mice, or within all downregulated genes in $CD4^+$ T-cells of aPV-vaccinated **(C)** or aPV+LpxL1-vaccinated **(D)** mice. A TFBS was considered over-represented when it met the following criteria, Z-score > 10 and Fischer score > 7, which are the recommended criteria at the oPOSSUM site.

Table S1 – Top 20 TFBS found in gene sets from CD4+ T-cells of aPV- or aPV+LpxL1-vaccinated mice.

Top 20 over-represented TFBS within upregulated genes in CD4+ T-cells of aPV vaccinated mice (A)							
Transcription factor	JASPAR ID	Class	Family	Target gene hits	Target TFBS hits	Z-score	Fisher score
REL	MA0101.1	Ig-fold	Rel	87	291	17.504	6.387
Pax4	MA0068.1	Helix-Turn-Helix	Homeo	3	3	16.198	4.191
IRF2	MA0051.1	Winged Helix-Turn-Helix	IRF	14	14	13.414	8.012
Stat3	MA0144.1	Ig-fold	Stat	79	227	12.747	4.469
SPIB	MA0081.1	Winged Helix-Turn-Helix	Ets	140	1449	11.833	10.628
RELA	MA0107.1	Ig-fold	Rel	65	131	11.748	8.211
FEV	MA0156.1	Winged Helix-Turn-Helix	Ets	115	693	11.428	3.568
NF-kappaB	MA0061.1	Ig-fold	Rel	69	172	11.185	5.745
ELK1	MA0028.1	Winged Helix-Turn-Helix	Ets	107	478	10.969	6.278
ELF5	MA0136.1	Winged Helix-Turn-Helix	Ets	133	959	9.624	9.058
STAT1	MA0137.2	Ig-fold	Stat	54	98	9.482	4.676
Pax6	MA0069.1	Helix-Turn-Helix	Homeo	17	17	8.211	6.710
Hand1::Tcfe2a	MA0092.1	Zipper-Type	Helix-Loop-Helix	105	477	8.111	3.784
MEF2A	MA0052.1	Other Alpha-Helix	MADS	64	121	7.405	8.167
EBF1	MA0154.1	Zipper-Type	Helix-Loop-Helix	91	324	6.954	4.987
SPI1	MA0080.2	Winged Helix-Turn-Helix	Ets	128	789	6.414	8.651
NFATC2	MA0152.1	Ig-fold	Rel	121	726	5.493	6.012
NR3C1	MA0113.1	Zinc-coordinating	Hormone-nuclear Receptor	22	28	5.094	3.164
EWSR1-FLI1	MA0149.1	Winged Helix-Turn-Helix	Ets	3	3	4.797	2.055
FOXF2	MA0030.1	Winged Helix-Turn-Helix	Forkhead	31	51	4.707	2.120

Top 20 over-represented TFBS within upregulated genes in CD4+ T-cells of aPV+Lpxl1 vaccinated mice (B)							
Transcription factor	JASPAR ID	Class	Family	Target gene hits	Target TFBS hits	Z-score	Fisher score
REL	MA0101.1	Ig-fold	Rel	142	427	20.407	10.808
NF-kappaB	MA0061.1	Ig-fold	Rel	114	270	16.938	10.145
Stat3	MA0144.1	Ig-fold	Stat	125	341	16.304	5.797
FEV	MA0156.1	Winged Helix-Turn-Helix	Ets	192	1036	14.583	8.724
SPIB	MA0081.1	Winged Helix-Turn-Helix	Ets	222	2152	14.425	14.405
RELA	MA0107.1	Ig-fold	Rel	103	193	13.908	11.579
Hand1::Tcfe2a	MA0092.1	Zipper-Type	Helix-Loop-Helix	165	737	13.518	4.257
ELF5	MA0136.1	Winged Helix-Turn-Helix	Ets	217	1444	13.409	17.278
STAT1	MA0137.2	Ig-fold	Stat	86	150	13.184	6.474
Klf4	MA0039.2	Zinc-coordinating	BetaBetaAlpha-zinc finger	181	1006	12.993	15.421
Pax4	MA0068.1	Helix-Turn-Helix	Homeo	3	3	11.558	3.002
ELK1	MA0028.1	Winged Helix-Turn-Helix	Ets	175	695	11.443	11.310
SPI1	MA0080.2	Winged Helix-Turn-Helix	Ets	208	1215	11.341	15.465
TP53	MA0106.1	Zinc-coordinating	Loop-Sheet-Helix	1	1	10.490	2.186
EBF1	MA0154.1	Zipper-Type	Helix-Loop-Helix	146	491	9.990	7.340
IRF2	MA0051.1	Winged Helix-Turn-Helix	IRF	15	15	8.227	4.583
SP1	MA0079.2	Zinc-coordinating	BetaBetaAlpha-zinc finger	164	792	8.115	14.017
Pax6	MA0069.1	Helix-Turn-Helix	Homeo	22	23	7.843	5.516
MEF2A	MA0052.1	Other Alpha-Helix	MADS	100	175	7.795	10.702
EWSR1-FLI1	MA0149.1	Winged Helix-Turn-Helix	Ets	5	5	7.401	2.985

Top 20 over-represented TFBS within downregulated genes in CD4+ T-cells of aPV vaccinated mice (C)							
Transcription factor	JASPAR ID	Class	Family	Target gene hits	Target TFBS hits	Z-score	Fisher score
RELA	MA0107.1	Ig-fold	Rel	82	160	15.089	7.836
CEBPA	MA0102.2	Zipper-Type	Leucine Zipper	132	512	13.306	4.313
IRF1	MA0050.1	Winged Helix-Turn-Helix	IRF	69	129	12.800	4.975
NF-kappaB	MA0061.1	Ig-fold	Rel	94	197	11.408	8.238
REL	MA0101.1	Ig-fold	Rel	104	298	10.831	3.265
Pou5f1	MA0142.1	Helix-Turn-Helix	Homeo	35	53	10.466	3.484
SRY	MA0084.1	Other Alpha-Helix	High Mobility Group	149	900	10.233	2.121
IRF2	MA0051.1	Winged Helix-Turn-Helix	IRF	12	13	9.305	3.641
Sox17	MA0078.1	Other Alpha-Helix	High Mobility Group	134	633	9.059	1.267
FOXI1	MA0042.1	Winged Helix-Turn-Helix	Forkhead	120	436	8.792	2.032
NFATC2	MA0152.1	Ig-fold	Rel	155	871	8.686	4.624
Pax4	MA0068.1	Helix-Turn-Helix	Homeo	2	2	7.997	1.911
MEF2A	MA0052.1	Other Alpha-Helix	MADS	67	140	7.877	2.385
AP1	MA0099.2	Zipper-Type	Leucine Zipper	168	1090	7.388	5.808
Foxq1	MA0040.1	Winged Helix-Turn-Helix	Forkhead	77	190	7.258	1.596
TAL1::TCF3	MA0091.1	Zipper-Type	Helix-Loop-Helix	72	138	7.064	2.383
CTCF	MA0139.1	Zinc-coordinating	BetaBetaAlpha-zinc finger	34	40	7.008	3.675
HLF	MA0043.1	Zipper-Type	Leucine Zipper	57	93	6.971	3.164
NFE2L2	MA0150.1	Zipper-Type	Leucine Zipper	64	98	6.156	4.404
FEV	MA0156.1	Winged Helix-Turn-Helix	Ets	151	746	6.033	3.577

Top 20 over-represented TFBS within downregulated genes in CD4+ T-cells of aPV+Lpxl1 vaccinated mice (D)							
Transcription factor	JASPAR ID	Class	Family	Target gene hits	Target TFBS hits	Z-score	Fisher score
CEBPA	MA0102.2	Zipper-Type	Leucine Zipper	55	211	8.947	2.472
HNF4A	MA0114.1	Zinc-coordinating	Hormone-nuclear Receptor	30	57	8.647	2.461
NR3C1	MA0113.1	Zinc-coordinating	Hormone-nuclear Receptor	13	17	8.374	2.699
IRF1	MA0050.1	Winged Helix-Turn-Helix	IRF	25	53	8.352	1.359
CTCF	MA0139.1	Zinc-coordinating	BetaBetaAlpha-zinc finger	18	19	7.731	4.622
IRF2	MA0051.1	Winged Helix-Turn-Helix	IRF	5	6	7.628	2.094
RELA	MA0107.1	Ig-fold	Rel	32	61	7.584	2.969
NF-kappaB	MA0061.1	Ig-fold	Rel	41	80	7.105	5.341
Hand1::Tcfe2a	MA0092.1	Zipper-Type	Helix-Loop-Helix	61	232	6.954	3.950
Pax4	MA0068.1	Helix-Turn-Helix	Homeo	1	1	6.848	1.405
ELF5	MA0136.1	Winged Helix-Turn-Helix	Ets	69	454	6.602	2.604
Foxq1	MA0040.1	Winged Helix-Turn-Helix	Forkhead	34	81	6.029	1.712
AP1	MA0099.2	Zipper-Type	Leucine Zipper	65	454	5.905	1.136
TAL1::TCF3	MA0091.1	Zipper-Type	Helix-Loop-Helix	30	59	5.843	1.561
SPI1	MA0080.2	Winged Helix-Turn-Helix	Ets	65	383	5.763	2.058
SPIB	MA0081.1	Winged Helix-Turn-Helix	Ets	74	663	5.619	3.587
MEF2A	MA0052.1	Other Alpha-Helix	MADS	25	57	4.946	0.794
EBF1	MA0154.1	Zipper-Type	Helix-Loop-Helix	47	154	4.936	1.926
znf143	MA0088.1	Zinc-coordinating	BetaBetaAlpha-zinc finger	7	8	4.731	1.652
Egr1	MA0162.1	Zinc-coordinating	BetaBetaAlpha-zinc finger	25	46	4.661	2.009

About the cover: The Perito Moreno glacier located in the Los Glaciares National Park in Patagonia, Argentina. Part of the Southern Patagonian Ice field which is the third largest reserve of fresh water. The end of the glacier is 5 km wide, with an average height of 74 metres and moves 1 - 2 metres each day. In 2016, René attended the 11th International Bordetella Symposium that was held in Buenos Aires, Argentina.

CHAPTER 7

Systems vaccinology reveals superior protection after pulmonary compared to subcutaneous administration of an outer membrane vesicle pertussis vaccine associated with local and systemic immune signatures in mice

René H.M. Raeven[1,5,#], Jolanda Brummelman[2,4,#], Jeroen L.A. Pennings[3], Larissa van der Maas[1], Kina Helm[2], Wichard Tilstra[1], Arno van der Ark[1], Arjen Sloots[1], Peter van der Ley[1], Willem van Eden[4], Wim Jiskoot[5], Elly van Riet[1], Cécile A.C.M. van Els[2], Gideon F.A. Kersten[1,5], Wanda G.H. Han[2,*], Bernard Metz[1,*]

[1]Intravacc, Institute for Translational Vaccinology, Bilthoven, The Netherlands,
[2]Centre for Infectious Disease Control, National Institute for Public Health and the Environment, Bilthoven, The Netherlands,
[3]Centre for Health Protection, National Institute for Public Health and the Environment, Bilthoven, The Netherlands,
[4]Department of Infectious Diseases and Immunology, Utrecht University, The Netherlands,
[5]Division of Drug Delivery Technology, Leiden Academic Centre for Drug Research, Leiden, The Netherlands
[#] Authors contributed equally
[*] Authors contributed equally

Submitted for publication

Abstract

Local immune responses in the lungs contribute to protection against *B. pertussis* infection and might improve the vaccine-elicited immunity. Therefore, the effect of the vaccine administration route on the degree of protection and the local and systemic immune response was investigated. Immunization of mice via the pulmonary route with a novel outer membrane vesicle pertussis vaccine (omvPV) led to faster clearance of *B. pertussis* upon intranasal challenge compared to immunization via the subcutaneous route. The local and systemic immune responses underlying this difference in protection were analyzed using a systems biology approach. Exclusively pulmonary immunization led to the presence of *B. pertussis*-specific IgA antibodies, IgA-producing plasma cells and Th17-cells in the lungs. Moreover, this route elicited increased levels of systemic specific IgG antibodies, IgG-producing plasma cells, memory B-cells, and Th17-cells. In addition, only pulmonary immunization elicited a rapid induction of pro-inflammatory cytokines and chemoattractants, e.g. IL-6 and CXCL10, observed on transcriptomic and proteomic levels, in the lungs. Distinct cytokine profiles were measured in sera, which were overall higher after subcutaneous immunization, e.g. G-CSF and IL-5. Transcriptome analysis of lungs and draining lymph nodes revealed differences in innate and adaptive responses between both administration routes e.g. the expression of *Igha* and *Rorc*, supporting the superior IgA, IgG, and Th17 responses detected in pulmonary-immunized mice. These results show that by administering the vaccine via the pulmonary as opposed to the subcutaneous route, an omvPV can elicit superior local and systemic immunity against *B. pertussis*, resembling immunity after primary infection. The study indicates that pulmonary immunization may be key to improve pertussis vaccination strategies.

Introduction

Currently, pertussis remains an endemic disease, even in highly vaccinated populations. Approaches to increase protection include the improvement of pertussis vaccines and vaccination strategies [1, 2]. The whole-cell and acellular pertussis vaccines induce a systemic immune response characterized by the formation of IgG antibodies and a T-helper (Th) response that is Th1/Th17 or Th2 dominated, respectively [3-6]. In contrast, a *B. pertussis* infection evokes a Th1/Th17 response both systemically and locally in the lungs [5, 7, 8]. Outer-membrane vesicle pertussis vaccines (omvPV) might be an improved alternative for the currently available vaccines. Subcutaneous immunization of omvPV elicited a systemic immune response comparable to that induced by *B. pertussis* infection, including high serum IgG levels against a broad antigen range [9] and a mixed Th1, Th17, and Th2 response [10]. Unfortunately, subcutaneous omvPV immunization does not induce local immune responses in the lungs that are thought to contribute to a better protection against *B. pertussis* [10].

Direct vaccine administration in the respiratory tract can lead to better protection compared to parenteral administration due to the induction of local immune responses as was shown for other respiratory pathogens, such as *M. tuberculosis* and influenza [11-13]. The feasibility of mucosal administration of different pertussis vaccines was proven as intranasal immunization provides protection against *B. pertussis* challenge [14-17]. Nonetheless, direct comparison of the local and systemic immune responses induced by parental and mucosal immunization of pertussis vaccines is not yet performed.

In the present study, we investigated in detail whether the route of immunization affects protection and the quality of the immune response in mice. A systems biology approach was used to compare immune responses following pulmonary and subcutaneous immunization with omvPV (**Figure 1A**). Such an approach was previously applied in vaccine research to predict vaccine responsiveness [18-21] and to unravel of molecular signatures of mucosal adjuvants [22] and respiratory pathogen infections [7, 23]. In our study, the novel omvPV-P93 with abolished Prn autocleavage was used, since it enables more specific readouts and provides better protection in a murine challenge model compared to the WT omvPV, even at a lower dose [24]. Besides *B. pertussis* clearance from the respiratory tract after intranasal challenge, gene expression profiles in draining lymph nodes and lungs, and cytokine profiles and antibody responses in serum and lungs of immunized mice were determined. Finally, specific B-cell and T-cell responses were investigated both locally and systemically. Our results demonstrate hallmarks of superior protective immunity to *B. pertussis* conferred by pulmonary vaccination with omvPV.

Materials and Methods

Vaccine and antigens

The outer membrane vesicle pertussis vaccine (omvPV) was prepared using a genetically modified *B. pertussis* B1917 strain lacking the autocleavage site in pertactin (Prn), as described previously [24]. 1 µg total protein omvPV was diluted in 50 µl and 300 µl PBS (Gibco) for pulmonary and subcutaneous immunization respectively. Pertussis antigens Ptx and FHA were obtained from Kaketsuken (Japan), Prn and Fim2/3 were kindly provided by Betsy Kuipers (National Institute for Public Health and the Environment, Bilthoven, the Netherlands).

B. pertussis challenge culture

The *B. pertussis* challenge culture was prepared as described in the literature [7], except that bacteria were grown in THIJS medium [25].

Ethics statement

An independent ethical committee for animal experimentations of the Institute for Translational Vaccinology (Intravacc) approved the animal experiments with identifiers 201400125 and 201400182. Animal handling in this study was carried out in accordance to the guidelines provided by the Dutch Act on Animal Experimentation.

Immunization and challenge of mice

Female BALB/c mice (Harlan, The Netherlands), 8-week-old, were immunized with 1 µg total protein omvPV either pulmonary (P.M.; 50 µl) or subcutaneously (S.C.; 300 µl) on day 0 and 28. Non-immunized (N.I.) mice were used as a control. Pulmonary administration was performed as described by Bivas-Benita *et al.* [26] using a MicroSprayer aerosolizer (IA-1C; Penn-Century, Philadelphia, PA, USA) supplied with a high-pressure syringe (FMJ-250; Penn-Century). Mice were intranasally challenged under anesthesia (isoflurane/oxygen), with 2×10^5 colony forming units (cfu) of *B. pertussis* B1917 in 20 µL of THIJS medium on day 56.

For gene expression in the lungs and draining lymph nodes (dLN), cytokine responses, and antibody responses, mice (n = 4 per group) were sacrificed 4 hours and 2, 7, 14 and 28 days after primary immunization. In addition, to investigate gene expression in the dLN, cytokine responses, and antibody responses after booster vaccination, mice (n = 4 per group) were sacrificed on day 35 and 56. Finally, mice (n = 4 per group) were sacrificed 4 hours after challenge and on day 58, 63, 70, and 84 to measure bacterial load in the respiratory tract, cytokine responses and antibody responses. For evaluation of B-cell responses, mice (n = 6 per group) were sacrificed on day 35 and 63 (plasma cells) and on day 56 and 84 (memory B-cells). For investigation of T-cell responses, mice (n = 6 per group) were sacrificed on day 28, 56, and 84. An additional control group (n = 6) of completely naive mice were included for B- and T-cell investigation on each time point. Mice were bled under anesthesia (isoflurane/

oxygen) by orbital bleeding and sacrificed by cervical dislocation for further sample collection. An overview of the study design of treatment and sample collection is schematically depicted in Figure 1A.

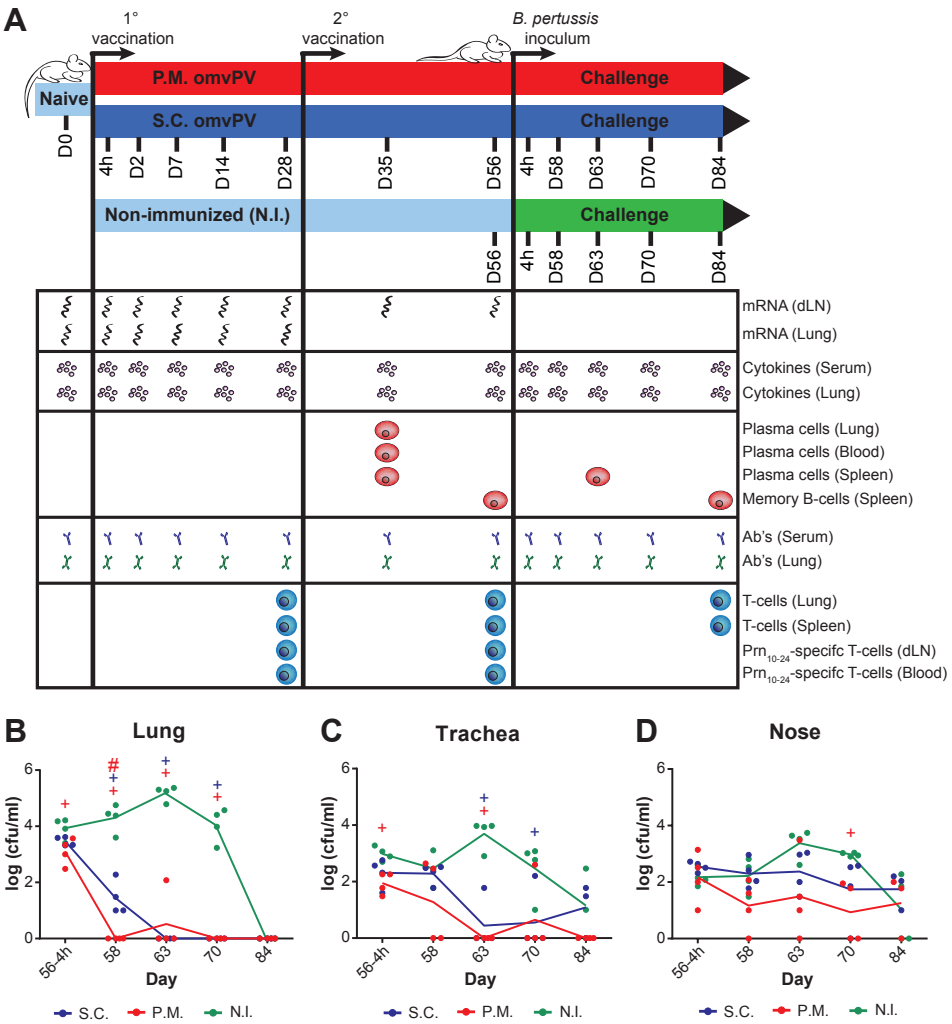

Figure 1 - Study design and *B. pertussis* colonization measured in the respiratory tract. **(A)** BALB/c mice were immunized with 1 µg omvPV pulmonary (P.M.; red) or subcutaneously (S.C.; blue) twice on day 0 and day 28. Subsequently, for both routes the vaccination-induced responses were characterized over a period of 56 days at 7 different time points. Additionally, a *B. pertussis* challenge ($2x10^5$ CFU) was performed on day 56 in both vaccinated groups and non-immunized (N.I.) mice (green). Vaccination responses and *in vivo* recall responses were characterized at the transcriptomic, proteomic and cellular level on given time points, as depicted. **(B-D)** The number of colony-forming units (cfu) were determined after *B. pertussis* challenge **(B)** in lungs, **(C)** trachea and **(D)** nose lavages of S.C. and P.M. immunized and N.I. mice. # $p \leq 0.05$ versus S.C. mice; + $p \leq 0.05$ versus N.I. mice.

Sample collection

From the lungs, the left lobe was placed in 1 ml RNAlater (Qiagen), incubated overnight at 4°C, and stored at -80°C for subsequent microarray analysis. The right lobe was collected in 900 µl THIJS medium and was homogenized using a Bio-Gen PRO200 Homogenizer (Pro Scientific Inc., Oxford, CT, USA) for the lung colonization assay after the challenge and after filtration (Millex GV Filter unit 0.22 µm, Millipore), lysates of all time points were used for pulmonary cytokine and antibody analysis. Complete lungs of mice used for T- and B-cell assays were collected in 5 ml RPMI-1640 medium (Gibco) supplemented with 10% FCS (Hyclone), 100 units penicillin, 100 units streptomycin, and 2.92 mg/ml L-glutamine (Invitrogen), hereafter named RPMI complete medium and kept on ice until use. The draining lymph nodes (dLN), bronchial LN for P.M. immunization and inguinal LN for S.C. immunization, were isolated and placed in 5 ml RPMI complete medium and kept on ice until use, for subsequent microarray analysis and T-cell analysis by tetramer staining. Whole blood for tetramer staining and analysis of B-cell responses was collected in heparin tubes (MiniCollect 1 ml LH Lithium Heparin, Greiner Bio-One, Austria). Serum for cytokine and antibody responses was obtained by collecting whole blood in a serum collection tube (MiniCollect 0.8 ml Z Serum Sep GOLD, Greiner Bio-One, Austria). After coagulation (10 min. at room temperature), sera were taken after centrifugation (10 min., 3000 g) and stored at -80°C. Spleens were placed in 5 ml RPMI complete medium and kept on ice for subsequent B- and T-cell assays. Trachea were collected in 900 µl THIJS medium and were homogenized using the Bio-Gen PRO200 Homogenizer for the trachea colonization assay. Nose lavage was obtained by flushing the nose with 1 ml THIJS medium after the trachea was removed for nose colonization assay. After filtration (Millex GV Filter unit 0.22 µm, Millipore), nose lavages were used to determine nasal antibody responses.

Colonization assays

The tissue lysates from lungs and trachea, and lavages of the nose were serially diluted (undiluted, 1:10, 1:100, and 1:1000) in THIJS medium. The diluted samples were plated on Bordet-Gengou agar plates and incubated for 5 days at 35°C. The number of cfu per ml was determined by using a colony counter (ProtoCOL, Synbiosis, Cambridge, United Kingdom).

B-cell ELISpot

Wells of filter plates (Multiscreen-HA 96 wells plates, Millipore) were coated (overnight, 4°C) with 5 µg/ml Prn (Sanofi) or 10 µg/ml wildtype B1917 OMV. As a positive control, wells were coated with a mixture of 7 µg/ml purified goat-anti-mouse kappa and 7 µg/ml purified goat-anti-mouse lambda (Southern Biotech). As a negative control, wells were left uncoated (PBS). After washing 3 times with PBS, the plates were blocked (1h, room temperature (RT)) with RPMI 1640 + 2% Protifar (Nutricia) and washed again.

Spleens and lungs were homogenized using a 70-µm cell strainer (BD Falcon, BD Biosciences) and cells were collected in RPMI complete medium. From whole blood, erythrocytes were lysed by using RBC lysis buffer (Pharm Lyse, BD Pharmingen). For detection of memory B-cells, $5x10^5$ splenocytes per well of a 24 well-plate were stimulated with CpG ODN 1826 (10 µg/mL, Invivogen), PWM (10 µg/mL), Staphylococcus aureus protein A of Cowan Strain (1:5000) and β-mercaptoethanol (1:25000) (all Sigma) in RPMI complete medium for 5 days at 37ºC to induce antibody secretion. Cells from blood ($0.75x10^5$ cells/well), lungs ($0.75x10^5$ cells/well), spleen ($5x10^5$ cells/well) or stimulated splenocytes ($5x10^5$ cells/well) were added to the coated plates and incubated overnight at 37°C. Plates were washed 7 times with PBS and 3 times with PBS-T (0.05% Tween-20). Then, the plates were incubated (1h, 37°C) with alkaline phosphatase-conjugated goat-anti-mouse IgA or IgG (Southern Biotech; 1:1000). Plates were washed 7 times with PBS, 3 times with PBS-T, and 5 times with tap water. Subsequently, filtered (0.45 µm) BCIP-NBT liquid substrate (Sigma) was added. Spot development was stopped by removing the substrate and extensively rinsing with distilled water. Plates were dried and stored at room temperature in the dark. Spots were counted with an AID iSpot reader (Autoimmun Diagnostika GmbH). The number of *B. pertussis* OMV-specific IgG- and IgA-secreting cells were indicated as antibody secreting cells (ASC) per 5 x 10^5 cells.

Antibody measurements

OMV-, Prn-, FHA-, Ptx-, and Fim2/3-specific antibodies were measured using an in-house developed mouse multiplex immunoassay, as described previously [27]. Serum samples were diluted 1:5000 for IgG (subclass) and 1:100 for IgM and IgA measurements. Lung lysate samples were diluted 1:100 and nose lavage samples were not diluted for measuring IgA levels. Reporter antibodies were R-PE-conjugated goat-anti-mouse IgA, IgG, IgG1, IgG2a, IgG2b, IgG3 or IgM (Southern Biotech). Data were acquired with a Bio-Plex 200, analyzed using Bio-Plex Manager software (version 5.0, Bio-Rad Laboratories), and presented as fluorescence intensities (FI).

Detection of Prn_{10-24} -specific $CD4^+$ T-cells

dLN were homogenized using a 70-µm cell strainer and cells were collected in RPMI complete medium. Blood was treated with erythrocyte-lysis buffer (10 g/L NH_4CL, 1.25 g/L $NaHCO_3$, 0.125 mM EDTA in dH_20; pH 7.4) for 10 minutes on ice, and then resuspended in RPMI complete medium. Cells were stained with APC-conjugated I-A^d tetramers specific for the Prn_{10-24} T-cell epitope [28] (NIH Tetramer Facility, Atlanta, Georgia, USA) in RPMI complete medium for 1 hour at 37°C. Next, cells were stained with Pacific blue-conjugated anti-CD4 (Biolegend), FITC-conjugated anti-CD44 (BD Biosciences), and LIVE/DEAD® Fixable Aqua Dead Cell Stain Kit for 30 minutes at 4°C in FACS buffer (PBS (pH 7.2) supplemented with 0.5% BSA (Sigma Aldrich) and 0.5 mM EDTA (ICN Biomedicals). Data were acquired on a FACS Canto II (BD Biosciences) and analyzed using FlowJo software (Tree Star).

Intracellular cytokine staining (ICS)

Lungs and spleens were homogenized using a 70-µm cell strainer and cells, collected in RPMI complete medium, were treated with erythrocyte lysis buffer. The cells were cultured in 24-well plates ($6x10^6$ cells/well) for 3 days at 37°C in the presence of IMDM complete medium (IMDM medium (Gibco) supplemented with 8% FCS, 100 units penicillin, 100 units streptomycin, 2.92 mg/ml L-glutamine, and 20 µM β-mercaptoethanol (Sigma)). For restimulation of cells, 1 µg/ml Prn or 1.5 µg/ml wildtype B1917 OMVs was added. On day 3, supernatant was collected for cytokine analysis, and the cells were transferred to U-bottom 96-well plates ($5x10^5$ cells/well) and restimulated overnight using the same antigen conditions.

ICS was performed on restimulated splenocytes and lung cells by using the BD Cytofix/Cytoperm Fixation/Permeabilization Solution Kit (BD Biosciences), according to the manufacturer's protocol. Briefly, cells were incubated with 10 µg/ml Golgiplug (BD Biosciences), 1 µg/ml αCD28 (BD Pharmingen), and 1 µg/ml αCD49d (BD Pharmingen) during the last 5 hours of restimulation. Cells were then stained in FACS buffer with Pacific blue-conjugated anti-CD4 (Biolegend), FITC-conjugated anti-CD44 (BD Biosciences), PE-Cy7-conjugated anti-CD103 (Biolegend; only the lung cells), and with LIVE/DEAD Fixable Aqua Dead Cell Stain Kit (Invitrogen). Thereafter, cells were fixed, permeabilized, and stained with PE-conjugated anti-IFNγ (BD Biosciences), APC-conjugated anti-IL-5 (Biolegend), and PerCP-Cy5.5-conjugated anti-IL-17A (eBioscience). Data were acquired on a FACS Canto II and analyzed by using FlowJo software.

Multiplex cytokine analysis (MIA)

Concentrations (pg/ml) of 32 cytokines (Eotaxin, G-CSF, GM-CSF, IFNγ, IL-10, IL-12 (p40), IL-12 (p70), IL-13, IL-15, IL-17A, IL- 1α, IL-1β, IL-2, IL-3, IL-4, IL-5, IL-6, IL-7, IL-9, IP-10, KC, LIF, LIX, M-CSF, MCP-1, MIG, MIP-1α, MIP-1β, MIP-2, RANTES, TNFα, and VEGF) present in serum and lung lysates were determined by using a MIA (Milliplex MAP Mouse Cytokine/ Chemokine - Premixed 32 Plex; Merck KGaA). The concentration of various Th subset cytokines (IL-4, IL-5, IL-10, IL-13, IL-17A, TNFα, and IFNγ) was determined in splenic culture supernatant using a Milliplex mouse cytokine 7-plex luminex kit (Millipore), according to the manufacturer's protocol. Measurements and data analysis were performed with a Bio-Plex 200 and using Bio-PlexManager software (version 5.0, Bio-Rad Laboratories). Results of the Th subset cytokines were corrected for the background (IMDM complete medium control) per mouse per stimulation per cytokine and calculated in pg/ml.

RNA isolation and microarray analysis

Isolation of RNA from lung tissue with additional determination of RNA concentrations and integrity was performed as described previously [7]. For isolation of RNA from cells in the dLN, the dLN were homogenized using a 70-µm cell strainer (BD Falcon, BD Biosciences) and cells were collected in RPMI complete medium and then washed with PBS. By using the MagNA Pure LC RNA Isolation High Performance kit (Roche) according to the manufactures protocol,

the cells were lysed, in 1 ml lysis buffer, and RNA was isolated with the MagNA Pure System (Roche). For lung tissue, samples of naive mice and P.M. vaccinated mice were analyzed as individual samples (n=3), whereas the RNA concentrates of S.C. vaccinated mice were pooled (n=3) for the following time points: Naive, 4 hours, 2 days, 7 days, 14 days, and 28 days post primary vaccination. RNA concentrates from the lymph node suspensions, bronchial for P.M. vaccination and inguinal for S.C. vaccination, of individual mice (n=3) were analyzed for eight time points (naive, 4 hours, 2 days, 7 days, 14 days, 28 days, 35 days and 56 days post primary vaccination). From the naive mice, both bronchial and inguinal lymph nodes were analyzed. Amplification, labeling and hybridization of RNA samples for either lung tissue or lymph nodes for microarray (HT MG-430 PM Array Plates, Affymetrix, Santa Clara, Calif, USA) was carried out at the Microarray Department of the University of Amsterdam, The Netherlands.

Transcriptomic data analysis

Quality control and normalization of raw Affymetrix CEL files were performed using the ArrayAnalysis website (www.arrayanalysis.org) [29], using the Robust Multichip Average (RMA) method [30] and the MBNI custom CDF version 19 [31]. Normalized data consisted of Log2 transformed signal values for 17856 genes. Subsequent analysis of normalized data was performed in R (www.r-project.org) and Microsoft Excel. To identify differentially expressed genes between experimental groups (naive and various time points post vaccination) an ANOVA was applied. The induction or repression of individual genes was expressed as fold ratio by comparing mean gene expression levels of experimental groups to the naive mice. For pulmonary transcriptome analysis, average normalized gene expression levels contain individual data of three mice per group (P.M. and naive mice) and pooled data of 3 mice for the S.C. group. For dLN transcriptome analysis, average normalized gene expression levels contain individual data of three mice per group. The criteria for differential expression for the pulmonary transcriptome analysis were *p*-value <0.01 (ANOVA) and an absolute fold ratio >2.0 (experimental groups compared to naive mice). For dLN transcriptome analysis, the criteria were set at *p*-value < 0.001 and fold ratio > 1.5. GeneMaths XT (Applied Maths, St-Martens-Latem, Belgium) was used to visualize differences in gene expression in heatmaps. Genes were arranged according to similar expression patterns in time at which genes exceeded the fold ratio cut-off. To facilitate visual interpretation of heatmaps, upregulation (red) and downregulation (green) of gene expression levels are only visualized above the fold ratio cutoffs and presenting fold ratios below the cutoffs as an unchanged value (black). Additional data visualization was done by principal component analysis based on expression profiles of all differentially expressed genes in R. Functional enrichment was determined with an over-representation analysis (ORA) based on Gene Ontology Biological Processes (GO-BP) and Kyoto Encyclopedia of Genes and Genomes (KEGG) by using DAVID [32]. Involvement of type I and II interferon-signaling pathway was performed by using the Interferome database (http://www.interferome.org/interferome/home.jspx) [33].

Gene network analysis

To construct a gene-function network, genes associated with five modules, namely acute phase, cytokine response, humoral response, pathogen recognition receptor (PRR) signaling, and T-cell responses, were determined using the ORA results and additional text mining. Interactions between genes were determined using the STRING database (http://string.embl.de/) with high confidence (0.700) and using co-occurrence, co-expression, experiments, databases, and text mining as types of evidence. Gene-function associations and gene-gene interactions were combined into one network file. The network visualization was performed using Cytoscape (version 2.8.3).

Immunoproteomic profiling

One-dimensional (1D) and two-dimensional (2D) electrophoresis in combination with Western blotting (1DEWB, 2DEWB) and LC-MS analysis were performed for the identification of antigen specificity of the antibody responses as described in the literature [9]. Acrylamide gels were loaded with 10-15 µg protein of a *B. pertussis* (B1917) lysate for 1D and with 25 µg protein of the lysate for 2D electrophoresis and blotted. Blots were treated with diluted sera (1:100), diluted lung lysates (1:10-1:50) and diluted nose lavages (1:10) prior to immunostaining with two different IR-800-labeled goat-anti-mouse secondary antibodies (anti-IgG or -IgA). Blots were scanned using an Odyssey infrared imager (Westburg) and analyzed with Delta2D software (Version 4.5) (Decodon, Germany).

Statistics

To determine significance of differences in the outcome of B-cell ELIspot, T-cell ICS, and T-cell tetramer analysis between groups, a Mann-Whitney t-test was used. Data of the cytokine, antibody, and colonization assays were log-transformed after which a t-test was performed. *p*-values ≤0.05 were considered to indicate significance of differences.

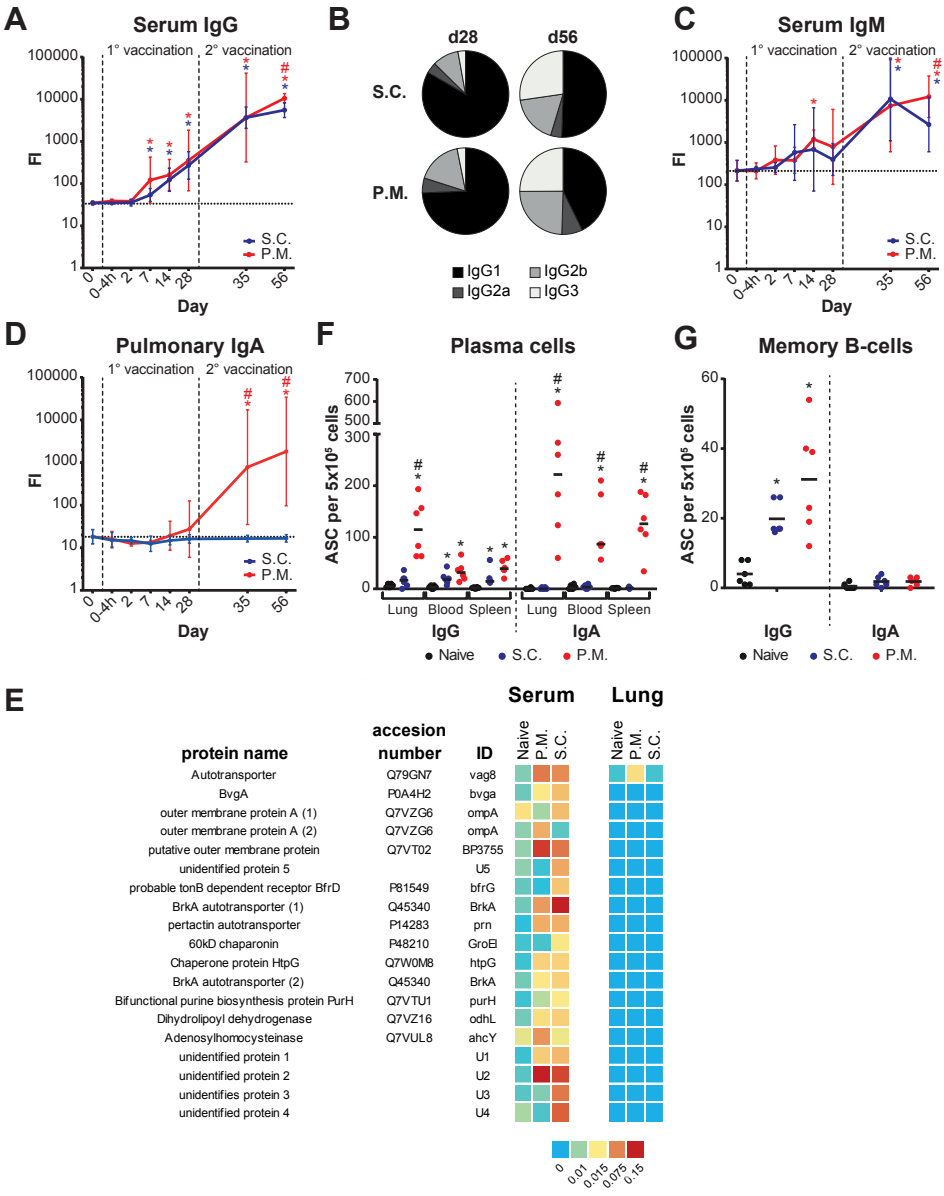

Figure 2 - *B. pertussis* OMV-specific B-cell responses induced by P.M. and S.C. immunization with omvPV. **(A-D)** By using MIA, **(A)** anti-OMV IgG antibody levels, **(B)** IgG subclass distribution, **(C)** IgM antibody levels were determined in sera and **(D)** anti-OMV IgA antibody levels in lung lysates. Results are expressed as fluorescence intensities (FI) of 4 mice per group per time point. **(E)** Specificity of serum IgG and pulmonary IgA elicited by P.M. and S.C. immunization as determined by 2DEWB. Analysis was performed using pooled serum and lung lysates of 4 mice per group. Fluorescence intensities for each spot were obtained from 1 blot for IgA and the average of 3 blots for IgG. * $p \leq 0.05$ versus naive mice (day 0); # $p \leq 0.05$ versus S.C. mice. **(F-G)** Numbers of **(F)** OMV-specific IgG- and IgA-secreting plasma cells in lungs, blood, and spleens and numbers of **(G)** IgG- and IgA-producing memory cells in spleens were determined by B-cell ELISpot of 6 mice per group at day 35 and day 56, respectively. Results are indicated as antibody secreting cells (ASC) per 5 x 10^5 cells. * $p \leq 0.05$ versus naive mice; # $p \leq 0.05$ versus S.C. mice.

Results

Superior protection against *B. pertussis* infection by P.M. compared to S.C. omvPV immunization

The colonization of the respiratory tract after intranasal *B. pertussis* challenge of pulmonary immunized mice (P.M. mice), subcutaneously immunized mice (S.C. mice), and non-immunized control mice (N.I. mice) differed substantially. Lungs, trachea, and noses of N.I. mice were heavily colonized by *B. pertussis* after a challenge. The highest numbers of colony forming units were found 7 days post challenge (p.c.) (**Figure 1B-D**). In contrast, *B. pertussis* was mostly cleared from lungs of P.M. mice already 2 days p.c., whereas bacteria from lungs of S.C. mice were cleared 5 days later (**Figure 1B**). In the trachea of both S.C. and P.M. mice, bacteria were mostly cleared 7 days p.c. (**Figure 1C**). In the nose, no complete clearance of *B. pertussis* was observed in the P.M., S.C., and N.I. mice within 28 days p.c. However, the number of bacteria in P.M. mice was significantly lower than in N.I. mice on day 70 (**Figure 1D**). Together, these data show that P.M. immunization with omvPV induced enhanced protection against *B. pertussis* infection compared to S.C. immunization.

IgG antibody responses

B. pertussis-specific antibodies are important contributors to pertussis immunity [34] and currently IgG serology still is the gold standard in pertussis vaccine research. The IgG (subclass) levels were determined after P.M. and S.C. immunization. Both immunization routes induced high and comparable levels of anti-OMV IgG antibodies in serum, but with significantly higher levels after P.M. immunization on day 56 (**Figure 2A**). S.C. immunization elicited already anti-Prn IgG antibodies after primary immunization, while these were observed only after a booster immunization in P.M. mice (**Figure S1A**).

The IgG subclasses distribution induced by P.M. and S.C. immunization were comparable for OMV-specific responses (**Figure 2B**). The primary immunization stimulated production of IgG1 antibodies, while the booster vaccination promoted the formation of IgG3 antibodies. For Prn-specific responses, booster P.M. immunization led to more IgG2a/b than S.C. immunization, while IgG1 still was the predominant subclass for both immunization routes (**Figure S1B**).

The immunogenic proteins to which the anti-OMV antibodies are directed were identified (**Figure 2E and Figure S3A-B**). On 2DEWB, twelve and seventeen immunogenic pertussis proteins were detected after P.M. and S.C. immunization, respectively (**Figure 2E and Table S1**). Spots showing high staining intensities in both groups corresponded with BP3755, Vag8, BrkA, and U2. Antibodies against ahcY, also visible at 55 kDa on 1DEWB (**Figure S3B**), and ompA(2) were solely induced by P.M. immunization, whereas antibody formation against ompA(1), U5, bfrG, GroEl, purH, U3, and U4 were only found after S.C. immunization. Additionally, anti-LPS antibodies (10 kDa) were observed after booster vaccination in both immunization groups (**Figure S3B**). Notably, following omvPV immunization via either route,

no IgG antibodies could be detected that were directed against Ptx, FHA, and Fim2/3 (data not shown), the antigens present in acellular pertussis vaccines in addition to Prn. Altogether, the systemic anti-OMV IgG response and subclass distribution after both P.M. and S.C. immunization were comparable and could not explain the increased protection of P.M. mice following challenge.

IgM antibody responses

Next, IgM antibodies were determined in sera from P.M. and S.C mice. IgM antibodies were only found directed against OMV and were induced significant on day 14 in P.M. mice. For both immunization routes, booster vaccination resulted in enhanced IgM antibody levels (**Figure 2C**). Similar to the findings for IgG, the level of anti-OMV IgM was significantly increased in P.M. versus S.C. immunized mice on day 56 (**Figure 2C**).

IgA antibody responses

IgA antibodies were found exclusively in P.M. mice, both in serum (**Figure S2A-B**) and lungs (**Figure 2D and S1D**). Serum IgA antibodies were directed against OMV and Prn, but not against other antigens present in acellular vaccines (**Figure S2A-E**). The specificity of pulmonary IgA was determined by immunoblotting and subsequent mass spectrometric identification of immunogenic proteins. The anti-OMV antibodies in the lungs were directed against Vag8 and LPS (**Figure 2E, S3A, and S3C**).

Pulmonary and systemic B-cell responses

The effect of the immunization route on the numbers of *B. pertussis*-specific plasma cells was investigated in cell suspensions from lungs, peripheral blood, and spleen. At the peak of the plasma cell response on day 35, anti-OMV and anti-Prn IgG-secreting cells were detected in the lungs of P.M. mice only (**Figure 2F and S1D**). However, in blood and spleen of S.C. and P.M. mice similar and modest numbers of IgG-secreting cells were found (**Figure 2F and S1D**). In addition, anti-OMV and anti-Prn IgA-secreting cells were detected in the lungs, spleen and blood, exclusively after P.M. immunization (**Figure 2F and S1D**).

Anti-OMV IgG-producing memory B-cells were measured in the spleen of P.M. and S.C. mice on day 56, with a trend towards higher numbers after P.M. immunization (**Figure 2G**). In contrast, anti-OMV IgA-producing memory B-cells could not be detected at all (**Figure 2G**). The Prn-specific memory B-cell responses on day 56 showed a similar trend as was found for the OMV-specific responses (**Figure S1G**). Thus, these data show that both S.C. and P.M. immunization elicited IgG-producing plasma and memory B-cells, while P.M. immunization also evoked IgA-producing plasma cells.

Pulmonary T-cell responses

Pulmonary *B. pertussis*-specific T-cell responses were investigated by analyzing cytokine

levels in the culture supernatants of lung cells that were restimulated with OMVs in vitro. Moderate IL-5 and vigorous IL-17A responses were detected after P.M. immunization only (Figure 3A). To investigate whether these cytokines were produced by $CD4^+$ T-cells, single cell analysis by ICS was performed on these cultured cells. Only P.M. immunization induced OMV-specific IL-17A-producing $CD4^+CD44^+$ T-cells in the lungs (Figure 3B). No OMV-specific IFNγ-producing and IL-5-producing $CD4^+CD44^+$ T-cells could be detected by ICS in the lungs of any of the immunized mice (data not shown).

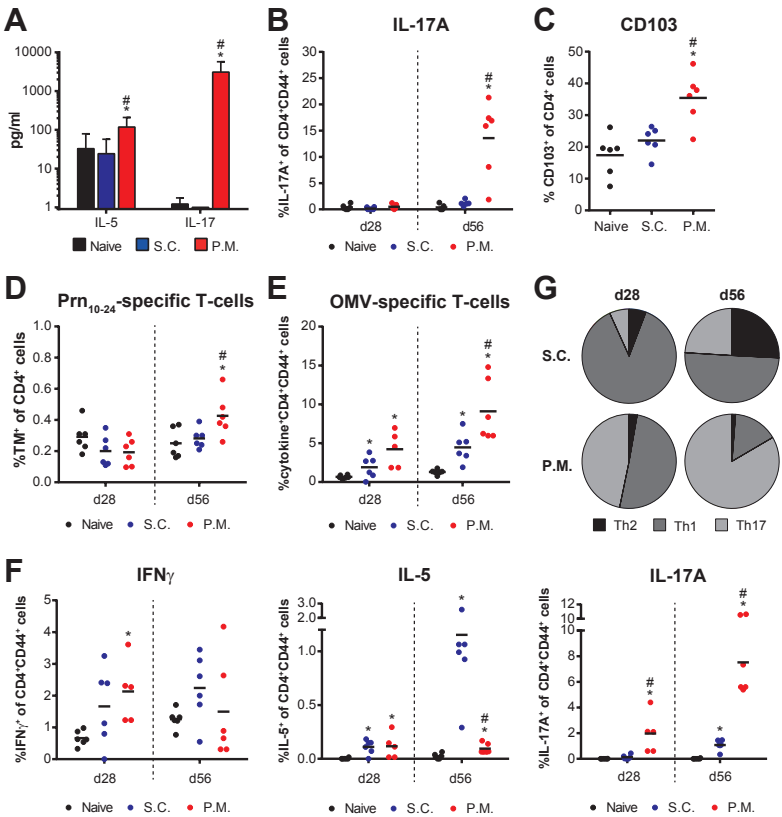

Figure 3 - Pulmonary and systemic *B. pertussis* OMV-specific T-cell responses induced by P.M. and S.C. omvPV immunization. **(A)** IL-5 and IL-17A levels in 3 day culture supernatant of lung cells, isolated on day 56, after *in vitro* stimulation with OMVs as determined by MIA. Results in pg/ml are corrected for the background level (IMDM complete medium control) and are given as mean ± SD of 6 mice per group. **(B)** Percentage of IL-17-producing $CD4^+CD44^+$ T-cells in the lungs, harvested on day 28 and day 56, as measured by ICS and flow cytometry after *in vitro* stimulation for 4 days with OMVs. **(C)** Flow cytometry for expression of CD103 on gated $CD4^+CD44^+$ T-cells in the lungs on day 56. **(D)** Frequency of Prn_{10-24}-specific $CD4^+$ T-cells in blood determined directly *ex vivo* on day 28 and day 56 using a tetramer staining and flow cytometry. **(E)** Magnitude of the systemic OMV-specific $CD4^+$ T-cell response after *in vitro* stimulation with OMV for 4 days was determined using ICS on splenocytes, calculated as the total percentage cytokine (IL-5, IFNγ, and IL-17A)-producing $CD4^+CD44^+$ T-cells. **(F)** Percentage IL-5-, IFNγ-, and IL-17-producing cells of $CD4^+CD44^+$ T-cells of spleens harvested on day 38 and day 56 and stimulated *in vitro* for 4 days with OMVs. Results of each analysis are given of 6 mice per group. **(G)** Distribution of Th subsets based on IL-5 (Th2), IFNγ (Th1), and IL-17A (Th17) production, as determined by ICS and flow cytometry. * $p \leq 0.05$ versus naive mice; # $p \leq 0.05$ versus S.C. mice.

Recently, it has been demonstrated that tissue-resident memory T-cells are important in the protection against respiratory pathogens [35]. Expression of CD103, a marker for tissue-resident memory T-cells, was determined on the OMV-specific IL-17A-producing $CD4^+CD44^+$ T-cells, which were solely detected in P.M. mice. Of these cells, 57 ± 24 percent expressed CD103 (data not shown). Moreover, an increased percentage of pulmonary $CD103^+CD4^+$ T-cells was detected in P.M. mice on day 56 compared to both S.C. and naive mice (**Figure 3C**). In conclusion, only P.M. immunization elicited pulmonary tissue-resident Th17 $CD4^+$ T-cells.

Magnitude of the systemic $CD4^+$ T-cell response

The magnitude of the Prn_{10-24}-specific $CD4^+$ T-cell response was determined *ex vivo* using tetramers specific for this immunodominant $I\text{-}A^d$ restricted T-cell epitope of Prn in BALB/c mice. No Prn_{10-24}-specific $CD4^+$ T-cells were detected in the dLN, bronchial and inguinal for P.M. and S.C. mice, respectively, on day 28 and day 56 (data not shown). However, Prn_{10-24}-specific $CD4^+$ T-cells were observed in blood of exclusively P.M. mice on day 56 (**Figure 3D**).

Furthermore, the magnitude of the $CD4^+$ T-cell response was investigated by determining the total percentage of *B. pertussis*-specific cytokine-producing (IFNγ, IL-5, or IL-17A) $CD4^+$ T-cells. Both P.M. and S.C. immunization induced a significant increase of OMV- and Prn-specific cytokine-producing $CD4^+CD44^+$ T-cells already on day 28 (**Figure 3E and S4B**). On day 56, a significantly higher percentage of these cells was detected after P.M. compared to S.C. immunization.

The effect of the immunization route on the Th-subset differentiation was determined. Analysis of cytokine levels in the culture supernatants of OMV-stimulated splenocytes revealed increased production of Th2 cytokine IL-4 and IL-5 after S.C. immunization, while the level of IL-13 was comparable after S.C. and P.M. immunization on day 28 and day 56 (**Figure S5A-B**). Stimulation of splenocytes with OMVs led to a high background production of Th1 cytokines IFNγ and TNFα of naive mice, possibly due to the presence of LPS in the OMVs (**Figure S5A-B**). Increased production of IFNγ by splenocytes from S.C. mice on day 28 and from P.M. on day 56 was still observed (**Figure S5A-B**). In addition, increased production of IL-17A and IL-10 was found by splenocytes of P.M. mice compared to S.C. mice on day 56. ICS analysis showed a significantly increased percentage of OMV-specific IFNγ-producing $CD4^+CD44^+$ T-cells after P.M. immunization on day 28 (**Figure 3F, left panel**). OMV-specific IL-5-producing $CD4^+CD44^+$ T-cells were detectable in P.M. and S.C. mice on day 28 and day 56. Notably, the percentage was significantly higher after S.C. immunization on day 56 (**Figure 3F, middle panel**). Significant OMV-specific IL-17A-producing $CD4^+CD44^+$ T-cells were induced after S.C. immunization on day 56. Notably, significantly higher percentages of these cells were detected after P.M. immunization at both day 28 and day 56 (**Figure 3F, right panel**). A similar trend for Prn-specific $CD4^+CD44^+$ T-cells were observed as the OMV-specific $CD4^+CD44^+$ T-cells (**Figure S4B**).

The distribution of OMV- and Prn-specific $CD4^+CD44^+$ T-cells, based on the production of

IFNγ, IL-5, or IL-17A, indicates that S.C. immunization induced systemically a Th1-dominated response on day 28 and a mixed Th1/Th17/Th2 response on day 56 (**Figure 3G and S4C**). In contrast, P.M. immunization induced a mixed Th1/Th17 response on day 28, which shifted towards a Th17-dominated response on day 56. In summary, more Th1/Th17-skewed $CD4^+$ T-cells were elicited by P.M. compared to S.C. immunization.

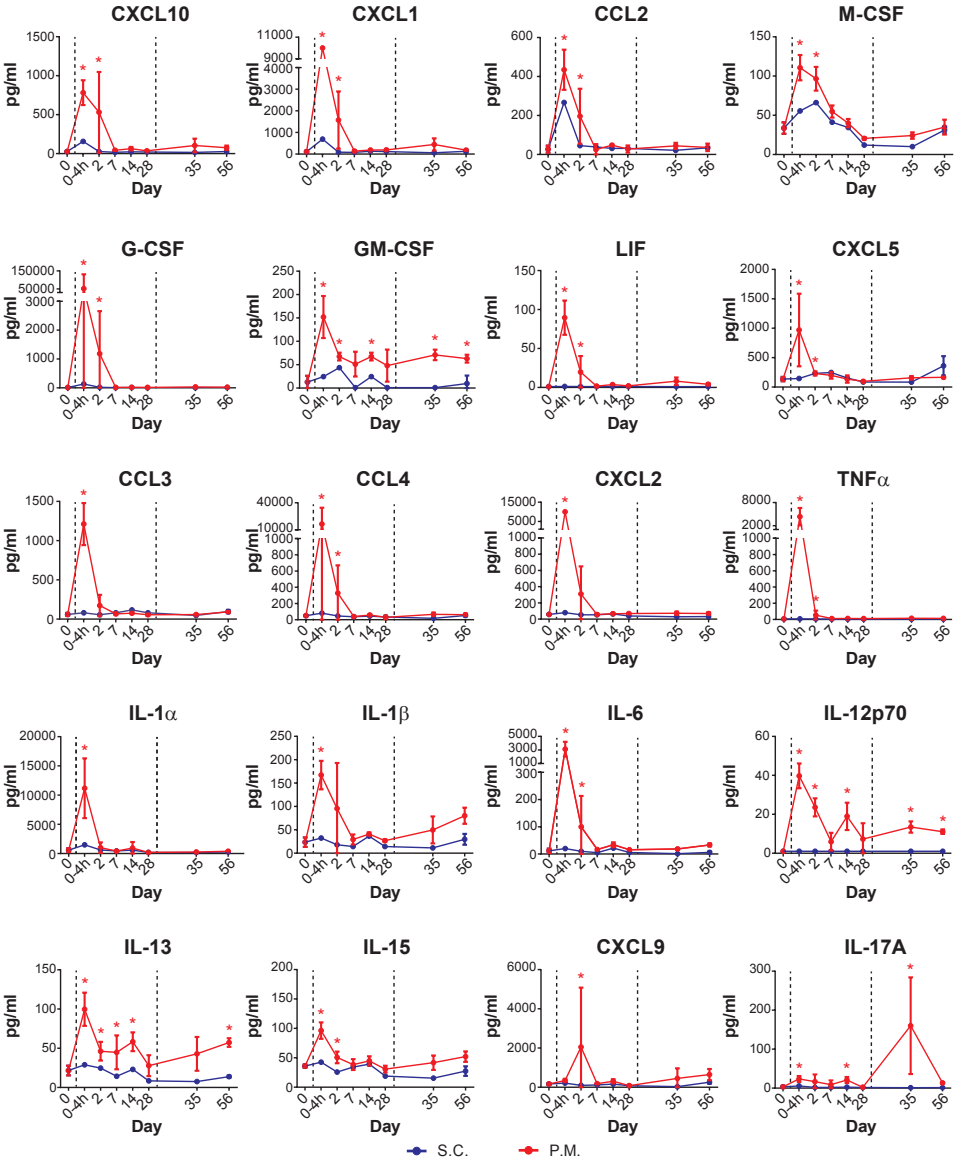

Figure 4 - Pulmonary cytokine responses after P.M. and S.C. omvPV immunization. The concentrations of cytokines in lung lysates of immunized mice were analyzed over time by using MIA. The cytokine concentrations were measured in the individual lung lysates of 4 mice per time point for P.M. mice and in a pool of the lung lysates of 4 mice per time point for S.C. mice.* $p \leq 0.05$ versus naive mice (day 0).

Cytokine profiles

The immunization-induced cytokine profile was determined in the lung lysates as well as serum. The largest differences were observed 4 hours post primary immunization (Figures 4 and 5). Concentrations of IL-6, IL-12p70, G-CSF, GM-CSF, IL-1α, IL-1β, IL-13, IL-15, LIF, CXCL5, CCL3, CCL4, CXCL2, CXCL10, CXCL1, CCL2, M-CSF, and TNFα were increased 4 hours post primary immunization in the lungs of P.M. mice. A trend towards increased levels of CXCL10, CXCL1, CCL2, and M-CSF was observed in the lungs of S.C. mice (Figure 4). At later time points, CXCL9 and IL-17A were found in P.M. mice on day 2 and day 35, respectively. In serum, increased levels of CXCL1, CCL4, TNFα, and IL-10 levels were found in both S.C. and P.M. mice (Figure 5A). In addition, higher levels of G-CSF, CXCL10, CCL2, CCL5, and IL-5 were detected after S.C. compared to P.M. immunization (Figure 5B), whereas the levels of IL-6 were higher in P.M mice (Figure 5C). Notably, CXCL1, CCL4, TNFα, G-CSF, CXCL10, CCL2, and IL-6 were found in both the lungs and sera of P.M. mice. Altogether, while S.C. induced only a systemic cytokine response, P.M. immunization induced a distinct systemic and pulmonary cytokine response.

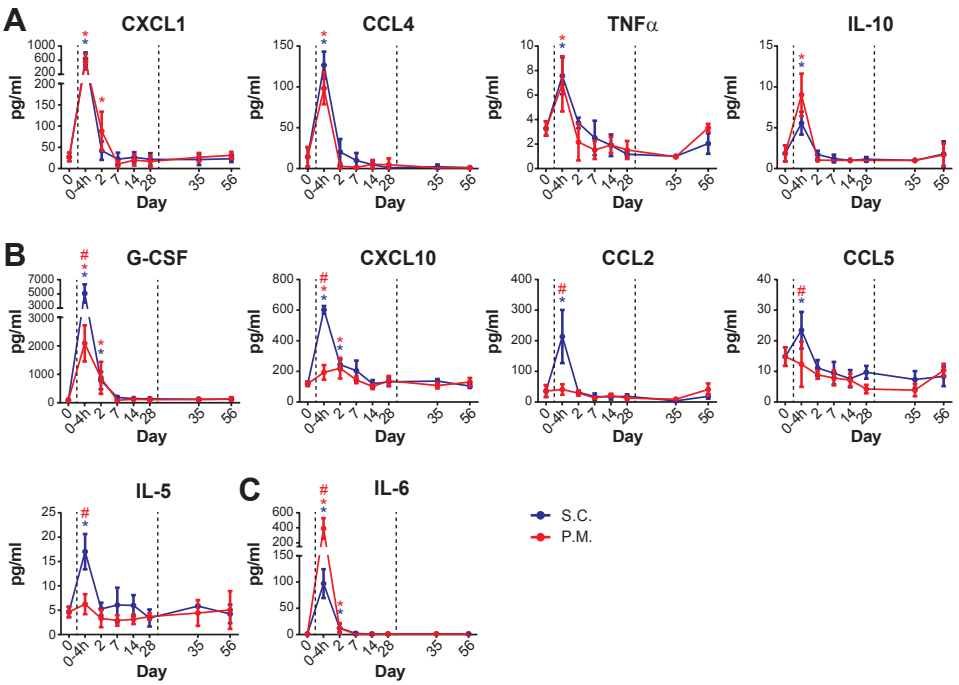

Figure 5 - Systemic cytokine responses after P.M. and S.C. omvPV immunization. The concentrations of cytokines in serum of immunized mice were analyzed over time by using MIA. **(A)** Cytokines with comparable levels in P.M. and S.C. mice. **(B)** Cytokines with elevated levels in S.C. compared to P.M. mice. **(C)** Cytokine with elevated level in P.M. compared to S.C. mice. Data is given as mean concentrations for 4 mice per group per time point. * $p \leq 0.05$ versus naive mice (day 0); # $p \leq 0.05$ versus S.C. mice.

Transcriptomic signatures in draining lymph nodes

Microarray analysis on bronchial and inguinal dLN from P.M. and S.C. mice, respectively, revealed 1921 genes that were differentially expressed (*p*-value ≤ 0.001, FR ≥ 1.5) over time compared to naive mice (**Figure 6A**). 951 genes were upregulated and 466 downregulated solely after P.M. immunization, 211 were upregulated and 145 were downregulated in both groups, and 109 were upregulated and 39 were downregulated exclusively after S.C. immunization. ORA using DAVID indicated enrichment of 141 GO-BP terms and KEGG pathways. A selection of these terms was sorted by the most significant enrichment and included Cell cycle, apoptosis, immune response, T-cell activation, and B-cell mediated immunity (**Figure 6B**). Cell cycle genes were mainly upregulated in P.M. mice. Innate signatures in the S.C. mice mainly involved genes downstream of IFN signaling (**Figure 6C**).

Genes related to T- and B-cells, based on gene ontology and text mining, are shown in **Figures 6D-E**. In total, 50 genes were related to T-cells of which many were associated with distinct Th subsets (**Figure 6D**). Upregulation of most genes occurred 4 hours after immunization and from day 7 onwards. More genes were upregulated in P.M. mice than in S.C. mice. The upregulated genes in P.M. mice included Th17-associated genes, such as the master regulator for Th17 differentiation (*Rorc*), *Hif1a*, and *Havcr1*. The few T-cell related genes exclusively expressed in S.C. mice comprised Th1- and Th17-associated genes, such as *Irf5, Ccr6,* and *Syt11*. Expression of B-cell related genes in S.C. mice mainly occurred on day 7 and day 35 (**Figure 6E**). In contrast, in P.M. mice elevated expression of B-cell related genes post primary immunization was detected earlier (4 hours) and persisted until day 28. Moreover, a smaller number of genes was induced on day 35 by booster immunization in P.M. compared to S.C. mice. Expression of *Mzb1, Ighm, Igkc, Ighg2b, Jchain, Ighg1,* and *Aicda* suggested antibody production and the presence of B-cells in dLN, which was more pronounced in P.M. mice. In addition, upregulation of specific B-cell membrane, activation, and homing markers were observed. Both immunization routes induced *Cxcr5, Cd22, Cd40,* and *Cd83* expression, while exclusively the S.C. route induced *Cd19, Cd72, Ccr6,* and *Siglecg* and exclusively the P.M. route induced *Cd38*.

In conclusion, P.M. and S.C. immunization with omvPV evoke distinct innate and adaptive responses in the dLN as detected on transcriptome level.

Figure 6 (Right) - Transcriptomic profiles in the draining lymph nodes following P.M. and S.C. omvPV immunization. **(A-E)** Gene expression in P.M. and S.C. mice was compared to naive mice (day 0) (FR ≥ 1.5, *p*-value ≤ 0.001). **(A)** 1921 genes upregulated (red) or downregulated (green) are visualized in heatmaps (mean of n = 3). Genes not surpassing a fold change of 1.5 are shown as basal level (black). The overlap (yellow) and the exclusive presence of genes in either the P.M. (blue) or S.C. (orange) immunization groups is depicted next to the heatmap. **(B)** Over-representation analysis on all 1921 genes revealed the involvement of specific GO-BP terms with corresponding total amount of genes (blue), upregulated (red) and downregulated (green) genes. **(C)** The 47 genes exclusively found upregulated during the innate response of the S.C. mice were shown in a heatmap (left panel) and the genes were compared to the Interferome database to determine involvement of the Type I IFN (IFNα and IFNβ) and/or Type II IFN (IFNγ) signaling pathway (right panel). **(D)** T-cell related genes, including association with distinct Th subsets, are depicted for P.M. and S.C. mice. **(E)** B-cell related genes are depicted for P.M. and S.C. mice.

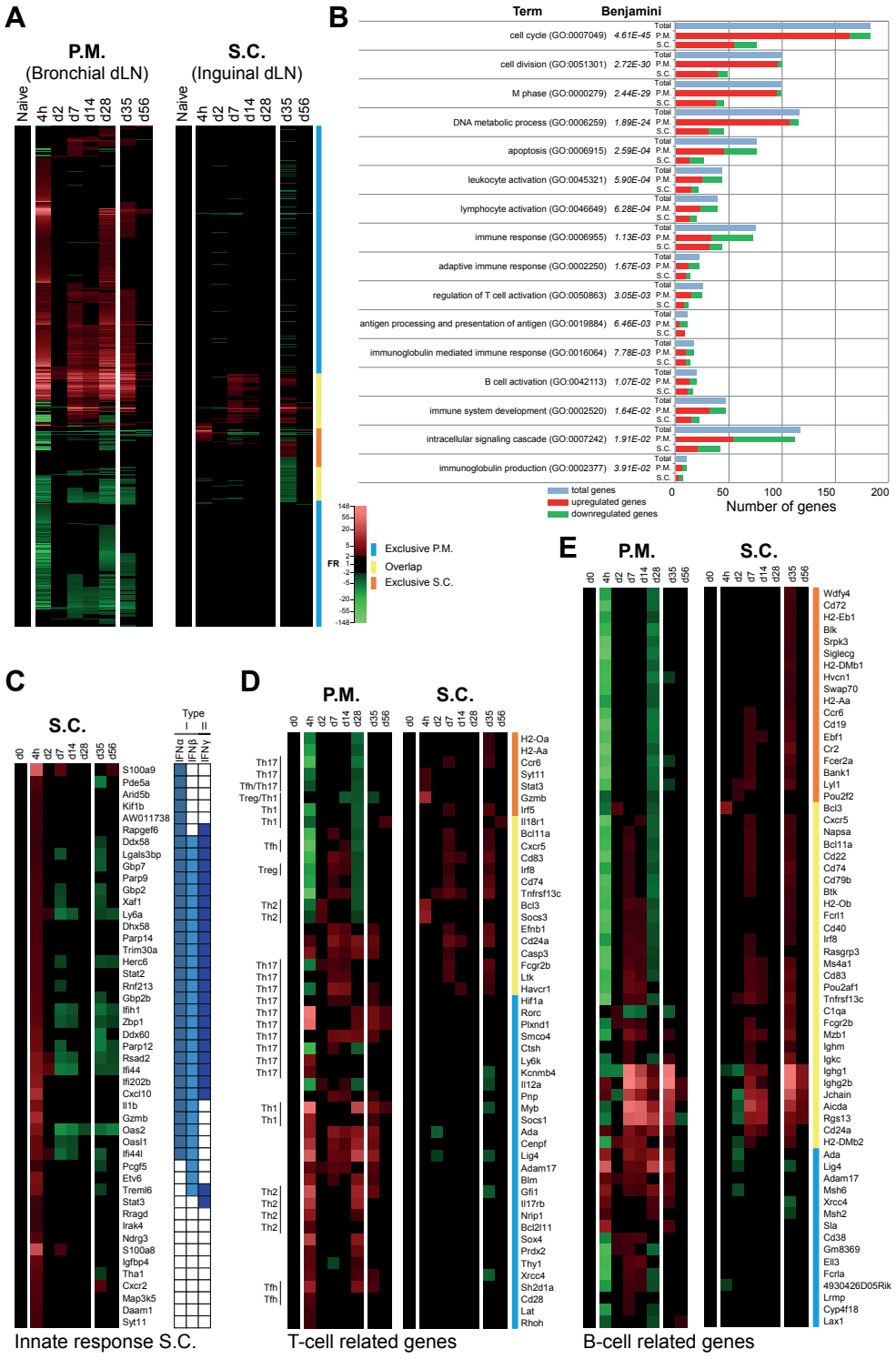
A
P.M.
(Bronchial dLN)
S.C.
(Inguinal dLN)
Naive
4h
d2
d7
d14
d28
d35
d56
B
Term
Benjamini
cell cycle (GO:0007049) 4.61E-45
cell division (GO:0051301) 2.72E-30
M phase (GO:0000279) 2.44E-29
DNA metabolic process (GO:0006259) 1.89E-24
apoptosis (GO:0006915) 2.59E-04
leukocyte activation (GO:0045321) 5.90E-04
lymphocyte activation (GO:0046649) 6.28E-04
immune response (GO:0006955) 1.13E-03
adaptive immune response (GO:0002250) 1.67E-03
regulation of T cell activation (GO:0050863) 3.05E-03
antigen processing and presentation of antigen (GO:0019884) 6.46E-03
immunoglobulin mediated immune response (GO:0016064) 7.78E-03
B cell activation (GO:0042113) 1.07E-02
immune system development (GO:0002520) 1.64E-02
intracellular signaling cascade (GO:0007242) 1.91E-02
immunoglobulin production (GO:0002377) 3.91E-02
Total
P.M.
S.C.
total genes
upregulated genes
downregulated genes
Number of genes
FR
Exclusive P.M.
Overlap
Exclusive S.C.
C
S.C.
Type
I
II
IFNα
IFNβ
IFNγ
Innate response S.C.
D
P.M.
S.C.
Th17
Tfh/Th17
Treg/Th1
Th1
Tfh
Treg
Th2
H2-Oa
H2-Aa
Ccr6
Syt11
Stat3
Gzmb
Irf5
Il18r1
Bcl11a
Cxcr5
Cd83
Irf8
Cd74
Tnfrsf13c
Bcl3
Socs3
Efnb1
Cd24a
Casp3
Fcgr2b
Ltk
Havcr1
Hif1a
Rorc
Plxnd1
Smco4
Ctsh
Ly6k
Kcnmb4
Il12a
Pnp
Myb
Socs1
Ada
Cenpf
Lig4
Adam17
Blm
Gfi1
Il17rb
Nrip1
Bcl2l11
Sox4
Prdx2
Thy1
Xrcc4
Sh2d1a
Cd28
Lat
Rhoh
T-cell related genes
E
P.M.
S.C.
Wdfy4
Cd72
H2-Eb1
Blk
Srpk3
Siglecg
H2-DMb1
Hvcn1
Swap70
H2-Aa
Ccr6
Cd19
Ebf1
Cr2
Fcer2a
Bank1
Lyl1
Pou2f2
Bcl3
Cxcr5
Napsa
Bcl11a
Cd22
Cd74
Cd79b
Btk
H2-Ob
Fcrl1
Cd40
Irf8
Rasgrp3
Ms4a1
Cd83
Pou2af1
Tnfrsf13c
C1qa
Fcgr2b
Mzb1
Ighm
Igkc
Ighg1
Ighg2b
Jchain
Aicda
Rgs13
Cd24a
H2-DMb2
Ada
Lig4
Adam17
Msh6
Xrcc4
Msh2
Sla
Cd38
Gm8369
Ell3
Fcrla
4930426D05Rik
Lrmp
Cyp4f18
Lax1
B-cell related genes

Pulmonary transcriptomic signatures

Microarray analysis was performed on lung tissue collected during the primary immunization and comprised 691 genes that were differentially expressed (*p*-value ≤ 0.01, FR ≥ 2.0) over time compared to naive mice (**Figure 7A**). The largest dissimilarity was observed 4 hours after P.M. immunization as revealed by a principal component analysis (PCA) (**Figure 7B**). Many of these genes were no longer expressed on day 2 and later, while upregulation of other genes was observed (**Figure 7A**), as was also observed in the direction of variance in the PCA (**Figure 7B**). The pulmonary gene expression on day 28 did not return completely to basal levels. Notably, also differential gene expression was observed mainly on day 2 in the lungs of S.C. mice (**Figure 7A-B**). ORA (Benjamini < 0.05) on the 691 genes revealed enrichment of 127 terms (11 KEGG Pathways, 116 GO-BP terms). A selection is shown in **Figure 7C**. Genes involved in pathogen recognition reflected by expression of PRR genes and members of corresponding downstream signaling pathways (inflammasome, TNF, NFκB, and MAPK) and effector molecules (e.g. pro-inflammatory responses) (**Figure 7C and S6A**). Moreover, genes involved in innate lymphoid cells (ILCs), CSF-signaling, T-cell activation, humoral response, and genes encoding complement, cytokines, cytokine receptors, and membrane markers were upregulated (**Figure 7C and S6B**).

The transcriptomic signatures obtained after P.M. immunization in the lungs (691 genes) were compared to the dataset of gene expression profiles (558 genes) discovered in the lungs of mice after experimental *B. pertussis* infection in a previous study [7]. In total, 98 genes were found in both datasets. A gene-function network analysis investigating the involvement of genes in modules PRR-signaling, acute phase, cytokine response, humoral response, and T-cell responses, showed differences between both datasets (**Figure 7D**). Notably, the infection dataset comprised more genes related to the modules acute phase and humoral response, whereas the P.M. immunization dataset included more genes related to cytokine response and PRR-signaling. Only a few shared genes (27 genes) were directly connected to the investigated modules. However, by using the STRING database many shared genes

Figure 7 (Right) - Pulmonary transcriptomic profiles following P.M. and S.C. omvPV immunization. **(A-C)** Gene expression was compared to naive mice (day 0) (FR ≥ 2.0, *p*-value ≤ 0.01). **(A)** 691 genes upregulated (red) or downregulated (green) are visualized in heatmaps (mean of n = 3 for P.M. mice and n = 1 (pool of 3 mice) for S.C. mice). Genes not surpassing a fold change of 2.0 are shown as basal level (black). **(B)** Principal component analysis (PC1 and PC2) shows the (dis)similarity of the five time points for both P.M. and S.C. mice. **(C)** ORA on 691 genes uncovered the involvement of specific GO-BP terms and KEGG pathways with corresponding total amount of genes (blue), upregulated (red) and downregulated (green) genes. **(D-E)** Pulmonary transcriptomes were compared after P.M. immunization and a *B. pertussis* infection [7]. **(D)** A gene-function network analysis showing the connection of genes, expressed within 28 days after P.M. immunization or infection, to a specific module (blue line) based on involvement in acute phase, cytokine response, humoral response, pathogen recognition receptor (PRR) signaling, and T-cell responses. Genes that were expressed in both datasets (shared, triangle, purple), exclusively expressed in infected mice (circle, green), or exclusively expressed in P.M. mice (circle, red) are depicted. Additional, indirect linkage of shared genes with other genes in the network (grey line) by using the STRING database are shown. **(E)** For infected mice (9 time points) and P.M. mice (6 time points) an average fold ratio (FR) (expressed as LN-transformed numbers) was calculated to determine the expression intensity and kinetics for each module corresponding to those included in the network analysis.

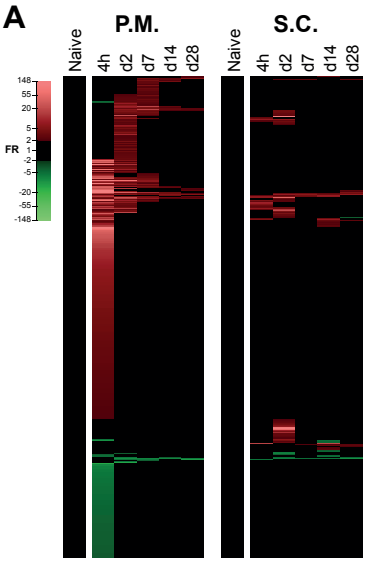
A
P.M.
S.C.
Naive
4h
d2
d7
d14
d28
FR
148
55
20
5
2
1
-2
-5
-20
-55
-148

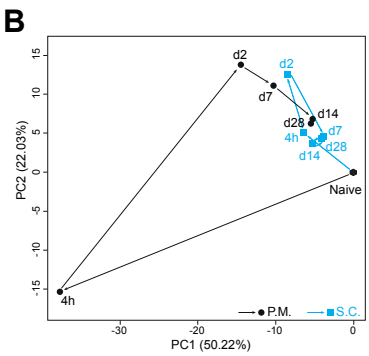
B
PC2 (22.03%)
PC1 (50.22%)
d2
d7
d14
d28
4h
Naive
P.M.
S.C.

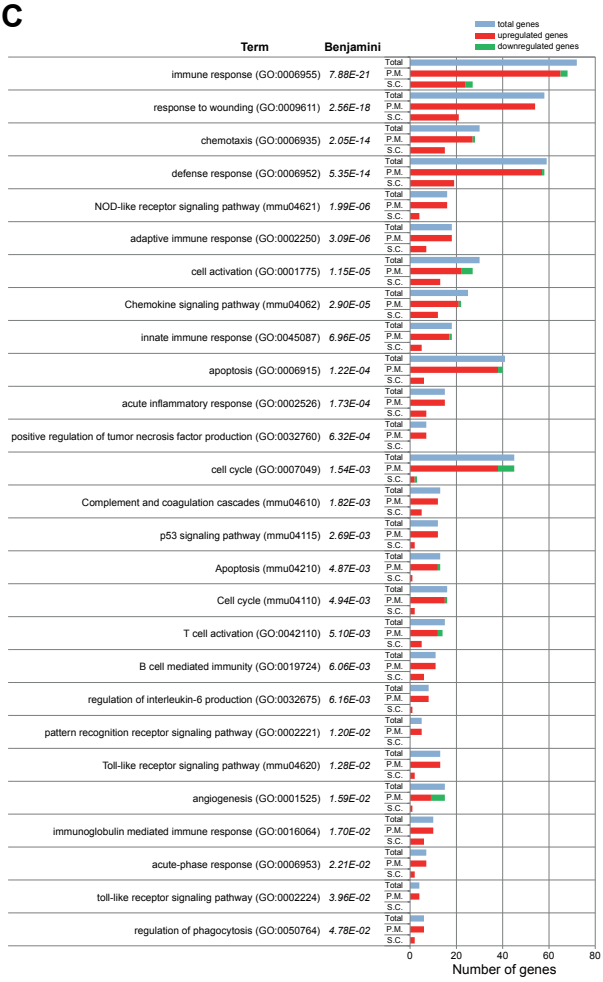
C
total genes
upregulated genes
downregulated genes
Term
Benjamini
immune response (GO:0006955) 7.88E-21
response to wounding (GO:0009611) 2.56E-18
chemotaxis (GO:0006935) 2.05E-14
defense response (GO:0006952) 5.35E-14
NOD-like receptor signaling pathway (mmu04621) 1.99E-06
adaptive immune response (GO:0002250) 3.09E-06
cell activation (GO:0001775) 1.15E-05
Chemokine signaling pathway (mmu04062) 2.90E-05
innate immune response (GO:0045087) 6.96E-05
apoptosis (GO:0006915) 1.22E-04
acute inflammatory response (GO:0002526) 1.73E-04
positive regulation of tumor necrosis factor production (GO:0032760) 6.32E-04
cell cycle (GO:0007049) 1.54E-03
Complement and coagulation cascades (mmu04610) 1.82E-03
p53 signaling pathway (mmu04115) 2.69E-03
Apoptosis (mmu04210) 4.87E-03
Cell cycle (mmu04110) 4.94E-03
T cell activation (GO:0042110) 5.10E-03
B cell mediated immunity (GO:0019724) 6.06E-03
regulation of interleukin-6 production (GO:0032675) 6.16E-03
pattern recognition receptor signaling pathway (GO:0002221) 1.20E-02
Toll-like receptor signaling pathway (mmu04620) 1.28E-02
angiogenesis (GO:0001525) 1.59E-02
immunoglobulin mediated immune response (GO:0016064) 1.70E-02
acute-phase response (GO:0006953) 2.21E-02
toll-like receptor signaling pathway (GO:0002224) 3.96E-02
regulation of phagocytosis (GO:0050764) 4.78E-02
Total
P.M.
S.C.
0
20
40
60
80
Number of genes

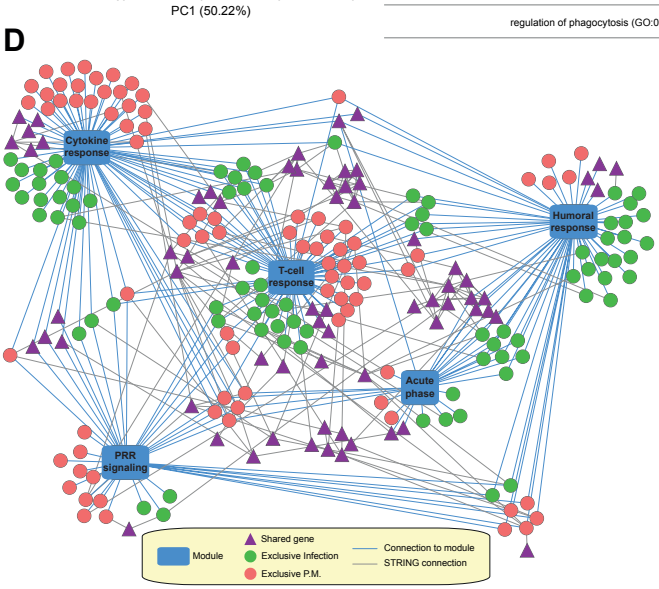
D
Cytokine response
T-cell response
Humoral response
Acute phase
PRR signaling
Module
Shared gene
Exclusive Infection
Exclusive P.M.
Connection to module
STRING connection

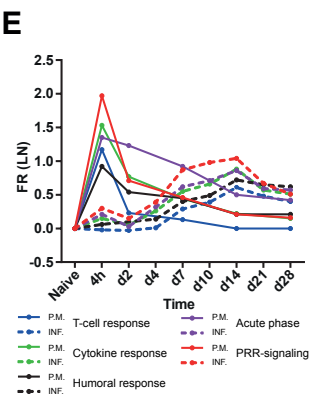
E
FR (LN)
2.5
2.0
1.5
1.0
0.5
0.0
-0.5
Naive
4h
d2
d4
d7
d10
d14
d21
d28
Time
P.M.
INF.
T-cell response
Acute phase
Cytokine response
PRR-signaling
Humoral response

(42 genes) could be indirectly linked to the modules by their interaction with other genes in the network. A comparison of intensity and kinetics of the average gene expression of each module revealed that P.M. immunization induced faster and more intense expression of all modules than infection (**Figure 7E**). In conclusion, both P.M. immunization and *B. pertussis* infection induced genes involved in PRR-signaling, acute phase, cytokine response, humoral response, and T-cell responses, yet with different intensity and kinetics. Moreover, the genes included in these modules are distinct for P.M. immunization and infection.

In vivo recall response after *B. pertussis* challenge

After unraveling the immune status of both of P.M. and S.C. mice on day 56, we determined the recall responses after an intranasal *B. pertussis* challenge. The serum anti-OMV IgG levels decreased after the challenge in P.M. and S.C. mice (**Figure 8A**). The challenge of non-immunized (N.I.) mice developed anti-OMV IgG and IgM, but the IgG levels remained lower compared to immunized mice (**Figure 8A**). For anti-Prn IgG levels a similar trend was observed after challenge (**Figure S1A**). However, no anti-Prn IgM was detected in any of the mice (data not shown). Further, no detectable levels of IgG and IgM to Ptx, FHA, or Fim2/3 were observed (data not shown). The challenge did not substantially alter the IgG subclass distribution of the anti-OMV and anti-Prn serum IgG response in P.M. and S.C. mice, present on day 56 (**Figure 2B and S1B**), since the IgG1 subclass remained dominant in both groups on day 84 (**Figure 8B and S1B**). However, a distinct distribution was found in challenged N.I. mice, since the IgG2b subclass response was more prominent in this group (**Figure 8B and S1B**). Enhanced serum IgA antibodies specific for OMV, Prn, and Fim2/3 were present in all challenged mice, whereas serum anti-Ptx and anti-FHA IgA were absent (**Figure S2A-E**). The pulmonary anti-OMV IgA antibody levels in P.M. mice remained high after the challenge, while in S.C. and N.I. mice these antibodies could only be detected on days 70 and day 84 (**Figure**

Figure 8 (Right) - *In vivo* recall response after *B. pertussis* challenge of P.M., S.C. and N.I. mice. **(A)** Serum anti-OMV IgG antibodies (left panel), IgM antibodies (middle panel), and pulmonary anti-OMV IgA antibodies (right panel) determined in time after *B. pertussis* challenge on day 56 using MIA. Results are expressed as fluorescence intensities (FI) of 4 mice per group per time point. * $p \leq 0.05$ versus levels on day 56; # $p \leq 0.05$ versus S.C. mice; + $p \leq 0.05$ versus N.I. mice. **(B)** Distribution of the anti-OMV IgG subclasses on day 84. **(C-D)** Numbers of OMV-specific IgG- and IgA-secreting plasma cells **(C)** and memory cells **(D)** in spleens on day 84, as determined by B-cell ELISpot of 6 mice per group. **(E)** Cytokine levels in 3 day culture supernatant of lung cells, isolated on day 84, after *in vitro* stimulation with OMVs, as determined by MIA. Results in pg/ml are corrected for the background level (IMDM complete medium control) and are given as mean ± SD of 6 mice per group. **(F)** Percentage of IL-17-producing $CD4^+CD44^+$ T-cells in the lungs, harvested on day 84, as measured by ICS and flow cytometry after *in vitro* stimulation for 4 days with OMVs. **(G)** Magnitude of the systemic OMV-specific $CD4^+$ T-cell response on day 84 after *in vitro* stimulation with OMV for 4 days, as determined by ICS on splenocytes and calculated as the total percentage cytokine (IL-5, IFNγ, and IL-17A)-producing $CD4^+CD44^+$ T-cells. **(H)** Distribution of Th subsets based on IL-5 (Th2), IFNγ (Th1), and IL-17A (Th17) production on day 84, as determined by using ICS and flow cytometry. * $p \leq 0.05$ versus naive mice; # $p \leq 0.05$ versus S.C. mice; + $p \leq 0.05$ versus N.I. mice. **(I)** The characteristics of the adaptive immune response obtained by primary (day 28) and booster (day 56) P.M. omvPV immunization in comparison to primary *B. pertussis* infection on day 28 and 56 are summarized. ‡ Obtained from a previous study [36]. N.D. = not determined.

8A). The same trend was observed for pulmonary anti-Prn IgA levels (Figure S1C). In addition, no pulmonary anti-Ptx and anti-FHA IgA antibodies were detected after challenge (data not shown), while pulmonary anti-Fim2/3 IgA antibodies were found in S.C. and N.I. mice on day 84 (Figure S2F). Anti-OMV IgA antibodies were only detected in nose lavages of P.M. mice 4 hours after challenge, which were most likely induced by the earlier immunization (Figure S7A). These nasal IgA antibodies were directed against Vag8 (Figure S3D) and Prn (Figure

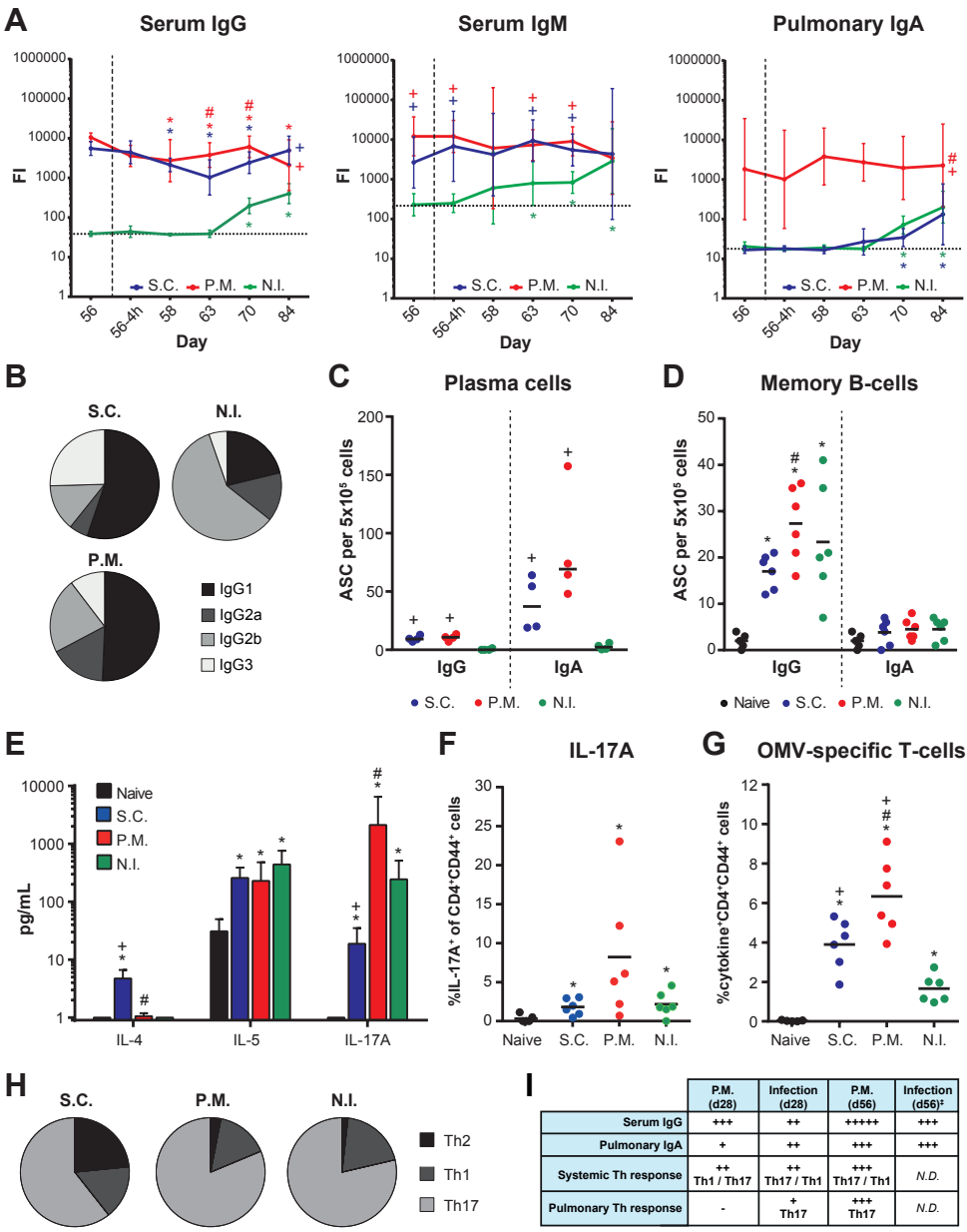

I

	P.M. (d28)	Infection (d28)	P.M. (d56)	Infection (d56)‡
Serum IgG	+++	++	+++++	+++
Pulmonary IgA	+	++	+++	+++
Systemic Th response	++ Th1 / Th17	++ Th17 / Th1	+++ Th17 / Th1	*N.D.*
Pulmonary Th response	-	+ Th17	+++ Th17	*N.D.*

S7B). The challenge led to enhanced anti-OMV IgA antibodies in all groups on day 84 (Figure S7A). In addition to higher anti-Vag8 IgA levels, the challenge induced anti-LPS antibodies in the P.M. and S.C. mice, but not in the N.I. control mice (Figure S3D). Furthermore, nasal anti-Prn, -Ptx, and -FHA IgA levels were significantly increased in S.C. mice following challenge (Figure S7B-D). Significantly higher anti-Fim2/3 IgA antibody concentrations were detected in N.I. mice on day 84 as compared to 4 hours after challenge, with the same trend in both immunized groups, but not significant (Figure S7E).

The numbers of anti-OMV IgG- and IgA-secreting plasma cells in the spleen of S.C. and P.M. mice were comparable and significantly higher than the numbers in N.I. mice on day 63 (Figure 8C). Furthermore, high numbers of anti-OMV IgG-producing memory B-cells were present in the spleen of P.M., S.C., and N.I. mice compared to the numbers in naive mice (Figure 8D). Moreover, higher numbers were induced by P.M. than S.C. immunization. In contrast, even after challenge, anti-OMV IgA-producing memory B-cells were not detected in any of the groups (Figure 8D). The Prn-specific antibody-secreting cells and memory B-cell responses showed a similar trend as found for the OMV-specific responses, except that no Prn-specific IgG-producing memory B-cells could be detected in challenged N.I. mice (Figure S1F-G).
Investigation of the culture supernatants of OMV-stimulated cells from the lungs showed IL-4 production solely by cells from S.C. mice (Figure 8E). In contrast, lung cells from all three challenged groups produced IL-5 and IL-17A, although IL-17A secretion by P.M. mice was significantly increased as compared to S.C. and N.I. mice (Figure 8E). However, a trend towards a higher percentage of OMV-specific IL-17A-producing $CD4^+CD44^+$ T-cells was observed in the lungs after challenge in P.M. compared to S.C. or N.I. mice (Figure 8F). Similar results were found after Prn stimulation, except that IL-17A-producing $CD4^+CD44^+$ T-cells were not detectable in N.I. mice (Figure S4C). OMV- and Prn-specific IFNγ- and IL-5-producing $CD4^+CD44^+$ T-cells were absent in the lungs of all challenged groups (data not shown). Systemic T-cell responses, as detected by ICS, showed a higher magnitude, as calculated by the total percentage of *B. pertussis*-specific cytokine-producing (IFNγ, IL-5, or IL-17A) splenic $CD4^+$ T-cells, in P.M. compared to S.C. and N.I. mice (Figure 8G). Moreover, distinct Th subset distributions were observed in S.C. and P.M. mice after challenge (Figure 8H). In S.C. mice, the pre-challenge Th response (Figure 3F) underwent a shift towards a Th17 response at the expense of the Th1 response. Notably, the Th2 component remained responsible for a quarter of the Th response. In P.M. mice, the Th response was not altered after challenge with little or no Th2 component (Figure 8H).

The systemic and local adaptive immune responses after a primary (day 28) and booster (day 56) P.M. immunization were schematically summarized and compared with those induced by a primary *B. pertussis* infection on day 28, obtained in this study, and day 56, obtained in our previous study [36]. The comparison demonstrated that the adaptive immune responses

were comparable after P.M. omvPV immunization and a *B. pertussis* infection (**Figure 8I**). Notably, there were however quantitative differences as the systemic IgG levels were higher after P.M. immunization compared to infection while pulmonary IgA levels were enhanced upon infection on day 28.

Collectively, the data of the *in vivo* recall responses indicate that the systemic and local memory B- and T-cell responses after P.M. versus S.C. omvPV-immunized mice were different in function and magnitude. The systemic ratio of the Th subsets and the IgA response induced by P.M. immunization was reminiscent of the response after primary *B. pertussis* infection.

Discussion

Pulmonary immunization induces local immunity important for protection as was demonstrated for several respiratory pathogens [11-13]. In this study, the immune responses evoked by pulmonary and subcutaneous immunization of an omvPV were compared in detail. Pulmonary immunization provided superior protection against *B. pertussis* challenge over the subcutaneous route. A systems biology approach revealed innate and adaptive immune signatures associated with this superior protection. The pulmonary gene expression and cytokine profiles exclusively evoked by P.M. immunization revealed omvPV recognition by PRRs, induction of pro-inflammatory and IL-17 effector cytokines, and IgA responses. Furthermore, in dLNs of S.C. mice, genes downstream of IFN signaling were expressed, while in dLNs of both P.M. and S.C. mice genes involved in the production of IgG were expressed. Moreover, based on gene expression, Th17-cells were detected in the dLNs of P.M. mice. The systemic cytokines, however, most were higher after S.C. immunization. Although both P.M. and S.C. immunization induced strong systemic adaptive immune response, P.M. immunization evoked higher IgM levels, IgG levels, and CD4+ T-cell responses. Moreover, the induced Th subsets differed, since P.M. immunization led to a mixed Th1/Th17, yet Th17 dominated, response, whereas S.C. immunization led to a mixed Th1/Th2/Th17 response. More importantly, P.M. immunization elicited a robust mucosal adaptive immune response as indicated by the presence of IgA antibodies, IgA- and IgG-producing plasma cells, and Th17 differentiated $CD4^+$ T-cells in the lungs of mice.

An overview of the main findings is presented in **Figure 9** and discussed in detail hereafter. During the innate phase, expression of genes associated with pathogen recognition and the PRR downstream-signaling cascade were detected in the lungs of P.M. mice, which included TLRs, MyD88, NFκB, and pro-inflammatory cytokines (**Figure 9A**). This demonstrates that the omvPV is sensed in the lung by TLR4, based on the expression of *Lbp* and *Cd14*, and by TLR2 on innate cells, which is similar to the recognition of wPV and whole bacteria [37-39]. Interestingly, also enhanced expression of *Tlr7* and *Nlrp3* was observed indicating activation of intracellular PRRs by omvPV. The expression of pro-inflammatory cytokines, such as *Il1b*, *Il6*, and *Cxcl10*, was also detected in the lungs on protein level. Multiple known IL-17 effector cytokines [8, 40] were measured in the lungs of P.M. mice, including CXCL1, CXCL2, CCL2, G-CSF, GM-CSF, and TNFα. These IL-17 effector cytokines facilitate, together with IL-1β and IL-6, a Th17-differentiating environment. This was reflected by the presence of Th17 cells in the dLN, based on expression of *Rorc*, *Hif1a*, and *Havcr1*. Moreover, Th17 cells were detected in the spleen and more importantly in the lungs on single cell level, suggesting induction of both systemic and tissue-resident cells. In addition, the presence of CCL3, CCL4, CXCL10, and IL-12p70 in the lungs promotes differentiation towards Th1 cells [41, 42]. Indeed Th1 differentiation was promoted, since Th1 cells were detected systemically on single cell level. A Th1/Th17 response is favorable for providing protection against *B. pertussis* infection [5, 7,

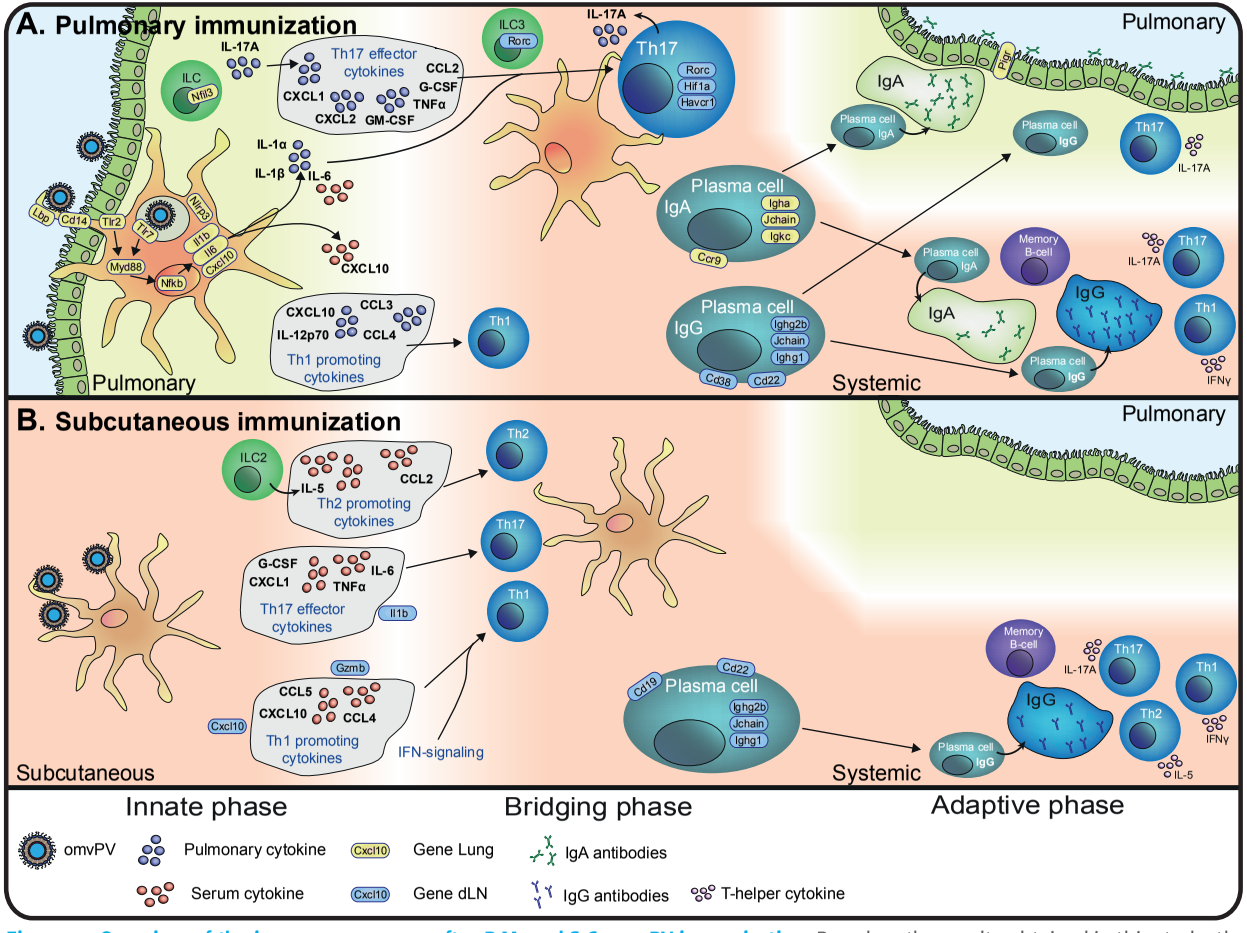

Figure 9 - Overview of the immune responses after P.M. and S.C. omvPV immunization. Based on the results obtained in this study, the main findings of the innate and adaptive immune responses were connected for **(A)** P.M. immunization and **(B)** S.C. immunization.

8] and additionally, the presence of tissue-resident T-cells in the lungs might even enhance protection [35]. The humoral response after P.M. immunization was characterized by pulmonary expression of IgA-related genes and the IgA transporter (*Pigr*) and the subsequent IgA presence in lungs and serum. In line with these findings, IgA-producing plasma cells were detected in spleen, blood, and lungs. Homing of these cells to the lungs may be enabled by CCR9, in our dataset found on gene expression level, which expression on IgA-producing memory B-cells is a mucosal homing marker. Furthermore, high serum IgG levels in P.M. mice corresponded with specific gene expression (*Ighg1, Igh2b,* and *Jchain*) of IgG-producing plasma cells in the dLN, and with detected IgG-producing plasma cells on single cell level in spleen, blood, and lungs. In addition, IgG-producing memory B-cells were detected in spleens of P.M. mice. Interestingly, pulmonary expression of *Nfil3* and early expression of *Rorc* in the dLN suggest involvement of ILCs in the immune response upon P.M. immunization. *Nfil3* is an ILC marker and *Rorc* is expressed by the ILC3 subset [43].

After S.C. immunization, omvPV is most likely sensed in a similar manner as after P.M. immunization, mainly by TLR2 and TLR4, although this was not investigated at the injection site in this study. The strong systemic cytokine response demonstrated a Th1- (CCL4, CCL5, and CXCL10), Th2- (IL-5 and CCL2), and Th17-differentiating (CXCL1, G-CSF, IL-6, and TNFα) environment, which was later reflected by presence of splenic Th1, Th2, and Th17 cells on single cell level (**Figure 9B**). Moreover, the induction of Th1 cells was linked to the early expression of genes downstream of IFN signaling found in the dLN [44]. The source of the early IL-5 production might be ILC2s [43], suggesting the involvement of these cells after S.C. omvPV immunization. Furthermore, the expression of B-cell markers (*Cd19* and *Cd22*) in addition to immunoglobulin-related genes (*Igh2b, Jchain,* and *Ighg1*) revealed the presence of IgG-producing plasma cells in the dLNs. Subsequently, IgG-producing plasma cells were detected on single cell level in spleen and blood. Additionally, S.C. omvPV immunization led to IgG-producing memory B-cells in the spleen and high serum IgG levels.

Based on the IgA responses, three interesting observations were revealed. First, full clearance of *B. pertussis* from the nose was not achieved despite the presence of anti-Vag8 IgA antibodies in the nose lavage in P.M. mice. This suggests that under the conditions used in our study with respect to vaccine and challenge dose, anti-Vag8 IgA induction in the nose alone may not be sufficient for prevention of nasal *B. pertussis* colonization. Second, 28 days after *B. pertussis* challenge, nasal anti-LPS IgA antibodies were detected in P.M. and S.C. mice, but not in non-immunized (N.I.) mice. Also, a lack of OMV-specific IgA-secreting plasma cells in N.I. mice after challenge was observed. Because no IgA response was detectable before challenge in S.C. mice, it was expected that challenge of S.C. and N.I. mice would evoke a similar IgA response. This faster induction of IgA responses in S.C. compared to N.I. mice may indicate the presence of low numbers of LPS-specific IgA-producing memory B-cells in S.C. mice stimulated upon a challenge. Third, large numbers of IgA-secreting plasma cells were present in the spleen 7 days post P.M. booster vaccination (day 35). However, IgA-producing

memory B-cells were non-detectable on day 56. Nonetheless, the recall of memory B-cells in response to infection led to a rapid increase in numbers of IgA-secreting plasma cells in the spleen (day 63). This suggests that IgA-producing memory B-cells may not reside in the spleen but elsewhere, presumably as tissue-resident IgA-producing memory B-cells in the mucosa [45]. Since IgA responses may contribute to protection against *B. pertussis* infection, these different aspects of the IgA responses require further investigation.

The immunity induced by P.M. immunization with an omvPV substantially resembles the infection-induced immunity, still considered as benchmark for optimal immunity. Interestingly, P.M. immunization with omvPV confers sterilizing immunity to a similar extent as is observed for infection-induced immunity in mice and baboons [5, 7, 8]. After both P.M. immunization and *B. pertussis* infection, a strong IgG response is induced. Furthermore, circulating and pulmonary IgA-producing B-cells were detected after P.M. immunization, leading to the production of mucosal IgA. This IgA was mainly directed against Vag8 as was observed after a challenge of mice with *B. pertussis* [36]. Moreover, both after P.M. immunization and *B. pertussis* infection, the $CD4^+$ T-cell responses, pulmonary and systemically, are Th17 dominated [5, 7, 8, 36].

Remarkably, there were also differences between P.M. immunization and infection-induced immunity. Serum IgG responses were already higher after primary P.M. immunization compared to *B. pertussis* infection on day 28. Moreover, increased IgG levels were found after booster immunization compared to the levels observed 56 days after infection [36]. Moreover, the omvPV vaccination in general evoked a distinct IgG subclass response compared to infection, which was partly caused by high anti-LPS IgG3 induction after the booster vaccination. IgG subclass distribution is thought to be indirect evidence for Th responses [46-48]. In our study the Th responses are not mirrored in the IgG subclass responses, since the Th responses are comparable after P.M. immunization and infection, while the IgG subclass distribution is distinct. Given that both S.C. and P.M. administration of omvPV result in an equal IgG subclass response, suggests that the differences compared to infection are probably caused by the vaccine composition and vaccination scheme rather than administration route. Furthermore, this study and our previous study [9] demonstrate that the antigen specificity of the serum IgG induced by P.M. immunization differs from infection, most likely due to distinct antigen composition. Whereas omvPV contains only outer-membrane and periplasmic proteins, live bacteria are comprised of additional cytosolic proteins and are capable of *de novo* production and secretion of antigens, such as Ptx [9]. Pulmonary IgA levels on day 28 induced by infection were higher compared to primary P.M. immunization. Booster P.M. immunization equalized the IgA levels with those after infection on day 56 [36].

Furthermore, with respect to cytokine profiles, P.M. immunization leads to faster and more intense pulmonary and serum cytokine production as compared to infection. However, higher

cytokine levels were expected during *B. pertussis* infection because of a prolonged antigen exposure [7] and a higher antigen dose compared to P.M. immunization with non-replicating omvPV. Weaker cytokine responses upon an infection might be explained by the immune evasion strategies of *B. pertussis* [49], such as dampening of host cytokine responses [50]. Extensive comparison of early pulmonary transcriptomic profiles induced by P.M. vaccination obtained from this study and those induced by *B. pertussis* infection [7] demonstrated that although both responses included genes involved in acute phase, PRR-signaling, cytokine responses, humoral response and T-cell responses, these responses comprised distinct genes. Moreover, P.M. immunization leads to faster and more intense pulmonary gene expression, which is in line with the cytokine profiles.
Together, the comparison of omvPV-induced immunity through P.M. administration and infection-induced immunity revealed overall comparability, notwithstanding some distinct innate responses.

Another advantage of pulmonary immunization, besides the induction of mucosal immune responses resembling that induced by *B. pertussis* infection, is that P.M. vaccine administration is needle-free. Currently, no pulmonary vaccines are licensed and only a few mucosal vaccines have been approved for human use. These include nasal vaccine against influenza virus and oral vaccines against poliovirus, rotavirus, *Salmonella typhi*, and *Vibrio cholerae* [51]. Pulmonary vaccine administration in humans is in early clinical development. Both powder inhalers [52] and fluid, nebulized vaccines are clinically tested, the latter in infants of 9 months of age [53]. Nasal vaccine administration might also be an option and may be suitable for infants. Intranasal immunization with an omvPV is also feasible since it provides protection against *B. pertussis* infection [14]. In addition, nasal immunization has been shown to result in IgA antibodies not only in the nasal cavity, but also lower in the respiratory tract [51, 54]. However, in depth analysis of the immune response induced by nasal immunization route in the context of pertussis is required.

In conclusion, this study showed that an omvPV can elicit superior local and systemic immunity against *B. pertussis* infection, with a similar type of adaptive immune response as induced by infection, by administering the vaccine pulmonary instead of subcutaneously. Therefore, pulmonary immunization may be key to the development of novel candidate pertussis vaccines. Further, in addition to serology, the gold standard in pertussis research, a systems biology approach is invaluable in order to unravel and understand the immunological signatures underlying the vaccine-induced immunity. In turn, this facilitates a rational choice for a vaccine candidate and route of administration, mitigating the risk of failure in the late-stage of development.

Acknowledgments

We are thankful to Tim Bindels and the employees of the Animal Research Centre (ARC) from Intravacc, Bilthoven, The Netherlands for respectively the production of the omvPV and performance of the animal experiments. We are grateful to Dale Long and Rick Willis of the NIH Tetramer Facility of Atlanta, Georgia, USA, for supplying the tetramers. We acknowledge the Microarray Department (MAD) of the University of Amsterdam, The Netherlands, for the performance of the microarray analyses.

References

1. Rumbo, M. and D. Hozbor, Development of improved pertussis vaccine. Hum Vaccin Immunother, 2014. 10(8): p. 2450-3.
2. Brummelman, J., *et al.*, Roads to the development of improved pertussis vaccines paved by immunology. Pathog Dis, 2015. 73(8): p. ftv067.
3. Mascart, F., *et al.*, Modulation of the infant immune responses by the first pertussis vaccine administrations. Vaccine, 2007. 25(2): p. 391-8.
4. Vermeulen, F., *et al.*, Cellular immune responses of preterm infants after vaccination with whole-cell or acellular pertussis vaccines. Clin Vaccine Immunol, 2010. 17(2): p. 258-62.
5. Ross, P.J., *et al.*, Relative contribution of Th1 and Th17 cells in adaptive immunity to *Bordetella pertussis*: towards the rational design of an improved acellular pertussis vaccine. PLoS Pathog, 2013. 9(4): p. e1003264.
6. Brummelman, J., *et al.*, Modulation of the CD4(+) T cell response after acellular pertussis vaccination in the presence of TLR4 ligation. Vaccine, 2015. 33(12): p. 1483-91.
7. Raeven, R.H.M., *et al.*, Molecular Signatures of the Evolving Immune Response in Mice following a *Bordetella pertussis* Infection. PLoS One, 2014. 9(8): p. e104548.
8. Warfel, J.M. and T.J. Merkel, *Bordetella pertussis* infection induces a mucosal IL-17 response and long-lived Th17 and Th1 immune memory cells in nonhuman primates. Mucosal Immunol, 2013. 6(4): p. 787-96.
9. Raeven, R.H.M., *et al.*, Immunoproteomic Profiling of *Bordetella pertussis* Outer Membrane Vesicle Vaccine Reveals Broad and Balanced Humoral Immunogenicity. J Proteome Res, 2015. 14(7): p. 2929-42.
10. Raeven, R.H.M., *et al.*, *Bordetella pertussis* outer membrane vesicle vaccine confers equal efficacy in mice with a lower inflammatory response compared to a classic whole-cell vaccine. Manuscript subitted.
11. Aguilo, N., *et al.*, Pulmonary but not subcutaneous vaccination confers protection to TB susceptible mice by an IL17-dependent mechanism. J Infect Dis, 2015.
12. Liu, H., *et al.*, Evaluation of mucosal and systemic immune responses elicited by GPI-0100- adjuvanted influenza vaccine delivered by different immunization strategies. PLoS One, 2013. 8(7): p. e69649.
13. Wang, J., *et al.*, Single mucosal, but not parenteral, immunization with recombinant adenoviral-based vaccine provides potent protection from pulmonary tuberculosis. J Immunol, 2004. 173(10): p. 6357-65.
14. Roberts, R., *et al.*, Outer membrane vesicles as acellular vaccine against pertussis. Vaccine, 2008. 26(36): p. 4639-46.
15. Asensio, C.J., *et al.*, Outer membrane vesicles obtained from *Bordetella pertussis* Tohama expressing the lipid A deacylase PagL as a novel acellular vaccine candidate. Vaccine, 2011. 29(8): p. 1649-56.
16. Asokanathan, C., M. Corbel, and D. Xing, A CpG-containing oligodeoxynucleotide adjuvant for acellular pertussis vaccine improves the protective response against *Bordetella pertussis*. Hum Vaccin Immunother, 2013. 9(2): p. 325-31.
17. Mielcarek, N., *et al.*, Live attenuated *B. pertussis* as a single-dose nasal vaccine against whooping cough. PLoS Pathog, 2006. 2(7): p. e65.
18. Querec, T.D., *et al.*, Systems biology approach predicts immunogenicity of the yellow fever vaccine in humans. Nat Immunol, 2009. 10(1): p. 116-25.
19. Furman, D., *et al.*, Apoptosis and other immune biomarkers predict influenza vaccine responsiveness. Mol Syst Biol, 2013. 9: p. 659.
20. Li, S., *et al.*, Molecular signatures of antibody responses derived from a systems biology study of five human vaccines. 2014. 15(2): p. 195-204.
21. Nakaya, H.I., *et al.*, Systems biology of vaccination for seasonal influenza in humans. Nat Immunol, 2011. 12(8): p. 786-95.
22. Lindqvist, M., *et al.*, Unraveling molecular signatures of immunostimulatory adjuvants in the female genital tract through systems biology. PLoS One, 2011. 6(6): p. e20448.
23. Brandes, M., *et al.*, A systems analysis identifies a feedforward inflammatory circuit leading to lethal influenza infection. Cell, 2013. 154(1): p. 197-212.
24. Sloots, A., *et al.*, Abolished pertactin cleavage enhances the immunogenicity and potency of a novel *B. pertussis* outer membrane vesicle vaccine: A proof of principle. Manuscript in preparation.
25. Thalen, M., *et al.*, Rational medium design for *Bordetella pertussis*: basic metabolism. J Biotechnol, 1999. 75(2-3): p. 147-59.
26. Bivas-Benita, M., *et al.*, Non-invasive pulmonary aerosol delivery in mice by the endotracheal route. Eur J Pharm Biopharm, 2005. 61(3): p. 214-8.
27. Stenger, R.M., *et al.*, Fast, antigen-saving multiplex immunoassay to determine levels and avidity of mouse serum antibodies to pertussis, diphtheria, and tetanus antigens. Clin Vaccine Immunol, 2011. 18(4): p. 595-603.
28. Stenger, R.M., *et al.*, Immunodominance in mouse and human CD4+ T-cell responses specific for the *Bordetella pertussis* virulence factor P.69 pertactin. Infect Immun, 2009. 77(2): p. 896-903.
29. Eijssen, L.M., *et al.*, User-friendly solutions for microarray quality control and pre-processing on ArrayAnalysis.org. Nucleic Acids Res, 2013. 41(Web Server issue): p. W71-6.
30. Bolstad, B.M., *et al.*, A comparison of normalization methods for high density oligonucleotide array data based on variance and bias. Bioinformatics, 2003. 19(2): p. 185-93.
31. Dai, M., *et al.*, Evolving gene/transcript definitions significantly alter the interpretation of GeneChip data. Nucleic Acids Res, 2005. 33(20): p. e175.
32. Huang da, W., B.T. Sherman, and R.A. Lempicki, Systematic and integrative analysis of large gene lists using DAVID bioinformatics resources. Nat Protoc, 2009. 4(1): p. 44-57.
33. Samarajiwa, S.A., *et al.*, INTERFEROME: the database of interferon regulated genes. Nucleic Acids Res, 2009. 37(Database issue): p. D852-7.
34. Plotkin, S.A., Complex correlates of protection after vaccination. Clin Infect Dis, 2013. 56(10): p. 1458-65.

35. Turner, D.L. and D.L. Farber, Mucosal resident memory CD4 T cells in protection and immunopathology. Front Immunol, 2014. 5: p. 331.
36. Raeven, R.H.M., *et al.*, Immunological signatures after *Bordetella pertussis* infection demonstrate importance of pulmonary innate immune cells. Manuscript subitted.
37. Brummelman, J., *et al.*, *Bordetella pertussis* naturally occurring isolates with altered lipooligosaccharide structure fail to fully mature human dendritic cells. Infect Immun, 2015. 83(1): p. 227-38.
38. Banus, S., *et al.*, The role of Toll-like receptor-4 in pertussis vaccine-induced immunity. BMC Immunol, 2008. 9: p. 21.
39. Higgins, S.C., *et al.*, TLR4 mediates vaccine-induced protective cellular immunity to *Bordetella pertussis*: role of IL-17-producing T cells. J Immunol, 2006. 177(11): p. 7980-9.
40. Tsai, H.C., *et al.*, IL-17A and Th17 cells in lung inflammation: an update on the role of Th17 cell differentiation and IL-17R signaling in host defense against infection. Clin Dev Immunol, 2013. 2013: p. 267971.
41. Rot, A. and U.H. von Andrian, Chemokines in innate and adaptive host defense: basic chemokinese grammar for immune cells. Annu Rev Immunol, 2004. 22: p. 891-928.
42. Christie, D. and J. Zhu, Transcriptional regulatory networks for CD4 T cell differentiation. Curr Top Microbiol Immunol, 2014. 381: p. 125-72.
43. Zhong, C. and J. Zhu, Transcriptional Regulatory Network for the Development of Innate Lymphoid Cells. Mediators Inflamm, 2015. 2015: p. 264502.
44. Huber, J.P. and J.D. Farrar, Regulation of effector and memory T-cell functions by type I interferon. Immunology, 2011. 132(4): p. 466-74.
45. Lamm, M.E. and J.M. Phillips-Quagliata, Origin and homing of intestinal IgA antibody-secreting cells. J Exp Med, 2002. 195(2): p. F5-8.
46. Mitsdoerffer, M., *et al.*, Proinflammatory T helper type 17 cells are effective B-cell helpers. Proc Natl Acad Sci U S A, 2010. 107(32): p. 14292-7.
47. Stevens, T.L., *et al.*, Regulation of antibody isotype secretion by subsets of antigen-specific helper T cells. Nature, 1988. 334(6179): p. 255-8.
48. Germann, T., *et al.*, Interleukin-12 profoundly up-regulates the synthesis of antigen-specific complement-fixing IgG2a, IgG2b and IgG3 antibody subclasses in vivo. Eur J Immunol, 1995. 25(3): p. 823-9.
49. de Gouw, D., *et al.*, Pertussis: a matter of immune modulation. FEMS Microbiol Rev, 2011. 35(3): p. 441-74.
50. Andreasen, C. and N.H. Carbonetti, Pertussis toxin inhibits early chemokine production to delay neutrophil recruitment in response to *Bordetella pertussis* respiratory tract infection in mice. Infect Immun, 2008. 76(11): p. 5139-48.
51. Holmgren, J. and C. Czerkinsky, Mucosal immunity and vaccines. Nat Med, 2005. 11(4 Suppl): p. S45-53.
52. Cape, S., *et al.*, Safety and immunogenicity of dry powder measles vaccine administered by inhalation: a randomized controlled Phase I clinical trial. Vaccine, 2014. 32(50): p. 6791-7.
53. Wong-Chew, R.M., *et al.*, Immunogenicity of aerosol measles vaccine given as the primary measles immunization to nine-month-old Mexican children. Vaccine, 2006. 24(5): p. 683-90.
54. Bergquist, C., *et al.*, Local and systemic antibody responses to dextran-cholera toxin B subunit conjugates. Infect Immun, 1995. 63(5): p. 2021-5.

Supplementary information

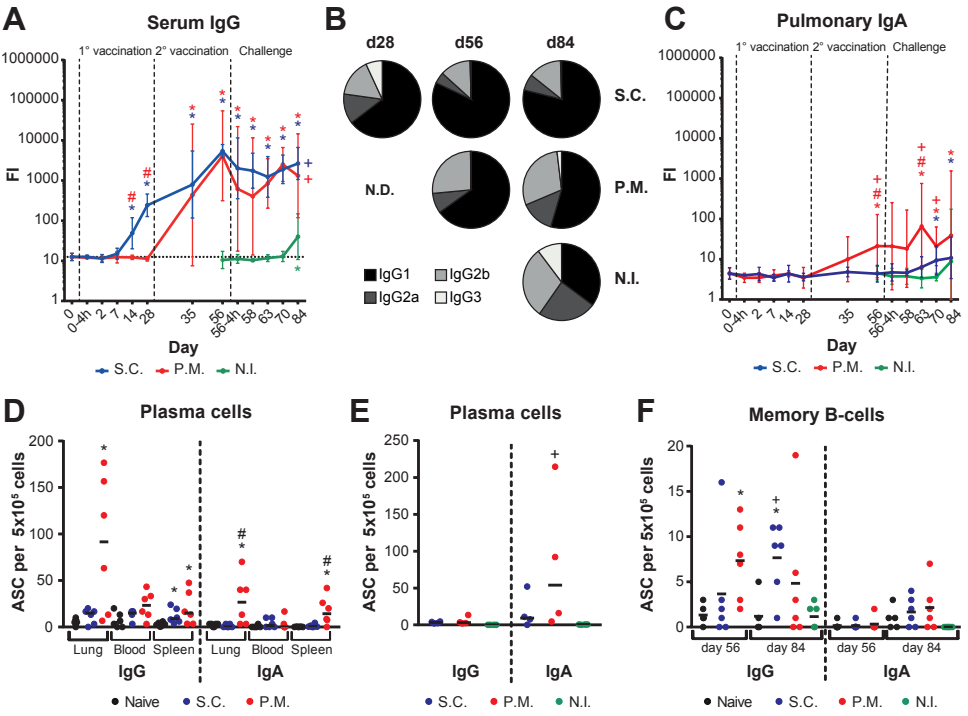

Figure S1 - Prn-specific B-cell responses induced by P.M. and S.C. omvPV immunization. **(A-C)** Serum anti-Prn IgG antibodies **(A)**, IgG subclass distribution **(B)**, and pulmonary anti-Prn IgA antibodies **(C)** were determined in immunized mice using MIA. Results are expressed as fluorescence intensities (FI) of 4 mice per group per time point. * $p \leq 0.05$ versus naive mice (day 0); # $p \leq 0.05$ versus S.C. mice; + $p \leq 0.05$ versus N.I. mice. **(D-E)** Numbers of Prn-specific IgG- and IgA-secreting plasma cells (n = 6) in **(D)** lungs, blood, and spleens on day 35 and in **(E)** spleens (n = 4) on day 63. **(F)** Numbers of Prn-specific IgG- and IgA-producing memory cells were determined in spleens (n = 6) on day 56 and 84. *$p \leq 0.05$ versus naive mice; # $p \leq 0.05$ versus S.C. mice; +$p \leq 0.05$ versus N.I. mice. N.D = not detected.

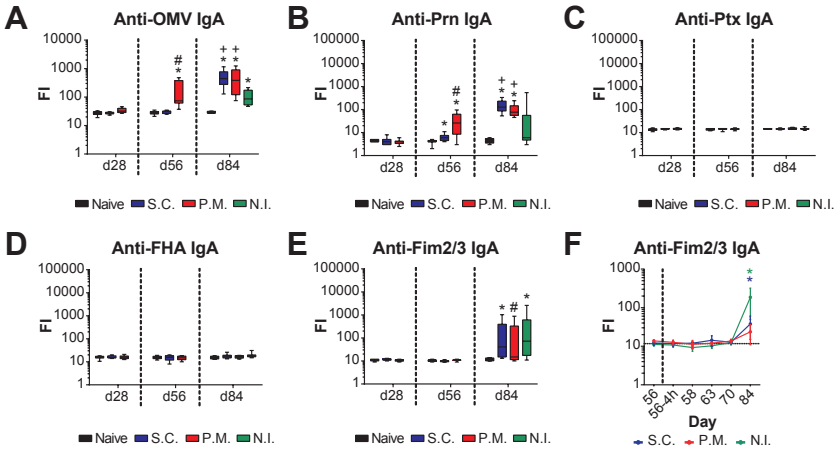

Figure S2 - Serum IgA levels against OMV, Prn, Ptx, FHA and Fim2/3 and pulmonary anti-Fim2/3 IgA induced by P.M. and S.C. omvPV immunization. **(A-E)** The levels of IgA antibodies directed against **(A)** OMV, **(B)** Prn, **(C)** Ptx, **(D)** FHA, and **(E)** Fim2/3 were determined in serum on day 28 and day 56 (vaccine-induced) and on day 84 (infection-induced) in naive, S.C., P.M., and N.I. mice. * $p \leq 0.05$ versus naive mice; # $p \leq 0.05$ versus S.C. mice; + $p \leq 0.05$ versus N.I. mice. **(F)** The levels of pulmonary anti-Fim2/3 IgA following challenge were determined in S.C., P.M. and N.I. mice. Results are expressed as fluorescence intensities (FI) of 4 mice per group per time point. * $p \leq 0.05$ versus levels day 56.

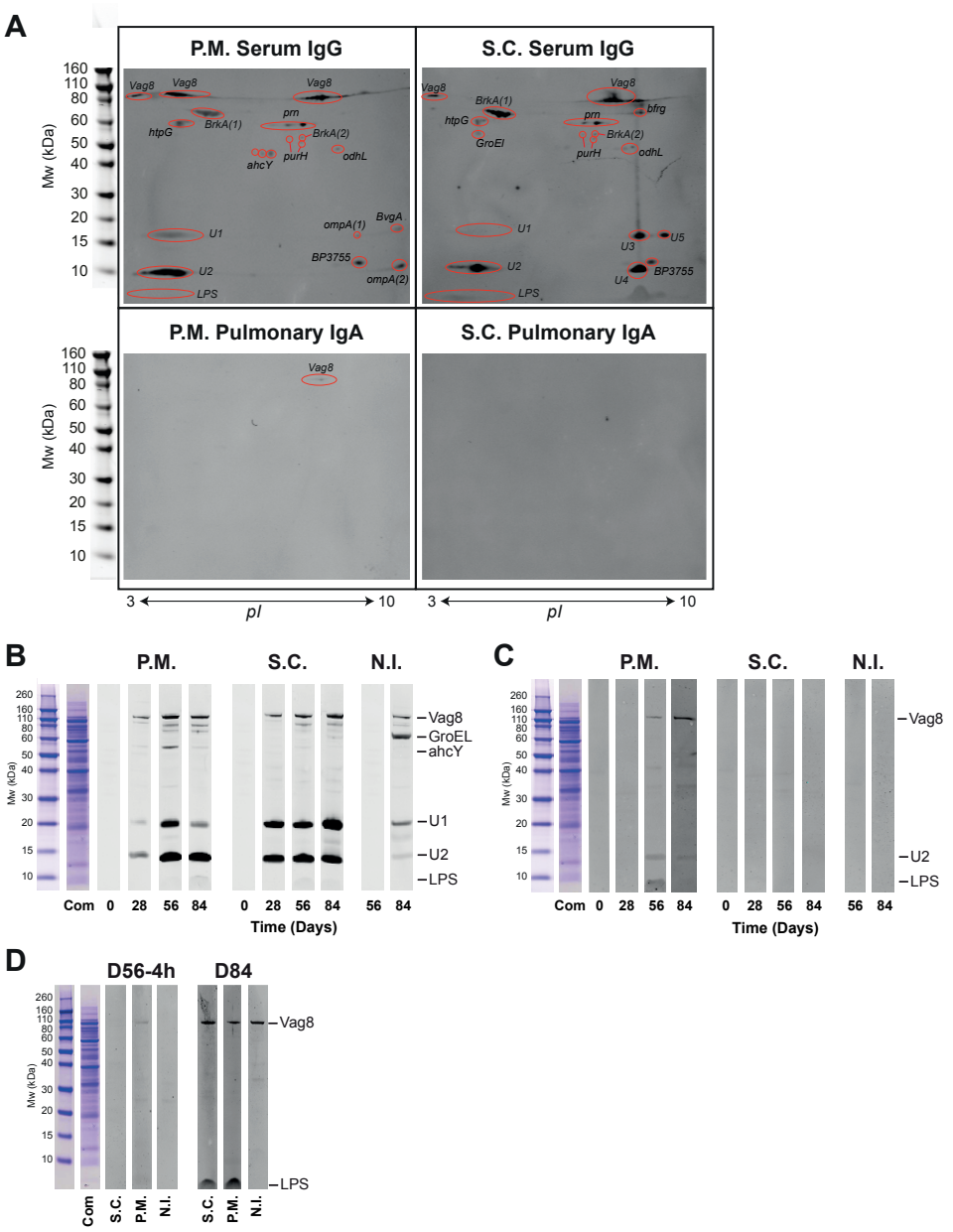

Figure S3 - Specificity of antibodies induced by P.M. and S.C. omvPV immunization. **(A)** Specificity of IgG and IgA in respectively serum and lung lysates of S.C. and P.M. mice on day 56 was determined using 2DEWB. Figure represents one blot for each condition. Individual spots with corresponding protein ID, as determined by LC-MS, are depicted. **(B-D)** Antibody specific as determined by 1DEWB for serum IgG **(B)** and pulmonary IgA **(C)** on day 28, 56, and 84 and nasal IgA **(D)** 4 hours and 28 days (day 84) after challenge. Identification of bands representing GroEL, LPS, Vag8, ahcY, and two unidentified antigens (U1-2) are shown. As a control a Coomassie staining (Com) was performed on the 1DE gel to stain the *B. pertussis* proteins.

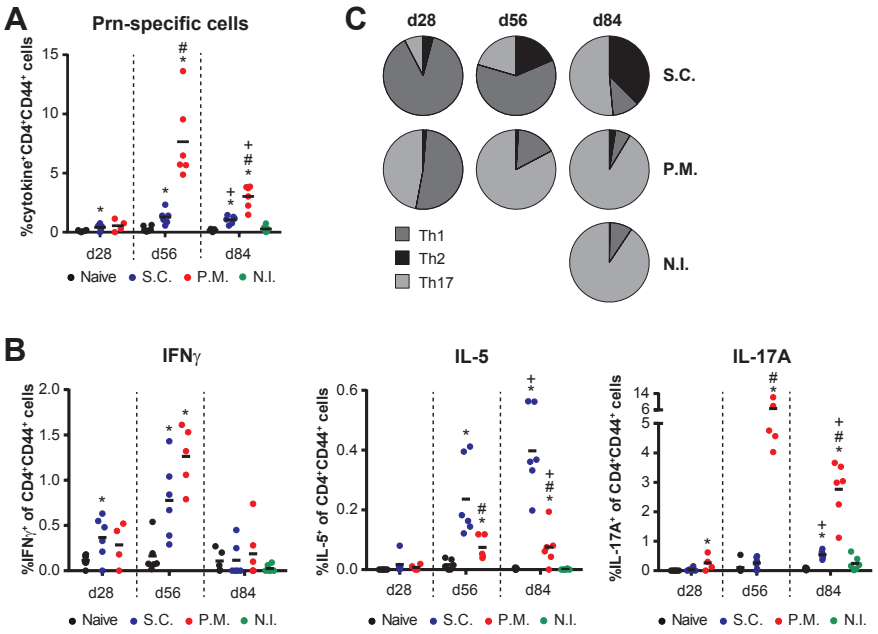

Figure S4 - Pulmonary and systemic Prn-specific T-cell responses induced by P.M. and S.C. omvPV immunization. **(A)** Magnitude of the Prn-specific $CD4^+$ T-cell response on day 28, 56, and 84 after *in vitro* stimulation with Prn for 4 days was determined using ICS and calculated as the total percentage cytokine (IL-5, IFNγ, and IL-17A)-producing $CD4^+CD44^+$ T-cells. **(B)** Percentage IL-5-, IFNγ-, and IL-17-producing cells of $CD4^+CD44^+$ T-cells of spleens harvested on day 38 and day 56 and stimulated *in vitro* for 4 days with Prn. Results of each analysis are given of 6 mice per group. **(C)** Distribution of Th subsets based on IL-5 (Th2), IFNγ (Th1), and IL-17A (Th17) production as determined using ICS and flow cytometry. * $p \leq 0.05$ versus naive mice; # $p \leq 0.05$ versus S.C. mice; + $p \leq 0.05$ versus S.C. mice.

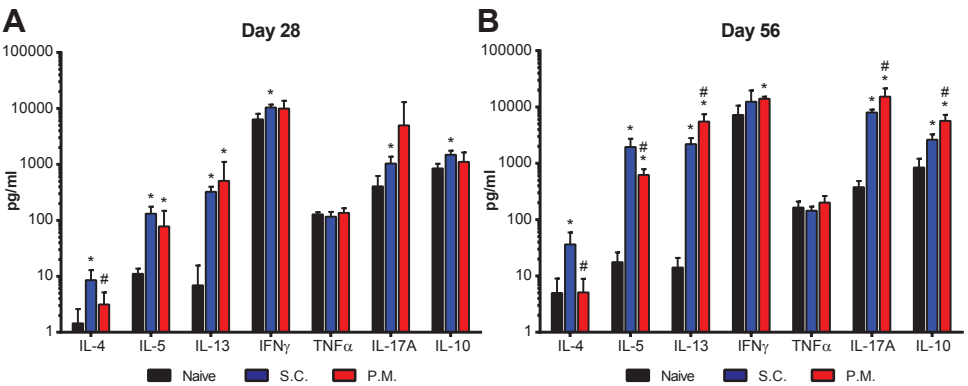

Figure S5 - Cytokine levels in supernatants of OMV stimulated splenocytes. **(A-B)** The presence of cytokines in day 3 culture supernatants of splenocytes collected on **(A)** day 28 and **(B)** day 56 was tested using a multiplex assay. Results in pg/ml are corrected for the background level (IMDM complete medium control) and are given as mean ± SD of 6 mice per group. * $p \leq 0.05$ versus naive mice; # $p \leq 0.05$ versus S.C. mice.

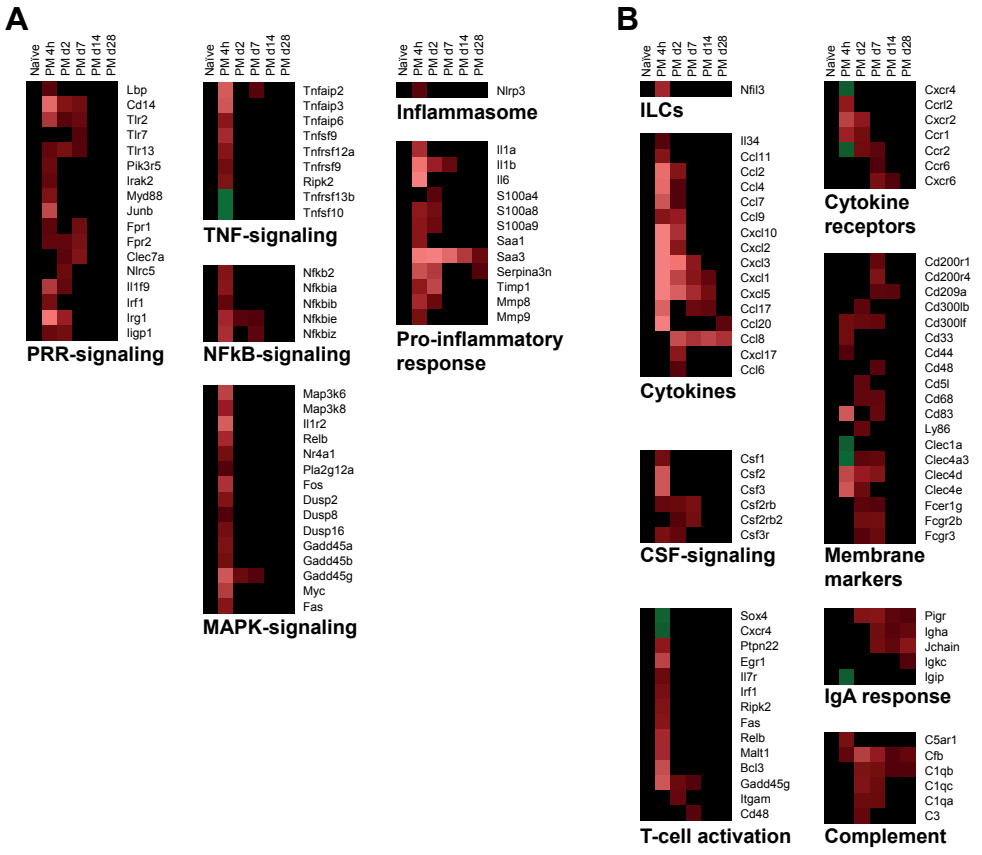

Figure S6 - Pulmonary transcriptome following P.M. immunization. **(A-B)** Differential upregulated (red) or downregulated (green) gene expression of P.M. mice (mean of n = 3) compared to naive mice (day 0) (FR ≥ 2.0, *p*-value ≤ 0.01). Genes not surpassing a fold change of 2.0 are shown as basal level (black). **(A)** Genes are depicted involved in pathogen recognition, such as the inflammasome and the pathogen recognition receptor (PRR)-, TNF-, NFκB-, and MAPK-signaling pathways and pro-inflammatory responses. **(B)** Genes are depicted involved in ILCs, CSF-signaling, T-cell activation, humoral response, and complement in addition to genes encoding for cytokines, cytokine receptors, and membrane markers.

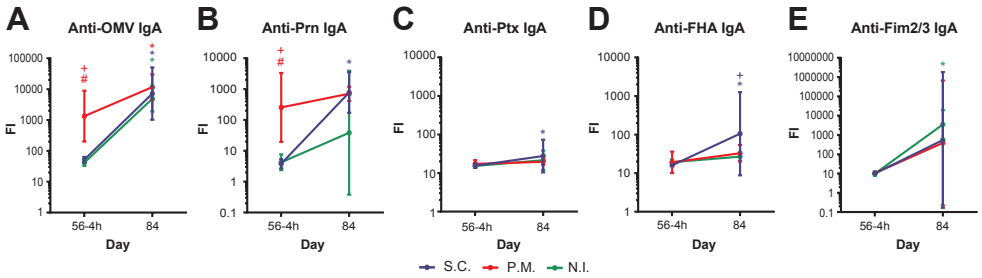

Figure S7 - IgA responses in the nose lavages of P.M., S.C., and N.I. mice. IgA antibodies specific for OMV **(A)**, Prn **(B)**, Ptx **(C)**, FHA **(D)**, and Fim2/3 **(E)** were determined in the nose lavage of P.M., S.C., and I.N. mice 4 hours after *B. pertussis* challenge (d56-4h) and at day 84. Results are expressed as fluorescence intensities (FI) of 4 mice per group per time point. * $p \leq 0.05$ versus levels on d56-4h; # $p \leq 0.05$ versus S.C. mice; + $p \leq 0.05$ versus N.I. mice.

Table S1 Immunogenic proteins determined by LC/MS of excised spots found by immunoblotting of 2DE gels

protein description[a]	accession number[b]	ID[b]	Mw (kDA)[c]	pI[c]	coverage (%)[d]	number of peptides assigned with high confidence[d]
60kD chaparonine	Q7W0M8	*GroEl*	57.4	5.2	69	33
adenosylhomocysteinase	Q7VUL8	*ahcY*	51.6	6.1	53	20
autotransporter	Q79GN7	*vag8*	94.8	6.8	41	27
bifunctional purine biosynthesis protein	Q7VTU1	*purH*	55.8	6.3	36	16
BrkA autotransporter (1)	Q45340	*BrkA*	103.3	7.1	30	21
BrkA autotransporter (2)	Q45340	*BrkA*	103.3	7.1	18	14
chaperonine protein HtpG	Q7W0M8	*htpG*	71.1	5.2	65	39
dihidrolipoyl dehydrogenase	Q7VZ16	*odhL*	50.1	6.8	61	25
outer membrane protein A (1)	Q7VZG6	*ompA*	21.0	8.7	17	3
outer membrane protein A (2)	Q7VZG6	*ompA*	21.0	8.7	35	5
pertactin autotransporter	P14283	*prn*	93.4	9.2	28	16
probable tonB dependent receptor	P81549	*BfrD*	79.3	8.2	58	37
putative outer membrane protein	Q7VT02	*BP3755*	23.0	9.2	26	5
Virulence factors putative positive transcription regulator	P0A4H2	*bvga*	22.9	8.4	78	14

a) Proteins in excised gel spots identified by LC–MS analysis.
b) Accession numbers of proteins and corresponding ID provided by uniprot (http://www.uniprot.org).
c) Molecular weight (Mw) and isoelectric point (pI) are calculated based on protein sequence.
d) Percentage of a protein sequence covered by identified peptides from the corresponding protein and the number of peptides assigned with high confidence.

About the cover: The Jet d' Eau fountain in Geneva, Switserland. The 140 metres high fountain is located in the Lake Geneva. In 2015, René was invited to participate in the roundtable discussion at the Foundation Merieux event "*Pertussis: biology, epidemiology and prevention*" that was held in Annecy, France.

CHAPTER 8

Meta-analysis of pulmonary transcriptomes from differently primed mice identifies molecular signatures to differentiate immune responses following *Bordetella pertussis* challenge

René H.M. Raeven[1,2,*], Jeroen L.A. Pennings[3,*], Elly van Riet[1], Gideon F.A. Kersten[1,2], Bernard Metz[1]

[1]Institute for Translational Vaccinology (Intravacc), Bilthoven, The Netherlands,
[2]Division of Drug Delivery Technology, Leiden Academic Centre for Drug Research, Leiden, The Netherlands
[3]Centre for Health Protection, National Institute for Public Health and the Environment, Bilthoven, The Netherlands,

[*] Both authors contributed equally

Manuscript submitted

Abstract

Respiratory infection with *Bordetella pertussis* leads to severe effects in the lungs. The resulting immunity and also immunization with pertussis vaccines protects against disease, but the induced type of immunity and longevity of the response are distinct. In this study the effect of priming, either by vaccination or infection, on a subsequent pathogen encounter were studied. To that end, three post-challenge transcriptome datasets of previously primed mice were combined and compared to the responses in unprimed control mice. In total, 205 genes showed different transcription activity. A co-expression network analysis assembled these genes into 27 clusters, combined into six groups with overlapping biological function. Local pulmonary immunity was only present in mice with infection-induced immunity. Complement-mediated responses were more prominent in mice immunized with an outer membrane vesicle pertussis vaccine than in mice that received a whole-cell pertussis vaccine. Additionally, 46 genes encoding for secreted proteins may serve as markers in blood for the degree of protection (*Cxcl9, Gp2, Pla2g2d*), intensity of infection (*Retnla, Saa3, Il6, Il1b*), or adaptive recall responses (*Ighg, C1qb*). The molecular signatures elucidated in this study contribute to better understanding of functional interactions in challenge-induced responses in relation to pertussis immunity.

Introduction

Whooping cough, caused by *Bordetella pertussis* is an endemic disease with considerable health impact [1, 2]. Several vaccines against *B. pertussis* are marketed or under development. These include whole-cell pertussis vaccine (wPV), acellular pertussis vaccine (aPV), live-attenuated pertussis vaccine (BPZE1), and vaccines based on outer membrane vesicles (omvPV) [3-6]. These vaccines are very different with regard to concept (whole-cell inactivated, subunit, live attenuated), composition and route of immunization. Although all vaccines confer protection in the mouse challenge model [3-7], the type and level of immunity is different [3-7]. This difference in immunity leads to distinct pulmonary immune responses upon subsequent *B. pertussis* encounter [7, 8].

Analysis of different transcriptome datasets is a tool for unbiased investigation of biological processes. It has been used to compare for instance the immune responses induced by different vaccines to identify universal vaccine-induced signatures [9-11]. Previously, differences in pulmonary gene expression of mice immunized with omvPV or wPV [7], and mice receiving a primary infection [8] were elucidated. However, the pulmonary transcriptome datasets obtained by challenge experiments may contain potential gene markers related to pertussis immunity. The identification of those markers may contribute to better understanding of pertussis immunity and as read-out in a human challenge model [12].

We performed an meta-analysis of pulmonary transcriptome datasets obtained after a *B. pertussis* challenge in mice with a different pertussis immune status. These included mice with infection-induced immunity, wPV-immunized mice (wPV-mice), omvPV-immunized mice (omvPV-mice), and non-immunized mice (N.I. mice) as control [7, 8]. The molecular signatures were characterized with special attention for secreted proteins, since these markers could potentially be useful for monitoring immune responses in blood samples to determine degree of protection, intensity of infection, or promptness of adaptive recall responses for later application in human challenge studies.

Methods

Datasets

We used gene expression datasets from four *B. pertussis* challenge experiments in mice. These included data from challenge studies performed 56 days after the primary immunization or infection [7, 8]. We included mice with (i) infection-induced immunity, mice immunized twice with (ii) wPV or (iii) omvPV, and (iv) non-immunized mice (**Figure 1A**).

Gene expression analysis

The flow diagram showing all stages of the gene expression analysis and the selection criteria is shown in **Figure 1B**. For all datasets, we included five time points: 56 days post primary infection (p.i.) or immunization, but before challenge (D0), and 4 hours, 2 days, 7 days and 14 days post intranasal *B. pertussis* challenge (p.c.). Gene expression profiles of non-challenged and non-immunized mice were used as a control. In each of the four experiments, differentially expressed genes (DEGs) were identified by using previously described methods [13, 14], namely a one-way ANOVA at a stringency value of $p \leq 0.001$ and an absolute Fold Ratio (FR, i.e. challenge response to the control group) ≥ 2.0. Data for the combined set of DEGs (across time points in one study) were merged. This set of DEGs was further refined by (i) identifying DEGs that differed by a FR ≥ 2.0 across studies at one time point; (ii) excluding genes that are not protein-coding (mainly genes annotated by NCBI as "gene model" or "hypothetical gene"); and (iii) excluding genes with batch-to-batch variation between arrays in the control groups.

Functional analysis

For the resulting datasets, a co-expression network was created, based on the Euclidean distance between their overall response patterns across all groups and time points. Genes were connected in a network if their co-expression similarity fell in the top 1% of overall most similar responses. Additionally, remaining genes were connected to genes with the most similar response over time in order to include each gene in the network. Further functional analysis and identification of genes that encode for secreted proteins based on the Uniprot-term 'secreted' were performed by using DAVID [15].

Data visualization

Data were visualized using Adobe Illustrator CC 2015, Cytoscape (version 2.8.3) (www.cytoscape.org), R (www.r-project.org), Genemaths XT (Applied Maths, St-Martens-Latem, Belgium), and Venny (http://bioinfogp.cnb.csic.es/tools/venny/index.html).

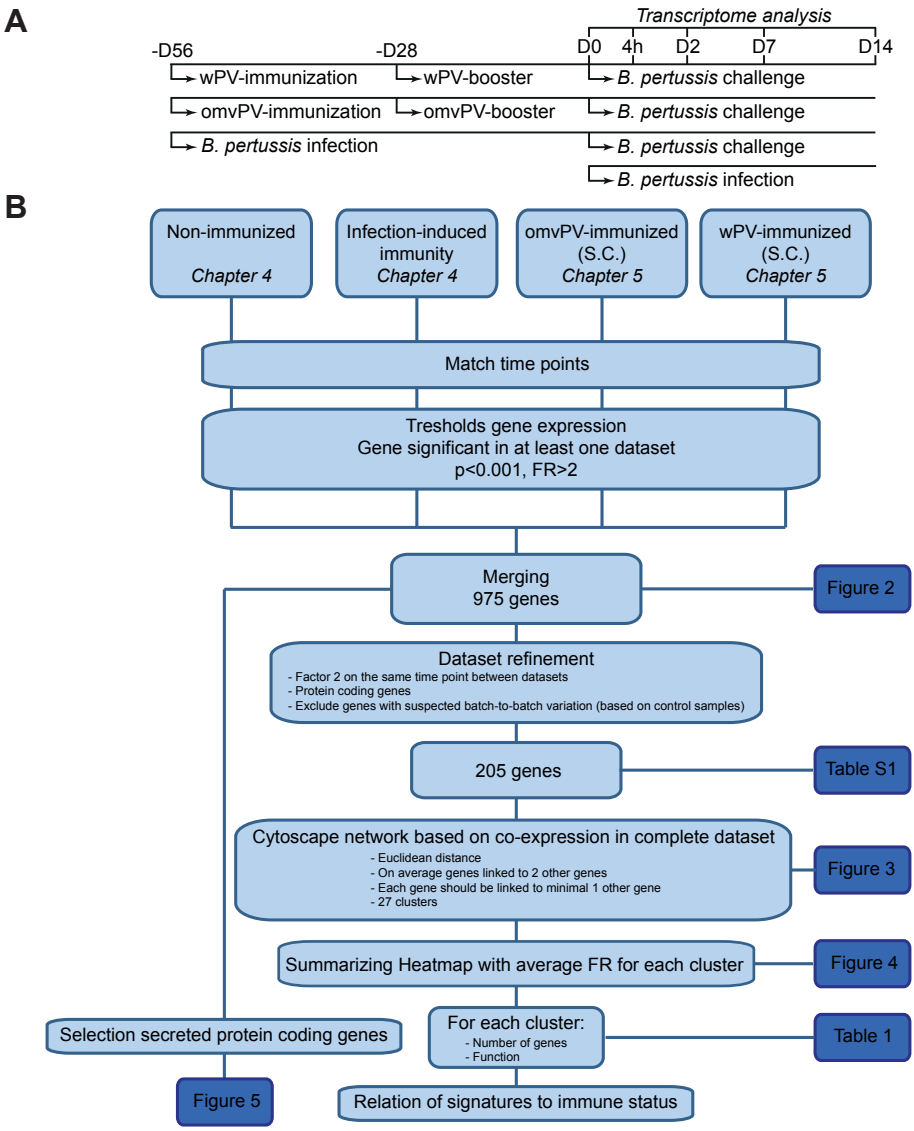

Figure 1 - Design and method used in this study. Four transcriptome datasets were included obtained after a *B. pertussis* challenge in the lungs of non-immunized mice, mice with infection-induced immunity, and mice immunized subcutaneously (S.C.) with omvPV or wPV. **(A)** The immunization and challenge scheme of these datasets is shown. The source of these datasets in the corresponding chapters of this thesis is depicted. **(B)** The different steps of the meta-analysis and criteria used are described and linked to the figures and tables in this chapter.

Results and Discussion

Identification of gene expression signature clusters

The pulmonary transcriptomes of four individual *B. pertussis* challenge experiments were merged. The immunization and *B. pertussis* challenge scheme of these studies is shown in **Figure 1A**. Individual datasets revealed 975 DEGs (FR ≥ 2.0, $p \leq 0.001$) in one or more datasets (**Figure 2**). In total, 627, 256, 169 and 280 genes were included in the non-immunized, omvPV-immunized and wPV-immunized mice, and mice with infection-induced immunity, respectively. Subsequently, we identified DEGs (FR ≥ 2.0, $p \leq 0.001$) between the datasets for each time point. This second round of identifying DEGs between studies, combined with a 'cleanup' by exclusion of functionally less relevant genes, i.e. hypothetical or non-protein coding genes (**Figure 1**), left 205 genes for further analysis (**Table 1**). Co-expression patterns for these 205 genes were determined and visualized in a network analysis (**Figure 3**). This analysis split the 205 genes into 27 signature clusters (A-AA) ranging in size from 2 to 75 genes (**Table 1**). The average gene expression was calculated for each gene cluster and visualized in a heatmap (**Figure 4**).

Function of clusters and relation to pertussis-vaccinated background

To determine the function of the individual clusters, an overrepresentation analysis was performed using DAVID. The different clusters were combined to six groups with overarching biological functions (group I-VI) (**Figure 3 and 4**). From these molecular signatures, we additionally identified the genes that encode for secreted proteins. Because they may serve as markers that can be analyzed in blood and could be interesting candidates for later

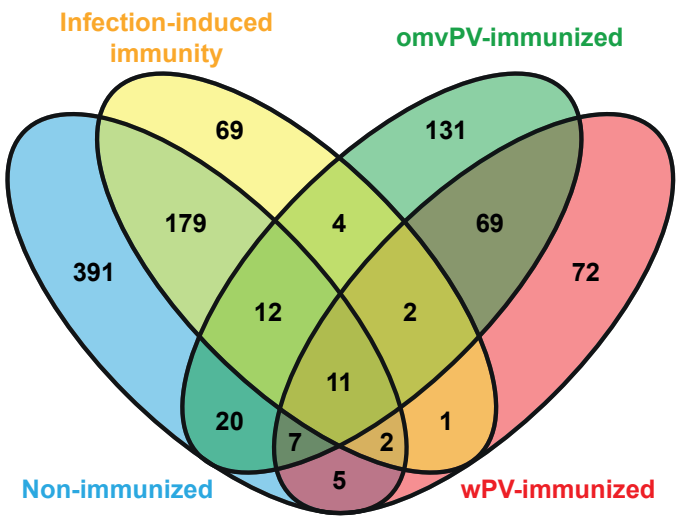

Figure 2 - Venn diagram. The overlap of differentially expressed genes between four datasets obtained from lungs of mice at different time points after *B. pertussis* challenge is depicted.

application in human studies. In total, 46 genes were identified to code for secreted proteins, which were present in the different groups, except for group III (Figure 5). Gene expression of clusters and single genes were compared with the number of colony forming units (cfu) in the lung (Figure 4 and 5) which were determined previously in primed and unprimed mice [7, 8].

At this point, we are able to isolate different molecular signatures from this analysis based on the gene expression kinetics. First, (i) signatures of local immunity induced by the primary vaccination or infection that are still active or present in the lungs on Do, just before challenge. Second, (ii) signatures of infection intensity. The N.I. mice have the highest number of bacteria in the lungs on 7 days p.i. whereas these are cleared faster in primed

Table 1 - Detailed information on the 27 gene clusters.

Clusters	Number of genes	Included genes
A	75	Abcf1, Abhd8, Agap3, Amotl2, Arap1, Arhgef40, Atp9a, B4galnt1, Cenpb, Cldn3, Cnp, Cpsf1, Cyp2s1, D17H6S56E-5, Dctn1, Ddr1, Egln2, Fasn, Flii, Lbp, Gadd45g, Gclc, Get4, Gpr56, Grn, Gstm1, Hgs, Hspb1, Itga3, Itga7, Itih4, Keap1, Kif1c, Lrp10, Mgll, Mmrn2, Nfe2l1, Os9, Pard6b, Parm1, Pex14, Piezo1, Pip4k2c, Pkm, Plbd2, Pnpla2, Por, Ralgds, Rbm19, Relb, Rftn1, Rgp1, Rgs12, Rnh1, Rptor, Rrp1, Rsph1, Rusc2, Sbno2, Sdc3, Sec61a1, Sema3b, Sh3tc1, Slc3a2, Spint2, Sqstm1, Stab1, Tap2, Tgm2, Tmbim6, Tnip1, Ucp2, Vars, Vpreb3, Zbtb7a
B	5	Crip2, Hdac5, Isyna1, Lrg1, Plxnb2
C	4	Prpf8, Psap, Psmd3, Shisa5
D	4	Cyba, Ehd1, Mvp, Myh14
E	2	Hadha, Man2b1
F	10	Ccl19, Ciita, Cxcl12, Cxcr2, Fam26f, Gm12407, Plbd1, Reg3g, Rrm2, BC048546
G	8	Cd74, H2-Ab1, H2-D1, H2-DMa, H2-Eb1, H2-K1, Nup62-il4i1, Steap4
H	7	Bpifb1, Cp, Cxcl17, Ltf, Prom1, Scgb3a1, Tmc5
I	5	Cdhr1, Clca4, Pglyrp1, Ubd, 4833428L15Rik
J	3	Ccar1, Gbp10, Gbp6
K	2	Iigp1, Mki67
L	2	Ccna2, Ckap2
M	10	Basp1, C1qb, Cd177, Cxcl13, Gm9758, Gp2, Pla2g2d, Speer4b, Speer4c, Speer4e
N	6	Ccl20, Ighg, Igj, Igk, Igkv4-59, Igkv8-30
O	5	Igh-VJ558, Ighm, Igkc, Igkv4-53, Pigr
P	4	C3, C4a, C4b, Tnfaip2
Q	4	Ccl8, Cxcl9, Retnla, Saa3
R	4	Cfb, Clca3, Lcn2, Tff2
S	14	Ank3, BC117090, Bcl2a1a, Bcl2a1b, Bcl2a1c, Bcl2a1d, Cd209f, Cxcl5, Fpr2, Mmp3, Rorc, Scel, Tspan2, A130040M12Rik
T	7	Chil3, Ear1, Ear10, Ear12, Ear2, Ear3, Rnase2a
U	6	Aif1, H2-Aa, H2-Ea-ps, Ms4a7, S100a4, Serpina3g
V	3	Ccl17, Clec4n, 2900060B14Rik
W	3	Ctss, Fcgr2b, Wfdc17
X	4	Agr2, Cxcl11, Igtp, Timp1
Y	3	Cd14, Cxcl2, Fgg
Z	3	Ccl2, Il1b, Il6
AA	2	Arntl, Lox

Group I
Group II
Group III
Group IV
Group V
Group VI
A
B
C
D
E
F
G
H
I
J
K
L
M
N
O
P
Q
R
S
T
U
V
W
X
Y
Z
AA

mice (**Figure 4 and 5**). Therefore the kinetics and/or intensity of gene expression of acute phase and pro-inflammatory proteins that are secreted during colonization could indicate the intensity of infection in the mouse model. Finally, (iii) signatures of recall responses of adaptive immunity. These are expressed earlier (within 2 days p.c.) in immunized mice, but are absent or expressed later on (7-14 days p.i.) in N.I. mice. The different, groups (I-VI), clusters (A-AA), and genes encoding secreted proteins will be described hereafter.

Group I - Innate activation

Clusters A-E were combined to group I and comprised genes involved in general immune responses or related to macrophages and T-cell activation. These clusters were exclusively upregulated in the lungs of N.I. mice and mice with infection-induced immunity mice 4 hours p.c. Cluster A is the largest cluster, with 75 genes, and included genes involved in cell activation (*Relb, Gadd45g, Lbp, Sbno2*). Lipopolysaccharide binding protein (*Lbp*) is involved in recognition of LPS. Moreover, two integrins (*Itga3, Itga7*) were detected in this group, which are cell membrane proteins but not specific for immune cells.

Group II – Pulmonary bridging phase

Clusters F-I are part of group II that was enriched for antigen processing and presentation. These clusters were induced 7-14 days p.c. in N.I. mice, whereas these clusters were constantly expressed in mice with infection-induced immunity. Cluster G more specifically included genes involved in MHC signaling (*H2-Ab1, H2-D1, H2-DMa, H2-Eb1, H2-K1*). Additionally, group II contains genes coding for proteins that are secreted. These are expressed earlier in mice with infection-induced immunity compared to the mice receiving a vaccination (*Cxcl12, Cxcl17, Ccl19, Pglyrp1*) (**Figure 5**). Cxcl17 is a mucosal cytokine that attracts lung macrophages [16].

Group III – Cell cycle and tissue remodeling

Group III comprised genes of clusters J-L, associated with the cell cycle, which were only upregulated 7-14 days p.c. in N.I. mice. This group was marked by high activation of the cell proliferation marker *Mki67*. In addition, this group comprised of interferon-induced GTPases such as *Gbp6* and *Gbp10*, which are involved in the innate response to protect against a bacterial infection [17] and *Iigp1*. Activation of these genes solely in N.I. mice suggests enhanced lung cell proliferation as a result of lung tissue damage. Therefore, the absence of this gene expression signature in protected mice might indicate less collateral lung damage as a result of a *B. pertussis* challenge and, accordingly, suggests that recall responses of the adaptive immune system are sufficient.

Figure 3 (Left) - Network analysis. The 205 differentially regulated genes formed 27 clusters (A-AA). According to overlap in function, the clusters were subsequently combined in six groups (I-VI).

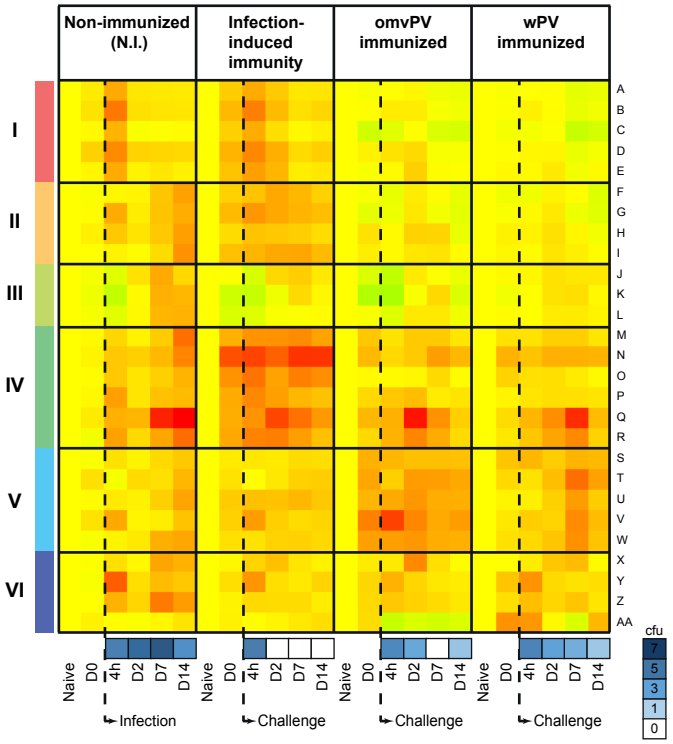

Figure 4 - Comparison of pulmonary gene expression profiles following a *B. pertussis* challenge in mice with different pertussis immunity background. Averaged fold changes of 27 clusters (A-AA) of infected non-immunized mice and challenged mice with infection-induced immunity, omvPV-immunization, or wPV-immunization background are depicted in a time course. Additionally, six groups (I-VI) with similarity in function are shown. The moment at which the *B. pertussis* infection or challenge was performed is depicted as well as the log10 number of colony forming units (cfu) for each time point post challenge as determined previously [7, 8].

Group IV – Mucosal and systemic adaptive recall responses

Clusters M-R were part of group IV of which the genes encode proteins with immunological functions, such as immunoglobulins, complement factors and acute inflammatory proteins. Clusters N-O both contain genes involved in antibody production. Cluster N is related to IgG production and more active in the lungs of mice with infection-induced immunity compared to omvPV- and wPV-immunized mice. Previously, we showed that pertussis immunization leads to higher total IgG levels compared to infection [18]. The higher expression of these genes in the lungs may suggest that the mice with infection-induced immunity have higher numbers of lung-resident IgG-producing B-cells, especially in combination with the co-clustering of these genes with Ccl20 that attracts CCR6^{+} B-cells. The genes (*Pigr*, *Igh-VJ558*) in cluster O are specifically related to IgA-production [19] and were strongly upregulated in mice with infection-induced immunity from 4 hours to 14 days p.c. This suggests that mice with infection-induced immunity have more intense and faster antibody production in the lungs compared to subcutaneously immunized mice. This was also shown at the functional level by the presence of specific-IgA in the lungs of mice with infection-induced immunity

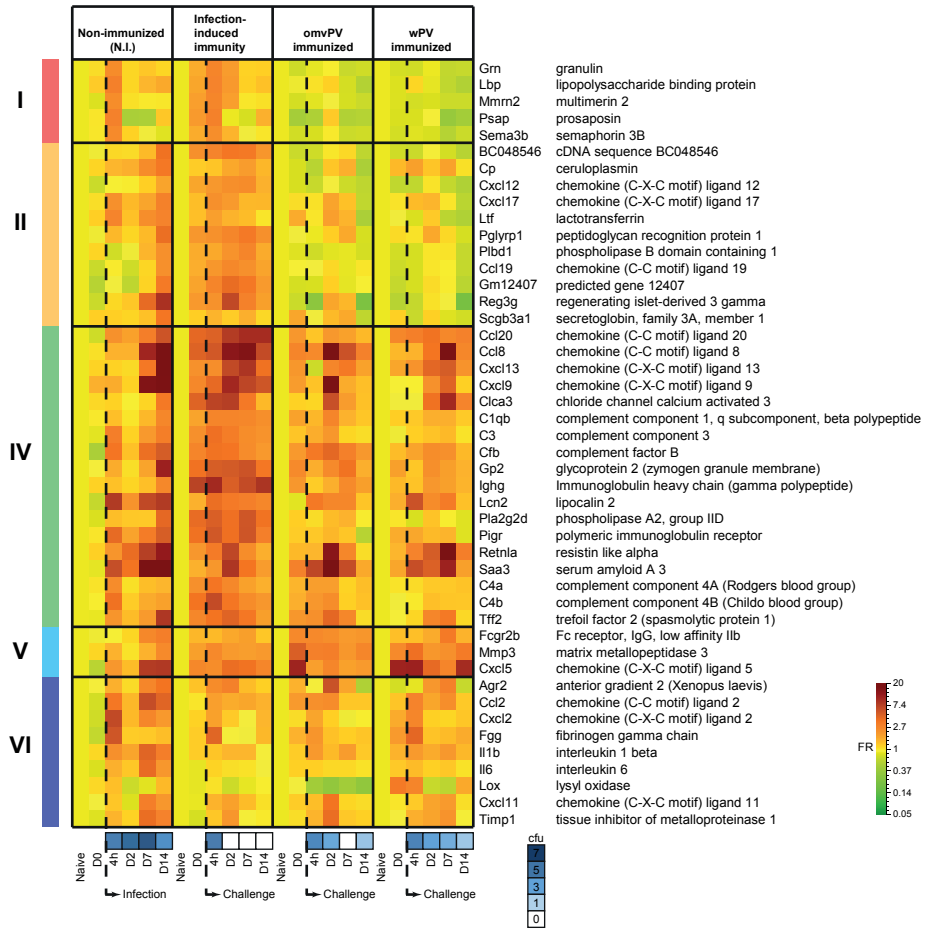

Figure 5 - Genes encoding for secreted proteins. Genes encoding for secreted proteins were retrieved from DAVID and illustrated as heatmap for the four pulmonary transcriptome datasets. The genes are clustered according to prevalence in the six function groups (I-VI), which is shown on the left. The moment at which the *B. pertussis* infection or challenge was performed is depicted as well as the log10 number of colony forming units (cfu) for each time point post challenge as determined previously [7, 8].

[8] and absence in wPV-mice and omvPV-mice [7]. Local stimulation of the immune system might be critical because the induction of antibody-related genes (*Iga, Pigr*) and mucosal IgA may lead to better protection. Cluster P contains three members of the complement system (*C3, C4a, C4b*). Members of complement systems (*C1qb, Cfb, C3, C4a, C4b*) were expressed most profound in the lungs of mice with infection-induced immunity and to a lesser extent in omvPV-immunized mice. Interestingly, these genes were hardly expressed in the lungs of wPV-immunized mice (**Figure 5**). This suggests that complement-mediated responses, which may contribute to clear *B. pertussis* from the lungs [20], are more prominent in omvPV-immunized mice. Cluster Q showed most pronounced expression in N.I. mice 7-14 days p.c., but was also present in wPV-mice 7 days p.c. In omvPV-mice and mice with infection-induced immunity, upregulated expression of cluster Q was observed 2 days p.c. This cluster included

Saa3, part of the acute phase response, *Cxcl9*, that attracts CXCR3$^+$ cells, a chemoattractant (*Ccl8*), and resistin-like molecule α (*Retnla*) that is important in lung pathology [21]. Notably, the expression of *Saa3* and *Retnla* follow the number of cfu in the lungs (**Figure 5**). Mice with infection-induced immunity show a limited induction of gene expression for *Saa3* and *Retnla*, which also peaks early, already 2 days p.c. In addition, they show the fastest lung clearance [8, 18]. On the contrary, the wPV-mice and N.I. mice showed later and more intense gene expression in accordance with prolonged lung clearance. The omvPV-mice revealed earlier expression compared to wPV-mice and N.I. mice conforming to the lower inflammatory responses observed in omvPV-immunized mice [7]. Both *Saa3* and *Retnla* encode for secreted proteins (**Figure 5**) and can therefore serve as a predictor of infection intensity when measured in blood.

Group V – Vaccine-primed innate responses

Cluster S-W were part of group V, which included genes associated with myeloid cells. These clusters were mainly upregulated in omvPV-mice 4 hours p.c. and in wPV-mice 7 days p.c. In cluster S, which is moderately expressed in omvPV-mice and wPV-mice, four members were identified belonging to the B cell leukemia/lymphoma 2 related proteins (*Bcl2a1a, Bcl2a1b, Bcl2a1c, Bcl2a1d*), a pathogen recognition receptor (*Fpr2*), a C-type lectin receptor (*Cd209f*), and matrix metallopeptidase 3 (*Mmp3*). Additionally, *Cxcl5*, a neutrophil attractant, was highly expressed before the challenge in the lungs of omvPV-mice and wPV-mice (**Figure 5**). Notably, this cluster also included the retinoic acid receptor (RAR)-related orphan receptor C (*Rorc*) that is essential for Th17 cell differentiation [22]. Cluster T included five members (*Ear1, Ear2, Ear3, Ear10, Ear12*) of the eosinophil-associated, ribonuclease A family. Cluster V was intensely upregulated in omvPV-mice 4 hours p.c. It contained *Ccl17*, and dendritic cell specific *Clec4n*. Together, these clusters represent an influx or higher proliferation of myeloid cells and DCs that are most profound in the omvPV-mice.

Group VI – Inflammation

Finally, cluster X-AA formed group VI that was enriched for the GO-term inflammatory response. Cluster Y was mainly upregulated 4 hours p.c. This was most intense in non-immunized mice and the lowest in omvPV-mice. This cluster contained the CD14 marker (*Cd14*) that is involved in LPS recognition, a neutrophil attractant (*Cxcl2*), and fibrinogen (*Fgg*), which is an important attenuator of LPS-mediated responses [23]. Cluster Z included *Ccl2* and the pro-inflammatory cytokines *Il6* and *Il1b* that were strongly induced in the N.I. mice and not in the three immunized groups. This indicates that previous exposure to either a vaccine or infection prevents induction of these pro-inflammatory markers in the lungs upon a *B. pertussis* challenge. Therefore, the presence of these signatures may serve as a marker for mice being unprotected against pertussis (**Figure 5**). Finally, cluster AA was only present in wPV-immunized mice.

Conclusions

This meta-analysis revealed molecular signatures specific for immune responses against pertussis. The signatures were measured in the lungs of mice that were previously exposed to either pertussis vaccination or infection. Comparison of the gene expression profiles in the lung of differently treated mice revealed that:

- Infection, but not subcutaneous vaccination, leads to induction of local immunity in the lungs. This local immunity is characterized by enhanced IgA production and involvement of 'trained' pulmonary innate cells [8].
- Responses to pertussis challenge in the lungs of omvPV-mice and wPV-mice were similar in nature, but the omvPV-mice respond slightly faster.
- Complement-mediated responses are more prominent in omvPV-immunized mice than in wPV-mice.
- Genes with unknown function (*Speer4b, Speer4c, Speer4e*) were associated with genes with well-known function (*C1qb, Cd177*) based on their co-expression, providing insight into their potential immunological functions.
- Genes of potentially secreted proteins were identified of which some may serve as markers in blood for analysis of degree of protection (*Cxcl9, Gp2, Pla2g2d*), intensity of infection (*Retnla, Saa3, Il6, Il1b*), or adaptive recall responses (*Ighg, C1qb*). This analysis can be performed by using an ELISA or multiplex immunoassay and for instance applied as readout in a human challenge model [12].

References

1. Cherry, J.D., Epidemic pertussis in 2012--the resurgence of a vaccine-preventable disease. N Engl J Med, 2012. 367(9): p. 785-7.
2. Tan, T., *et al.*, Pertussis Across the Globe: Recent Epidemiologic Trends From 2000-2013. Pediatr Infect Dis J, 2015. 34(9): p. e222-32.
3. Brummelman, J., *et al.*, Modulation of the CD4 T cell response after acellular pertussis vaccination in the presence of TLR4 ligation. Vaccine, 2015. 33(12): p. 1483-91.
4. Mielcarek, N., et al., Live attenuated *B. pertussis* as a single-dose nasal vaccine against whooping cough. PLoS Pathog, 2006. 2(7): p. e65.
5. Roberts, R., *et al.*, Outer membrane vesicles as acellular vaccine against pertussis. Vaccine, 2008. 26(36): p. 4639-46.
6. Ross, P.J., *et al.*, Relative contribution of Th1 and Th17 cells in adaptive immunity to *Bordetella pertussis*: towards the rational design of an improved acellular pertussis vaccine. PLoS Pathog, 2013. 9(4): p. e1003264.
7. Raeven, R.H.M., *et al.*, *Bordetella pertussis* outer membrane vesicle vaccine confers equal efficacy in mice with a lower inflammatory response compared to a classic whole-cell vaccine. Manuscript submitted.
8. Raeven, R.H.M., *et al.*, Immunological signatures after *Bordetella pertussis* infection demonstrate importance of pulmonary innate immune cells. Manuscript submitted.
9. Li, S., *et al.*, Molecular signatures of antibody responses derived from a systems biology study of five human vaccines. Nat Immunol, 2014. 15(2): p. 195-204.
10. Obermoser, G., *et al.*, Systems scale interactive exploration reveals quantitative and qualitative differences in response to influenza and pneumococcal vaccines. Immunity, 2013. 38(4): p. 831-44.
11. Wang, I.M., *et al.*, Transcriptional profiling of vaccine-induced immune responses in humans and non-human primates. Microb Biotechnol, 2012. 5(2): p. 177-87.
12. Merkel, T.J. and S.A. Halperin, Nonhuman primate and human challenge models of pertussis. J Infect Dis, 2014. 209 Suppl 1: p. S20-3.
13. Pennings, J.L., *et al.*, Gene expression profiling in a mouse model identifies fetal liver- and placenta-derived potential biomarkers for Down Syndrome screening. PLoS One, 2011. 6(4): p. e18866.
14. Raeven, R.H.M., *et al.*, Molecular Signatures of the Evolving Immune Response in Mice following a *Bordetella pertussis* Infection. PLoS One, 2014. 9(8): p. e104548.
15. Huang da, W., B.T. Sherman, and R.A. Lempicki, Systematic and integrative analysis of large gene lists using DAVID bioinformatics resources. Nat Protoc, 2009. 4(1): p. 44-57.
16. Burkhardt, A.M., *et al.*, CXCL17 is a major chemotactic factor for lung macrophages. J Immunol, 2014. 193(3): p. 1468-74.
17. Kim, B.H., *et al.*, A family of IFN-gamma-inducible 65-kD GTPases protects against bacterial infection. Science, 2011. 332(6030): p. 717-21.
18. Raeven, R.H.M., *et al.*, Immunoproteomic Profiling of *Bordetella pertussis* Outer Membrane Vesicle Vaccine Reveals Broad and Balanced Humoral Immunogenicity. J Proteome Res, 2015. 14(7): p. 2929-42.
19. Norderhaug, I.N., *et al.*, Regulation of the formation and external transport of secretory immunoglobulins. Crit Rev Immunol, 1999. 19(5-6): p. 481-508.
20. Jongerius, I., *et al.*, Complement evasion by *Bordetella pertussis*: implications for improving current vaccines. J Mol Med (Berl), 2015. 93(4): p. 395-402.
21. Fan, C., *et al.*, Resistin-Like Molecule alpha in Allergen-Induced Pulmonary Vascular Remodeling. Am J Respir Cell Mol Biol, 2015. 53(3): p. 303-13.
22. Ivanov, II, *et al.*, The orphan nuclear receptor RORgammat directs the differentiation program of proinflammatory IL-17+ T helper cells. Cell, 2006. 126(6): p. 1121-33.
23. Cruz-Topete, D., *et al.*, Delayed inflammatory responses to endotoxin in fibrinogen-deficient mice. J Pathol, 2006. 210(3): p. 325-33.

About the cover: Mount Fitz Roy ("Cerro Chalten"), seen from the Lagoon de los Tres, located in the Los Glaciares National Park in Patagonia on the border of Chile and Argentina. With a height of 3,405 metres, sheer mountain face, and harsh weather conditions it is considered one of the world's most difficult mountains to climb. In 2016, René attended the 11th International Bordetella Symposium that was held in Buenos Aires, Argentina.

CHAPTER 9

General discussion

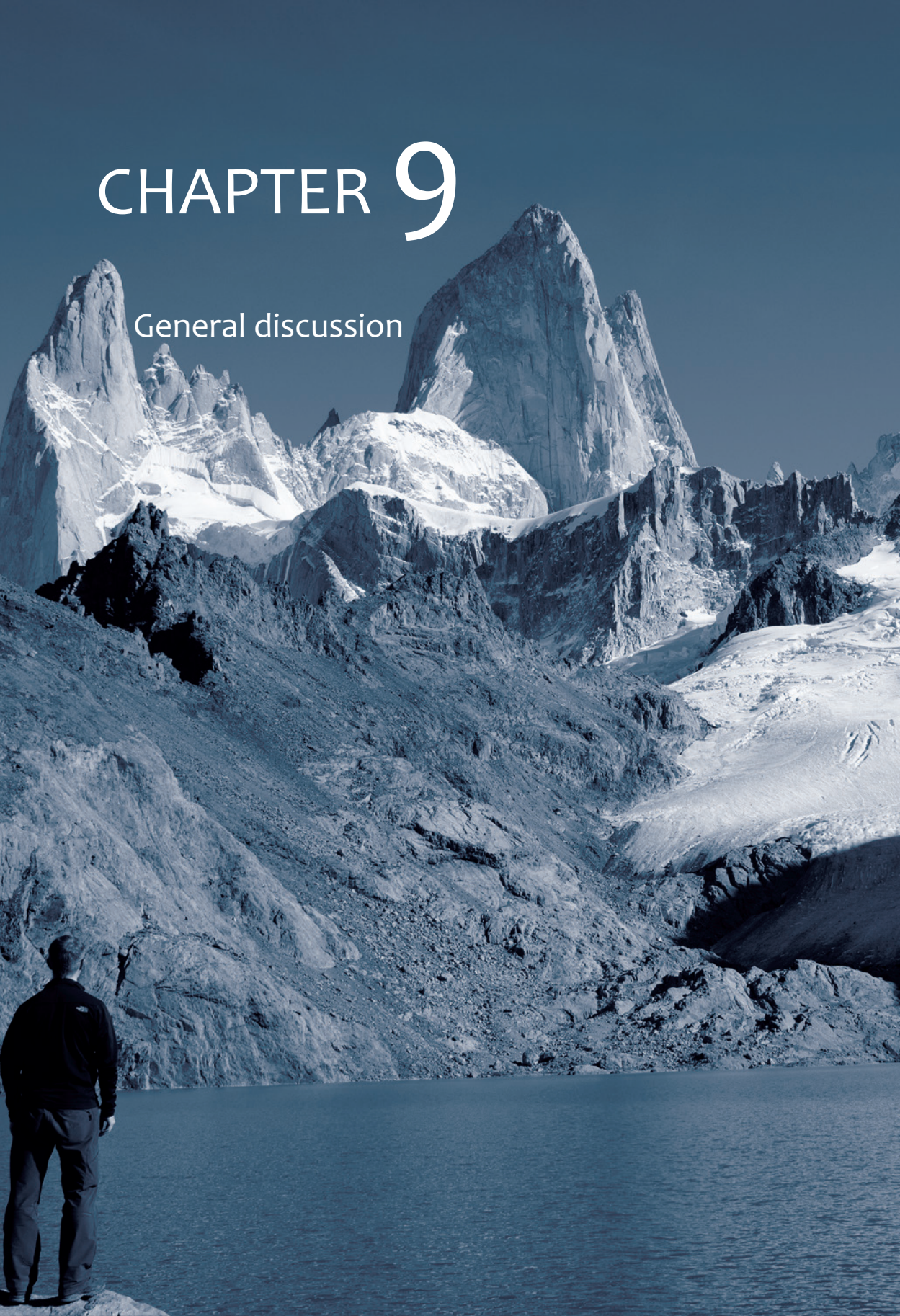

Summary

In this thesis a systems vaccinology approach is described to deepen knowledge of the immune responses evoked by different pertussis vaccines and compare this with a *Bordetella pertussis* infection since the latter induces robust, sterilizing immunity in the lungs of mice. We unraveled distinct immunity profiles elicited by different pertussis vaccines that were accompanied by various molecular signatures.

The immunological processes occurring during a *B. pertussis* infection are analyzed in detail and described in **Chapter 2**. Numerous new responses were identified within the innate, bridging and adaptive phases. These include extended duration of innate (cytokine) responses well into the second week of the infection. Since infection-induced immunity confers sterilizing immunity and provides preferable adaptive immunity against *B. pertussis*, it is used as benchmark throughout the thesis.

Infection-induced immunity is further investigated in **Chapter 3**. Here, mice with infection-induced immunity were challenged with a second infection. The molecular background of these mice revealed high activity of innate immune cells that specifically reside in the lungs. We suggest that these innate immune cells may represent 'trained' innate immunity [1, 2]. This included for instance gene markers for M-cells (*Gp2*, *Umod*). Additionally, the early expression of *Thy1* and *Il7r* and IL-5 secretion in the lungs suggested presence of innate lymphoid cells (ILCs) [3]. ILCs but also NK-cells are associated with 'trained' innate immunity [4].

The candidate vaccine of interest in this thesis is outer membrane vesicle pertussis vaccine (omvPV). This is a complex vaccine, containing hundreds of protein antigens. The immunogenicity of the individual antigens was assessed by immunoproteomic profiling anti-sera by using 2-D electrophoresis, Western blotting, and mass spectrometry (**Chapter 4**). The omvPV elicits a broader subclass distribution than whole-cell pertussis (wPV) and acellular pertussis (aPV) vaccines and most immunogenic antigens were Vag8, BrkA and LPS (**Table 1**).

In **Chapter 5** the immunogenicity of omvPV is compared with wPV, probably the most potent pertussis vaccine currently on the market, after subcutaneous immunization. OmvPV immunized mice developed higher systemic IgG titers and cleared bacteria slightly faster than wPV immunized mice from the lungs. Both groups evoked a mixed Th1/Th2/Th17 response (**Table 1**). The omvPV induced significantly lower systemic pro-inflammatory cytokine responses than wPV. The transcriptome showed that many genes expressed in the spleen were markers for the activation of IFN-signaling pathways and involvement of myeloid cells, such as neutrophils. Additionally, the omvPV-response comprised upregulation of genes with anti-inflammatory functions such as *Fpr2* [5] and *Steap4* [6].

Chapter 6 addresses immunological responses evoked by aPV. The $CD4^+$ T-cell response induced by aPV is Th2-dominated. Previously it was shown that supplementing aPV with with a non-toxic toll-like receptor 4 (TLR4) ligand, Lpxl1, leads to the formation of Th1/Th17 cells instead of strictly Th2 cells [7]. We isolated these $CD4^+$ T-cells and analyzed the transcriptome, which unraveled distinct molecular signatures between both groups. The addition of Lpxl1 to the aPV leads to upregulation of cytokines and transcription factors specific for Th1 and Th17 cells, such as *Ifng* and *Il17a*. Additionally, upregulation of less familiar Th1-associated genes, such as *Havcr2*, *Ccl5*, and *Cxcl9*, were detected.

Since infection induces robust immunity, including strong local IgA and Th17 responses, mice were immunized with the vaccine candidate omvPV by the pulmonary route (**Chapter 7**). Indeed, pulmonary administration of omvPV induced superior protection comparable as caused by infection and better than subcutaneously administered omvPV. The bacterial clearance rate from the lungs was reduced from 7 days to 2 days (**Table 1**). The pulmonary route elicited increased levels of systemic IgG antibodies, IgG-producing plasma cells, memory B-cells, and Th17-cells. More importantly, pulmonary immunization but not subcutaneous injection led to the presence of IgA antibodies, IgA-producing plasma cells and Th17-cells in the lungs. These adaptive responses were preceded by distinct serum and pulmonary cytokine profiles and transcriptome profiles in the dLN and lungs. The activation of TLRs and the downstream signaling pathways were detected in the lungs of pulmonary immunized mice. Signatures of ILC3s expressing *Rorc* [8] and IL-5-secreting ILC2s may correlate with the more dominant Th17 response after pulmonary immunization and systemic Th2 response after subcutaneous immunization respectively.

In **Chapter 8**, an *in silico* analysis was performed, which compared the transcriptome profiles of the lungs of mice with a different immune status after they received a *B. pertussis* challenge. This revealed 27 gene clusters with distinct patterns between immunized mice and non-immunized mice. The molecular patterns in the lungs of mice with infection-induced immunity revealed more specific markers of local immunity, which were absent in the mice that were systemically immunized with omvPV or wPV. This supported the importance of induction of local immunity. Specific molecular signatures that encode secreted proteins were detected that may serve as potential markers in blood for analysis of degree of protection (*Cxcl9, Gp2, Pla2g2d*), severity of infection (*Retnla, Saa3, Il6, Il1b*), or adaptive recall responses (*Ighg, C1qb*) in challenge studies.

Major findings

- The application of systems vaccinology in pertussis research revealed molecular signatures of pathogen-recognition, inflammatory responses, involvement and interaction of immune cells. The comprehensive dataset provided insight into the construction of immunity against *B. pertussis*.
- Infection-induced responses confer sterilizing protection that is caused by systemic immunity but more importantly by mucosal IgA, Th1/Th17 responses, and 'trained' innate immune cells in the lungs (**Chapters 2 and 3**).
- The omvPV elicits a broad and balanced immunoproteomic profile that differs from the profile induced by aPV, wPV, and infection with respect to antibody levels, antigen specificity, and subclass distribution (**Chapter 4**).
- Subcutaneous immunization of omvPV confers equal efficacy in mice but with a lower inflammatory response compared to wPV (**Chapter 5**).
- Addition of a non-toxic TLR4 ligand to aPV dampens the formation of Th2 cells and stimulates Th1/Th17 cells (**Chapter 6**).
- In contrast to subcutaneous immunization, the pulmonary administration of omvPV leads to superior protection in mice that is similar to the protection conferred by infection-induced immunity (**Chapter 7**).
- Distinct kinetics and intensity of innate immune responses between pulmonary omvPV immunization and *B. pertussis* infection lead to similar adaptive immunity (**Chapter 7**).
- Th17 and mucosal IgA are important contributors to enhanced pertussis immunity and hallmarks of responses evoked by both pulmonary administration of omvPV and *B. pertussis* infection (**Chapters 3 and 7**).

General discussion

The world is currently facing resurgence of pertussis [9-11] caused by pathogen adaptation and waning immunity [12]. This situation calls for re-evaluation of pertussis vaccines.

(i) Immunity induced by infection and pulmonary omvPV immunization

Infection-induced immunity in humans remains for 4-20 years [13] or even 50 years [14]. Immunity induced by marketed pertussis vaccines wanes after 4-12 years [13, 14]. In **Chapter 2** we showed that infection-induced immunity confers sterilizing immunity in the lungs of mice, which is consistent with the findings found in two studies with mice and baboons [15, 16]. The results in this thesis indicate that systemic IgG, and mucosal IgA (**Chapters 3 and 4**), Th17 cells in the lungs (**Chapters 2, 3 and 7**), and prolonged activity of pulmonary innate cells such as alveolar macrophages, M-cells and goblet cells (**Chapter 3**) contribute to robust protection against *B. pertussis*. The induction of local immune responses might improve vaccine-elicited immunity in a similar way. Indeed, pulmonary administration of omvPV led to faster clearance of *B. pertussis* after intranasal challenge than subcutaneous immunization (**Chapter 7**). The clearance is comparable to infection-induced immunity (**Chapter 2**). Although both immunization routes for omvPV induced strong systemic adaptive immune response, pulmonary immunization evoked a robust mucosal adaptive immune response that included IgA antibodies, IgA- and IgG-producing plasma cells, and Th17 cells in the lungs of mice. These findings as well as transcriptome analysis in the lungs suggest that infection and pulmonary immunization of omvPV confer comparable immunity (**Table 1**), yet with different intensity and kinetics. The responses were more intense and faster in the pulmonary immunized mice. Like other studies [15-18], our findings stress the importance of local induction of Th17 cells and induction of mucosal IgA in the lungs for optimal pertussis immunity. The molecular signatures of **Chapters 2, 3 and 7** provide insight in the underlying mechanisms preceding these adaptive responses. Infection-induced immunity (**Chapter 3**) and omvPV immunization (**Chapter 7**) showed markers of innate lymphoid cells (ILCs) that have important functions in orchestrating immunity i.e. by directing the Th-subset distribution [19]. Furthermore, the *B. pertussis* infection and the pertussis immunization studies (**Chapters 2, 3, 5 and 7**) demonstrated the involvement of the CCR6/CCL20 pathway [20], important for attracting B-cells [21] and Th17 cells [22, 23] towards the lung. Finally, infection-induced immunity involved $CXCR6^{+}$ T-cells that could serve as lung protection marker as was shown for *mycobacterium tuberculosis* [24].

(ii) Outer membrane vesicle vaccine

OmvPV contain hundreds of protein antigens with membrane proteins Vag8 and BrkA as main components (**Chapter 3**). In **Chapter 5**, we confirmed the protective capacity after subcutaneous immunization with omvPV. Construction of omvPV-P93 with abolished Prn

Table 1. Summary of the results of the pertussis immunization and infection studies in mice described in this thesis.

	Non-immunized	aPV (DTP3)*	wPV (WT B1917)*	omvPV (WT B1917)*	omvPV (Prn-B1917)*	omvPV (Prn-B1917)*	Infection (B1917)*
Chapter	1	3 and 6	3 and 5	3 and 5	7	7	4 and 7
Administration route#	-	S.C.	S.C.	S.C.	S.C.	P.M.	I.N.
Dose and dosing schedule	-	2 x 1/4HD (do and d28)	2 x 4 µg (do and d28)	2 x 4 µg (do and d28)	2 x 1 µg (do and d28)	2 x 1 µg (do and d28)	1 x $2x10^5$ CFU (do)
Antigens	-	FHA, Prn, Ptx	~1000 proteins	~500 proteins	~500 proteins	~500 proteins	~1000 proteins
Co-stimulatory components	-	Alum	LPS, DNA	LPS	LPS	LPS	LPS, DNA
Lung clearance	28 days	N.D.‡	7-14 days	7 days	7 days	2 days	2 days
Location immunity	-	Systemic	Systemic	Systemic	Systemic	Local, systemic	Local, systemic
IgA	-	-	-	-	-	+++	+++
IgA specificity	-	-	-	-	-	Vag8	Vag8, Ptx
IgG and subclass Total	-	++++	+++	++++	++++	+++++	+++
IgG and subclass IgG1	-	++++	+++	+++	++++	++++	+
IgG and subclass IgG2a	-	-	+	+++	+++	+++	+++
IgG and subclass IgG2b	-	-	++	+++	++	++	+++
IgG and subclass IgG3	-	-	+++	++++	+++	+++	-
IgG specificity	-	FHA, Prn, Ptx	Vag8, BrkA, GroEl, LPS	Vag8, BrkA, LPS	Vag8, BrkA, Prn	Vag8, BrkA, Prn	Vag8, BrkA, GroEl
Pulmonary Th-cells	-	-	-	-	-	Th17	Th17
Systemic Th-flavor (specificity)	-	Th2 (FHA, Prn, Ptx)	Th1, Th17, Th2 (wP, OMV, FHA)	Th1, Th17, Th2 (wP, OMV)	Th1, Th2, Th17 (Prn, OMV)	Th1, Th2, Th17 (Prn, OMV)	Th1, Th17 (FHA, Ptx, Prn, OMV)

* *B. pertussis* B1917, clinical isolate from the Netherlands (2000), WT B1917 = omvPV from wild type B1917 strain, Prn-B1917 = omvPV from strain with abolished Prn autocleavage [25].
# Subcutaneous (S.C.), pulmonary (P.M.), intranasal (I.N.)
‡ N.D. = not determined

autocleavage [25], resulted in dose reduction from 4 µg to 1 µg total protein content, with a comparable lung clearance rate of 7 days (**Chapter 7**)(**Table 1**). Remarkably, pulmonary immunization of omvPV-P93 caused lung clearance in only 2 days after challenge (**Chapter 7**), comparable to infection-induced immunity (**Chapter 2**). Furthermore, omvPV induce higher serum IgG levels after subcutaneous immunization than aPV and wPV (**Chapter 3**). The omvPV induced antibodies of all IgG subclasses directed against a broad range of antigens, e.g. Vag8 and BrkA. Apart from anti-protein responses, omvPV induced anti-LPS IgG3 antibodies that are bactericidal [26, 27]. Strong antibody responses against antigens that cause complement evasion by *B. pertussis*, such as Vag8 [28], may be beneficial as well as the broad subclass distribution that facilitates formation of antibodies with different functions [29].

The omvPV contains several intrinsic pathogen-associated molecular patterns (PAMPs) like LPS and bacterial DNA although less than wPV (**Chapter 3**). This presence of LPS in omvPV may still be a concern given its relation to adverse effects induced by wPV [30-33]. In **Chapter 5**, we demonstrate that the omvPV induces less systemic pro-inflammatory cytokines such as IL-6 and IL-1β, than wPV. These inflammatory responses caused by immunization are often related to adverse effects like fever [30-33]. Especially, the lower levels of IL-1β are preferable in relation to the rare induction of neurological effects by wPV [32]. However, the question remains whether the lower IL-1β induction by omvPV in mice is also observed in humans. Whereas the induction of pro-inflammatory cytokines is already reduced significantly compared to wPV, the remaining LPS contributes to Th1/Th17 skewed responses [34, 35] that are considered optimal for pertussis immunity [15, 16, 36]. Indeed, subcutaneous immunization with omvPV led to a mixed systemic Th1/Th2/Th17 response as seen in **Chapter 5** and **Chapter 7**, whereas pulmonary immunization even led to a more Th17-dominated systemic response. In addition, the pulmonary immunization conferred lung-resident Th17 cells (**Chapter 7**).

Vesicles are nanoparticles, which enables better uptake by DCs, in contrast to the larger whole-cell particles [37]. Additionally, the size [38] and cationic charge [39] of vesicles might be optimal to stimulate mucosal immune responses. This is in line with the mucosal immunity obtained after pulmonary immunization of omvPV (**Chapter 7**).

Further molecular engineering may optimize the use of omvPV as vaccine candidate. For instance, if necessary, PAMPs such as LPS can be modified to balance adjuvant activity and undesired inflammatory responses. Moreover, the presence of particular pertussis antigens can be increased as was shown for Prn [25] or even constructions can be made that allow heterologous antigen expression of different pathogens [40] as combination vaccine.

(iii) Preferred composition of pertussis vaccines

Based on the results described in this thesis we can speculate on the components that should be in the pertussis vaccine. The presence of LPS in pertussis vaccines will remain a point of debate. It is associated with adverse effects, but also acts as an adjuvant. As discussed above, LPS in omvPV induces lower pro-inflammatory profiles as compared to wPV, which may

indicate fewer adverse effects. Interestingly, a booster immunization with omvPV and wPV and a second infection of *B. pertussis* induced high levels of anti-LPS IgG3 (**Chapters 3, 4, 5 and 7**) that have bactericidal activity [26, 27]. The IgG3 subclass suggests that these antibodies are mainly formed in a T-cell independent manner [41]. Additionally, LPS as adjuvant improves the Th1/Th17 balance [34, 35] (**Chapters 3, 4, 5 and 7**). Interestingly, addition of the LPS-derivative Lpxl1 to aPV caused a shift from a strong Th2-dominated response towards an additional profound Th1/Th17 response [7]. In **Chapter 6**, we confirmed these Th1/Th17 responses on molecular level specifically in isolated $CD4^+$ T-cells. These studies confirm the importance of LPS as an adjuvant.

We demonstrated that B-cell and T-cell responses directed against multiple other antigens, i.e. Vag8 and BrkA, in omvPV and wPV contribute to protection against *B. pertussis* (**Chapters 5 and 7**). The small numbers of antigens in aPV stimulates vaccine-induced adaptation as was recently demonstrated by increased circulation of Prn-deficient strains [42, 43]. This suggests that Prn should be replaced, or that additional antigens should be added to the aPV. According to our results and those of others, possible candidate antigens would be adenylate cyclase toxin-hemolysin (Act) [44], BrkA [45], BvgA, TCF, and Vag8 [28, 46]. However, addition of antigens would further increase the cost of the aPV and more importantly would probably not improve the Th-balance. Changing the Th-response could be overcome by addition or replacement of the adjuvant in the aPV [7, 47]. Antibody responses against *B. pertussis* should preferably be directed against antigens such as Ptx, FHA, Vag8, BrkA because they have immune evasive properties [28, 48]. In addition, the IgG subclass distribution should be broad to fight the bacteria on multiple fronts through direct killing or with help of phagocytes.

Summarizing conclusion and perspectives

This thesis demonstrated the advantage of a systems vaccinology approach [49] in early vaccine development. Numerous molecular signatures were identified that are involved in pertussis immunization and *B. pertussis* infection. The next step is to confirm the functionality of these molecular signatures in relation to pertussis immunity in dedicated knockout studies. Furthermore, upcoming systems vaccinology pillars such as microRNAs [50], unbiased proteomics, and investigating purified cell populations [51], can be explored. Finally, new initiatives should be sought for more effective and faster retrieval of functional annotation of data from public databases.

Effective pertussis immunity comprises of systemic humoral and cellular responses that consist of memory B-cells, plasma cells that produce a broad IgG subclass response, and antigen-specific Th1/Th17-cells against multiple antigens. We demonstrated the importance of local immunity in the lungs, which should include IgA-producing memory B-cells and widespread IgA in the mucosa in addition to lung-resident memory Th17-cells. To limit vaccine-induced selection a broad antibody and preferably T-cell specificity directed against a combination of the following antigens is probably important; Ptx, Vag8, Prn, FHA, Fim2, Fim3, BrkA, LPS, BvgA, and TCF. Additionally, the induction of 'trained' innate immune cells, such as ILCs and NK-cells in the lungs may contribute to optimal pertussis immunity.
Re-introduction of wPVs in high-income countries in not expected, as it requires engineered strains that are less reactogenic with consistent expression of virulence factors. Altering current aPVs by changing adjuvants and/or antigens, i.e. Vag8, BrkA, are plausible options for increased efficacy of these vaccines. However, this most likely would only partly solve current problems, such as vaccine-induced pathogen evolution, waning immunity, and continued transmission in the vaccinated population [12, 52]. Third-generation pertussis vaccines like live-attenuated vaccine (BPZE1) [53] and omvPV, the latter especially in combination with mucosal immunization, confer better immunity profiles compared to wPVs and aPVs, at least in mice. The broad antigen content, intrinsic adjuvants, ideal presentation form as nanoparticle, and the possibilities of product engineering, make omvPV a promising vaccine candidate.

References

1. Netea, M.G., Training innate immunity: the changing concept of immunological memory in innate host defence. Eur J Clin Invest, 2013. 43(8): p. 881-4.
2. Netea, M.G., J. Quintin, and J.W. van der Meer, Trained immunity: a memory for innate host defense. Cell Host Microbe, 2011. 9(5): p. 355-61.
3. Monticelli, L.A., *et al.*, Innate lymphoid cells promote lung-tissue homeostasis after infection with influenza virus. Nat Immunol, 2011. 12(11): p. 1045-54.
4. Netea, M.G., *et al.*, Innate immune memory: a paradigm shift in understanding host defense. Nat Immunol, 2015. 16(7): p. 675-9.
5. Dufton, N., *et al.*, Anti-inflammatory role of the murine formyl-peptide receptor 2: ligand-specific effects on leukocyte responses and experimental inflammation. J Immunol, 2010. 184(5): p. 2611-9.
6. Inoue, A., *et al.*, Murine tumor necrosis factor alpha-induced adipose-related protein (tumor necrosis factor alpha-induced protein 9) deficiency leads to arthritis via interleukin-6 overproduction with enhanced NF-kappaB, STAT-3 signaling, and dysregulated apoptosis of macrophages. Arthritis Rheum, 2012. 64(12): p. 3877-85.
7. Brummelman, J., *et al.*, Modulation of the CD4(+) T cell response after acellular pertussis vaccination in the presence of TLR4 ligation. Vaccine, 2015. 33(12): p. 1483-91.
8. Mackley, E.C., *et al.*, CCR7-dependent trafficking of RORgamma(+) ILCs creates a unique microenvironment within mucosal draining lymph nodes. Nat Commun, 2015. 6: p. 5862.
9. Tan, T., *et al.*, Pertussis Across the Globe: Recent Epidemiologic Trends From 2000-2013. Pediatr Infect Dis J, 2015. 34(9):e222-32.
10. Cherry, J.D., Epidemic pertussis in 2012--the resurgence of a vaccine-preventable disease. N Engl J Med, 2012. 367(9): p. 785-7.
11. Celentano, L.P., *et al.*, Resurgence of pertussis in Europe. Pediatr Infect Dis J, 2005. 24(9): p. 761-5.
12. Mooi, F.R., N.A.T. van der Maas, and H.E. De Melker, Pertussis resurgence: waning immunity and pathogen adaptation - two sides of the same coin. Epidemiol Infect, 2013: p. 1-10.
13. Wendelboe, A.M., *et al.*, Duration of immunity against pertussis after natural infection or vaccination. Pediatr Infect Dis J, 2005. 24(5 Suppl): p. S58-61.
14. Campbell, P.T., *et al.*, Defining long-term drivers of pertussis resurgence, and optimal vaccine control strategies. Vaccine, 2015. 33(43): p. 5794-800.
15. Ross, P.J., *et al.*, Relative contribution of Th1 and Th17 cells in adaptive immunity to *Bordetella pertussis*: towards the rational design of an improved acellular pertussis vaccine. PLoS Pathog, 2013. 9(4): p. e1003264.
16. Warfel, J.M. and T.J. Merkel, *Bordetella pertussis* infection induces a mucosal IL-17 response and long-lived Th17 and Th1 immune memory cells in nonhuman primates. Mucosal Immunol, 2013. 6(4): p. 787-96.
17. Wolfe, D.N., *et al.*, Comparative role of immunoglobulin A in protective immunity against the Bordetellae. Infect Immun, 2007. 75(9): p. 4416-22.
18. Hellwig, S.M., *et al.*, Immunoglobulin A-mediated protection against *Bordetella pertussis* infection. Infect Immun, 2001. 69(8): p. 4846-50.
19. Artis, D. and H. Spits, The biology of innate lymphoid cells. Nature, 2015. 517(7534): p. 293-301.
20. Liao, F., *et al.*, CC-chemokine receptor 6 is expressed on diverse memory subsets of T cells and determines responsiveness to macrophage inflammatory protein 3 alpha. J Immunol, 1999. 162(1): p. 186-94.
21. Elgueta, R., *et al.*, CCR6-dependent positioning of memory B cells is essential for their ability to mount a recall response to antigen. J Immunol, 2015. 194(2): p. 505-13.
22. Hirota, K., *et al.*, Preferential recruitment of CCR6-expressing Th17 cells to inflamed joints via CCL20 in rheumatoid arthritis and its animal model. J Exp Med, 2007. 204(12): p. 2803-12.
23. Alcaide, P., *et al.*, Difference in Th1 and Th17 lymphocyte adhesion to endothelium. J Immunol, 2012. 188(3): p. 1421-30.
24. Lee, L.N., *et al.*, CXCR6 is a marker for protective antigen-specific cells in the lungs after intranasal immunization against *Mycobacterium tuberculosis*. Infect Immun, 2011. 79(8): p. 3328-37.
25. Sloots, A., *et al.*, Abolished pertactin cleavage enhances the immunogenicity and potency of a novel *B. pertussis* outer membrane vesicle vaccine: A proof of principle. Manuscript in preparation.
26. Mountzouros, K.T., A. Kimura, and J.L. Cowell, A bactericidal monoclonal antibody specific for the lipooligosaccharide of *Bordetella pertussis* reduces colonization of the respiratory tract of mice after aerosol infection with *B. pertussis*. Infect Immun, 1992. 60(12): p. 5316-8.
27. Kubler-Kielb, J., *et al.*, Oligosaccharide conjugates of *Bordetella pertussis* and bronchiseptica induce bactericidal antibodies, an addition to pertussis vaccine. Proc Natl Acad Sci U S A, 2011. 108(10): p. 4087-92.
28. Jongerius, I., *et al.*, Complement evasion by *Bordetella pertussis*: implications for improving current vaccines. J Mol Med (Berl), 2015. 93(4): p. 395-402.
29. Geurtsen, J., K.C. Fae, and G.P. van den Dobbelsteen, Importance of (antibody-dependent) complement-mediated serum killing in protection against *Bordetella pertussis*. Expert Rev Vaccines, 2014: p. 1-12.
30. Jefferson, T., M. Rudin, and C. DiPietrantonj, Systematic review of the effects of pertussis vaccines in children. Vaccine, 2003. 21(17-18): p. 2003-14.
31. David, S., P.E. Vermeer-de Bondt, and N.A. van der Maas, Reactogenicity of infant whole cell pertussis combination vaccine compared with acellular pertussis vaccines with or without simultaneous pneumococcal vaccine in the Netherlands. Vaccine, 2008. 26(46): p. 5883-7.
32. Armstrong, M.E., *et al.*, IL-1beta-dependent neurological effects of the whole cell pertussis vaccine: a role for IL-1-associated signalling components in vaccine reactogenicity. J Neuroimmunol, 2003. 136(1-2): p. 25-33.
33. Loscher, C.E., *et al.*, Proinflammatory cytokines in the adverse systemic and neurologic effects associated with parenteral injection of a whole cell pertussis vaccine. Ann N Y Acad Sci, 1998. 856: p. 274-7.
34. Banus, S., *et al.*, The role of Toll-like receptor-4 in pertussis vaccine-induced immunity. BMC Immunol, 2008. 9: p. 21.

35. Higgins, S.C., *et al.*, TLR4 mediates vaccine-induced protective cellular immunity to *Bordetella pertussis*: role of IL-17-producing T cells. J Immunol, 2006. 177(11): p. 7980-9.
36. Raeven, R.H.M., *et al.*, Molecular signatures of the evolving immune response in mice following a *Bordetella pertussis* infection. PLoS One, 2014. 9(8): p. e104548.
37. Kuehn, M.J. and N.C. Kesty, Bacterial outer membrane vesicles and the host-pathogen interaction. Genes Dev, 2005. 19(22): p. 2645-55.
38. Stano, A., *et al.*, Nanoparticle size influences the magnitude and quality of mucosal immune responses after intranasal immunization. Vaccine, 2012. 30(52): p. 7541-6.
39. Fromen, C.A., *et al.*, Controlled analysis of nanoparticle charge on mucosal and systemic antibody responses following pulmonary immunization. Proc Natl Acad Sci U S A, 2015. 112(2): p. 488-93.
40. Salverda, M.L., *et al.*, Surface display of a borrelial lipoprotein on meningococcal outer membrane vesicles. Vaccine, 2016. 34(8):1025-33.
41. Quintana, F.J., *et al.*, Induction of IgG3 to LPS via Toll-like receptor 4 co-stimulation. PLoS One, 2008. 3(10): p. e3509.
42. Pawloski, L.C., *et al.*, Prevalence and molecular characterization of pertactin-deficient *Bordetella pertussis* in the United States. Clin Vaccine Immunol, 2014. 21(2): p. 119-25.
43. Lam, C., *et al.*, Rapid increase in pertactin-deficient *Bordetella pertussis* isolates, Australia. Emerg Infect Dis, 2014. 20(4): p. 626-33.
44. Sebo, P., R. Osicka, and J. Masin, Adenylate cyclase toxin-hemolysin relevance for pertussis vaccines. Expert Rev Vaccines, 2014. 13(10): p. 1215-27.
45. Marr, N., *et al.*, Protective activity of the *Bordetella pertussis* BrkA autotransporter in the murine lung colonization model. Vaccine, 2008. 26(34): p. 4306-11.
46. Gouw, D., *et al.*, Proteomics-Identified Bvg-Activated Autotransporters Protect against *Bordetella pertussis* in a Mouse Model. PLoS One, 2014. 9(8): p. e105011.
47. Dunne, A., *et al.*, A novel TLR2 agonist from *Bordetella pertussis* is a potent adjuvant that promotes protective immunity with an acellular pertussis vaccine. Mucosal Immunol, 2015. 8(3): p. 607-17.
48. de Gouw, D., *et al.*, Pertussis: a matter of immune modulation. FEMS Microbiol Rev, 2011. 35(3): p. 441-74.
49. Pulendran, B., S. Li, and H.I. Nakaya, Systems vaccinology. Immunity, 2010. 33(4): p. 516-29.
50. Filipowicz, W., S.N. Bhattacharyya, and N. Sonenberg, Mechanisms of post-transcriptional regulation by microRNAs: are the answers in sight? Nat Rev Genet, 2008. 9(2): p. 102-14.
51. Touzot, M., *et al.*, Using Transcriptional Signatures to Assess Immune Cell Function: From Basic Mechanisms to Immune-Related Disease. J Mol Biol, 2015. 427(21): p. 3356-67.
52. Warfel, J.M., L.I. Zimmerman, and T.J. Merkel, Acellular pertussis vaccines protect against disease but fail to prevent infection and transmission in a nonhuman primate model. Proc Natl Acad Sci U S A, 2014. 111(2): p. 787-92.
53. Mielcarek, N., *et al.*, Live attenuated *B. pertussis* as a single-dose nasal vaccine against whooping cough. PLoS Pathog, 2006. 2(7): p. e65.

About the cover: Al-Khazneh ("The Treasury") in the ancient city of Petra, Jordan. Build in approximately 312 BC by the Nabateans. Part of the UNESCO World Heritage and among the New 7 Wonders of the World.

APPENDICES

Nederlandse samenvatting

Curriculum vitae

List of publications

Nederlandse samenvatting

Roodgedrukte woorden zijn opgenomen in de verklarende woordenlijst.

Kinkhoest

Kinkhoest is een luchtweginfectie die wordt veroorzaakt door de **gram-negatieve bacterie** *Bordetella pertussis*. *B. pertussis* werd in 1906 ontdekt en geïsoleerd door de Bordet en Gengou. Een infectie met *B. pertussis* komt in de natuur alleen voor bij mensen. Hoewel de ziekte vóórkomt bij alle leeftijdsgroepen, lopen pasgeborenen het grootste risico. Bepalen of iemand kinkhoest heeft is erg lastig aangezien in het vroege stadium van de infectie vaak alleen een milde hoest aanwezig is en geen koorts. In een latere fase van de infectie nemen de klachten toe met overgeven, ademnood en intensief hoesten, hetgeen bij baby's uiteindelijk kan leiden tot de dood. Deze intensieve hoest houdt een lange tijd aan. Daarom noemen de Chinezen het de "hoest van 100 dagen".

Kinkhoest epidemiologie

Kinkhoest is een ziekte die voorkómen kan worden door vaccinatie. Vaccinatie tegen kinkhoest vanaf 1940 heeft wereldwijd geleid tot een drastische afname van het aantal kinkhoestgevallen. Volgens een schatting van de Wereld Gezondheidsorganisatie voorkomt vaccinatie tegen kinkhoest circa 700.000 sterfgevallen per jaar. Volgens de huidige schattingen ontvangt 86% (115 miljoen) van alle kinderen drie kinkhoestvaccinaties. Ondanks deze hoge vaccinatiegraad komt kinkhoest nog steeds voor en zijn er regelmatig grote uitbraken. Ook in Nederland is het aantal gevallen van kinkhoest de afgelopen jaren drastisch gestegen (**Zie Hoofdstuk 1, Figuur 2A**). Mogelijke oorzaken zijn verandering van de circulerende stammen, maar ook de beperkte beschermingsduur van de huidige kinkhoestvaccins.

Kinkhoestbacterie

De kinkhoestbacterie wordt omgeven door een binnenmembraan en buitenmembraan. Het binnenmembraan omsluit het **cytoplasma**. De ruimte tussen het binnen- en buitenmembraan wordt het **periplasma** genoemd. Elk compartiment (cytoplasma, periplasma, binnen- en buitenmembraan) bevat unieke eiwitten met verschillende functies (**Zie Hoofdstuk 1, Figuur 1A**). Zo zijn er eiwitten in de buitenmembraan die helpen bij het hechten aan de **mucosa**. Andere eiwitten worden tijdens een infectie uitgescheiden, zoals pertussis toxine (Ptx). Onderzoek heeft tevens laten zien dat verschillende eiwitten van *B. pertussis* in staat zijn om het immuunsysteem van de gastheer te onderdrukken of omzeilen, waardoor de bacterie beter kan overleven. Kennis over deze eiwitten draagt bij aan het optimaliseren van vaccins tegen kinkhoest.

Kinkhoestvaccins

Momenteel zijn verschillende kinkhoestvaccins op de markt. Daarnaast worden nieuwe, betere kinkhoestvaccins ontwikkeld. Een belangrijk gegeven is dat al deze vaccins verschillen in hun samenstelling.

Het eerste kinkhoestvaccin dat op de markt kwam, bestond uit geïnactiveerde bacteriën (whole cell pertussis vaccin, wPV). Momenteel ontvangt naar schatting 75% van de wereldbevolking dit vaccin. Omdat wPV bestaat uit de volledige gedode bacterie bevat het veel verschillende **antigenen**. Hierdoor werken deze vaccins goed, maar gaat vaccinatie met wPV vaak gepaard met bijwerkingen zoals lokale zwelling op de plaats van injectie en koorts. Deze bijwerkingen lijken in ernst toe te nemen met het aantal vaccinaties en met de leeftijd waarop gevaccineerd wordt. Vandaar dat vaccinatie met wPV wordt afgeraden bij jongvolwassenen en volwassenen. Dit heeft geleid tot de vraag naar veiligere kinkhoestvaccins.

Deze vraag naar veiliger kinkhoestvaccins heeft de ontwikkeling gestimuleerd van accelulaire pertussis vaccins (aPV). Deze vaccins bestaan uit één tot vijf gezuiverde eiwitten van de kinkhoestbacterie, die aan aluminiumzouten worden **geadsorbeerd** (**Zie Hoofdstuk 1, Figuur 1B**). Het aluminiumzout is een hulpstof die het immuunsyteem prikkelt tot een betere reactie tegen de antigenen. In Nederland is het wPV in 2005 vervangen door een aPV met drie componenten. Deze vaccins geven tijdelijk een goede bescherming, maar recent onderzoek laat zien dat de beschermingsduur van aPVs maar beperkt is. De kosten van deze vaccins zijn hoog waardoor veel ontwikkelingslanden niet in staat zijn deze vaccins te gebruiken. De meest recente strategie met aPVs is maternale vaccinatie, waarbij zwangere vrouwen worden gevaccineerd waardoor kinkhoest-specifieke **antistoffen** worden overgedragen aan het ongeboren kind. Deze strategie is vooral gericht om de baby's in de eerste maanden van hun leven te beschermen tegen een kinkhoestinfectie.

Een van de vaccins die momenteel in ontwikkeling is, is een levend verzwakt kinkhoestvaccin. Dit vaccin bestaat uit levende bacteriën die in staat zijn om te delen maar dusdanig zijn aangepast dat een individu er niet ziek van wordt. Anders dan de huidige vaccins op de markt wordt dit vaccin via de neus (intranasaal) toegediend. In een muizenmodel geeft een eenmalige dosis van dit vaccin goede bescherming tegen een infectie. De ontwikkeling van dit vaccin is momenteel in de vroege klinische fase.

Een ander kinkhoestvaccin, het outer membrane vesicle pertussis vaccin (omvPV) dat momenteel in ontwikkeling is, bestaat uit buitenmembraan vesicles (outer membrane vesicles, OMVs). OMVs zijn blaasjes, zogenaamde vesicles, die zijn afgesnoerd van de buitenmembraan van de bacterie (**Zie Hoofdstuk 1, Figuur 1C**). Deze OMVs zijn ongeveer 10x kleiner dan de bacterie en bevatten voornamelijk eiwitten uit de buitenmembraan en lipiden,

zoals het immuunstimulerende **lipopolysaccharide** (LPS). OMVs worden van nature ook aangemaakt door bacteriën voor overdracht van stoffen tussen de bacteriën maar ze kunnen ook het immuunsysteem afleiden tijdens een infectie. Het omvPV is een vaccin dat centraal staat in dit proefschrift.

Vaccinatie en het immuunsysteem

Vaccinatie is een van de succesvolste medische interventies ter voorkoming van infectieziekten. Jaarlijks worden hierdoor miljoenen levens gered en een enorme ziektelast voorkomen. Anders dan bij therapeutische medicijnen, zijn vaccins tegen infectieziekten preventief en beschermen dus tegen een toekomstige infectie. Tijdens de vaccinatie wordt als het ware een infectie nagebootst met een veilig product. Het immuunsysteem bestaat o.a. uit vele soorten cellen met specifieke functies. De wijze waarop het immuunsysteem op een vaccin reageert, is voor een groot gedeelte afhankelijk van de componenten die zich in een vaccin bevinden, maar ook welke immuuncellen worden geactiveerd. Kennis over het vaccin en de interactie met het immuunsysteem van de gastheer zijn daarom van cruciaal belang om tot een effectief vaccin te komen.

Het immuunsysteem van de gastheer is onder te verdelen in twee gedeeltes. Het **aangeboren immuunsysteem**, dat snel reageert en als functie heeft om als eerste **pathogenen** te herkennen en uit te schakelen via b.v. **fagocyterende cellen**. Cellen van het aangeboren immuunsysteem hebben sensoren (**PRRs**) voor moleculen (**PAMPs**) die uniek zijn voor microben. Een voorbeeld van een PAMP voor *B. pertussis* is het hierboven genoemde LPS dat herkend wordt door Toll-like receptor 4 (TLR4). Na herkenning gaan deze cellen **cytokines** produceren, die vervolgens andere immuuncellen naar de plek van infectie sturen. Vaccins moeten in het algemeen deze stimulatoren ook bevatten om goed te kunnen werken. Deze toevoegingen worden **adjuvantia** genoemd. Echter, wanneer deze signalen te intens zijn, kunnen bijwerkingen, zoals koorts optreden. Bij vaccinatie is het daarom van belang dat deze signalen gereguleerd worden.
Naast het aangeboren immuunsysteem bestaat het **adaptieve immuunsysteem** dat bestaat uit immuuncellen zoals **B-cellen** en **T-cellen**. De **antigeen-presenterende cellen** (APCs), onderdeel van het aangeboren immuunsysteem, nemen het pathogeen of het vaccin op en selecteren bepaalde stukken die ze gaan presenteren aan B-cellen en T-cellen. B-cellen maken antistoffen zoals **immunoglobuline** G (IgG) of IgA terwijl **cytotoxische T-cellen** cellen kunnen opruimen die besmet zijn of tot kankercel zijn getransformeerd. Daarnaast spelen **T-helper (Th) cellen**, een belangrijke rol bij een goede bescherming tegen pathogenen zoals kinkhoestbacterieen. Th-cellen produceren cytokines op het moment dat ze het antigeen herkennen. Aan de hand van de cytokine productie worden ze getypeerd, b.v. **Th1**, **Th2**, **Th17**. De effectiviteit van de T-cellen en B-cellen is afhankelijk van aantallen, type, locatie en levensduur.

Systeem vaccinologie

Hoewel de meeste vaccins goed werken, is het werkingsmechanisme vaak slechts ten dele bekend. Daarnaast zijn er veel infectieziektes waar nog geen vaccins voor bestaan. Soms zijn verbeterde vaccins nodig. Het ontwikkelen en verbeteren van vaccins is tijdrovend en kostbaar. Een nieuwe strategie in biologisch onderzoek dat zich richt op het zo volledig mogelijk ontrafelen van biologische responsen kan de kans op succesvolle vaccinontwikkeling vergroten. Binnen het vaccinonderzoek wordt deze aanpak 'systeemvaccinologie' genoemd. Hierbij wordt de immuunrespons na vaccinatie tot in detail geanalyseerd. Daarbij worden de verschillende lagen van het immuunsysteem onderzocht met diverse technieken. Zo wordt er gekeken naar de expressie van genen, productie van eiwitten of de betrokkenheid van bepaalde cellen (**Zie Hoofdstuk 1, Figuur 3**). Tijdens dit onderzoek worden grote hoeveelheden data gegenereerd die met bio-informatica wordt geanalyseerd met als doel verbanden te leggen tussen vaccinatie en de immuunrespons. Met deze informatie kan de werking van vaccins beter begrepen worden. Ook kan de aanpak van 'systeemvaccinologie' de ontwikkeling van nieuwe vaccins bevorderen.

Dit proefschift

In dit proefschrift hebben we 'systeemvaccinologie' toegepast om een gedetailleerd beeld te schetsen van de immuunrespons na vaccinatie met verschillende kinkhoestvaccins in vergelijk met een kinkhoestinfectie in een muizenmodel.

In **Hoofdstuk 2** is de immuunrespons onderzocht die plaatsvindt tijdens een *B. pertussis* infectie in onbeschermde muizen. Het doorlopen van een kinkhoestinfectie is uiteraard geen reële vaccinatiestrategie maar voorgaand epidemiologisch onderzoek laat zien dat mensen na een kinkhoestinfectie langer beschermd zijn dan na vaccinatie met de huidige vaccins. Terwijl de immuniteit van kinkhoestvaccins afneemt na 4 tot 12 jaar, blijft de immuniteit na infectie 4 tot 20 jaar aanwezig. Daarnaast wordt in dit proefschrift een kinkhoestinfectie gebruikt om de mate van bescherming geïnduceerd door verschillende vaccins te bepalen in het muizenmodel. Het geldt dus als een soort van benchmark. In deze studie hebben we verschillende processen geïdentificeerd en aan elkaar gekoppeld die plaatsvinden in de verschillende fases van de immuunrespons na een primaire kinkhoestinfectie.

In **Hoofdstuk 3** zijn vervolgens de verschillen in de immuunrespons onderzocht bij muizen, die al eerder een infectie hebben doorlopen (dus goed beschermd zijn) en bij onbeschermde muizen. De beschermde muizen hebben immuniteit opgebouwd die bestaat uit voornamelijk Th17 cellen en specifieke antistoffen in het bloed en lokaal in de longen. Opmerkelijk is dat er ook cellen uit het aangeboren immuunsysteem in de longen gevonden werden in beschermde muizen. Dit betreft **goblet cellen**, **M-cellen** en **alveolaire macrofagen**. Dit geeft aan dat ook cellen van het aangeboren immuunsysteem in de longen mogelijk getraind worden door de eerste kinkhoestinfectie en bijdragen aan de goede bescherming.

Het omvPV is een kandidaat vaccin dat centraal staat in dit proefschrift. In **Hoofdstuk 4** wordt aangetoond dat het omvPV net als het wPV een complex vaccin is dat bestaat uit honderden eiwitten, en dus potentiele antigenen. In deze studie zijn muizen gevaccineerd met omvPV. Vervolgens hebben we met een combinatie van verschillende methodes, zoals **2D-elektroforese**, **Western blot** en **massaspectrometrie** bepaald tegen welke antigenen uit de OMVs de in het bloed aanwezige antistoffen gericht zijn. Dit is vergeleken met muizen die zijn gevaccineerd met een aPV of wPV, of muizen die een infectie hebben doorlopen. De resultaten laten niet alleen zien dat de vaccinsamenstelling bepaalt tegen welke eiwitten antistoffen worden gemaakt, maar ook invloed heeft op het **antistof subtype**. Deze antistof subtypes hebben een eigen functie bij de bescherming tegen kinkhoest. De resultaten van de studie laten zien dat vaccinatie met omvPV leidt tot een breed antistofprofiel tegen antigenen als Vag8, BrkA en LPS, maar tevens uit alle subtypes bestaat. In tegenstelling daarmee staat het aPV dat weliswaar hoge antistofniveaus tegen de drie antigenen FHA, Prn en Ptx induceert, maar die zijn alleen van het IgG1 subtype. Dit geeft mogelijk aan dat door het opwekken van verschillende IgG subtypes met meerdere functies, het omvPV een bredere type bescherming geeft.

In **Hoofdstuk 5** is de immuunrespons na vaccinatie met omvPV verder vergeleken met die na vaccinatie met een wPV. Het wPV geeft bescherming maar is ook geassocieerd met bijwerkingen. In deze studie laten we zien dat het omvPV een gelijke bescherming biedt tegen een kinkhoestinfectie met dezelfde type T-cellen en een hoger antistofniveau als het wPV. Maar wat opmerkelijk en belangrijker is, is dat na omvPV vaccinatie minder cytokines worden geproduceerd die geassocieerd worden met bijwerkingen. Daarnaast werden er op het niveau van genexpressie, genen geïdentificeerd met anti-inflammatoire functies na vaccinatie met omvPV.

Naast de specifieke antistoffen wordt er steeds meer aandacht geschonken aan T-cellen en specifiek de $CD4^+$ T-cellen, bij de bescherming tegen kinkhoest. De $CD4^+$ T-cel respons na aPV vaccinatie wordt gedomineerd door het Th2 type. In **Hoofdstuk 6** is het adjuvant Lpxl1 toegevoegd aan het aPV om te bepalen welke invloed dit heeft op de type T-cellen en welke genen hierbij tot expressie komen in de T-cellen. Lpxl1 is een niet-toxisch LPS die bindt aan TLR4 op immuuncellen die de richting van het immuunsysteem bepalen. Na vaccinatie zijn de T-cellen geïsoleerd uit muizen om vervolgens de genexpressie profielen te vergelijken met muizen die alleen met aPV zijn gevaccineerd. De resultaten van deze studie laten zien dat er meer genen, zoals **transcriptiefactoren** en cytokines tot expressie komen die geassocieerd worden met Th1 en Th17 cellen. Daarnaast werden andere minder bekende genen gevonden die gekoppeld kunnen worden aan de Th1/Th17 respons. Deze studie laat tevens zien dat het aanpassen van het adjuvans in aPV een invloed heeft op het type T-cellen dat wordt gevormd.

De verschillende kinkhoestvaccins die onderhuids worden ingespoten geven dus allen een ander type immuniteit. Een overeenkomst is echter dat ze geen van alle lokale immuniteit opwekken in de luchtwegen, zoals dat wel het geval is na een kinkhoestinfectie. In **Hoofdstuk 7** is daarom bepaald of de toedieningsroute van het omvPV invloed heeft op het type immuniteit en de mate van bescherming. Het omvPV werd pulmonaal, diep in de longen, toegediend en de immuunrespons werd in detail vergeleken met de onderhuidse toediening. De muizen die pulmonaal waren gevaccineerd met omvPV waren in staat om een kinkhoestinfectie in 2 dagen te klaren, terwijl dat na onderhuidse toediening 7 dagen duurde. In deze studie hebben we tevens laten zien dat beide toedieningsroutes leiden tot de inductie van **systemische immuniteit**, maar dat alleen de pulmonale toediening leidt tot **lokale immuniteit**. Deze lokale immuniteit in de long bestaat uit specifieke IgA antistoffen en Th17 cellen.

In **Hoofdstukken 2, 3 en 5** is de genexpressie gemeten in de longen tijdens het doorlopen van een kinkhoestinfectie bij muizen met een verschillende vaccinatieachtergrond. In **Hoofdstuk 8** is een meta-analyse uitgevoerd op deze datasets. Hierdoor waren we in staat om specifieke genen te groeperen en te koppelen aan immunologische functies die gelokaliseerd zijn in de long. Daarnaast zijn genen beschreven die mogelijk in het bloed gemeten kunnen worden om bijvoorbeeld de mate van bescherming te meten of de intensiteit van de infectie.

Conclusie en vooruitblik

In dit proefschrift wordt met de toepassing van 'systeemvaccinologie' geprobeerd een onderbouwing te geven voor de kenmerken waaraan een verbeterd kinkhoestvaccin moet voldoen. We hebben laten zien dat de diverse kinkhoestvaccins maar ook de kinkhoestinfectie een andere type immuunrespons opwekken en dat ook de mate van bescherming varieert in een muizenmodel. Er zijn daarnaast verschillende nieuwe markers (genen, eiwitten, cellen) geïdentificeerd als onderdeel van de immuunrespons van de gastheer die door vaccinatie met verschillende kinkhoestvaccins en een kinkhoestinfectie worden aangemaakt. We hebben in dit proefschrift nog niet specifiek kunnen kijken naar de rol van deze markers bij de bescherming tegen kinkhoest. Daarom zou een volgende stap in het onderzoek zich kunnen richten op infectie- of vaccinatie-experimenten waarbij specifieke markers worden uitgeschakeld om zo de rol van deze specifieke marker te ontrafelen.

Effectieve volwaardige immuniteit tegen kinkhoest bestaat uit systemische humorale en cellulaire immuunresponsen. Mogelijk dient deze immuniteit te bestaan uit **B-geheugencellen** en **plasmacellen** die IgG antistoffen maken van verschillende subtypen tegen meerdere antigenen maar ook antigeen-specifieke Th1/Th17 cellen. Wij hebben daarnaast laten zien dat de ontwikkeling van lokale immuniteit in de luchtwegen een belangrijke toevoeging is aan de bescherming tegen een *B. pertussis* infectie. Mogelijk dient dit te bestaan uit IgA-producerende B-geheugencellen en IgA antistoffen in de mucosa en Th17 cellen die zijn gelokaliseerd in de longen. Het in dit proefschrift beschreven onderzoek geeft aanwijzingen dat een goed beschermend vaccin antistoffen en T-cellen moet opwekken tegen de volgende antigenen: Ptx, Vag8, Prn, FHA, Fim2, Fim3, BrkA, LPS, BvgA en TCF. In ieder geval hebben beschermde muizen immuunresponsen gevormd tegen deze antigenen.

De herintroductie van wPVs in hoge-inkomenslanden is onwaarschijnlijk, omdat dit vaccin veel bijwerkingen geeft. Door de bacteriën genetisch aan te passen, bijvoorbeeld genen betrokken bij de LPS synthese, kunnen bijwerkingen van wPVs verminderd worden. Het aanpassen van de huidige aPVs is ook een mogelijkheid om de werkzaamheid van de vaccins te verbeteren. Bijvoorbeeld door het adjuvans te veranderen of het vaccin uit te breiden door andere gezuiverde kinkhoesteiwitten toe te voegen. De aanpassingen zullen de huidige problemen met kinkhoestvaccinatie wellicht niet volledig oplossen, waaronder de beperkte beschermingsduur, de kinkhoesttransmissie door gevaccineerden en de genetische adaptatie van de kinkhoestbacterie. De ontwikkeling van een volgende generatie kinkhoestvaccins, zoals omvPV, in combinatie met pulmonale of intranasale toediening bieden mogelijk betere immuniteit.

Verklarende woordelijst bij Nederlandse samenvatting

Aangeboren immuunsysteem	Afweersysteem dat al bij de geboorte aanwezig is. Reageert snel maar vaak aspecifiek.
Adaptieve immuunsysteem	Afweersysteem dat wordt verworven door het trainen van naïeve adaptieve immuuncellen d.m.v. blootstelling aan antigenen. Bij een tweede blootstelling aan hetzelfde antigeen, kan een getrainde adaptieve immuuncel sneller reageren.
Adjuvantia	Stof die het aangeboren immuunsysteem kan stimuleren.
Adsorberen	Hechten van moleculen aan het oppervlak van een vaste stof of vloeistof.
Alveolaire macrofagen	Long-specifieke macrofagen (fagocyten).
Antigeen-presenterende cellen	Immuuncel van het aangeboren immuunsysteem dat antigenen van een pathogeen opneemt en presenteert aan cellen van het adaptieve immuunsysteem.
Antigenen	Macromoleculen, vaak eiwitten waar het immuunsysteem op reageert.
Antistof	Eiwit, gemaakt door een B-cel, dat een antigeen kan herkennen en het onschadelijk kan maken.
Antistof subtype	Bij de muis zijn de IgG antistoffen onderverdeeld in 4 subtypen (IgG1, IgG2a, IgG2b, IgG3). Elk subtype heeft een eigen functie zoals binding van pathogenen of interactie met complement en Fc-receptoren.
B-cellen	Immuuncellen die antistoffen kunnen produceren.
B-geheugencellen	B-cellen die antistoffen produceren en een lange levensduur hebben.
Cytokines	Eiwitten die worden geproduceerd tijdens een immuunrespons en als boodschapper fungeren om cellen te beïnvloeden of op afstand aan te trekken.
Cytoplasma	De ruimte binnen de binnenmembraan m.u.v. de celkern.
Cytotoxische T-cellen	T-cellen met de CD8 receptor op het oppervlak. Binden aan cellen die geïnfecteerd zijn door een pathogeen en zorgen dat deze cellen doodgaan.
Fagocytose	Het omsluiten en afbreken van een pathogeen door fagocyterende cellen.
Goblet cellen	Epitheelcel die slijm produceert.
Gram-negatieve bacterie	Bacterie met een binnen- en buitenmembraan. De buitenmembraan bestaat uit een combinatie van eiwitten en lipopolysaccharide.
Immunoglobuline	Antistof. Er bestaan meerdere types waaronder IgG, voornamelijk aanwezig in het bloed en IgA, voornamelijk in de mucosa.
Lokale immuniteit	Afweer die specifiek aanwezig is op een bepaalde plek in het lichaam zoals bijv. de longen.
Lipopolysaccharide	LPS; moleculen in de buitenmembraan van gramnegatieve bacteriën die bestaan uit lipiden en polysaccharide (koolhydraten).
Massaspectrometrie	Techniek voor het kwantificeren en identificeren van moleculen op basis van massa.
M-cellen	Microfold cellen; specifieke immuuncellen in het epitheellaag.
Mucosa	Slijmvlies.
PAMPs	Pathogen-associated molecular patterns; Moleculen van het pathogeen die herkend worden door cellen van het aangeboren immuunsysteem d.m.v specifieke receptoren (PRRs).
Pathogeen	Microbiële ziekteverwekker.

Periplasma	Ruimte tussen de binnen- en buitenmembraan van de bacterie.
Plasmacellen	Gedifferentieerde B-cellen die grote hoeveelheden specifieke antistoffen produceren maar alleen overleven zolang er antigen aanwezig zijn.
PRRs	Pathogen-recognition receptors; Receptoren op en in bepaalde (immuun) cellen die PAMPs herkennen om vervolgens het aangeboren immuunsysteem te activeren.
T-cellen	Cellen van het adaptieve immuunsysteem die een onderdeel zijn van de cellulaire afweer welke o.a zijn onderverdeeld in T-helper cellen ($CD4^+$) en cytotoxische cellen ($CD8^+$).
T-helper (Th) cellen Th1, Th2 en Th17	T-cellen met de CD4 receptor op het oppervlak. Helpen bijvoorbeeld B-cellen en cytotoxische T-cellen. De verschillende type Th-cellen produceren specifieke cytokines die belangrijke processen in de immuunrespons beïnvloeden. De Th1-cellen maken o.a. IFNγ, Th2-cellen maken IL-4, IL-5 en IL-13 terwijl Th17-cellen IL-17 maken.
Transcriptiefactor	Eiwit dat de aanmaak van vele andere eiwitten bepaalt.
Systemische immuniteit	Afweer die aanwezig is in de bloedbaan.
Western blot	Techniek om de binding van antistoffen aan antigenen zichtbaar te maken.
2D-elektroforese	Techniek voor het scheiden van eiwitten in twee dimensies op basis van grootte en lading.

Curriculum vitae

René Raeven was born on August 18, 1982 in Geleen, The Netherlands. After graduating from the Mavo St. Anna in Geleen in 1998 he obtained a dual MBO Chemistry degree at the Leeuwenborgh College, Sittard (Netherlands) and Rheinwestfalische Technische Hochschule (RWTH), Aachen (Germany) in 2001. In 2004 he obtained a Bachelor degree in Biochemistry at the Hogeschool Zuyd in Heerlen, The Netherlands. During this study he performed an internship at the Arkansas State University in Jonesboro, USA on the effects of phytoestrogens in the reproductive tract of sheep. In 2005 he continued for a Master Degree Nutrition and Health at the Wageningen University, The Netherlands which he obtained in 2008. During this study he performed two internships. The first was at the Nutrigenomics Department at the Wageningen University where he investigated the role of transcription factor PPARα in obesitas-induced inflammation in hepatic and adipose tissue. His second internship was at the Nanyang Technological University in Singapore where he performed research on the role of FIAF/Angptl4 in the development and regeneration of villi in small intestine of mice. Subsequently, he worked as a researcher at DSM Dyneema and the Netherlands Vaccine Institute (NVI). In September 2011 he started his PhD project on systems vaccinology and the molecular signatures of immunity to *Bordetella pertussis* at the Institute of Translational Vaccinology (Intravacc) and Leiden University under the supervision of Prof. Dr. Gideon Kersten, Prof. Dr. Wim Jiskoot and Dr. Bernard Metz, which resulted in this thesis. In January 2016 he started working as a scientist at Intravacc continuing his work on systems vaccinology.

List of publications

Raeven RHM, Brummelman J, Pennings JLA, Nijst OEM, Kuipers B, Blok LER, Helm K, van Riet E, Jiskoot W, van Els CACM, Han WGH, Kersten GFA, Metz B. Molecular Signatures of the Evolving Immune Response in Mice following a *Bordetella pertussis* Infection. *PLoS One, 2014. 9(8): p. e104548.*

Raeven RHM, van der Maas L, Tilstra W, Uittenbogaard JP, Bindels THE, Kuipers B, van der Ark A, Pennings JLA, van Riet E, Jiskoot W, Kersten GFA, Metz B. Immunoproteomic Profiling of *Bordetella pertussis* Outer Membrane Vesicle Vaccine Reveals Broad and Balanced Humoral Immunogenicity. *J Proteome Res. 2015. 14(7):2929-42.*

Brummelman J, **Raeven RHM**, Helm K, Pennings JLA, Metz B, van Eden W, van Els CACM, Han WGH. Transcriptome signature for dampened Th2 dominance in acellular pertussis vaccine-induced CD4(+) T-cell responses through TLR4 ligation. *Sci Rep. 2016. 6:25064.*

Raeven RHM, Brummelman J, van der Maas L, Tilstra W, Pennings JLA, Han WGH, van Els CACM, van Riet E, Kersten GFA, Metz B. Immunological signatures after *Bordetella pertussis* infection demonstrate importance of pulmonary innate immune cells. *Manuscript submitted*

Raeven RHM, Brummelman J, Pennings JLA, van der Maas L, Tilstra W, Helm K, van Riet E, Jiskoot W, van Els CACM, Han WGH, Kersten GFA, Metz B. *Bordetella pertussis* outer membrane vesicle vaccine confers equal efficacy in mice with a lower inflammatory response compared to a classic whole-cell vaccine. *Manuscript submitted*

Raeven RHM, Brummelman J, Pennings JLA, van der Maas L, Helm K, Tilstra W,van der Ark A, Sloots A, van der Ley P, van Eden W, Jiskoot W, van Riet E, van Els CACM, Kersten GFA, Han WGH, Metz B. Systems vaccinology reveals superior protection after pulmonary compared to subcutaneous administration of an outer membrane vesicle pertussis vaccine associated with local and systemic immune signatures in mice. *Manuscript submitted*

Raeven RHM, Pennings JLA, van Riet E, Kersten GFA, Metz B. Meta-analysis of pulmonary transcriptomes from differently primed mice identifies molecular signatures to differentiate immune responses following *Bordetella pertussis* challenge. *Manuscript submitted*